

EXPERIMENTAL INVESTIGATION OF HYBRID COLD STORAGE CUM POWER GENERATOR

THESIS

Submitted in fulfillment of the requirement of the degree of

DOCTOR OF PHILOSOPHY

to

YMCA UNIVERSITY OF SCIENCE & TECHNOLOGY

by

ANIL KUMAR

Registration No.: YMCAUST/Ph35/2011

Under the Supervision of

DR. RAJ KUMAR

PROFESSOR



**Department of Mechanical Engineering
Faculty of Engineering & Technology
YMCA University of Science & Technology
Sector-6, Mathura Road, Faridabad, Haryana, India**

MAY, 2017



सत्यमेव जयते

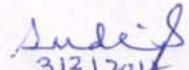
CERTIFICATE

TO WHOM IT MAY CONCERN

This is to certify that **ANIL KUMAR**, Ph.D. Scholar of Department of Mechanical Engineering, YMCA University of Science & Technology, Faridabad (HR) has successfully completed his Research Work on “**EXPERIMENTAL INVESTIGATION OF HYBRID COLD STORAGE CUM POWER GENERATOR**” in the National Institute of Solar Energy, Gwalpahari, Gurgaon, Harayana-122003, An Autonomous Institute of Ministry of New and Renewable Energy, New Delhi.

He worked very well under the above project as a fulfillment of the requirement for the degree of Doctor of Philosophy. He is sincere, hardworking and dedicated candidate.

I wish all the best for his future endeavours.


3/3/2014
(S.K. Singh)

Director General
National Institute of Solar Energy
Harayana-122003

DECLARATION

I hereby declare that this thesis entitled “**EXPERIMENTAL INVESTIGATION OF HYBRID COLD STORAGE CUM POWER GENERATOR**” by **ANIL KUMAR** being submitted in fulfilment of the requirements for the Degree of Doctor of Philosophy in “**DEPARTMENT OF MECHANICAL ENGINEERING**” under Faculty of “**ENGINEERING & TECHNOLOGY**” of YMCA University of Science & Technology Faridabad, during the academic year **2016-2017**, is a bonafide record of my original work carried out under guidance and supervision of **DR. RAJ KUMAR, PROFESSOR, DEPARTMENT OF MECHANICAL ENGINEERING** and has not been presented elsewhere.

I further declare that the thesis does not contain any part of any work which has been submitted for the award of any degree either in this university or in any other university.

(ANIL KUMAR)
Registration No.: YMCAUST/Ph.35/2011

CERTIFICATE

This is to certify that this Thesis entitled “**EXPERIMENTAL INVESTIGATION OF HYBRID COLD STORAGE CUM POWER GENERATOR**” by **ANIL KUMAR**, submitted in fulfillment of the requirement for the Degree of Doctor of Philosophy in “**DEPARTMENT OF MECHANICAL ENGINEERING**” under Faculty of “**ENGINEERING & TECHNOLOGY**” of YMCA University of Science & Technology Faridabad, during the academic year **2016-2017** is a bonafide record of work carried out under my guidance and supervision.

I further declare that to the best of my knowledge, the thesis does not contain any part of any work which has been submitted for the award of any degree either in this university or in any other university.

Dr. Raj Kumar

PROFESSOR

Department of Mechanical Engineering

Faculty of Engineering & Technology

Date:

YMCA University of Science & Technology Faridabad

ACKNOWLEDGEMENT

I would like to express my sincere gratitude to my Supervisor **Dr. Raj Kumar** for giving me the opportunity to work in this area. It would never be possible for me to take this thesis to this level without his/her innovative ideas and his/her relentless support and encouragement.

I also wish to offer my warm expression of thanks to, **Er. S.K. Singh, Director General, National Institute of Solar Energy, Gurgaon** for his unflinching assistance, guidance and pearls of wisdom to enable me to complete this thesis. He provided me all the facilities and academic environment at the various stages for completing this dissertation work in the Research Centre.

I am also thankful to all staff members of Department of Mechanical Engineering, YMCA University of Science & Technology, Faridabad and National Institute of Solar Energy, Gurgaon for their cooperation in my research work.

Finally, I would like to express my gratitude to my family members and friends for their support and encouragement.

(ANIL KUMAR)

Registration No.: YMCAUST/Ph.35/2011

ABSTRACT

In the recent years, the cogeneration technology has been broadening for the utilization of both the renewable energy and waste heat to reduce the serious global environmental related issues. The renewable energy resources have been discovered as the best option to meet the constant increasing demand of power and cooling simultaneously. There are many renewable energy technologies for the utilization of existing resources but two kinds of technologies such as biomass gasification technology and solar technology have been used in this thesis.

In the biomass gasification technology, the processed producer gas is provided to the IC engine coupled with AC generator. This renewable energy power generator has been employed with an $\text{NH}_3\text{-H}_2\text{O}$ vapor absorption refrigeration machine, which is operated by the ‘hybrid solar energy-exhaust gas waste heat’ and thus a ‘new hybrid cold storage cum power generation system’ has been explored. This thesis describes an individual and combined experimental investigation of the ‘hybrid system’ on the basis of energy and exergy analysis. The whole unit has been tested with gradually increasing resistive load from 15.24 kW to 38.86 kW. In the individual investigation, the energy and exergy gasification efficiencies lie between 70.22–81.22% and 62.73–77.75% respectively, with the grate temperature of 1310–1360°C. The tar level after gas cooling-cleaning unit has been obtained 8 mg/Nm³, which is significantly lower than that of the ‘wet packed bed scrubber-based producer gas cooling and cleaning system’.

Similarly the results analysis of the scheffler collector (solar technology), the HRU (Heat Recovery Unit) and the VAM (Vapour Absorption Machine) also show the better performance than the previously coined analogous research literature. The scheffler collector’s technology is effectively used in the winter season due to the less value of cosine losses. The performance of the VAM is higher at the “higher value of the evaporator and generator’s temperatures” or at the “lower value of condenser and absorber’s temperatures”, while the HRU shows the effective utilization of the hybrid solar energy-exhaust gas waste heat extracted from the renewable energy operated Internal Combustion Engine (I.C. Engine). The combined investigation shows that the exergy analysis of the system leads to a possible performance improvement. Nearly 86.35% of the input exergy is destructed due to irreversibilities in the different

components. The engine shows the biggest exergy loss due to the irreversibility occurring in the various processes (such as combustion, heat transfer, mixing, friction, etc.), while the gasifier, scheffler collector, absorber, generator, electric generator and the HRU follow the next largest exergy loss. Around 9.68% is available as the useful exergy output. The exhaust exergy lost to 'the environment and as unaccounted exergy' is 3.99%, which is lower than the corresponding exhaust energy loss of 15.03%, while the useful energy output is 14.83%. It has been observed that the electric load, exhaust gas temperature, condenser and evaporator temperature have significant effects on the total power output, refrigeration output, energy and exergy efficiency. The refrigerants used are of zero ODP and negligible GWP, and the CO₂ emission of the exhaust gases is very small as compared to that of the fossil fuel run engine, hence, this hybrid system is favorable to the global environment along with saving of the fossil fuel. The results also show that the 'new hybrid cold storage cum power generation system' has slightly higher overall energy efficiency and significantly higher overall exergy efficiency than the earlier investigated 'the novel combined power and ejector-refrigeration cycle' and, 'the combined power and ejector-absorption refrigeration cycle'.

TABLE OF CONTENTS

Candidate's Declaration	i
Certificate of the Supervisor	ii
Acknowledgement	iii
Abstract	iv
Table of Contents	vi
List of Tables	xi
List of Figures	xiii
List of Photographs	xv
List of Abbreviations	xvi
CHAPTER-I. INTRODUCTION	1
CHAPTER-II. LITERATURE SURVEY	7
2.1 PERFORMANCE INVESTIGATION OF GASIFIER	7
2.2 QUALITY OF PRODUCER GAS	9
2.3 EFFECT OF FUEL (PRODUCER GAS/FOSSIL FUEL) ON ENGINE'S EXHAUST AND ITS EMISSIONS CHARACTERISTICS WITH PERFORMANCE PARAMETERS	11
2.4 PERFORMANCE EVALUATION OF SOLAR COLLECTOR	14
2.5 PERFORMANCE ANALYSIS OF HEAT EXCHANGER	16
2.5.1 Counter Flow Heat Exchanger	16
2.5.2 Multi-Passes and Cross Flow/Shell & Tube Heat Exchanger	18
2.6 ASSESSMENT OF COLD STORAGE SYSTEM	20
2.6.1 Performance of Vapour Absorption Machine	20
2.6.2 Environmental Impacts from Chiller's Refrigerants	22
2.7 PERFORMANCE STUDY OF THE COMBINED CO-GENERATION SYSTEM	24
CHAPTER-III. THEORY OF HYBRID SYSTEM	29
3.1 PRINCIPLES OF BIOMASS GASIFICATION	29

3.1.1	Types of Gasifier	31
3.1.1.1	Updraft or Counter-Current Gasifier	31
3.1.1.2	Downdraft or Co-Current Gasifier	32
3.1.1.3	Cross-Draft Gasifier	33
3.1.2	Process Zones	33
3.1.2.1	Drying Zone	34
3.1.2.2	Pyrolysis Zone	34
3.1.2.3	Oxidation (Combustion) Zone	34
3.1.2.4	Reduction Zone	35
3.2	PRINCIPLES OF GAS ENGINE-GENERATOR	35
3.2.1	Producer Gas Engine	35
3.2.2	Alternating Current Generator	36
3.3	PRINCIPLES OF SCHEFFLER COLLECTOR WITH SYSTEM OPERATION	37
3.4	PRINCIPLES OF WASTE HEAT RECOVERY UNIT	39
3.4.1	Counter Flow Heat Exchanger	39
3.4.2	Multiple-Passes and Cross Flow Heat Exchanger	40
3.5	PRINCIPLES OF VAPOUR ABSORPTION MACHINE	41
3.6	PRINCIPLES OF CO-GENERATION SYSTEM	42
	CHAPTER-IV. MATERIALS AND METHODOLOGY	45
4.1	DESCRIPTION OF EXPERIMENTAL SET-UP	45
4.1.1	Biomass Gasifier	46
4.1.2	Gas Engine-Generator	47
4.1.3	Scheffler's Collectors	47
4.1.4	Waste Heat Recovery Unit	49
4.1.5	Vapour Absorption Machine	50
4.2	THE TECHNICAL SPECIFICATIONS AND THE EXPERIMENTAL PROCEDURE	51
4.2.1	Specification of Hybrid System	51
4.2.2	Specification of Electric Generator	51
4.2.3	Specification of Engine	51

4.2.4	Specification of Gasifier	52
4.2.5	Specification of Scheffler Collector	52
4.2.6	Specification of Vapour Absorption Machine	52
4.2.7	Experimental Procedure	53
4.3	MEASURING DEVICES AND METHODS USED	55
4.3.1	Fuel	55
4.3.2	Resistive Loading Device	55
4.3.3	Gas Analyzer	56
4.3.4	Measurement of Tar	56
4.3.5	Air Flow Rate	57
4.3.6	Producer Gas Discharge	57
4.3.7	Measurement of Pressure	58
4.3.8	Measurement of Temperature	58
4.3.9	Measurement of Moisture	59
4.3.10	Power Output Measurement	59
4.3.11	Engine Emission Measurement	59
4.3.12	Pyrheliometer, Pyranometer and Ultrasonic Anemometer	59
4.3.13	Design and Calibration of Orifice Plate	61
4.3.13.1	Design Consideration	61
4.3.13.2	Calibration Procedure	61
4.3.13.3	Calculation for Coefficient of Discharge	61
4.4	DEFINITIONS AND MEASUREMENT OF DIFFERENT PARAMETERS	62
4.5	ASSUMPTIONS FOR EVALUATION OF THE HYBRID SYSTEM	67
4.6	FORMULAE USED IN ENERGY AND EXERGY ANALYSIS	68
CHAPTER-V. RESULTS AND DISCUSSION		85
5.1	EVALUATION OF GASIFIER	86
5.1.1	Biomass Consumption Rate and Specific Fuel Consumption	86
5.1.2	Temperature, Reactor Pressure, Calorific Value of Producer Gas and Specific Gas Production	88
5.1.3	Energy and Exergy Efficiency of Downdraft Gasifier	90

5.2	EVALUATION OF GAS COOLING & CLEANING UNIT AND SCHEFFLER SOLAR DISC	91
	5.2.1 Evaluation of Gas Cooling & Cleaning Unit	
	(Condition of Producer Gas)	91
	5.2.1.1 Temperature and Pressure of Producer Gas	91
	5.2.1.2 Tar Contents and Composition of Producer Gas	93
	5.2.2 Evaluation of Scheffler Disc	94
	5.2.2.1 Solar Temperature, Radiations and Solar Power	94
	5.2.2.2 Heat Loss Factor and Heat Absorbed by Receiver	96
	5.2.2.3 Energy and exergy efficiency of Scheffler Collector	98
5.3	PERFORMANCE ANALYSIS OF EXHAUST GAS AND ITS EMISSION CHARACTERISTICS	99
	5.3.1 Exhaust Gas and Mass Flow Rate	99
	5.3.2 Exhaust Gas Emission	100
5.4	ASSESSMENT OF HEAT RECOVERY UNIT	102
	5.4.1. On the Basis of Solar Energy and Engine's Exhaust	102
	5.4.1.1 LMTD and Heat Capacity Ratio (R)	102
	5.4.1.2 Efficiencies and Overall Heat Transfer Coefficient (U)	102
	5.4.2. On the Basis of Producer Gas	103
	5.4.2.2 LMTD and Heat Capacity Ratio (R)	103
	5.4.2.2 Efficiencies and Overall Heat Transfer Coefficient (U)	104
	5.4.3. Comparison of Waste Heat Recovery with Overall Energy and Exergy Loss	105
5.5	PERFORMANCE EVALUATION OF COLD STORAGE SYSTEM	107
	5.5.1 Generator Temperature and Absorber Temperature	107
	5.5.2 Evaporator Temperature and Condenser Temperature	108
	5.5.3 Ambient Temperature and Time for Steady State	110
5.6	COMBINED ANALYSIS OF THE SYSTEM	111
	5.6.1. Energy and Exergy Analysis	111
	5.6.2. Gasifier Output, Brake Power and Exhaust Gas Temperature	115
	5.6.3. Power Outputs/Overall Efficiency at Exhaust Gas Temperature	115

5.6.4. Power Outputs and Overall Efficiency at Evaporator Temperature	117
5.6.5. Power Outputs and Overall Efficiency at Condenser Temperature	118
CHAPTER-VI. CONCLUSIONS	121
6.1 For Gasifier and Producer Gas	121
6.2 For Scheffler Collector	121
6.3 For Vapour Absorption Machine	122
6.4 For Exhaust Heat and Waste Heat Recovery Unit	122
6.5 For Combined Analysis of the Hybrid System	123
CHAPTER-VII. SCOPE FOR FUTURE WORK	125
7.1 Extended Heat Recovery Unit Design for Multi-heat Resources	125
7.2 System Integration for Application	125
7.3 Formation of Chemical and Fertilizers	125
7.4 Co-generation Technology for Residential Use	126
7.5 Integration with Energy Storage	126
LIMITATIONS	127
CONTRIBUTIONS	129
REFERENCES	131
Appendix-A (Sample calculations)	149
Appendix-B (Tables)	174
Appendix-C (Uncertainty analysis)	190
Appendix-D (Brief Biodata)	194
Appendix-E (List of Publications)	196

LIST OF TABLES

Table	Description	Page No.
Table-1 (Gasifier)	Pressure level measurement (mm of water gauge)	174
Table-2 (Gasifier and filters)	Temperature measurement in (°C)	174
Table-3 (Engine and generator)	Power generation sheet	175
Table-4	PG/Biomass requirement/gasifier efficiency	175
Table-4a	Calibration data for air	176
Table-4b	Calibration data for PG	176
Table-5	PG chemical exergy calculation	177
Table-6	Thermal properties of PG	177
Table-7	Thermal properties of constituents of PG	178
Table-8	Average chemical contents of wood fuels	178
Table-9	ED of gasifier	179
Table-10	EDs of filters	179
Table-11 ED of engine	ED of engine	180
Table-12	scheffler collector efficiency calculation	180
Table-13	scheffler collector's heat loss factor calculation	181
Table-14	Exhaust gas calculation	181
Table-15	Exhaust gas emissions calculation	182

LIST OF TABLES

Table	Description	Page No.
Table-16	HRU ED evaluation for exhaust and solar energy	182
Table-17	HRU evaluation for exhaust and solar energy	183
Table-18	HRU ED evaluation for producer gas	183
Table-19	HRU evaluation for producer gas	184
Table-20	Evaluation of VAM	184
Table-21	COP Evaluation of VAM	185
Table-22	Entropy Evaluation of VAM	185
Table- 23	EDs Evaluation of VAM	186
Table-24	VAM calculation with respect to atmosphere	186
Table-25	(Combined analysis)	187
Table-26	Combined analysis at constant load	187
Table-27	Overall heat balance at different loads	188
Table-28	Overall exergy balance at different loads	189

LIST OF FIGURES/GRAPHS

Figure	Description	Page No.
Fig 3.1	Updraft or counter-current gasifier	31
Fig 3.2	Downdraft or co-current gasifier	32
Fig 3.3	Cross draft gasifier	33
Fig 3.4	Schematic view of scheffler collector	37
Fig 3.5	Counter Flow Heat Exchanger	39
Fig 3.6	Multiple-pass and cross flow heat exchanger	40
Fig 3.7	Vapor absorption system with aqua-ammonia solution	41
Fig 4.1	Schematic diagram of a hybrid cold storage cum power generator	53
Fig 5.1	Variation of Biomass Consumption Rate at different loads	86
Fig 5.2	Variation of Specific fuel consumption at different loads	87
Fig 5.3	Variation of CV and PG temperature at different loads	88
Fig 5.4	Variation of reactor pressure and specific gas production with load	88
Fig 5.5	Variation of reactor temperature above the grate	89
Fig 5.6	Effect of load on energy and exergy efficiency	90
Fig 5.7	Variation of temperature of producer gas at different loads	91
Fig 5.8	Variation in pressure of gasifier and different filters	92
Fig 5.9	Variation of tar content of producer gas at different filters	93
Fig 5.10	Variation of composition of producer gas at different loads	94
Fig.5.11	Variation of solar temperature gain and beam radiations with time	95
Fig 5.12	Variation of power obtained and given by radiations with time	95
Fig 5.13	Variation of heat loss with receiver temperature	96
Fig 5.14	Variation of heat absorbed by receiver with wind velocity	97
Fig 5.15	Variation of energy and exergy efficiency with receiver temperature	97
Fig 5.16	Variation of exhaust gas temperature and mass flow rate with load	98
Fig 5.17	Variation of air-fuel ratio and brake power output with load	99

LIST OF FIGURES/GRAPHS

Figure	Description	Page No.
Fig 5.18	Variation of exhaust gas heat used with exhaust gas temperature	100
Fig 5.19	Variation of oxygen and carbon dioxide with load	100
Fig 5.20	Variation of Nitrous oxide with load	101
Fig 5.21	Effect of input temperature on LMTD and heat capacity ratio	101
Fig 5.22	Effect of input temperature on efficiencies and overall heat transfer coefficient	103
Fig 5.23	Effect of input temperature on LMTD and heat capacity ratio	103
Fig 5.24	Effect of input temperature on efficiencies and overall heat transfer coefficient	104
Fig 5.25	Variation of exhaust heat used or lost at different loads	105
Fig 5.26	Percentage distribution of input energy at different loads	106
Fig 5.27	Percentage distribution of input exergy at different loads	106
Fig 5.28	Variation of heat used and performance with generator temperature	107
Fig 5.29	Variation of absorber heat and performance with absorber temperature	108
Fig 5.30	Variation of Coefficient of Performances with evaporator temperature	109
Fig 5.31	Variation of Coefficient of Performances with condenser temperature	109
Fig 5.32	Variation of Coefficient of Performances with ambient temperature	110
Fig 5.33	Variation of evaporator temperature with time	111
Fig 5.34	Percentage distribution of total input energy for the hybrid system	112
Fig 5.35	Percentage distribution of total input exergy for the hybrid system	114
Fig 5.36	Effect of electric load on gasifier output, brake power and exhaust gas temperature	114
Fig 5.37	Effect of exhaust gas temperature on electric output, refrigeration and total output	115
Fig 5.38	Effect of exhaust gas temperature on overall energy and exergy efficiency	116
Fig 5.39	Effect of evaporator temperature on electric output, refrigeration and total output	117
Fig 5.40	Effect of evaporator temperature on overall energy and exergy efficiency	118
Fig 5.41	Effect of condenser temperature on electric output, refrigeration and total output	119
Fig 5.42	Effect of condenser temperature on overall energy and exergy efficiency	119

LIST OF PHOTOGRAPHS

Photograph	Description	Page No.
Photograph 4.1	Pictorial view of hybrid cold storage cum power generator	45
Photograph 4.2	Pictorial Views of double ignition downdraft gasifier	46
Photograph 4.3	Pictorial Views of Gas engine-gen set with spark plugs	47
Photograph 4.4	Pictorial Views of scheffler collectors	48
Photograph 4.5	Pictorial Views of heat recovery unit	49
Photograph 4.6	Pictorial Views of vapour absorption machine and cold storage	50
Photograph 4.7	View of different kind of filters	54
Photograph 4.8	View of biomass used as fuel and wood cutter	55
Photograph 4.9	View of loading device and Gas Chromatograph	56
Photograph 4.10	View of tar measuring device	56
Photograph 4.11	View of vane type anemometer, orifice plate with U-tube Manometer and electronic manometer	57
Photograph 4.12	View of control panel, data logger and temperature indicator	58
Photograph 4.13	View of control panel and gas analyzer	59
Photograph 4.14	Set up view of pyrhelimeter with pyranometer and ultrasonic anemometer	60

LIST OF ABBREVIATIONS

Nomenclature

$\dot{E} / \dot{E}_x / \varepsilon$	Exergy rate [kJ s ⁻¹]
\dot{Q}	Heat/Energy rate [kJ s ⁻¹]
\dot{Q}	Discharge [m ³ s ⁻¹]
\dot{W} / P	Work done [kW]/ Power [kW]
T	Absolute temperature [K]
h	Enthalpy [kJ kg ⁻¹]
\dot{m}	Mass flow rate [kg s ⁻¹]
s	Entropy [kJ kg ⁻¹ K ⁻¹]
P	Pressure [Nm ⁻²]
NH ₃ -H ₂ O	Ammonia-water
COP	Coefficient of Performance
VAM	Vapour Absorption Machine
ODP	Ozone Depletion Potentials
GWP	Global Warming Potentials
DNI	Direct Normal Irradiation

Greek symbols

ρ	Density [kg m ⁻³]
ε	Effectiveness
η	Efficiency [%]

LIST OF ABBREVIATIONS

Subscript

B	Brake
I.C. Engine	Internal Combustion Engine
HRU	Heat Recovery Unit
TV/V	Throttle Valve/Velocity
G, gen	Generator
h/c , E	Hot/Cold, Engine/Electric
P	Pump/Power/Pressure
a/amb	Air/Ambient
SHE	Solution Heat Exchanger
PG, pg, g	Producer gas
CV	Calorific Value
act/th	Actual/Theoretical
i/f	Initial/Final
m	Moisture/Mean/Mass Fraction
O, in, O/P	Overall, Input, Output
ss/ws	Strong/Weak Solution
C _d	Coefficient of discharge
a/avg	Absorber/Average
c, con	Condenser
E, e, evp, w	Evaporator, Water/Weight
r/s'	Refrigerant/Isentropic process
1,2,3..i,j,k..	State points in Figures

CHAPTER-I

INTRODUCTION

India has a unique geographical position and a wide range of soil thus producing variety of fruits and vegetables like apples, oranges, grapes, potatoes, ginger, chillies, etc is favourable. Marine products are also being produced in the large amount due to the widespread coastal areas. The present production level of the fruits and vegetables is more than 100 million tones. However, the growth rate of the population is even higher in the India, due to which the consumption and demand of the perishable commodities (such as fruits, dry fruits, marine products, vegetables, processed foods, dairy products etc.) have been increasing day by day. Presently, the storage of these products is the biggest problem. The cold storage facilities are the prime infrastructural component for such kind of perishable commodities. Obviously, the power demand together with the cooling demand has also been increasing rapidly. Moreover, there are also the grim global environmental related issues because of the exhaust gas and use of refrigerants. Nonetheless, the chlorofluorocarbon refrigerants are also currently considered responsible for the ozone layer depletion and the increase in the global warming.

In the recent years, many great efforts are being done for the production of power from the renewable energy resources. The utilization of both the renewable energy and the exhaust gas waste heat of renewable energy power plant can tackle the serious global environmental related problems, such as green house effect from CO₂ emissions due to the combustion of the fossil fuels in the utility power plants.

In order to utilize the hybrid renewable energy and exhaust gas waste heat, which comes from the producer gas engine, a 'new hybrid cold storage cum power generation system' has been explored and proved the best effort for reducing the above cited environmental related problems by the exhaust gas and refrigerants with improvement of the overall efficiency. This cogeneration system has the potential to meet the requirement of both, rapidly increasing demand of power and cooling simultaneously. The power production by the producer gas run engine and the cooling production from its exhaust gas waste heat have the potential to reduce the global environmental related problems. Obvious in the above system, the depletion of the

ozone layer and increase in the global warming can significantly be controlled by the use of suitable refrigerants.

In this context, Calm (2006) summarized the atmospheric (combined stratospheric and tropospheric) lifetimes, global warming potentials (GWPs) and ozone depletion potentials (ODPs) of refrigerants. The comparative efficiencies and the implications of greenhouse gas emissions of the chiller refrigerants with their relative importance were also discussed. McLinden et al. (2014) explored the possibilities for low GWP refrigerants. A set of 1200 refrigerants was selected for screening criteria such as estimation for GWP, stability, flammability, critical temperature and toxicity etc. based on earlier research works. There is an almost common consent in toxicity and stability. From the literature's review, there is no existence of ideal refrigerant. They have at least one or more negative characteristics.

In the regard of co-generation technology, Khaliq et al. (2012) represented the first and second law investigation of industrial waste heat based combined power and ejector-absorption refrigeration cycle. In this cycle, 77.3% of the total input exergy was lost, in which around 53.6% of the total input exergy was destroyed due to the irreversibilities (maximum in condenser, heat exchanger and ejector) in the different components of the cycle and 23.7% was as the exhaust exergy lost to the environment, while the useful exergy output was 22.7%. In the energy analysis context, the exhaust energy lost to the environment was calculated 44% and, 19.7% was available as the useful energy output, while 36.3% energy was associated with the use or loss among various components of cycle. The thermodynamic analysis of the combined power and ejector refrigeration cycles was presented by Dai et al. (2009). This cycle could be run either by one of the energy (the flue gases, solar energy, industrial waste heats and the geothermal energy) or by the input resource of the hybrid energy. The performance of the systems was evaluated on the basis of the exergy analysis and found that 77.8% of the total input exergy was lost, in which 41.6% due to the irreversibilities in the components and 36.2% exhaust exergy lost to the environment, while the exergy output was 22.19%. The biggest exergy loss due to the irreversibility occurred in the heat addition and rejection processes whereas; ejector was the next largest exergy loser. A significant amount of the heat wasted to the environment which reduced the energy and exergy efficiency of the combined power and ejector refrigeration cycle.

An elaborate research of the combined co-generation system has been remarked in the literature for the development and analysis of combined power and absorption refrigeration cycle, which operates on the waste heat, but hardly any information is available on the analysis of a 'new hybrid cold storage cum power generation system'. However, high performance cooling cycles have also been rarely presented by researchers in the earlier investigation. It has been seen recently that a great interest has grown among the researchers in adopting the cogeneration system; due to their ability to operate the cooling system at relatively low source temperature.

Since, to ensure the best performance of the 'new hybrid cold storage cum power generation system', it is necessary to investigate the individual components of this system. This system consists of the components; a downdraft gasifier, four scheffler collectors, a gas-engine gen set, a waste heat recovery unit and a vapour absorption machine.

In the connection of gasifier, Martinez et al. (2012) reviewed the feasibility of the 'Biomass downdraft gasifier coupled with the reciprocating internal combustion engines' (RICEs) for the production of heat and power at the small scale. The biomass material with the moisture content less than 25% provided the cold gasification efficiency of 50-70%, while the low heating value of the producer gas was around 4-6 MJ/Nm³ at average temperature in the combustion zone of about 1000°C. Rathore et al. (2008) reported the performance of a gasification system. The temperature above the grate had been found with the variation of 800-1143°C. The producer gas temperature at the outlet of gasifier varied from 380-440°C during the experimental analysis. The heating value of producer gas was found to be 4.35 MJ/Nm³. The variation in the efficiency of gasifier was between 65-70%. Zhang et al. (2013) discussed gasification by the phase change material technique. The energy and exergy of the gasification system were 50.8% and 44.9% respectively for the base case. A parametric study showed the influences of power, air flow rate and feed stock consumption rate on the energetic and the exergetic efficiency of process, while Bhave et al. (2008) reported the development as well as assessment of a compact, "wet packed bed scrubber-based producer gas cooling and cleaning system" for quality evaluation of the producer gas, which was suitable for small-scale applications. This unit gave a clean gas with 'tar and dust' content below the limit of 150 mg/Nm³ as long as the inlet gas 'tar and dust' content was below about 600 mg/Nm³.

In concern of solar collector' literature, Patil et al. (2011) investigated the performance of the scheffler reflector, which revealed that the average power gained by sun and thermal efficiency were 1.30 kW and 21.61% respectively. The maximum water temperature achieved through the receiver in the storage tank was obtained 98°C on a clear day operation with the ambient temperature between 28°C to 31°C. Tyagi et al. (2007) presented an exergetic and parametric performance of concentrating type solar collector. The large variations in the energy and exergy efficiencies could be observed with change in mass flow rate of the working fluid. At the normal mass flow rate conditions; the variations in efficiencies were moderate.

In the consideration of the engine performance and emission characteristics, Prasad et al. (2009) reported the performance of castor non-edible vegetable oil and its blend with diesel engine. At the rated load, the emissions i.e. carbon monoxide, hydrocarbon, smoke were 56.41%, 20.27%, 31.32% respectively higher and NO_x was 44% lower as compared to diesel fuelled engine. This was due to incomplete combustion of the dual fuel. Its brake thermal efficiency was 54.76% higher than the diesel run engine. Ghazikhani et al. (2014) experimentally investigated the effects of ethanol additives on the performance and emissions (HCs, CO, CO₂ and NO_x) of a SI two stroke engine at variable loads and speeds. The sample data of emissions for pure gasoline provided the range of CO: 06 to 1.24%, CO₂: 8.1 to 9.5% and NO_x: 76 to 71 ppm. There was a significant reduction in pollutants emissions from engine using ethanol additives. Although as the exhaust temperature increased, most emissions increased, but hydrocarbons (HCs) decreased.

In literature study of heat exchangers, Ghazikhani et al. (2014) used a 'counter current flow double pipe heat exchanger' for the recovery of exergy from a direct injection (DI) Diesel engine. The exergy recovery through heat exchanger increased with increased in engine load and speed, which contributed the reduction in brake specific fuel consumption (bsfc) from 10-15%. This reduction in the bsfc is showing the fact that the exergy was recovered in the heat exchanger. Al-attab and Zainal (2010) analysed the performance of a high temperature 'stainless steel heat exchanger' for rejecting the heat from a biomass gasifier combustor to the working fluid of the turbine. The average effectiveness of heat exchanger for the steady state operation was found to be 62.5% at 694°C turbine inlet temperature.

In the literature survey of the vapour absorption machine; Kong et al. (2010) thermodynamically investigated a single stage ammonia-water absorption system of a

rated cooling capacity of 2814 W. The experimental results revealed the cooling capacity of 1900 W to 2200 W with the actual COP of 0.32 to 0.36. The exergy destruction of the each component had been evaluated. The irreversibility was occurred due to the temperature difference and heat dissipation. Pridasawas and Lundqvist (2004) represented the exergy analysis of solar energy operated ejector refrigeration cycle. The operating conditions for the analysis of cycle were: atmospheric temperature of 30°C, a solar radiation of 700 W/m², a cooling capacity of 5 kW and an evaporator temperature of 10°C. In the exergy analysis, the most significant exergy losses occurred in the ejector and solar collector, while the energy and exergy efficiency of the cycle were found to be 27.41% and 4.39%.

In the literature, the thermodynamic analysis of the above described components of the system has been stated broadly due to their specific applications of each component. The biomass gasification and solar technology are increasing interests exhaustively as a forthcoming way to provide electricity in remote areas using local renewable fuels with huge reduction in pollution, while an efficient heat exchanger can perform promptly and very effectively in a combined system.

Therefore, the aim of this dissertation is to evaluate the feasibility of the 'new hybrid cold storage cum power generation system, and to obtain further improvements in the efficiency to some extent. To meet the requirement of cooling and power generation, the investigation has been done with the following **objectives**.

- (i) Performance evaluation of gasifier at different rating conditions.
- (ii) To assess the exhaust heat and its emission characteristics.
- (iii) To assess the waste heat recovery unit (heat from the producer gas, heat from hybrid solar energy and engine exhaust) at the different operating conditions and compare it with the overall heat loss to the atmosphere.
- (iv) To assess the performance of cold storage system.
- (v) To assess the conditions of producer gas and performance of scheffler solar disc system at different intensity of the radiation.
- (vi) To evaluate the performance of the combined cogeneration system

The analysis of this hybrid system has been performed on the basis of the energy and exergy methods. The irreversibilities in the each components of the system have been calculated for the effective utilization of the hybrid solar energy- exhaust gas waste heat of Internal Combustion Engine.

CHAPTER-II

LITERATURE SURVEY

The following literature survey has been carried out to collect the information of the work done in the previous years:

2.1 PERFORMANCE INVESTIGATION OF GASIFIER

Mukunda & Paul et al. (1994): The system developed at IISc, Bangalore, Dasag, Switzerland and ETH, Switzerland and test conducted were in thermal mode of analysis. These tests gave the performance of the reactor, quality of producer gas and the energy balance at the different loads. At the partial load, the average cold gas efficiency was about 49%. The tar and particulates levels were independent of the load and the average tar and particulate of 20 ± 10 and 60 ± 20 mg/m³ were noted at the cold end. These results indicate higher tar level and lower cold gas efficiency. Future a hybrid system installed and carried out few tests which gave satisfactory higher performance of the double ignition downdraft gasifier.

Reed et al. (1999): Specific gasification rate of down draft gasifier is the most important measure for checking the performance. A low specific gasification rate causes slow pyrolysis conditions at around 600°C and produces high charcoal 20-30%, large quantities of unburned tar, and a gas with high hydrocarbon content and volatile (tar) content. A high specific gasification rate causes very fast pyrolysis (>800°C), heated the surface of particles not center which permit to react with charcoal and due to produce less than 10% charcoal at 1050°C and hot gases at 1200-1400°C in pyrolysis zone. These gases then react with the remaining char-ash to yield tars less than 1000 ppm, 5-7% char-ash and a producer gas with less energy. As specific gasification rate varied from 180-936 m³/hr/m² of the grate, the gas production rate increased from 0.3672-2.444 m³/hr, charcoal production rate decreased from 13-4.7% and tar decreased 8330-300 mg/kg of producer gas. So these results show the maximum values of performance. The limitations have been expanded by using the the double ignition downdraft gasifier.

Rutherford and Williamson (2006): The biomass gasification systems transform a solid fuel into a gaseous fuel which retains 75-88% of the heating value of original. A gaseous fuel offers easier handling and the ability to be utilized in either a gas engine

or a gas turbine. The Conventional biomass co-generation plants utilize the steam turbines, while integration of a gasifier with a gas turbine or an engine provides efficiencies of 25-40%. This paper presents the peak load supply for the plant by biomass gasification. At the maximum electric load, the range of gasification efficiency has been found around 70-80%.

Rathore et al. (2008): The study of this paper deals with the thermal performance of the gasification system installed at M/S Phosphate India Pvt. Limited, Udaipur. The biomass consumption rate of the gasifier was found 100-120 kg/hr. The average air and gas flow rate was 92.69-99.20 m³/hr and 204-210.26 m³/hr respectively. The temperature above the grate varied from 800-1143°C. The gas outlet and flame temperature varied during the test from 380-440°C and 690-740°C respectively. The quality of gas samples were analyzed and heat value of producer gas was observed 4.35 MJ/Nm³. The test was performed for 50 hours continuously. The cold gas efficiency was varied from 65-70%. The better performance of the gasification system has been demonstrated with technically feasible in this experimental investigation.

Sharma and Panwar (2009): The biomass based natural down draft gasifier had been tested and run for over a cumulative period of about 30 hours. The overall thermal efficiency was determined with the help of water boiling test and found around 39.53%. The thermal capacity of the gasifier was measured 14.54 kW, which was the total energy produced in 1 hour. At 30 kg loading rate; the temperature was in the range of 685-1142°C, 541-1086°C, 380-788°C, 212-519°C and 102-362°C at 20 mm, 200 mm, 400 mm, 600 mm and 800 mm above the grate respectively. The gas outlet temperature ranged from 112- 432°C. From the test, it has been found that the quality of the producer gas improves for the smooth longer operation of the gasifier.

Garg and Sharma (2013): Biomass gasification converts the solid biomass into Producer gas that can be used for mechanical, electrical and thermal energy production. The proximate and ultimate analysis of the biomass feed stocks like pine wood, sawdust, eucalyptus, sal wood and popular wood had been represented in this paper. These fuels had been used for the operation of 5 kW biomass gasifier coupled with engine-electric power generator. The performance of this system could not be enhanced due to its design considerations but the evaluation of gasifier of hybrid system is in acceptable performance range.

The researchers like **McKendry (2002)**, **Belgiorno et al. (2003)**, **Mukhopadhyay (2004)**, **Franco and Giannini (2005)**, **Mountouris et al. (2006)**, **Mountouris et al.**

(2008), Vaezi et al. (2008), Gassner and Marechal (2009), Rathore et al. (2009), Sohel and Jack (2011), Varshney et al. (2010), Varshney et al. (2011), Arena (2012), Centeno et al. (2012), Panwar et al. (2012), Pirc et al. (2012), Vaezi et al. (2012), Yoon and Lee (2012), Barea et al. (2013), Garg and Sharma (2013), Malik and Mohapatra (2013), Zhang et al. (2013) have represented the nearly same work of performance investigation of the gasifier but no work related to the performance evaluation of the double ignition gasifier has been found in the above literature.

2.2 QUALITY OF PRODUCER GAS

Mukunda et al. (1994): This paper deals with biomass-based energy devices. In the developing countries this technology is very needful, which has been highlighted. The biomass was classified into the woody (solid) and powdery (pulverized) form along with comparison of its energetics with fossil fuels. The involved technologies were namely gasifier-engine-alternator combinations, gasifier-combustor and for generation of heat and electricity in this paper, which were discussed for both woody biomass and powdery biomass in some detail. The importance of biomass to obtain high-grade heat by using the pulverized biomass in the cyclone combustors was emphasized. The true potential of the system is not discussed to the current world situation in this paper, while quality of producer gas has been found favourable for the hybrid technology.

Bhattacharya and Dutta (2000): This paper presents the results of an experimental study on two-stage gasification of wood with preheated air. Very clean gas had a tar content of about 10 mg/Nm³ or lower could be obtained from such gasification. For an increase airflow rate of the two-stage gasifier results in decrease of the tar content and CO₂ concentration whereas the concentration of CO and H₂ increased. The experimental results have been found in proportionate range to the installed system.

Hasler and Nussbaumer (2000): Tars and particles were considered as harmful components of biomass derived producer gas in internal combustion engine applications. Since the gas cleaning devices could reach upto particularly lower particle and tar levels than previous coined units, long duration sampling periods were needed for the determination of the producer gas contaminants due to stable state. A new sampling method had been developed which used several classes of 'tar' components and allowed long duration sampling. The new displacement method has

been used to measure tar at eight different gasifier locations and found better results regarding quality of producer gas so far.

Zainal et al. (2002): An experimental investigation of a downdraft biomass gasifier was carried out with the use of furniture wood and wood chips as a fuel in gasifier. The effect of the equivalence ratio on the gas composition, Calorific Value and the gas production rate was studied in this paper. Initially, the calorific value of the producer gas increased with increase in equivalence ratio and attained a peak; subsequently, decreased with the increase in equivalence ratio. The gas flow rate/unit weight of the fuel increased linearly with increase in equivalence ratio. There was no complete conversion of carbon into a gaseous fuel in this paper but wood has been found effective fuel for generation of producer gas in this experimental analysis.

Pathak et al. (2007): Engine quality producer gas must be almost free of solid matters (tar and particulate) to minimize engine wear and maintenance. This paper presented a design and development work of sand filter for upgrading the PG to IC engine quality renewable energy fuel. The developed sand filter was tested for its performance with SPRERI'S 20 kW_e downdraft gasifier with engine set up. The percentage reduction in tar and particulate matters was 319 mg/Nm³ and 53 mg/Nm³ before and after filter respectively, which is far higher than existing quality of PG.

Bhave et al. (2008): Biomass gasifiers are playing an increasing and important role as decentralized energy sources particularly in the rural India. When this technology is used for power generation through IC engines or for assured thermal applications, it is required a clean flue gas. For this, it is required to cool biomass-based producer gas to atmospheric temperature and clean it from tar and particulates before it can be used as a fuel. This paper reported the development and evaluation of a compact, "wet packed bed scrubber-based producer gas cooling-cleaning system", which gave lower value of tar, However this value is much more than quality of PG of hybrid system.

Shabangu et al. (2014): This paper evaluates the feasibility of co-production of methanol and biochar from thermal treatment of pine in a two-stage process; first stage is pyrolysis or gasification to produce biochar and volatiles, while second stage is the processing of the volatiles to produce methanol. In this work, three concepts were studied: (a) slow pyrolysis at 300°C; (b) slow pyrolysis at 450°C; and (c) gasification at 800°C, all of them followed by processing of the volatiles into producer gas and the conversion of the producer gas into methanol. Gasification was able to generate methanol at lower prices than fossil fuel. The slow pyrolysis is

responsible for the production of tar so the double ignition downdraft gasifier has been suggested for complete combustion of fuel.

The above researcher's work done of the quality of producer gas has the approximately similarity with the following research articles:

Bliek et al. (1984), Hasler and Nussbaumer (1999), Chen et al. (2003), Prins et al. (2003), Bhoi and Channiwala (2008), Sheth and Babu (2009), Fagernas et al. (2010), Rapagna et al. (2010), Anis and Zainal (2011), Simeone et al. (2011), Jordan and Akay (2012), Paethanom et al. (2012), Shackley et al. (2012), Jaojaruek et al. (2013), Yan et al. (2013), Asadullah (2014). However, no work related to the performance analysis of the cyclone coupled with heat exchangers cooling and cleaning system has been found in the above research literature.

2.3 EFFECT OF FUEL (PRODUCER GAS/FOSSIL FUEL) ON ENGINE'S EXHAUST AND ITS EMISSIONS CHARACTERISTICS WITH PERFORMANCE PARAMETERS

Sridhar et al. (2001): This paper reveals the performance of producer gas with a lower calorific run reciprocating engine and also the use of producer gas in multi-cylinder spark ignition reciprocating engines with varying compression ratio from the 17:1 to 12:1. This restriction in compression ratio has been mainly attributed to find the auto-ignition tendency of the fuel. The current work clearly indicates that the engine operates efficiently at higher compression ratio without any tendency of auto-ignition. As estimated, working at a higher compression ratio becomes more efficient and also produced greater brake power. A maximum brake power of 17.5 kW_e was acquired at an overall efficiency of 21% at the highest compression ratio. The maximum de-rating of power of engine in gas mode was 16% as compared to the normal diesel mode of operation at comparable compression ratio, whereas, the overall efficiency of system declined by 32.5%. A careful analysis of energy balance shows that the excess energy loss to the coolant due to the existing combustion chamber design occurs. Addressing the combustion chamber design for producer gas run engine should form a part of future work in improving the overall efficiency. In the present experimental work, venturi-carburettor has been used for proper mixing in the modified diesel engine to achieve the better performance of the engine.

Zheng et al. (2004): In Diesel Engine, Exhaust gas recirculation (EGR) is effective to reduce nitrogen oxides (NO_x) because it lowers the oxygen concentration and the

flame temperature of the working fluid in combustion chamber and increases the particulate matter (PM). When EGR further increases, the engine operation reaches at higher instabilities with increased carbonaceous emissions and even losses of power. In this research, the inevitable uses of EGR were highlighted. The implementation of EGR in different ways was done and impact of EGR on Diesel engine operations was investigated. Since, new concepts' regarding EGR increases the carbonaceous emissions so the PG has been projected as a favourable fuel.

Kanoglu et al. (2005): Performance of a Diesel engine power plant with a rated output of 120 MW was examined based on the energy and exergy analysis. The power plant consisted of seven identical Diesel engines. Each engine consisted of various subsystems including fuel heating units, turbochargers and heat exchangers perform numerous valuable jobs. The engine operated on heavy fuel oil, and gave emissions at the low level by the effective treatment of the systems. The mass, energy and exergy balances were evaluated for each flow stream in the power generation unit. The energy and the exergy efficiencies of the power plant were determined to be 47% and 44%, respectively. The exergy destruction of engine is mostly due to the irreversible combustion process. It was accounted for 32% of the total input exergy and 57% of the total irreversibilities in the power plant. Most irreversibilities in the power plant occurred in the desulphurization, compressor, intercooler and lubrication oil cooler units, while the engine used in this hybrid experimental investigation system shows about 40% exergy destruction.

Ohta et al. (2006): A waste heat recovering device for an internal combustion engine was designed and manufactured. It consisted of an internal combustion engine and an evaporator. In the evaporator, the exhaust gas from the internal combustion engine was introduced, which was as a high temperature hot fluid. To avoid the loss of heat, the exhaust gas inlet of the evaporator was placed adjacent to an exhaust valve of the internal combustion engine. Thus, a waste heat recovering device could work efficiently in highest recovery of waste heat. In the experimental work of this thesis, the hybrid waste heat recover has been done effectively from pollution free fuel.

Hassan et al. (2011): The performance and emission characteristics for the dual fuel engine were analysed by supercharged producer gas-diesel dual fuel mode. The engine was tested at constant engine speed and different loads operated with premixed producer gas-diesel dual fuel. It was found that the use of supercharged producer gas-diesel fuel mixture increases the brake thermal efficiency and specific energy

consumption of engine, while there is a reduction in carbon monoxide emission. The main reason for this type of emission is relatively complete combustion occurred due to more air utilization, which increases the volumetric efficiency under these operating conditions. Therefore, the experimental investigation indicates towards the use of venturi associated with carburettor in an engine for an effective combustion characteristic, so that best engine performance of hybrid system can be obtained.

Martinez et al. (2012): Biomass downdraft gasifier coupled with reciprocating internal combustion engines (RICEs) is a feasible technology for the production of heat and power at small scale. This paper contains information gathered from a review of published papers, which shows the effects of the particle and dust size, the moisture content of biomass material and the air/fuel equivalence ratio utilized in the gasification process with regard to the quality of the producer gas. Furthermore, value of the parameters of producer gas, such as its energy density, knock tendency, flame speed, auto-ignition delay period and the typical spark ignition timing, were systematized and summarized. Finally, information on the typical performance of numerous diesel and spark ignition RICEs powered with producer gas was presented, in which the spark ignition engine fuelled with producer gas had better performance than producer gas operated diesel engine.

Ghazikhani (2014): In this work, the effects of ethanol additives (5%, 10% and 15% in volume) on the engine's performance and its emissions (CO, HCs, CO₂ and NO_x) of a SI two stroke engine was experimentally investigated at different diverges loads and speeds. Also, the influence of delivery ratio and exhaust temperature on emissions characteristics and engine performance was described. The obtained results showed that when alcoholic fuel was used, delivery ratio and scavenging efficiency increased because of the rapid evaporation of ethanol subsequently, outcomes of scavenging and trapping efficiencies were in greater amount accordance with the flawless mixing model additives with fuel. There was a significant reduction in pollutions released from engine utilizing ethanol additives; CO emission with 35% reduction, which was the most reduction percentage among other pollutants emissions. Similarly the emission characteristics of the hybrid system have much reduction in green house gases with different performance parameters.

Moreover, almost similar research work has been done by the researchers like **Baliga et al. (1993)**, **Boyle (1994)**, **Shashikantha et al. (1994)**, **Hsieh et al. (2002)**, **Mohod et al., (2003)**, **Murillo et al. (2005)**, **Sridhar et al. (2005)**, **Mustafi et al. (2006)**,

Singh et al. (2007), Singh (2007), Sovacool (2008), Banapurmath and Tewari (2009), Prasad et al. (2009), Sahoo (2009), Kumar and Reddy (2010), Dasappa et al. (2011), Kalam and Masjuki (2011), Korakianitis et al. (2011), Sezer (2011), Gonzalez et al. (2013), Liaquat et al. (2013), Raman and Ram (2013), Balki et al. (2014), Dweepson et al. (2014), Faith et al. (2014), Hagos et al. (2014), Hagos et al. (2014), Yaliwal et al. (2014), Dutsadee et al. (2015), Homdoun et al. (2015), Homdoun et al. (2015).

In the above literature, there is no description of the quality of the exhaust heat and even a single emission sample does not represent so drastical reduction in the green house gases.

2.4 PERFORMANCE EVALUATION OF SOLAR COLLECTOR

Bhirud and Tandale (2006): A fixed focus concentrator is called Scheffler collector. At present, this type of collector is extensively used for cooking applications. These can also be used for industrial heating applications. This paper describes a field assessment of two fixed-focus collectors for heating of mild steel plates to 135°C in an oven. For evaluating the performance of the concentrating scheffler collectors, through cooling and heating processes, two concentrators with total 20 m² aperture area were used for heating of 75-150 Kg mild steel plates. Achieved results show that the batch size of 100 Kg is required time of 27 minutes. Using the heating and cooling curves the heat removal factor and optical efficiency factor were calculated for each case and compared. Tests results show better performance of scheffler collectors used in hybrid energy co-generation system than the scheffler collector presented in this research article.

Scheffler (2006): About half of the solar power which is collected by the reflector becomes finally available in the cooking vessel. The power output varies with the season. A sun which shines more from the front into the reflector sees a larger reflector (large aperture), and so more power is produced. In the similar way, a sun shining more from behind sees a smaller reflector and less power is produced. A reflector of 2.7 m² could typically bring 1.2 lts of water to boiling point within 10 minutes. The bigger reflectors (12.6 m², 16 m²) were also used to produce steam, either for cooking or for industrial purposes, while four reflectors have been used in the present hybrid system for the heating applications.

Munir et al. (2010): The paper represents a complete explanation about the design principles and construction details of an 8 m^2 surface area Scheffler concentrator. In the first part of the paper, the mathematical calculations is presented to the design of the reflector parabola curve and reflector elliptical frame with regard to equinox (solar declination = 0) by selecting a specific lateral part of a paraboloid. Arc lengths, crossbar equations and their ellipses and their radii are also calculated to form the required lateral section of the paraboloid. Subsequently, the seasonal parabola equations are calculated for two extreme positions of the summer and winter in the northern hemisphere (standing reflectors). The parabola equations' slopes for equinox (solar declination = 0), summer (solar declination = +23.5) and winter (solar declination = -23.5) for the Scheffler reflector (8 m^2 surface area) are calculated 0.17, 0.28 and 0.13 respectively. The y-intercepts for the parabola equations for equinox, summer and winter are calculated as 0, 0.54 and -0.53 respectively. By the comparison to the equinox parabola curve, the summer parabola is found smaller in size and used as the top part of the parabola curve whereas the winter parabola is larger in size and used as the lower part of the parabola curve to give the fixed focus. For this aim, the reflector assembly is composed of flexible crossbars and a frame to induce the essential modification of the parabola curves with the altering solar declination. For the daily tracking, these collectors rotate along an axis parallel to the polar axis of the earth at an angular velocity of one rotation per day with the help of simpler and cheaper self-tracking devices. During the seasonal tracking, the reflector rotates at half the solar declination angle with the help of a telescopic clamp mechanism. The scheffler collector's design procedure does not need any special computational setup, thus providing the potential use in domestic as well as industrial configurations.

Patil et al. (2011): The performance of Scheffler collector had been investigated. In that system, the drum installed at served the dual purpose of absorber tube and storage tank. Its storage capacity was kept 20 litres for experimental analysis. Performance analysis of the scheffler reflector had revealed that the average power storage and efficiency in terms of water boiling test were 1.30 kW and 21.61% respectively against an average value of beam radiations intensity of 742 W/m^2 . The maximum water temperature achieved in the storage tank was 98°C on a clear day operation with the ambient temperature between 28°C to 31°C . However the greater efficiency of the scheffler collector used in hybrid system is obtained around 27%.

Dafle and Shinde (2012): This study discloses the Design, Fabrication and Performance Evaluation for 2 bar pressure and 110°C temperature cooking applications using 16 m² Scheffler reflectors. The Scheffler along with mild steel absorber plate of size, 18 cm diameter and 2.5 cm thick was evaluated for performance in month of February 2012 at composite climate zone. It was seen during evaluation that solar radiation over the day changes from 620 W/m² to 937 W/m². The instantaneous efficiency drops with rise in radiation. Absorber plate temperature changes from 138°C to 235°C, whereas maximum temperature of steam achieved was 107°C at the outlet of the boiler. The overall efficiency achieved was 57.41% which seems on higher than that of the parabolic trough devices. This paper determines accomplishment of concentrating solar thermal devices using the Scheffler collector technology similar in that of the hybrid system for water heating and low pressure, temperature steam applications in industries.

Phate et al. (2014): The performance of 2.7 m² Scheffler reflector had been investigated in this article. Scheffler Reflector is parabolic dish collector type, which was designed to collect energy from sunlight. In this System, storage vessel was installed at focus point of the collector. Vessel stores capacity is 10 ltr, in which water was filled for the purpose of experimental analysis. The performance analysis of the scheffler reflector showed that average power and energy efficiency were 550 W and 19% respectively (which is lower than solar collector of hybrid system). Maximum temperature of water was found to be 94°C at ambient temperature of 32°C to 40°C.

Some researchers such as **Jayasimha (2006), Tyagi et al. (2007), Dorfling et al. (2010), Chandak et al. (2011), Kumar et al. (2011), Prasanna and Umanand (2011), Tao et al. (2011), Nene and Suyambazhahan (2012), Huang et al. (2012), Patil et al. (2012), Saidura et al. (2012), Sardeshpande and Pillai (2012), Suple and Suraskar (2012), Thakkar (2013), Abdollahpour et al. (2014), Mawire and Taole (2014), Phate and Bhortake (2014)** have almost same research's work, but no effort related to the use of scheffler collectors in the hybrid technology can be seen in the above literature survey.

2.5 PERFORMANCE ANALYSIS OF HEAT EXCHANGER

2.5.1 Counter Flow Heat Exchanger

Gupta and Atrey (2000): Due to the high effectiveness of the counter flow heat exchanger; it is commonly used in cryogenic systems. In addition, the thermal

performance depends upon various heat losses such as longitudinal conduction through wall, heat leakage from atmosphere, flow mal-distribution, etc. The conventional design procedure does not consider these losses, which is misleading the actual performance of heat exchanger. The exergy analysis has been carried out to get the real performance of heat exchanger in the thesis experimental work. In this paper, the numerical model was developed with the consideration of heat loss and leak and subsequently, the predictions were compared with the experimental data. Further, the heat leak from ambient and longitudinal conduction parameters on degradation of heat exchanger performance for 300-80 K and 80-20 K temperature range were studied.

Al-attab and Zainal (2010): Recently, there has been wide-ranging research on the idea of biomass fuel powered externally firing micro gas turbines; but only a small subset of these studies has used experimental work for performance evaluation of the systems. The thermal energy or power generation has not yet been produced in Malaysia by these systems. The aim of this paper is to evaluate the performance of a high temperature stainless steel heat exchanger. It was built to transfer heat energy in terms of power from a biomass gasifier to the working fluid of pure air turbine. The analysis was based on experimental results using air blower with different air supplied capacities. The average effectiveness of heat exchanger was obtained 62.5% at 694°C turbine inlet temperature (significantly lower than the effectiveness of the HRU).

Mondol et al. (2011): The performance of a novel heat exchanger unit ('Solasyphon') with a customed twin-coil ('coil') system was experimentally analysed under indoor and outdoor operating conditions. It was developed for a solar hot water system. It can easily be associated with an existing single-coil hot water cylinder to avoid the need for costly twin-coil solar hot water storage. The investigation was based on experimental results collected under various operating conditions including different primary supply temperatures (solar simulated); heating with a partially stratified storage from ambient, heating from ambient and finally no draw-off and standard draw-off patterns are used for examination. The outdoor testing was conducted on both the systems separately over Summer/Autumn conditions (Northern Ireland). The consequences showed that the 'Solasyphon' system is more effective compared to a customed twin-coil system for a domestic use where intermittent hot water demand is predominant and on intermediate or poor solar days, a transient solar input particularly occurs. It has been found that the results of the HRU are more efficient than the 'Solasyphon' system under the same heating duration.

Tighe et al. (2012): Temperature profiles inside a counter-current mixer for the continuous hydrothermal synthesis of inorganic nanoparticles had been measured under the conditions (10–25 ml/min superheated water, referred density of 1 g/ml, at 350–450°C and 24.1 MPa, mixed with precursors at 10–20 ml/min) used in published author's and other's literature work. Owing to internal heat transfer through the inner wall of the tube to the products flowing around it, the superheated water was cooled significantly before meeting the precursors. Subsequently, the fluids had fully mixed and the region immediately was at a lower temperature than that determined from an overall heat balance sheet. The relevant results of the HRU are found to be better than counter-current heat exchanger studied in this research article.

Patel and Ramana (2013): The development of any country can be done by the development of the Energy sector. The energy planners have the challenge to meeting the growing demands at acceptable costs in various sectors like industries, commercial, transport etc. This heat exchanger was installed at power plant of M/S Vardhaman Acrylics Ltd, Jhagadia, Bharuch, Gujarat, India. The power plant was made of 5.5 MW turbine-generator set with two extraction points which supplied the heat energy to meet process demand. The steam was generated at the capacity of 45 kg/cm² pressure, the ambient pressure fluidized bed combustion boiler supplied by the M/S Thermax Babcock & Wilcox Ltd, Pune, India. The overall energy & exergy analysis of Heat Exchanger was carried out based on massive data collection over a period of 90 days. The energy and exergy losses of different components were calculated and suggestions were provided for improving energy & exergy efficiency of the plant work. Similar energy and exergy analysis in heat exchanger has been done for its effective utilization in hybrid system.

The basically similar kind of research work has been done in the research articles such as **Narayanan and Venkatarathnam (1999)**, **Shiba and Bejan (2001)**, **Khan et al. (2003)**, **Islam et al. (2006)**, **Guo et al. (2010)**, **Sahin et al. (2010)**.

2.5.2 Multi-passes and Cross Flow/Shell & Tube Heat Exchanger

Ogulata and Doba (1998): A cross-flow plate type heat exchanger had been designed, fabricated and studied in laboratory conditions for effective utilization of waste heat. The experimental analysis of this heat exchanger was conducted based on parameters such as temperatures, the pressure losses occurring in the system and velocity of the air. Subsequent measurement of these variables, the efficiency of the

heat exchanger had been evaluated. The irreversibility of the heat exchanger had also been calculated, while its consideration in the design of the heat exchanger minimized the entropy generation number according to second law of thermodynamics. Parameters like optimum flow path length, dimensionless heat transfer area and dimensionless mass velocity were responsible for the minimizing the entropy generation number. The graphical presentation of the different HRU parameters shows the ever lasting performance of the hybrid technology.

Luo et al. (2002): A mathematical model was developed for forecasting the one-dimensional (co-current and counter-current) or multi-stream steady-state thermal performance of heat exchangers. This model was analytically solved for constant physical properties of multi-streams. The general solution was applied to calculate the different types of one-dimensional multi-stream heat exchangers as well as their networks by introduction of three matching matrices. The numerical examples were provided to explain the detailed procedures. A few required mathematical models have been used for analysis of cross flow heat exchanger of the hybrid system.

Alotaibi et al. (2004): The parameters like inlet fluid temperatures or mass flow rates can be used to control the operation of heat exchangers under the variable loads. An approximate infinite-dimensional equation by finite-dimensions was used to develop a numerical method based on finite-differences. This had been used for the study of a conduction–convection system. The dynamics of a single-pass cross-flow heat exchanger was represented by a coupled set of partial differential equations. Simultaneously convection, conduction and advection were also demonstrated in which water and air was the in- and over-tube fluids, respectively. The behavior of the heat exchanger equations was analyzed by the numerical method. The experimental results of the cross flow/ shell and tube type heat exchanger of the hybrid co-generation technology for the different inlet temperature of the exhaust gas/producer gas has been presented with good performance in the thesis.

Gomez et al. (2009): A new cross-flow arrangement was featured to thermally characterize a cross-flow heat exchanger for the applications in industries of refrigeration and automobile. This new flow arrangement had two fluid circuits in the form of two tube rows with two tube lines. The comparative performance study was done with standard two-pass counter-cross-flow arrangement based on the thermal effectiveness and the heat exchanger efficiency for several combinations of the number of transfer units and the heat capacity rate ratio. Moreover, there was the third

comparison of “heat exchanger exergy destruction norm” (HERN) through the effect of different parameters such as the heat capacity rate ratio and the inlet temperature ratio for several fixed number of transfer units. The new featured flow arrangement provided higher heat exchanger efficiency and higher thermal effectiveness. The exergy destruction was lesser over a wide range of the number of transfer units and the heat capacity rate ratio. This new featured flow arrangement with a promising way in the cross-flow heat exchanger for a single-phase fluid has been used in heat recovery unit of the experimental set up.

Ghazikhani et al. (2014): In the experimental analysis, the recovery of exergy from a direct injection Diesel engine was analysed where a turbocharged (OM314 DIMLER) of diesel engine was tested at various engine speeds and torques. To meet this purpose, a counter current flow double pipe heat exchanger was fitted at the exhaust of engine and analysed. Obtained results showed that exergy recovery increased with increase in engine load and speed. Additionally, increased use of exergy recovery gave the reduction in brake specific fuel consumption (bsfc). The reduction in bsfc was nearly 10% by using recovered exergy from the exhaust gas of engine. However, exergy recovered in the hybrid experimental work is obtained nearly 59%.

Almost same research work has been found in articles **Beziel and Stephan (1995)**, **Navarro and Gomez (2005)**, **Kapale and Chand (2006)**, **Lee and Bae (2008)**, **Pulat et al. (2009)**, **Buckinx et al. (2013)**, **Dixit and Ghosh (2013)**, **Fakheri (2014)**.

In the above literature of the heat exchangers, there is no explanation of the performance analysis of the HRU, which is a combination of counter flow heat exchanger and cross flow heat exchanger.

2.6 ASSESSMENT OF COLD STORAGE SYSTEM

2.6.1 Performance of Vapour Absorption Machine (VAM)

Chua et al. (2000): In this research work, a general thermodynamic definition for understanding the behaviour of absorber was generated and studied the effect of the various dissipative mechanisms on performance of the chiller. The assumptions regarding the absorption machine could be removed this black box analysis. In this analysis, the mass transfer resistance was also considered to get a more realistic cooling effect. Lastly, T-S diagram for the absorption machine was plotted for the theoretical foundation. This graphical approach of the VAM of hybrid system

indicates better performance than the chiller studied in this research paper. It could be used as a practical tool for analysis of any system.

Pridasawas and Lundqvist (2004): Solar energy operated ejector refrigeration cycle was investigated on the basis of exergy analysis. The considered operating conditions for the analysis were: ambient temperature of 30°C as the reference temperature, a solar radiation of 700 W/m², a cooling capacity of 5 kW, an evaporator temperature of 10°C, and butane as the refrigerant in the refrigeration cycle. The irreversibilities depended on the operating temperatures and exergy was destructed in components of cycle. The most significant exergy losses were occurred in the ejector and the solar collector of the cycle. The optimization of the generator temperature for a specific evaporation temperature was achieved with the minimization of the entire losses in the system. The optimized generator temperature was considered nearly 80°C for the above operating conditions. The cooling temperature in VAM has been found -5°C, which shows the better cooling effect than the solar operated refrigeration cycle.

Sun (2008): A gas engine, a shaft power operated vapor-compression refrigeration chiller and a waste heat run absorption refrigeration chiller were associated to make an integrated refrigeration system (IRS). The assessment of the IRS showed that 596 kW was the cooling capacity of the IRS, and 1.84 was primary energy ratio (PER) at air-conditioning rated conditions. The refrigerating capacity of the prototype rises and PER of prototype reduces with the rise of the gas engine speed. For operating the prototype at high-energy efficiency, the gas engine speed was used as a regulator at partial load. The IRS had proved a cost saving system with the use of waste heat. To make hybrid energy operated co-generation system, shaft power has been given to engine coupled with generator in the experimental work.

Kong et al. (2010): With the complete condensation a single stage ammonia-water absorption system was designed and fabricated. The performance of the system was experimentally investigated. The designed system operated by electric heater as heating source had cooling capacity of 2814 W. The mathematical models had been derived from the First and Second Laws of thermodynamics. The calculated data by these models were compared with experimental results. The results display that the experimental cooling capacity was obtained between 1900 W and 2200 W with the actual COP established between 0.32 and 0.36. The internal entropy generation of the components was evaluated. It showed that the larger irreversibility was due to the largest temperature difference and heat dissipation by the generator and evaporator. In

the experimental analysis, the COP of the VAM is found between 0.45-0.62. This reflects the better performance than a single stage ammonia-water absorption system.

Sedigh and Saffari (2012): In this article, the single, double and triple effect absorption cycles had been thoroughly examined. The working fluid in these cycles was a pair of water-lithium bromide with one condenser in first both cycles, three condensers in last cycle. Thermodynamic analysis was used for examining of both these cycles. The results showed that these cycles could be used for massive purposes. The research on the triple effect cycles was being done for industrial utilization. The cycle had evaporator, absorber, high temperature generator (HTG), intermediate temperature generator, three condensers, three heat exchangers and low temperature generator. The equations of conservation of mass and energy were applied for each component of the system and, then the COP of system and thermodynamic properties at every point of the cycle were calculated. The exergy analysis was also performed for the cycle. The mathematical models of this absorption cycle have been used in analysis of the VAM of the hybrid energy operated cold storage cum power generator. Nearly Similar research literature can be seen in **Dincer et al. (1995)**, **Sun (1999)**, **Srikhirin et al. (2001)**, **Wang (2001)**, **Dawoud (2007)**, **Kaynakli and Yamankaradeniz (2007)**, **Pratihari et al. (2012)**, **Mazouz et al. (2014)**.

2.6.2 Environmental Impacts From Chiller's Refrigerants

Andersen and Lupinacci (1988): A Montreal Protocol on Substances that Deplete the Ozone Layer had been signed by the US, the European Economic Community and 23 other nations on 16 September, 1987 to protect the ozone layer. This is an international platform for all countries of the world to control the production and consumption of certain halon and chlorofluorocarbon (CFC) compounds. 35% of all CFC is used in refrigeration and air conditioning in the USA only; therefore there is a need of quick efforts by the refrigeration engineers and government to protect the ozone layer. This Paper briefly proposes the norms as well as scientific approaches on international and domestic level must be taken to protect the ozone layer. Owing to it, the refrigerants used in VAM of hybrid system are of zero ODP and negligible GWP.

Calm (2002): This paper reviews the current and historical status of the refrigerants for chillers and project new one for future. It investigates the global environmental issues that emphasize on recent changes. It then reported candidate refrigerants for future availability (or phaseout) based on controls for environmental protection,

toxicity, efficiency, escalating future costs and flammability. It was noted that negative marketing and conflicting approach, intended to discredit competitor's approaches, create confusion and delay replacement of older with new one efficient compound. The result also affects the environment, increment in costs, and chokes the market of chiller. The building owners, Engineers and others involved in refrigeration's decisions should return to traditional chiller refrigerant based on cost, local manufacturer support, performance, reliability and service options. It was concluded that there was no ideal refrigerant and that none is likely to be found. Therefore, the pair of working fluid ammonia-water has been used in the VAM, which meets the requirement of ideal condition to some extent.

McMullan (2002): The debate to control of the GWP and ODP on global platform leads to social responses and legislative measures by government for the industries. In this paper, problems were reported and the ways in which the industry could contribute to meeting the lower amount of the GWP and ODP. This paper also reported the choice and availability of working mediums, the risk of losing the simplicity in design and fabrication, and the increment in complexity of using fluid mixtures. The training with some course work must be provided by the government for adoption of the required changes in technology to save the globe.

Calm (2006): This article presents the different refrigerant options for chillers in tabulated form with the environmental data and global warming potentials. The paper also reports briefly the historic development of different refrigerants. The comparative performance of 28 refrigerants including chlorofluorocarbon (CFC), hydrofluorocarbon (HFC), hydro chlorofluorocarbon (HCFC), hydrocarbon (HC), and inorganic (such as ammonia) refrigerant was too reported in the paper. The relative importance of the refrigerant and energy related components of chiller emissions were described. This paper gave the idea to take iorganic refrigerant in the VAM.

Calm (2008): This paper reviews the development of refrigerants from past to the present time, and then addresses future directions for it. The history of the refrigerant has been broken into four refrigerant generation's criteria and discussed. This paper shows successive development with replacement of refrigerant, such as why the interest was earlier in natural refrigerants. The paper reviews the current options with international agreements according to Montreal and Kyoto Protocols to avoid ODP and GWP. It also provides the other international and local environmental concerns with control measures. The results also show the unintended environmental harm that

almost certainly will be future problems. It defines new policy and regulatory for the next generation refrigerants to be adopted to avoid the global environmental issues.

McLinden et al. (2014): This paper explores the possibilities for low GWP refrigerants. A set of 1200 refrigerants was identified from 56000 refrigerants and examined by applying screening criteria (parameters) such as estimation for GWP, stability, flammability and critical temperature and toxicity. The methods for this screening of refrigerants had been reported in earlier research works and it was summarized in this paper. 62 refrigerants with critical temperatures between 300 K and 400 K were selected, which could be used in current equipment with minor changes. These above refrigerants included halogenated olefins; compounds containing N₂, O₂ or S; as well as CO₂. There is an almost common consent of these refrigerants considering their thermodynamic properties, toxicity and stability. So far, ideal refrigerant is not identified in all respects. All the refrigerants have one or more negative characteristics such as poor thermodynamic properties, chemical instability, toxicity, very high operating pressures, low to moderate flammability etc. Therefore the refrigerant has been selected for the VAM, which will phase out in long time.

The approximate similarity in research work can be seen in the articles such as **Fischer (1993), Wuebbles (1994), Mangani et al. (2000), Calm (2002), Devotta et al. (2004), Mohanraj (2009).**

In the above literature survey of vapour absorption machine and chiller's refrigerants, there is no studied of the hybrid energy operated vapour absorption machine with refrigerant of zero ODP and negligible GWP.

2.7 PERFORMANCE STUDY OF COMBINED CO-GENERATION SYSTEM

Kong et al. (2005): The performance of a micro-combined cooling, heating and power (CCHP) system was experimentally investigated in this paper. The micro-CCHP system is driven by natural gas and LPG. A small-scale generator set driven by a gas engine had rated electricity power of 12 kW, while a new small-scale adsorption chiller was of rated cooling and heating capacity of 9 kW and 28 kW respectively. A pair of silica gel–water was used as working fluid in the adsorption refrigeration machine. The COP of the adsorption refrigeration chiller was more than 0.3 for 13.8°C evaporation temperature. The materials and methodology were applied to make a better test-rig platform for combined cooling, heating and power generation

system. The experimental analysis of the hybrid system describes the pollution free power and cooling production.

Wu and Wang (2006): Combined cooling, heating and power (CCHP) systems technologies has proved a best alternative to meet the energy requirement as well as to control the emission of the world. The clarification of the definition and benefits of CCHP systems were discussed in the first part of paper; then the technical performance characteristics of CCHP system were presented with utilization and developments in second part. In the third part, the four typical systems of various size ranges with existing diverse CCHP configurations were reported in the paper. The world had been divided into four main sections such as the US, Europe, Asia and the Pacific and rest of the world and the worldwide status of CCHP development was briefly introduced. It is concluded after going through the research article that this promising CCHP technologies can be as a tri-generation technology, which has been described in the future scope of the hybrid cold storage cum power generation system. It can run with the cooperation of government, energy-related enterprises etc.

Dai et al. (2009): A new proposed combined power and refrigeration cycle was made of the Rankine cycle and the ejector refrigeration cycle. The power output and refrigeration output could be produced by this combined cycle simultaneously. The exhaust gas waste heat generated by gas turbine or engine, industrial waste heats, and geothermal energy, solar energy could be used to operate this cycle. The second law analysis was performed to improve the cycle thermodynamically, while a parametric analysis studied the variations of the key thermodynamic parameters on the performance of the system. Moreover, a genetic algorithm could be made to the parametric optimization for achieving the maximum exergy efficiency. The outcomes of this paper showed that the biggest exergy losses occurred in the ejector and in heat addition processes due to the irreversibility. It was also observed that the turbine back pressure, turbine inlet pressure, the condenser and evaporator temperature had significant effects on refrigeration output, the turbine power output and exergy efficiency of the system. The exergy efficiency of 27.10% was obtained under the given condition of cycle, while the exergy efficiency of the hybrid system has been found significantly higher than that of the combined power and refrigeration cycle.

Kanogolu and Dincer (2009): In this paper, performance evaluation of different cogeneration system was carried out on the basis of first and second law thermodynamics. The cogeneration plants were gas turbine system, steam-turbine

system, geothermal system and diesel-engine system. Here, the simultaneous generation of electrical power and heating occurred in the cogeneration plant. The comparison was made on the basis of same amount of electrical and thermal power output for all the systems except the diesel. The diesel engine and geothermal systems were more attractive due to their higher exergy efficiencies than that of gas turbine and steam turbine systems. The exergy analysis is a powerful tool to analysis of any system. The large energy of hybrid system has been configured in this research work for more advantages as well as these direct towards the drops in all kind of fuel use and environmental related issues.

Coronado et al. (2011): Wood gasification technologies can be used to produce the electrical energy from stationary engine for particularly rural or small social group of people where the supply of electricity's network doesn't be present. The recovery of exhaust gases (engine) makes the system efficient and attractive. In this paper, a fixed bed gasifier with a compact cogeneration system has been used in order to cover electrical and thermal demands (hot and cold energy) by renewable resources. The results analysis showed that the energy balance provided the energy efficiency (electric as well as hot/cold water generation; performance coefficient and the heat exchanger). After considering the annual interest rates the investment, the operational and the maintenance cost; the payback periods, hot and cold water production costs, the costs of production of electrical energy had been calculated. A few points of biomass gasification theory have been considered in the thesis from this article.

Agarwal and Karimi (2012): A natural refrigerant based N_2O compression cycle and the combined absorption cycle with an ejector refrigeration cycle were employed to make a proposed triple effect refrigeration cycle. The combined advantages of the above three cycles reflected in a single triple effect refrigeration cycle. The different refrigeration output at different temperature of the combined cycle was achieved. This cycle was driven by the abundantly available industrial waste heat. The thermodynamic analysis was performed, in which energetic, exergetic parameters with exergy losses were demonstrated. The results showed that the refrigeration outputs, thermal efficiency and exergy efficiency were significantly affected by turbine inlet pressure, turbine outlet pressure, the waste flue gas temperature, compressor discharge pressure and ejector evaporator temperature. The energy and exergy efficiency of the hybrid system have been found significantly higher than this tri-generation cycle during the experimental evaluation.

Khaliq et al. (2012): The cogeneration cycle was proposed and consisted of ‘a LiBr-H₂O absorption refrigeration system’ and ‘the combined power and ejector refrigeration system’, wherein R141b was used as a working fluid. The results of exergy analysis showed that about 53.6% of the input exergy was destroyed due to irreversibilities in the different components, 23.7% exhaust exergy was lost to the environment and useful exergy output was 22.7% whereas 44% energy was distributed to different components and the useful energy output was 19.7%. The results also showed that this combined cycle was better than the previously coined combined power and ejector refrigeration cycle in terms of thermal and exergy efficiencies. The exergy analysis has shown better performance of the hybrid cogeneration system than this combined power and ejector refrigeration cycle.

Kumar et al. (2015): In the regard of promotion of biomass energy utilization, the attempts made by Indian government have been communicated in this article. The total capacity of all installed plants from all the resources for electricity generation is 2666.64 GW as on 31st March 2013 in India. The all resources of the renewable energy contribute 10.5% in total power generation, out of which 12.83% power is only being generated by the biomass material utilization. Nearly 500 million metric tons of biomass per year including surplus agricultural and forest area is available in India. 17,500 MW is generated by the all biomass power generation units in India. At present the total cogeneration power is 2665 MW in which 1666 MW is included by the biomass cogeneration power plants. The different species of biomass materials are described in this research paper and the investigation reveals that India has more than abundant biomass feed stock. The Indian Government has executed many policies and strategies for the development program of the generation of the power by the biomass materials. These norms include the entire biomass energy sector such as solid fuels, bio gas, bio diesel etc. These should be implemented strictly for effective results.

The almost same research work has been studied in the research papers such as **Lior (2002), Jurado et al. (2003), Minciuc et al. (2003), Baratieri et al. (2009), Cho et al. (2009), Padilla et al. (2010), Pihl et al. (2010), Jankes et al. (2012), Kawabata et al. (2012), Rashidi et al. (2012), Rocha et al. (2012), Sadhukhan et al. (2012), Ahrenfeldt et al. (2013), Strzalka et al. (2013).**

In the above literature, there is no renewable energy-waste heat operated new hybrid cold storage cum power generation system, which is admissible from the view point of global environment, thermodynamics and the technology.

CHAPTER-III

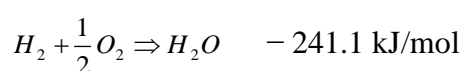
THEORY OF HYBRID SYSTEM

Hybrid renewable energy and waste heat technology for combined cooling and power (CCP) production is a promising technology which, especially in micro-scale plants with a power output less than 500 kW, provides an attractive alternative to conventional cogeneration plant. The combination of biomass gasification and a gas engine for CCP is a logical choice in the small-scale range as compared to conventional technology; these plants can be very competitive. The emerging hybrid technology makes it possible to build decentralized cogeneration plants that have not been sufficiently efficient before. Therefore, the following paragraphs focus on the principle of the building parts of the ‘new hybrid cold storage cum power generator’ which is explored in this research work:

3.1 PRINCIPLES OF BIOMASS GASIFICATION

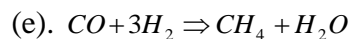
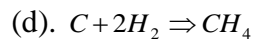
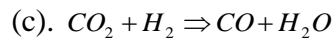
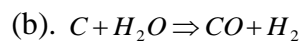
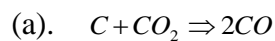
McKendry (2002) introduced the theory of biomass gasification in which, the gasification was a chemical process during which biomass converted into carbon monoxide and hydrogen by reacting the raw material (biomass) with a limited amount of oxygen. The substance of a solid fuel is usually composed of the elements hydrogen, carbon and oxygen. Additionally there may be nitrogen and sulfur. The occurring gasification reactions need high operating temperatures (800-1300°C) and pressures. The reactor is called a gasifier and the resulting gas mixture is called syngas or producer gas and is itself a fuel.

When the complete combustion takes place, water is obtained from the hydrogen and carbon dioxide from the carbon. Oxygen from the fuel is also incorporated in the combustion products and decreases the amount of combustion air needed. Combustion is described by the following chemical reaction formulae:



This means that burning 1 gram atom, i.e. 12.00 gm of carbon, to dioxide, a heat quantity of 401.9 kJ is released, and that a heat amount of 241.1 kJ is rejected during the oxidation of 1 gram molecule, i.e. 2.016 gm of hydrogen to water vapour.

In all kinds of gasifiers, the carbon dioxide (CO_2) and water vapour (H_2O) are reduced (as much as possible) to carbon monoxide (CO), methane (CH_4) and hydrogen (H_2), which are the key combustible components of producer gas. Reactions of the gasification process (they are taking place in the reduction zone of a gasifier between the gaseous and solid reactants) are given below:



So, the steps of the gasification process are the following:

- Biomass heating and converting volatile compounds to gas (when heated, biomass releases volatile matter leaving fixed carbon: app.20-25%).
- Combustion of the volatile compounds with air (volatile compounds react with air, provide energy for the heating of biomass and rise the temperature of gases to 1200-1300°C).
- Reduction of combustion products CO_2 and H_2O to CO , H_2 and CH_4 (the hot gases, contained CO_2 and water vapour, react with the fixed carbon or glowing layer of charcoal) - these reactions are endothermic – the reduction necessitates heat and so, the temperature of producer gas decreases (app.600-700°C).
- The rate of reactions decreases with decreasing temperature. In the condition of the water-gas equilibrium, the reaction rate becomes very low below 700°C (reaches equilibrium very fast). The composition of gas (the concentrations of steam, carbon monoxide, carbon dioxide and hydrogen are now balanced) then remains unchanged.

So, the essence of the gasification process is a sub-stoichiometric combustion of the fuel: controlled amount of air or oxygen is supplied to the oxidation zone of the gasifier to allow some of the organic material to be "burned", thus generating carbon monoxide and energy, that induces the next reaction that further converts organic material to hydrogen (H_2) and additional carbon dioxide (CO_2).

3.1.1 Types of Gasifier

The choice of the one particular gasifier depends on type of fuel used (its final available form, size, moisture and ash content) and on the application. These may be portable or stationary. The classification of gasifier and mechanism of its process zones have been taken from the References such as Vaezi et al. (2012), Varshney et al. (2010), Zhang et al. (2013) and it's literature. In the exhaustive literature survey, gasifiers are classified according to the way in which air is introduced in the fuel column. Thus, there exist three main gasifiers; Updraft, Downdraft, Cross draft.

3.1.1.1 Updraft or Counter-Current Gasifier

The counter current or updraft gasifier is the oldest and the most simple gasifier type. Following figure 3.1 shows the schematic diagram of this gasifier.

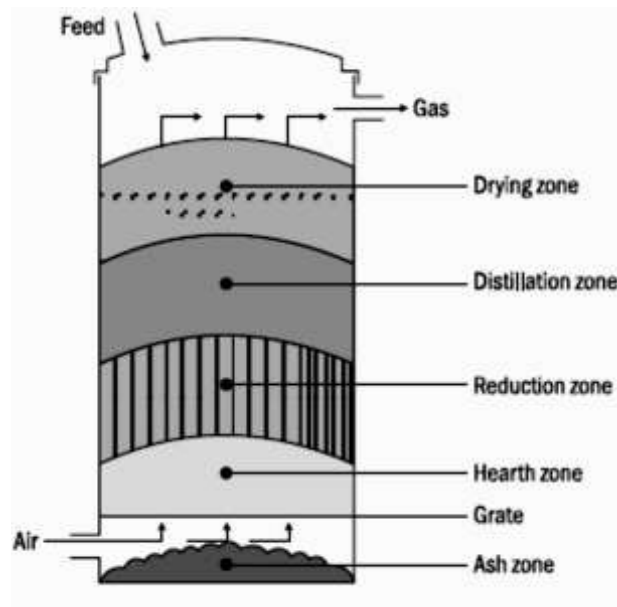


Fig 3.1 Updraft or counter-current gasifier

An updraft gasifier has evidently defined the partial combustion or hearth, reduction, and pyrolysis or distillation zones. The intake of air takes place at the bottom and the gas leaves from the top of the gasifier (so, the air flow is counter current to the fuel

flow). The combustion reactions occur near the grate at the bottom. Then the reduction reactions take place a little higher up in the gasifier, chased by heating and pyrolysis of the fuel in the upper part (accordingly of “heat transfer by radiation and forced convection from the lower zones”). The updraft gasifier allows achieving the greatest efficiency as the hot gas passes through the fuel bed and leaves the gasifier at low temperature. But in this occasion the tar, produced during the gasification process is carried out with the gas stream while, ash is removed from the bottom of the gasifier.

3.1.1.2 Downdraft or Co-Current Gasifier

In the case of the updraft gasifier, producer gas has very high tar content which can cause serious problems during the internal combustion engine operation. The tar existence problem in the gas stream is diminished in co-current or downdraft gasifiers, in which primary gasification air is acquainted at or above the gasifier’s oxidation zone and the producer gas leaves from the bottom of the gasifier (so, the air and fuel flow move in the same direction – co-current). Tarry distillation products from the fuel in this gasifier types have to pass through the burning bed of charcoal and by means of this they are converted into gases: carbon dioxide, carbon monoxide, hydrogen and methane. The tar decomposition degree depends on the gasifier hot zone temperature and on the residence time of tarry vapours there.

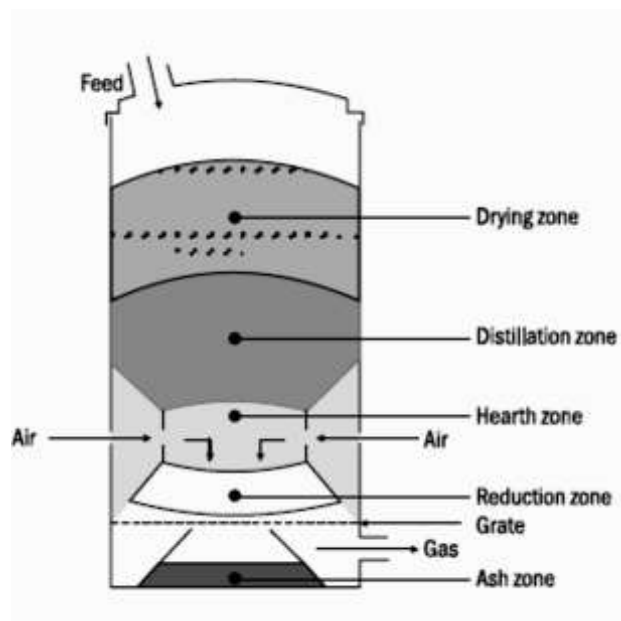


Fig 3.2 Downdraft or co-current gasifier

The main disadvantages are lower overall efficiency (comparing with the updraft gasifier), the lower heating value of the gas, inability to operate on a number of unprocessed fuels and difficulties in handling high ash and moisture content fuels (slagging).

3.1.1.3 Cross-Draft Gasifier

Cross-draft gas producers were adapted for the use of charcoal as a fuel. They have assured benefits over both of the updraft and down-draft gasifiers. Charcoal gasification results in very high temperatures (1500°C and even higher) in the oxidation zone which can lead to material problems and affect the producer gas composition, higher CO content, low H₂ and CH₄ content.

Advantages of the system lie in the very small scale upon which it can be run. Its installations under 10 kW (shaft power) can under certain conditions be economically viable. The reason for this is that it has the very simple gas-cleaning unit (only a cyclone and a hot filter) which can be employed during the use of this kind of Cross-Draft gasifier in combination with small engines. A disadvantage of this type of gasifiers is their minimum tar-converting proficiencies and the subsequent requisite for the highest quality (low volatile content) charcoal.

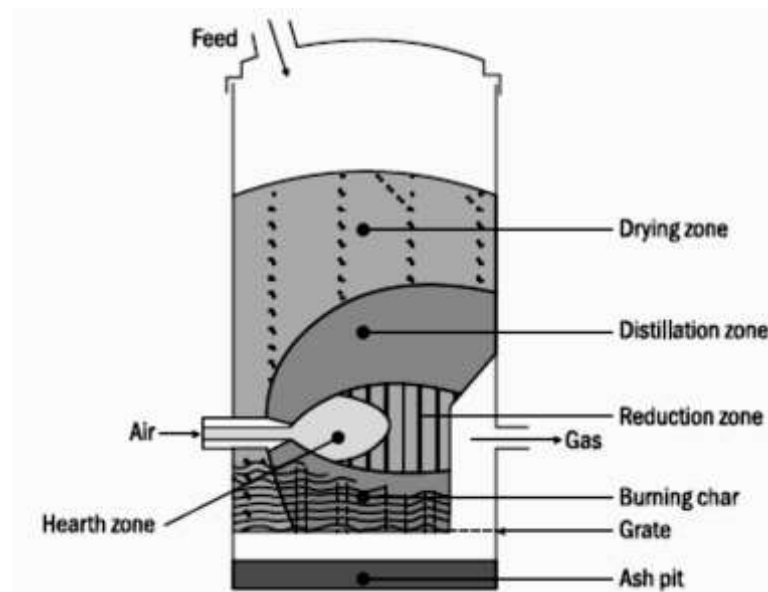


Fig 3.3 cross draft gasifier

3.1.2 PROCESS ZONES

It is possible to distinguish four separate zones in the gasifier: Drying zone, Pyrolysis zone, Oxidation (combustion) zone & Reduction zone.

3.1.2.1 Drying Zone

Solid fuel is introduced into the gasifier at the top. Biomass fuel entering the gasifier has variable moisture content of about 5-30% (depending on the fuel type) and in this gasifier zone drying of the fuel takes place (as a result of heat transfer from the lower parts of the gasifier). Then the water vapour flows downwards and is added to the water vapour formed in the oxidation (combustion) zone. Part of this vapour may be reduced to hydrogen while the rest will end up as a moisture content of the producer gas. Some organic acids that can result in gasifier corrosion are also released during the drying process.

3.1.2.2 Pyrolysis Zone

At the temperature range between 280°C and 500°C pyrolysis of the biomass fuel occurs. The details of the pyrolysis reactions are not yet well known, but it can be assumed that the large molecules (e.g., cellulose, hemi-cellulose and lignin) break down into the medium size molecules and carbon (char) during the fuel heating. Then the products of the pyrolysis process flow downwards into the hotter zones of the gasifier. Some of them will be burned in the combustion zone, and the rest (depending on the residence time in the hot gasifier zone) will break down to even small size molecules of methane, hydrogen, carbon monoxide, ethane, ethylene, etc. If the residence time will be too short or the temperature too low, then medium sized molecules can escape and condense as tars and oils, in the low temperature parts of the system.

3.1.2.3 Oxidation (Combustion) Zone

The oxidation zone is formed at the air intake level of the gasifier. Reactions that take place in this zone (reactions with oxygen) are highly exothermic and raise the temperature up to 1200–1500°C. Oxidation zone has two important functions; heat generation, conversion and oxidation of condensable products from the pyrolysis zone. To help gasifier establish its functions well, cold spots in the oxidation zone must be avoided. It is for this reason, two parameters – air inlet velocities and the reactor geometry must be carefully chosen.

3.1.2.4 Reduction Zone

The products of partial combustion move downwards through the red-hot charcoal bed, where reduction reactions take place. These reactions are endothermic – the reduction reaction necessitates heat and so, the producer gas temperature reduces (app. 600–700°C). “In this zone the sensible heat of the gases and charcoal is converted as much as possible into the chemical energy of the producer gas”. The end product of the chemical reactions that take place in the gasifier reduction zone is a producer (wood) gas which can be used (after dust and tar removal and cooling) as a fuel for internal combustion engines.

3.2 PRINCIPLES OF GAS ENGINE-GENERATOR

It is basically an engine-generator set for power generation application. It consists of following two systems.

3.2.1 Producer Gas Engine

Many researchers such as Banapurmath and Tewari (2009), Bhattacharya and Dutta (2000), Garg and Sharma (2013), Homdoun et al. (2015), Martinez et al. (2012), Mukunda et al. (1994), Zheng et al. (2004) etc. have been trying to develop a modified internal combustion engine for producer gas utilization from the long time. According to suggestions of researchers, the diesel engine has been converted into producer gas engine with slight changes. First, the spark plugs are fitted at the place of diesel injection nozzles, and then the plugs are connected to an ignition system, which controls the ignition timing and generates electricity to produce the spark in spark plugs. Second, a venturi has been installed for connecting the downdraft gasifier and the engine. The discharge valve connected in venturi can cut the gas supply in situation of an engine has to stop running. Third, the homogenous air-fuel mixture is prepared before entering the engine. This is usually done by a carburettor. To supply the constant pressure gas, a regulator is coupled to a carburettor. When an engine is coupled to electric generator with resistive load device, the volumetric flow of air-fuel mixture into the engine is constant, due to the constant rpm of engine with the corresponding frequency of the resistive load device. If the producer gas flow is low, the engine will compensate it by sucking in more air to maintain a constant volumetric flow. Thus, the air-fuel ratio is changed. These changes can be made through adjusting the regulator of the air and gas. When an engine operates on the producer

gas, the oxygen content in the exhaust gas changes, which is an indication of change in A/F ratio. This results in change of the CV, ideal A/F ratio and air intake. For a precise control of A/F ratio, the measurements of the A/F mixture must be made before the intake manifold with adjustments of the regulator of air and gas. In the diesel engine, the temperature of the air must be high in combustion chamber to ignite the diesel. Usually, the compression ratio is very high (14:1-25:1) for the diesel engine. Most of the diesel engines are made of a compression ratio around 17:1-18:1, which is higher than that of a petrol or natural gas engine. Since, a diesel engine has been converted into producer gas run engine without change in the compression ratio, which improves the efficiency drastically. The producer gas is fed to engine at a slightly above atmospheric pressure. The venturi for producer gas also needs a constant pressure. This venturi lowers the pressure of the producer gas to just above atmospheric pressure, so that the mixing of the air and gas can be made in a venturi there by the homogeneous mixture formation become easier in the carburettor. This constant A/F mixture is fed to the engine cylinder, where it is ignited by means of a spark produced at the spark plug. During this heat addition process, chemical energy of the producer gas is converted into heat which produces a temperature increase of around 2000°C. The pressure at the end of combustion process is considerably increased due to the heat released from the producer gas. This high pressure pushes the piston toward the bottom dead centre and power is produced. Now, both pressure and temperature decrease inside the cylinder during expansion. At the end of expansion stroke, pressure falls to atmospheric pressure. The piston starts moving up and sweeps the burnt gases out from the cylinder almost at atmospheric pressure. Thus, for one complete cycle, the power is obtained at the crankshaft.

3.2.2 Alternating Current Generator

A wired coil rotates inside the magnetic field generated by a magnet, which induces a voltage between the terminals coil. The periodic change in voltage happens due to change in position of the coil with respect to the magnetic poles. The amplitude of voltage depends upon the strength of magnetic field. It is directly proportional to rotational speed of the coil and its frequency is equal to revolution per second executed by the coil. If the rotational speed of the coil is constant and the magnetic field is uniform, the voltage induced between the terminals is sinusoidal with zero mean value. Each terminal of the coil is connected to a metallic ring. The contact of

the metallic rings is made with the fixed brushes. These brushes are connected to an electric load to establish the alternating current in the circuit. This information is collected from the literature survey of effect of the fuel on IC Engine.

The make of electric alternating current generator coupled to the engine is Kirloskar electric Co. Ltd. It is highly efficient, self-Excited, Self-Regulated and suitable for continuous operation. Its specification and pictorial view (Photograph 4.3) has been given in the next chapter.

3.3 PRINCIPLES OF SCHEFFLER COLLECTOR WITH SYSTEM OPERATION

The scheffler concentrating technology is one of the better technologies for the different kind of applications. In industries, it can meet the demand of water heating and steam applications. It is made of number of flexible parabolas or the combination of these gives a paraboloid shape. The fixed focus reflectors were developed by Mr. Wolfgang Scheffler and have proved to be a mile stone in solar thermal energy utilization technology.

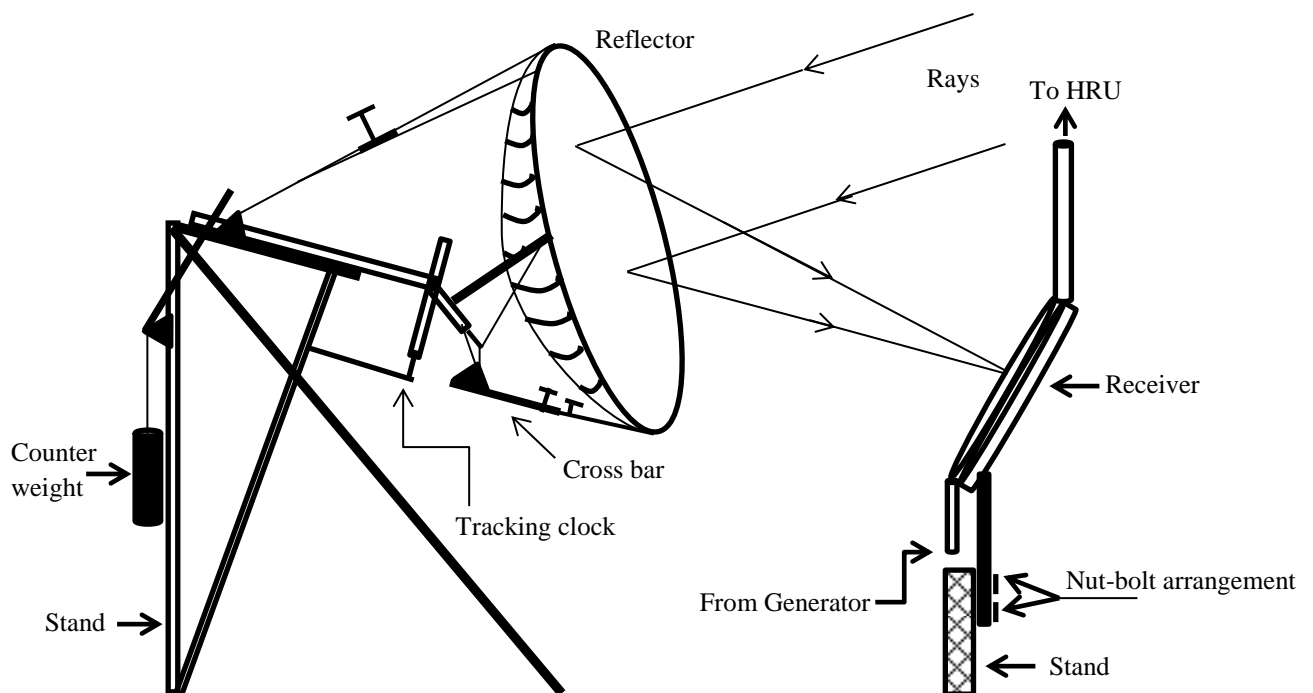


Fig 3.4 Schematic view of scheffler collector

Since the earth spins around an axis which passes through the North Pole and the South Pole while, the scheffler collector is used to spin around an axis parallel to the above axis, just in the opposite direction. Thus, it counteracts the earth's rotation and

cancels it out; as a result, the reflector keeps facing the sun in a constant manner. This is called the polar mounting or mounting on a polar axis. The distance between focus and center of the reflector depends on the selected parabola. During the day, the concentrated light on receiver will only rotate around its own center but not move sideways in any direction there by the focus stays fixed, which is very beneficial because the receiver have not to be moved either. The speed is one revolution per day or better to say, half a revolution in half a day because we do not use it at night. The constant speed of reflector is controlled with mechanical tracking device, which is called clockwork (or tracking clock). Changing the inclination of the reflector and deforming the reflector are the mechanically combined work: the two pivots, one is at each side of the reflector-frame, and other one is in the center of the reflector, do not form a line, but second one is located below it. This way inclines the reflector and leads to a change in its depth; thus, the center of the reflector is lifted up (big radius of crossbars) or pressed down (small radius of crossbars) relative to the reflector frame. It is enough to adjust the upper and lower end of the reflector to their correct position to obtain a sufficient exact reflector-shape. The setting is done by the adjustment of a telescopic bar at the each end of the reflector.

To adjust the reflector shape has to be done manually every 2-3 days. When all concentrated light incident on the focal point, where the receiver is fitted, this shows that the correct reflector shape has been achieved.

Once the receiver is illuminated and the clockwork is in motion, the spot of focused light remains on the receiver throughout the day. The seasonal variation in the height of the sun requires changing not only the angle between the reflector and its axis of rotation, but also the shape of the reflector. The scheffler collector comprises a number of flat glass mirror or acrylic mirror facets. The axis of daily rotation runs through the center of gravity of the reflector. Thus the reflector always maintains its gravitational equilibrium and the mechanical tracking device (i.e. clock mechanism) doesn't need to be driven by much force to rotate the reflector. The inclined cut creates the specific elliptical shape of the concentrationg Scheffler reflector. The heat generated by the solar energy is taken through the water into receiver to the heat recovery unit. For practical reasons, the shape of the reflector is made in such way that the focus is outside of the reflector, either on the north side or the south side. In this way, the focus can be even inside a building while the reflector remains outside. The above discussion regarding the scheffler collector is presented on the basis of the

references such as Bhirud and Tandale (2006), Jayasimha (2006), Scheffler (2006), Dafle and Shinde (2012), while the overall acute observation of its literature is made from the references of the performance evaluation of solar collectors.

3.4 PRINCIPLES OF WASTE HEAT RECOVERY UNIT (HRU)

The researchers like Luo et al. (2002) and Pulat et al. (2009) introduced the heat recovery unit (HRU), it is an equipment that transmit heat content (enthalpy or energy) of a comparatively high temperature hot fluid to a lower temperature cold fluid in which the hot fluid temperature decreases (or remain constant in case of losing the latent heat of condensation) and the cold fluid temperature increases (or remain constant in case of gaining latent heat of vaporization). Thus the HRU works as the heat exchanger. A heat exchanger normally provides indirect contact heating between two streams of fluids. For instance, a cooling tower cannot be termed a heat exchanger in which the water is cooled by direct contact with air. The proper design, operation and maintenance of the HRU can make the process of energy transfer efficient, minimize the energy losses and increase the HRU life. The HRU performance can deteriorate with time, off design operations and other interferences such as scaling, fouling etc. It is essential to evaluate periodically the performance of the HRU in order to maintain them at a high efficiency level. Mainly, two types of heat exchanger have been comprised in the HRU for two different types of hot fluid.

3.4.1 Counter Flow Heat Exchanger

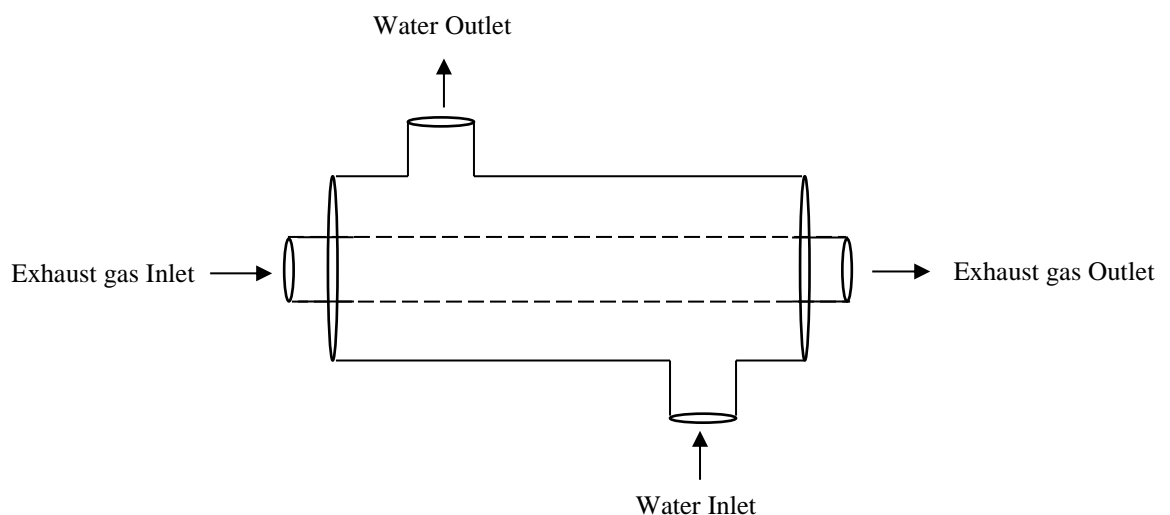


Fig 3.5 Counter flow heat exchanger

Al-attab and Zainal (2010) and its related literature reviews reported the counter flow heat exchanger. These are the heat exchangers in which the fluid flow directions of the cold and hot fluids are opposite to each other. In this heat recovery unit, the water is utilized as the cold fluid, while the exhaust gases are used as the hot fluid. These heat exchanging devices are cheap for both in designing and maintenance, making them a good choice for small scale applications. The flow of fluids is considered to be counter current flow for enhanced heat transfer from exhaust gases to the cooling water. It can be seen for the same terminal temperatures of cold and hot fluids, the LMTD for a counter flow heat exchanger is more than that for the parallel flow heat exchanger for a given same heat transfer rate. If the heat capacity rates are equal, the LMTD is equal to zero but the temperature difference is constant throughout the heat exchanger.

3.4.2 Multiple-Passes and Cross Flow Heat Exchanger

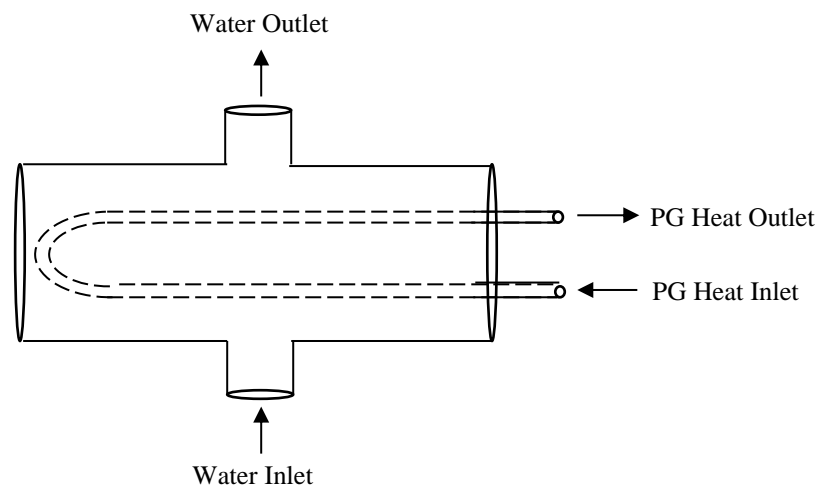


Fig 3.6 Multiple-pass and cross flow heat exchanger

Ghazikhani et al. (2014) and its relevant literature survey presented a double pipe cross flow heat exchanger. When large amount of heat has to be transferred, the heat exchanger area should be large. The small shell in a big shell in the heat exchanger is called pass. In the single tube pass heat exchanger, this requirement can be met either increasing the length of tubes or by decreasing their diameter and increasing the number of tubes at the same time but practically it is not possible due to the limitation of the size of the heat exchanger. The multiple passes arrangement has been developed owing to this difficulty. The multiple tubes per pass can increase the

required heat transfer area. It is calculated during the determination of heat transfer rate. There may also be the cross flow of the fluids (i.e. at right angle to each other) along with the multiple passes. The flow conditions for multiple-passes and cross flow heat exchangers are more complex than the concentric tube, single pass heat exchangers. For dealing this complex situation, the LMTD for this heat exchanger is determined by the multiplication of it with a correction factor, F , while the LMTD is determined just like it is done in the counter flow heat exchanger. The correction factor, F is calculated analytically or graphically, which is greater than 0.75 for the good design of heat exchanger.

3.5 PRINCIPLES OF VAPOUR ABSORPTION MACHINE (VAM)

The universal truth is that the ammonia boils at -33.34°C at the atmospheric pressure. When the pressure in a vessel is higher than the atmospheric pressure, the ammonia boils at a temperature higher than -33.34°C in that vessel, while when the pressure is lower than atmospheric pressure, the ammonia boils at a temperature lower than -33.34°C .

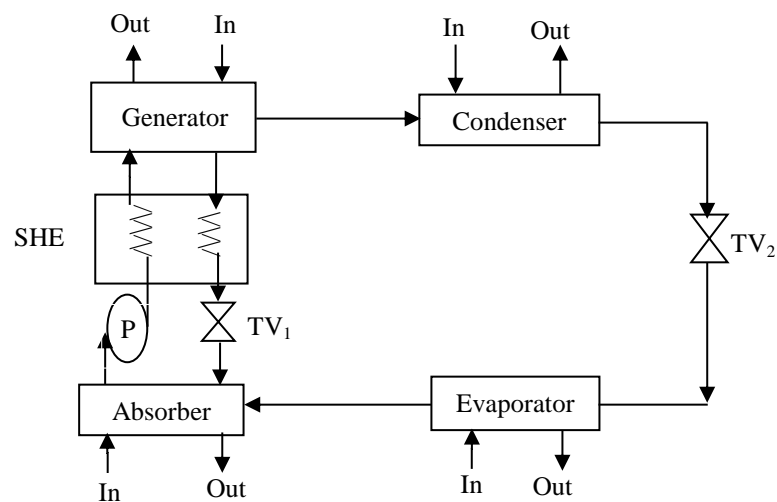


Fig 3.7 Vapor absorption system with aqua-ammonia solution

There are the two basic principles for the operation of the VAM, which are as follows:

- The first principle is that ammonia boils at -5°C at higher pressure than the atmospheric pressure, which is known as gauge pressure.
- The second principle is that the evaporation of refrigerant results in cooling of the cold body or contacted body.

The basic principles of the vapour absorption machine are generated by the acute analysis of the several researchers such as Chua et al. (2000), Srihirin et al. (2001), Kaynakli and Yamankaradeniz (2007), Kong et al. (2010), Mazouz et al. (2014) and its literature's study. To give it a practical feasibility, consider a closed vessel (evaporator) placed under the gauge pressure. It is kept in the cold storage and air is blown on it at atmospheric pressure. The following phenomenon will occur there:

- Since the pressure inside the vessel is maintained above the atmospheric pressure, there is no problem of leakage of refrigerant from the evaporator. The air runs over the vessel and gets cool through evaporation of refrigerant at -5°C taking an evaporation heat from running air in the cold storage. In such a way, the temperature lower than the atmospheric temperature is maintained inside the cold storage.
- The vapours of refrigerant ammonia so produced after the evaporation will immediately be absorbed by the cold water. This ensures the pressure decrease inside the vessel and increases the cooling effect.

The cold water in the absorber is always circulated because this has capability to absorb more ammonia from the evaporator. To recover the absorbent, aqua-solution is heated that causes the solution release the absorbent. The mixture is again made and is recirculated back to the vessel called generator, while the released refrigerant vapour is condensed in a separate vessel and sent to the evaporation.

3.6 PRINCIPLES OF CO-GENERATION SYSTEM

The cogeneration technology attracts numerous researchers like Cho et al. (2009), Dai et al. (2009), Kanogolu and Dincer (2009), Khaliq et al. (2012), Kumar et al. (2015) etc. due to their various quality applications at economical price rates. In the co-generation system, the chronological generation of two different kinds of valuable energy takes place from a single source of energy. Generally, the mechanical energy and thermal energy (exhaust gas waste heat) are generated by the co-generation system. The mechanical power generation equipment could be a steam turbine, combustion turbine; producer gas operated reciprocating spark ignition, Diesel engine, or fuel cell. The generated mechanical energy from the above equipment may be used to drive an electric generator (for producing electricity), motor, pump, compressor, fan or for various end services. The engine coupled to generators

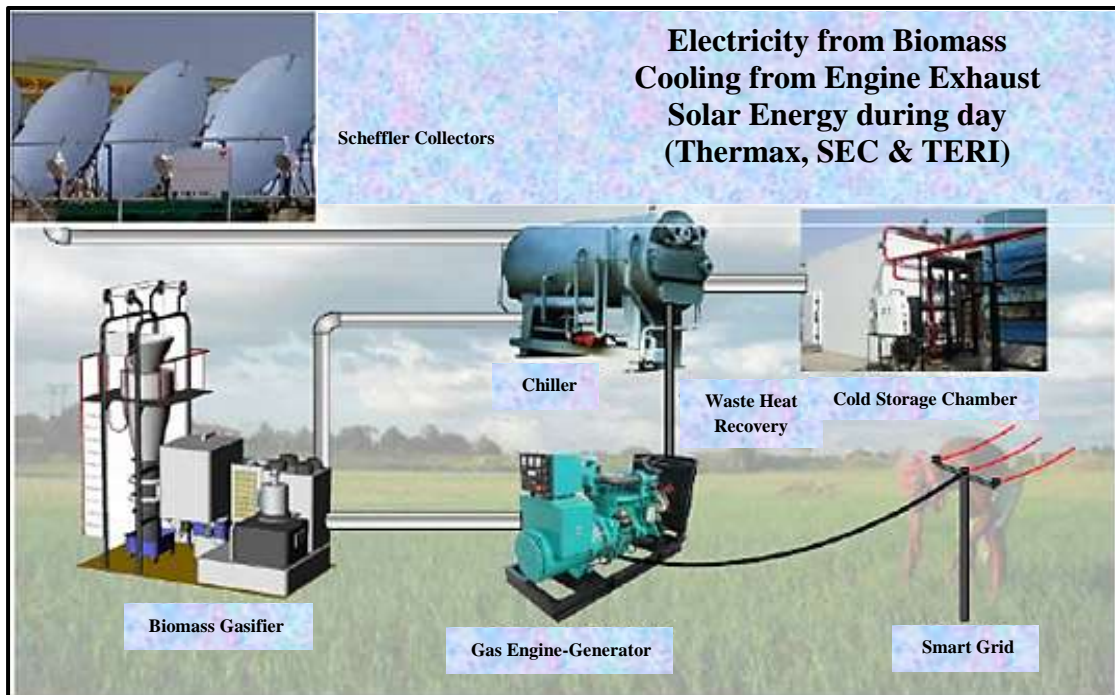
produces electric power and reject heat in various quantities at various temperatures that can be used for the required operation. Heat recovery exchangers or boilers, absorption chillers, and desiccant dehumidifiers are used for heating, cooling, or ventilation to the building space respectively. The thermal energy can be used either for the direct or for indirect process applications. In the direct use of thermal energy, energy for heating can be used for the required space, producing steam, hot water, hot air for dryer etc., while in case of indirect use, the system like chiller is used to generate the cooling effect. Heat-driven absorption chiller technology plays a prominent role in making use of the reject heat as well as solar energy, for space and ventilation air cooling. In this way, the overall efficiency of the co-generation system can reach up to 80% and more in some of the cases. A small scale generation gas turbine operated co-generation power plant can save about 40% of the total energy input as compared to a fossil fuel run conventional power plant with a boiler for heating. It indicates towards the decentralization of power plant. The decentralized co-generation system reduces the losses related to the transmission and distribution of the electricity as well as using the exhaust heat for cooling or heating. These transmission and distribution losses are around 5-10% in conventional power plant. These losses become greater, when electricity is supplied to remote and smallest consumers. These can be eliminated using the hybrid system. The production of electricity has been done on-site so the burden on the utility network is reduced. Moreover, co-generation systems save the fossil fuels along with the reduction of the emission of greenhouse gases such as CO₂ per unit volume of energy output. The schematic diagram of the hybrid system or co-generation for power as well as cooling generation has been shown in figure 4.1 in the next Chapter No.- 4.

The cogeneration technology plays an important role from macroscopic and microscopic point of view. At the macroscopic level, the power can be decentralized and shared by private sector, thus it would reduce the financial burden of the nation for the power utility. Additionally, it can preserve the traditional energy resources and reduce the import fuel price rate. At the microscopic level, the overall energy bill price rate of the consumers can be reduced, specially, when there is the need of both kinds of energy at one place and thus a rational energy tariff can be practised in the country.

CHAPTER-IV

MATERIALS AND METHODOLOGY

The cold storage cum power generator based on hybrid renewable energy resources with exhaust gas waste heat is installed at the R&D campus of the SEC (Solar Energy Centre), which is located at Gwalpahari, Gurgaon (HR). It is a combined collaboration of the SEC (MNRE), TERI and Thermax Limited, Pune with 15 kW rated cooling capacity of the VAM. This test rig has been studied at the above centre. This chapter shows the different instruments used in the experiments and method of experiments carried out to investigate the performance of system.



Photograph 4.1 Pictorial view of hybrid cold storage cum power generator

4.1 DESCRIPTION OF EXPERIMENTAL SET-UP:

The test unit consists of the Biomass gasifier, Gas Engine-Generator, Scheffler's collectors, Waste heat recovery unit and Cold storage system. In the above photograph 4.1, the real pictures of each component of this test rig have been depicted. The description of the different components used in the test rig for the investigation is being represented as follows:

4.1.1 Biomass Gasifier:



Photograph 4.2 Pictorial Views of double ignition downdraft gasifier

There are the four zones in any gasifier namely: Drying zone, Pyrolysis zone, Oxidation (combustion) zone and Reduction zone. The tarry products are the biggest problem in a gasifier. In this system, the double ignition downdraft gasifier is being prominently used because the tar entrainment problem in the gas stream can be minimized by the use of this type of gasifier. In the double ignition downdraft gasifier, the air is supplied in two stages; the first stage of the air is provided at the nozzle, where the biomass is fed into the reactor, while the second stage of the air supply take place at the oxidation zone level where together with oxidation of a part of the char the volatiles are released into the upper zone of the reactor. The first air supply stage is located near the top of the reactor where the biomass is partially oxidized and the thermal energy is released. This is needed for the drying and pyrolysis phases occurring above the combustion zone. The second air supply stage is in the middle of the reactor, more precisely, in the oxidation zone where the tar decomposition into lighter size molecules occurs. This results in the reduction of the tar content in the volatiles and in the generation of thermal energy for the endothermic char gasification. Since the partially oxidized pyrolysis products pass through the char bed in the char gasification reactor, the tar content is further reduced in second stage air supply or ignition. Despite a comparatively low content of tar in the producer gas than the downdraft gasifiers, this must be further reduced using the different filters such as regenerator as a scrubber, air cooler, water cooler, cyclones, fabric filter and paper filter. Finally, the processed gas should be brought to the gas engine-gen set.

4.1.2 Gas Engine-Generator:

The producer gas outlet of the gasifier via different filters is connected to the Engine gas control valve. The air is then sucked into the Engine through a mixer butterfly consisting of piping and valves arrangement. The shaft of the gas engine is coupled with the electric generator. When the shaft rotates, the electricity is produced by the generator. The double ignition gasifier coupled with gas engine generator set is started with a heavy duty Battery (12 V+12 V), in which first 12 V battery is initially used to operate the blower of the gasifier to produce the ignition in the gasifier, while the second 12 V battery is used for running the gas engine-gen set. The regenerator is used as a main scrubber for cooling of the gas. The air is used as the cooling medium for the producer gas in regenerator (HE-1). Further for cooling and cleaning, the PG passes through the different filters such as: cyclone, fabric filter, HE-2 (air cooler), HE-2 (water cooler), paper filter and then finally to the engine. The producer gas then starts the engine on the gas mode. The governor linked control butterfly is provided to vary the gas quantity according to the electrical load on the power generator, keeping frequency within limits. Negligible portion of the generated electricity is used in the pump of the cold storage system and rest of the electricity can be given to the **Smart Grid**. The electricity can be used for other ends purposes from the smart grid.



Photograph 4.3 Pictorial Views of Gas engine-gen set with spark plugs

4.1.3 Scheffler's Collectors:

A scheffler's collector tracks the sun and focus sunlight on a fixed receiver. The reflector produces a converging beam of sun-light aligned with an axis of rotation.

The axis of rotation is parallel to the axis of the earth. The clock mechanism rotates the reflector around its axis of rotation at a rate of one revolution per day. It keeps the reflected beam aligned with the axis of rotation as the sun moves. Each morning, the operator has to rotate the reflector back to its starting position in which the receiver is illuminated and switch on the clockwork. After few days the operator has to adjust the angle between the axis of rotation and reflector to accommodate the seasonal variation in the height of the sun.



Photograph 4.4 Pictorial Views of scheffler collectors

In the hybrid system, first the stored water from raw water tank passes through the softener where all the impurities and the hardness are removed. Again, this water is stored in the pure water tank and from here; it is pumped in the insulated spread pipe line around the reflectors. The water from the pure water tank passes through the receivers, which are in the fixed position and at the focus of the reflector. The collector concentrates sunlight on the receivers, where the water gets heated due to the high temperature of the reflector and then the heated water is circulated through the

generator of the vapour absorption machine (VAM) via the heat recovery unit (HRU). The nitrogen gas is used in the pipe line with water so there is no conversion of water into vapour. The exhaust gas waste heat from the engine is also used to heat the water in the HRU.

4.1.4 Waste Heat Recovery Unit (HRU):



Photograph 4.5 Pictorial Views of heat recovery unit

Waste heat recovery unit (HRU) is nothing but a combination of counter flow heat exchanger and single pass-cross flow heat exchanger. During the solar hours (day), the HRU works as counter flow heat exchanger, the ‘hybrid solar energy-engine exhaust waste heat’ and ‘water’ are used as the hot and cold fluid respectively, while during the non-solar hours (night), the mechanism of the HRU treats as a single pass-cross flow heat exchanger, either hybrid engine exhaust heat and auxiliary firing of producer gas or only combustion heat of producer gas can be used to provide the heat to the water into the heat recovery unit. There are the two tubes in a pass, in which the hot fluid flows, while the single stream of water circulates at right angle over these tubes. This single stream of water also passes through the HRU, solar collector and generator of the VAM. The cold fluid (water) always flows towards the generator of the VAM from the HRU, where it imparts the heat to the generator of the VAM. Additionally, the thrice sources of energy can be utilized simultaneously but the system will not be economical viable.

4.1.5 Vapour Absorption Machine (VAM):



Photograph 4.6 Pictorial View of vapour absorption machine and cold storage

In the vapour absorption machine, the compressor is replaced by an absorber, a pump, a generator and pressure reducing valve. These components in this system perform the same function as that of a compressor in the vapour compression refrigeration system. The heat of the HRU is imparted to the generator of the VAM, where the vapour ammonia refrigerant drives off the solution and enters into the condenser with high pressure and velocity, here it is liquefied. The liquid refrigerant then flows into the evaporator through throttle valve and thus the cooling effect can be seen at the evaporator. It is connected to a container, known as cold storage. In this system the low pressure vapour refrigerant from the evaporator has been drawn into an absorber where it is absorbed by the weak solution of the refrigerant forming a strong solution. This strong solution is pumped to the generator where again it is heated by the heat of the HRU and thus the cycle is repeated. In the system the low pressure ammonia vapour leaving the evaporator, enters the absorber where it is absorbed by the cold weak solution (or that is called cold water) in the absorber. Owing to this, a separate arrangement for cold water circulation over the absorber is done. The cold water has the ability to absorb the very large quantities of ammonia vapour and the solution thus formed, is known as aqua-ammonia solution. The absorption of ammonia vapour in water lowers the pressure in the absorber which in turn draws more ammonia vapour from the evaporator and thus raises more heat from the hot body. The pump can increase the pressure of the aqua-ammonia solution upto 10 bar.

4.2 THE TECHNICAL SPECIFICATIONS AND THE EXPERIMENTAL PROCEDURE

4.2.1 Specification of Hybrid System

Cooling Capacity	15 kW
Cold storage Temperature	0°C to -5°C
Gas Engine capacity	50 kWe
Biomass consumption	70 kg/hr
Heat source for VAM	
During solar hours	Solar and producer gas engine exhaust.
During non-solar hours	Producer gas engine exhaust/ auxiliary firing.

4.2.2 Specification of Electric Generator

Type of generator:	A.C. generator (Kirloskar electric Co. Ltd.)
Rated capacity:	50 kWe
R.P.M.	1500
Voltage:	415
Alternator efficiency	80% (As per manufacturer specification)

4.2.3 Specification of Engine

Type of engine:	6R1080TA (Kirloskar oil engine Ltd.)
Governing class:	M ₂
Engine No.	6H.2510/1000003
No. of cylinders:	06
Rated power:	115 kW
R.P.M.	1500

4.2.4 Specification of Gasifier

Type of gasifier	Downdraft gasifier (Ankur from TERI)
Model	WBG-40
Gasification temperature	1050°C-1150°C
Fuel storage capacity	200 kg
Fuel type	Wood with 5-30% with Permissible moisture content
Biomass charging	On-line batch mode by topping up once every one hour

4.2.5 Specification of Scheffler Collector

Make with No. of collectors	Thermax Pvt. Ltd. installed 04 collectors
Maximum temperature at focal point	1020°C
Maximum efficiency	84%
Aperture area of each collector	16 m ²
Average DNI/Used materials	700 W/m ² / Steel profiles and glass mirror
Used materials	Steel profiles and glass mirror

4.2.6 Specification of VAM

Make	Thermax Pvt. Ltd.
Type of model	Single effect absorption chiller (KG-111A/B)
Cooling capacity	15 kW
Refrigerant used	NH ₃ -H ₂ O mixture
Evaporator temperature	-5°C ($\dot{m}_{exf} = 905\text{kg} / h$ with $t_{inex} = 30.65^\circ\text{C}$, $t_{exout} = -3.83^\circ\text{C}$)
Condenser temperature	35°C ($\dot{m}_{exf} = 816\text{kg} / h$ with $t_{inex} = 29.56^\circ\text{C}$, $t_{exout} = 38.57^\circ\text{C}$)
Absorber temperature	25°C ($\dot{m}_{exf} = 25.92\text{kg} / h$ with $t_{inex} = 33.4^\circ\text{C}$, $t_{exout} = 40.21^\circ\text{C}$)
Heating medium in generator	Water ($\dot{m}_{exf} = 1814\text{kg} / h$ with $t_{inex} = 119^\circ\text{C}$, $t_{exout} = 109^\circ\text{C}$)
HRU/generator efficiency	100%

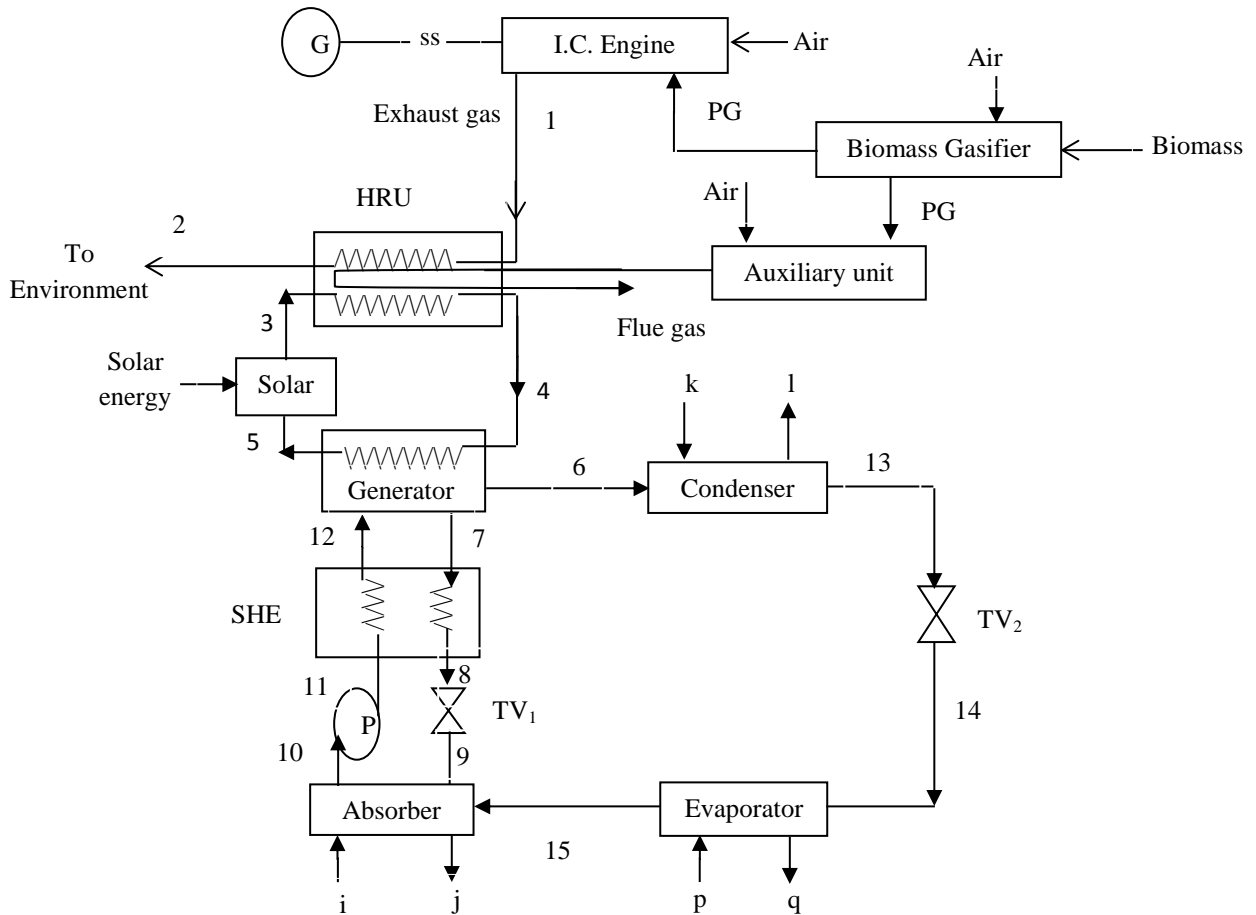


Fig 4.1 Schematic diagram of a hybrid cold storage cum power generator

4.2.7 Experimental Procedure

Figure 4.1 shows a schematic diagram of the ‘hybrid cold storage cum power generator’ wherein the critical components are identified. The biomass is fed through the feed door and is stored in the hopper of the gasifier. The limited and controlled amount of air for partial combustion enters through Air Nozzles. The throat (or hearth) makes sure relatively clean and good quality gas production. The Reactor holds charcoal for reduction of partial combustion products whereas allowing the ash to drop off in the ash pond. The gas passes through the annulus area of reactor from upper portion of the perforated sheet. The gas outlet is connected with the various downstream systems viz. HE-1 (regenerator) as a scrubber, cyclone, fabric filter, HE-2 (air cooler), HE-2 (water cooler), paper filter and Engine shut-off valve. Gas produced in the Gasifier is scrubbed and cooled in HE-1 (regenerator) with recirculating air with the help of blower. Gas is separated from particulates in the cyclone and introduced in the fabric filter, HE-2 (air cooler), HE-2 (water cooler) and

paper filter. The cool-clean Gas and Air is then sucked into the Engine through a mixer butterfly be made up of piping and valves arrangement.



Photograph 4.7 View of different kind of filters

The Gasifier is started with the help of a Battery (12 V), which initially provides auxiliaries power to run the blower for starting the Gasifier System. A Battery based Electric Starter to starts the engine. The producer gas then starts engine on gas mode. The governor linked control butterfly valve is provided to vary the gas quantity as per electrical load on the generator, keeping frequency within limits.

During solar hours, the hybrid exhaust waste heat gases (1-2) and the solar energy (3-4) from the Scheffler collector (which is a fixed focus collector), while during non-solar hours, the hybrid exhaust waste heat gases (1-2) and combustion heat of the PG in the HRU through auxiliary firing, first go to the HRU and finally to the generator (4-5). The high velocity refrigerant saturated vapor (6) of ammonia from the generator goes to the condenser where the heat is rejected at the condenser pressure. Now the saturated liquid (13) from the condenser passes through the throttle valve (TV_2), where the pressure reduces equal to the evaporator pressure and goes to the evaporator of the VAM. The saturated vapor (15) after receiving heat, enters into the absorber, where it is absorbed by the absorbent water, which lowers the pressure in the absorber and, draws more ammonia vapor from the evaporator, thus a solution is formed. The hot weak solution (7) passes through the solution heat exchanger (SHE) and cooled to (8), and then passes through the throttle valve (TV_1) to reduce its pressure (9) i.e., absorber pressure. Two streams (15, 9) get mixed at absorber and form a solution (10), which is pumped by the solution pump (P) and passes through

the SHE, then finally enters, to the generator (12), where it is heated. The ammonia vapor drives off the solution due to this heat at high pressure leaving behind the hot weak solution (7) in the generator. Now, the high velocity refrigerant ammonia vapor (6), coming from the generator goes to the condenser again, thus the cycle is repeated. The VAM, scheffler collector, Engine and Gasifier Control panels are equipped with all kind of switching facilities, indications and safety of operation. An electric driven biomass cutter and reactor heat recovery established wood pieces drying arrangement are as well provided to make the system self-sufficient.

4.3 MEASURING DEVICES AND METHODS USED:

The experiment has been initiated on the ‘hybrid cold storage cum power generator system’ after attaining the steady state operation in terms of generation of consistent cooling and electric power. The hybrid system has been tested with varying electric load from 15.24 kW to 38.86 kW. The experiment has been made with the help of the following devices.



Photograph 4.8 View of biomass used as fuel and wood cutter

4.3.1 Fuel: The biomass ‘firewood chips’ of approximately size $65 \times 40 \times 35 \text{ mm}^3$ with moisture content 25% has been used as a fuel for testing of the system.

4.3.2 Resistive Loading Device: The loading device has been developed in R&D campus, which has star connection with 15 heaters of 5 kW capacity each. These heaters have been well distributed on each phase through 14 MCV kept ON or OFF to load the engine gradually.



Photograph 4.9 View of loading device and Gas Chromatograph

4.3.3 Gas Analyzer: The producer gas leaving the gasifier has been collected in the gas samplers and analyzed the gas composition using gas chromatograph. The chemical composition by volume is maximum for the nitrogen gas, while it is minimum for the methane gas. However, the chemical composition of all constituents of producer gas is in stable state. The make of the gas chromatograph is "CHEMITO, Model No.8510" collaboration with USA.



Photograph 4.10 View of tar measuring device

4.3.4 Measurement of Tar: The tar samples have been collected in copper tube condenser dipped in ice bath. The length of condenser is 5 m. The temperature of water bath in which the copper tube condenser is placed, has been maintained to be $5\pm 1^{\circ}\text{C}$ to cool the gasses passing through the condenser. This tar has been collected by the displacement method in which it is displaced for the 100 liters of water and then it is washed with acetone from the condenser. Subsequently, it is kept in oven at 60°C up to the evaporation and weighed. Then, the beaker weight is subtracted from

this weighed value. The final value is the weight of tar. This tar has been collected from outlet of gasifier and each filter.



Photograph 4.11 View of vane type anemometer, orifice plate with U-tube manometer and electronic manometer

4.3.5 Air Flow Rate: The air flow to all the devices has been measured using vane type digital anemometer make “**Leda -1000 Electronic anemometer**”. For the evaluation of discharge, the following continuity equation has been used:

$$\dot{Q}_{air} = \text{Density} \times \text{Area} \times \text{velocity}_{air} = \rho \times \frac{\pi}{4} \times d^2 \times V$$

Where, ρ = Density of air (kg/m^3) d = Diameter of the pipe (m),

V = velocity of air (m/s)

4.3.6 Producer Gas Discharge: The discharge of producer gas from gasifier outlet is measured using the calibrated orifice plate fitted with water column U-tube manometer. The design and manufacturing of this orifice plate has been done in the research workshop of solar energy center. The difference of manometer height (Δh) can give the discharge using following formula:

$$\dot{Q}_{PG} = \frac{C_d \times A_o}{\sqrt{1-\beta^4}} \times \sqrt{\left\{ 2g \times \Delta h \times \left(\frac{\rho_w}{\rho_g} - 1 \right) \times \sin \theta \right\}} \times 3600 \text{ (m}^3\text{/hr)}$$

Where, $C_d = 0.66$ (From the calibration of the orifice plate)

A_o = area of orifice plate = $\pi/4 \times d^2$,

$d = \text{Diameter of orifice plate} = 3.75 \times 10^{-2} \text{ m}$

$\beta = \frac{d}{D} = 0.5, D = \text{Diameter of the pipe} = 7.5 \times 10^{-2} \text{ m}$

$\rho_g = \text{Density of producer gas} = 1.09 \text{ kg/m}^3,$

$\theta = 90^\circ, \Delta h = \text{Manometer height (m)}$

Therefore, the final formula is: $\dot{Q}_{PG} = 364.4 \times \sqrt{\Delta h} \text{ (m}^3/\text{hr)}$

4.3.7 Measurement of Pressure: The pressure at the different filters has been measured using the electronic manometer and the make of the manometer “COMARK C9507/IS-MANOMETER INTR SAFE”.



Photograph 4.12 View of control panel, data logger and temperature indicator

4.3.8 Measurement of Temperature: The temperature profile of the gasifier has been measured using K-type chromel-alumel thermocouple (1250 mm length & 8 mm diameter) at eight different locations above the grate. The temperature at the different locations has been measured with the help of J-type thermocouples. The make of these is “EMSON Pvt. Ltd. Ajmer”. These fitted thermocouples have been connected with the control panel, which is installed by Thermax limited, Pune. This control panel also shows the temperature at different locations of the whole co-generation system. The data logger has also been used for measurement of temperature. The make of Data logger is “DATA TAKER, Model No.-DT600 and Series-3”.

4.3.9 Measurement of Moisture: First of all, the biomass is weighed and kept in oven for 24 hours at 100°C. After this period, it is again weighed and deducted from the previous weight and divided by the original weight, in this way it would give the percentage of moisture reduction with time.

4.3.10 Power Output Measurement: The electric power output is measured by recording the voltages across the three phases of the AC generator and the current drawn by the resistive load device. In the resistive load device, star connections have been made. The voltage, current, frequency, power factor and power output can be recorded directly from the control panel. The power supplied to the grid is measured by using the following formula:

$$P = VI\sqrt{3} \text{ (Watt)}$$

Where, v = Voltage (V) and I = Current (A)



Photograph 4.13 View of control panel and gas analyser

4.3.11 Engine Emission Measurement: Exhaust emission has been measured with the help of the gas analyzer (Endee Make model no PA-2400) in the exhaust manifold, which is an on-line gas analyzer, sucks the exhaust gas sample and displays the proposition of gas constituents in the screen. The gases analyzed have oxygen (O₂), carbon dioxide (CO₂), nitrogen oxide (NO) on an intermittent basis.

4.3.12 Pyrheliometer, Pyranometer and Ultrasonic Anemometer: A pyrheliometer is an instrument for measuring the direct beam solar irradiance at

normal incidence. Sunlight enters into the instruments through a window and it's directed to the thermopile, which converts heat into electrical energy by seebeck effect, which display in watt per square meter. It is so designed that it measures only the radiation from sun's disk (which has an apparent diameter of $\frac{1}{2}^\circ$) and from a narrow annulus of sky of diameter 5° around the sun's disk. A pyr heliometer is often used with same set up of pyranometer. (DNI)



Photograph 4.14 Set up view of pyr heliometer with pyranometer and ultrasonic anemometer

A **pyranometer** is an instrument for measuring the global (direct and diffuse) solar radiation. If it is provided with a shadow band that prevents direct beam solar radiation from reaching the receiver, it measures diffuse solar radiation. The whole set up is used with solar tracking system to keep the system towards the sun. The make of pyr heliometer and pyranometer is Kipp & zonen with model number CMP3 and SPH1 respectively. (Global)

Ultrasonic anemometer: The Ultrasonic Anemometer is a 2-axis, no-moving-parts with wind sensor. It is ideal and reliable for general meteorological applications and measurement. It measures wind based on the transit time of ultrasonic pulses between four transducers. Air flow alters the transit time which is used to calculate flow velocity. Wind direction is determined from relative velocities along each acoustic path. Measured results are displayed on the Wind Tracker displays, data loggers, etc. The sensor is constructed using ultra-violet stabilized thermoplastic, stainless steel, and anodized aluminium for superior environmental resistance. It can easily be mounted on 1 inch pipe. The Make of Ultrasonic anemometer is the R.M. YOUNG COMPANY, USA and Model No. YOUNG 85000.

4.3.13 Design and Calibration of Orifice Plate:

4.3.13.1 Design Consideration: An orifice flow meter is installed between flanges connecting two pipes of upstream & downstream and downstream pressure tapping threaded $\frac{1}{2}$ of pipe diameter while upstream pressure tapping threaded at equal to diameter of pipe. The orifice diameter is taken $\frac{1}{2}$ of the diameter of pipe. One side of the orifice is chamfered with 45° . This chamfer should be towards the downstream. The hole in the orifice plate must coincide with flange hole to ensure precise centering of the orifice plate in the pipe line. The position of the pressure tappings is vertical. A U-tube differential manometer with water in the column was used to measure the pressure difference between upstream and downstream side of the pipe.

4.3.13.2 Calibration Procedure: The entire orifice plate assembly is installed in the Lab and calibrated with air blower. A valve was provided to change the air flow rate. At the different valve opening, the air flow rate was varied and velocity was measured with the help of vane type anemometer. Water column height was also measured in the U-tube manometer.

4.3.13.3 Calculation for Coefficient of Discharge: Coefficient of discharge can be calculated as follows;

$$C_d = \frac{(\dot{Q}_a)_{act}}{(\dot{Q}_a)_{th}}$$

Where C_d = Coefficient of Discharge

$(\dot{Q}_a)_{act}$ = Actual Discharge of air (kg/sec)

$(\dot{Q}_a)_{th}$ = Theoretical Discharge of air (kg/sec)

Actual Discharge of air can be calculated as:

$$(\dot{Q}_a)_{act} = \rho_a \times \frac{\pi}{4} \times D_1^2 \times V_a$$

Where, $\rho_a = 1.18 \text{ kg/m}^3$, $D_1 = 0.06875 \text{ m}$

On putting the value of above parameter, the formula can be written as

$$(\dot{Q}_a)_{act} = 0.00438 \times V_a \quad (1)$$

Where ρ_a = Density of air (kg/m³)

D_1 = Diameter of Van type Anemometer

V_a = Velocity of air measured by Van type Anemometer

Theoretical discharge of air can be calculated as

$$(\dot{Q}_a)_{th} = \frac{\rho_a \times A_o}{\sqrt{(1-\beta^4)}} \times \sqrt{\left\{ 2g \times \Delta h \times \left(\frac{\rho_w}{\rho_a} - 1 \right) \times \sin \theta \right\}}$$

Where,

A_o = area of orifice plate = $\pi/4 \times d^2$,

d = Diameter of orifice plate = 3.75×10^{-2} m

$\beta = \frac{d}{D} = 0.5$, D = Diameter of the pipe = 7.5×10^{-2} m

ρ_a = Density of air = 1.18 kg/m³

ρ_w = Density of water = 1000 kg/m³

$\theta = 90^\circ$, Δh = Manometer height (m) and $g = 9.81$ m/s².

On putting the value of above parameter formula can be written as

$$(\dot{Q}_a)_{th} = 0.1734 \times \sqrt{\Delta h} \quad (2)$$

Where, Δh = Different of manometer height of water column (m)

From equation (1) and (2) Coefficient of discharge can be calculated as

$$C_d = \frac{0.00438 \times V_a}{0.1734 \times \sqrt{\Delta h}}$$

The average manometer height and air flow rate is taken from table-4a:

$$C_d = \frac{0.00438 \times 4.8}{0.1734 \times \sqrt{0.0334}} = 0.6634$$

4.4 DEFINITIONS AND MEASUREMENT OF DIFFERENT

PARAMETERS: Following parameters have been calculated for analyzing the performance of the hybrid system:

4.4.1 Biomass Consumption Rate (BCR): The biomass consumption rate has been estimated by dividing the weight of total biomass poured in the gasifier with the total time of operation.

$$BCR = \frac{\dot{m}_b}{t_o} \text{ (kg/hr)}$$

Where, \dot{m}_b = Biomass poured (kg)

t_o = Time of Operation (hr)

4.4.2 Brake Power (P_B): It is the measurement of rotational force available at the output of the engine crank shaft and the power corresponding to it is known as the brake power.

4.4.3 Specific Fuel Consumption (SFC): It is expressed as the ratio of biomass consumed in kilogram in unit time to the power output. It gives required fuel consumption rate at particular load.

$$SFC = \frac{BCR}{\dot{P}_E}$$

4.4.4 Air-Fuel Ratio (A/F): It is the ratio of mass of the air to the mass of the producer gas. It is also known as specific air consumption. As the load increases, the A/F ratio decreases.

$$A / F = \frac{\dot{m}_{air}}{\dot{m}_{PG}}$$

4.4.5 Co-efficient of Discharge (C_d): It is the ratio of actual discharge of fluid to the theoretical discharge of fluid in the pipe. It gives the exact value of discharge.

$$C_d = \frac{\dot{Q}_{actual}}{\dot{Q}_{theoretical}}$$

4.4.6 Generator Efficiency (η_{gen}): It is the ratio of electric power output to the brake power of the engine. The installed generator is highly efficient.

$$\eta_{gen} = \frac{\dot{P}_E}{\dot{P}_B}$$

4.4.7 Mass Flow Rate: The mass flow rate is the product of density and discharge of fluid. It is based on principle of continuity. It can be calculated as:

$$\dot{m} = \rho \times \dot{Q}$$

4.4.8 Density of Producer Gas (ρ_g):-Average chemical composition of producer gas by volume is given as follows:-

$$CO = 20 \pm 2\% \quad (\text{Molecular weight} = 28.01 \text{ gm/mole})$$

$$CO_2 = 12 \pm 1\% \quad (\text{Molecular weight} = 44.01 \text{ gm/mole})$$

$$H_2 = 20 \pm 2\% \quad (\text{Molecular weight} = 2.016 \text{ gm/mole})$$

$$CH_4 = 3 \pm 1\% \quad (\text{Molecular weight} = 16.043 \text{ gm/mole})$$

$$N_2 = 45\% \quad (\text{Molecular weight} = 28.01 \text{ gm/mole})$$

At NTP, 1mole =22.4 liter, assume the quantity of producer gas is 100 liters

Then, No. of moles (n) for gas constituents are

For CO	No. of moles = Volume of gas / 22.4 =20/22.4 = 0.89 moles
For CO_2	No. of moles = Volume of gas / 22.4 =12/22.4 = 0.536 moles
For H_2	No. of moles = Volume of gas / 22.4 =20/22.4 = 0.89 moles
For CH_4	No. of moles = Volume of gas / 22.4 =3/22.4 = 0.134 moles
For N_2	No. of moles = Volume of gas / 22.4 =45/22.4 = 2.01 moles

Mass of the gas constituents: Mass = No. of moles \times Molecular weight

For CO	Mass = 0.89 \times 28.01 = 24.93 gm
For CO_2	Mass = 0.536 \times 44.01= 23.59 gm
For H_2	Mass = 0.89 \times 2.016 = 1.8 gm
For CH_4	Mass = 0.134 \times 16.043 =2.15 gm
For N_2	Mass = 2.01 \times 28.0134 =56.31 gm

Total mass $m = 108.78 \text{ gm}$

Density of the producer gas =Total mass / Total volume

$$\rho_g = 108.78/100$$

$$\rho_g = \mathbf{1.09 \text{ kg/m}^3}$$

4.4.9 Specific Heat of Producer Gas:-The producer gas constituents are carbon monoxide (CO), carbon dioxide (CO_2), hydrogen (H_2), methane (CH_4) and nitrogen

(N_2). The specific heat of these constituents are taken from gas table and calculated at NTP. These values are as follows:-

$$CO = 1.048 \text{ kJ/m}^3 \text{ }^\circ\text{C}, CO_2 = 0.839 \text{ kJ/m}^3 \text{ }^\circ\text{C}, H_2 = 14.14 \text{ kJ/m}^3 \text{ }^\circ\text{C}, CH_4 = 2.233 \text{ kJ/m}^3 \text{ }^\circ\text{C}$$

$$\text{and } N_2 = 1.029 \text{ kJ/m}^3 \text{ }^\circ\text{C}.$$

$$C_p = \frac{m_{CO} C_{p,CO} + m_{CO_2} C_{p,CO_2} + m_{H_2} C_{p,H_2} + m_{CH_4} C_{p,CH_4} + m_{N_2} C_{p,N_2}}{m}$$

$$C_p = \frac{24.93 \times 1.048 + 23.59 \times 0.839 + 1.8 \times 14.14 + 2.15 \times 2.233 + 56.31 \times 1.029}{108.86}$$

$$C_p = 1.232 \text{ kJ/m}^3 \text{ }^\circ\text{C}$$

So the specific heat of the producer gas is **1.232 kJ/m³ °C**.

4.4.10 Energy Content: The choice of a fuel is based on its heating value. If the heating value (energy content) of the fuel is higher, the higher is the efficiency of the system “for one charge one can get power for the longer time”. The higher heating value (HHV) is determined by the bomb calorimeter, while the lower heating value (LHV) is determined as follows:

$$LHV = HHV - w_m h_{fg}$$

Where, w_m = Weight fraction of moisture produced in combustion

h_{fg} = Heat of vaporization of water

4.4.11 Specific Gas Production: It is the ratio of producer gas production per unit time to biomass consumption rate. It's expression is:

$$SGP = \frac{\dot{Q}_{PG}}{BCR}$$

4.4.12 Heat Loss Factor (F_{U_L}): The heat loss factor, determines the energy lost from the absorber to ambient by a combined process of convection and radiation between the receiver plate and the solar collector along with conduction losses across the receiver and radiation losses between the solar collector and the surroundings. The

heat loss factor of a collector is defined as the ratio of the DNI to the temperature difference between mean and ambient temperature.

$$FU_L = \frac{DNI}{(T_m - T_a)}$$

4.4.13 Coefficient of Performance (COP): It is the ratio of amount of heat absorbed into the evaporator from the cold body to the heat supplied in the generator. It reflects the interest to maintain the temperature inside the evaporator below the atmospheric temperature.

$$COP = \frac{\text{Desired}_{O/P}}{\text{Expenditure}}$$

4.4.14 Heat Capacity Ratio (R): It is the ratio of the minimum heat duty to the maximum heat duty. Also calculated by the ratio of temperature range of the hot fluid to that of the cold fluid. Higher the heat capacity ratio, greater will be size of the exchanger.

$$R = \frac{C_{\min}}{C_{\max}}$$

4.4.15 Logarithmic Mean Temperature Difference (LMTD): The logarithmic average of the terminal temperature approaches across a heat exchanger.

$$(\Delta T)_{LMTD} = \frac{\theta_i - \theta_o}{\ln\left(\frac{\theta_i}{\theta_o}\right)} = \frac{(T_{h1} - T_{c2}) - (T_{h2} - T_{c1})}{\ln\left\{\frac{(T_{h1} - T_{c2})}{(T_{h2} - T_{c1})}\right\}}$$

4.4.16 Effectiveness (ε): It is the ratio of the actual heat transfer to the maximum heat transfer. Higher the effectiveness shows the lesser will be the requirement of heat transfer surface.

$$\varepsilon = \frac{q_{\text{actual}}}{q_{\max}}$$

4.4.17 LMTD Correction Factor (F): When it is multiplied with LMTD, gives the corrected LMTD thus accounting for the temperature driving force for the cross flow pattern as applicable inside the exchanger.

$$F = \frac{\sqrt{(1+R)}}{(1-R)} \times \frac{\ln\left\{\frac{1-\varepsilon R}{1-\varepsilon}\right\}}{\ln\left[\frac{2-\varepsilon\left\{(1+R)-\sqrt{(R+1)}\right\}}{2-\varepsilon\left\{(1+R)+\sqrt{(R+1)}\right\}}\right]}$$

4.4.18 Overall Heat Transfer Coefficient (U): It is the ratio of heat flux per unit difference in approach across heat exchange in terms of temperature. The magnitude of it indicates the ability of heat transfer for a given surface. If the heat transfer coefficient (U) is higher, lesser will be the heat transfer surface requirement.

$$U = \frac{\dot{Q}}{A \times (\Delta T)_{LMTD}}$$

4.5 ASSUMPTIONS FOR EVALUATION OF HYBRID SYSTEM

The main components of this hybrid co-generation system are vapour absorption machine, double ignition downdraft gasifier, gas engine gen set and scheffler collectors. These are similar in configuration and working process with the different components, which are analysed on the basis of numerous theories in the existing various references such as McKendry (2002), Varshney (2010), Garg and Sharma (2013), Zhang et al. (2013), Boyle (1994), Kalam and Masjuki (2011), Jayasimha (2006), Luo et al. (2002), Chua et al. (2000), Lior (2002) etc. The following assumptions are made for the analysis of the ‘hybrid cold storage cum power generation system’;

- There is the steady state flow in the each components of the system.
- The strong solution leaving the absorber and weak solution leaving the generator are accounted in the saturated state.
- The pressure drop in the pipes and heat losses to the environment in the HRU, engine, condensers and the evaporators are neglected.
- The flow through the throttle valve is isenthalpic.
- The solution in the generator and absorber is in the equilibrium state at their respective temperature and pressure.
- The power consumed by the pumps is considered negligible.
- The kinetic, potential and chemical exergies of the substances are neglected.
- At the outlet of the condenser, there is saturated liquid state.
- At the outlet of the evaporator, there is saturated vapour state.

- Only physical exergies are considered for engine's exhaust gas waste heat and vapour flows.
- It is assumed that CO, CO₂ and H₂O produced during oxidation are added to the corresponding values of the same substances produced during pyrolysis.
- It is assumed that N₂ entering the oxidation zone is an inert gas.
- The ideal gas principles are applied to air and exhaust gases.
- The combustion reaction in producer gas engine is complete.
- Because the water in the exhaust is generally vapour state in internal combustion engines, the lower heating value (LHV) of the fuel is used.
- Specific heat of exhaust gases is temperature-dependent.
- The combustion products are assumed as an ideal gas such as air for the calculation results.

4.6 FORMULAE USED IN ENERGY AND EXERGY ANALYSIS: Apart from the above analysis, various following parameters have been calculated to predict the individual and combined performance of the system on the basis of the energy and the exergy methods:

4.6.1. Exhaust Gas Calculation:

Khaliq et al. (2012) provides the actual heat of exhaust gas: By Energy Balance

$$\dot{Q}_{actual\ exhaust} + \dot{Q}_{solar} = \dot{Q}_{gen.} + \dot{Q}_{sensible\ gain}$$

$$\dot{Q}_{actual\ exhaust} = \dot{Q}_{gen.} + \dot{Q}_{sensible\ gain} - \dot{Q}_{solar}$$

Where, Heat supplied by solar; $\dot{Q}_{solar} = \dot{m}_{water} \times C_{p,water} \times \Delta T_{solar}$

Heat gained by exhaust in HRU; $\dot{Q}_{HRU} = \dot{m}_{water} \times C_{p,water} \times \Delta T_{HRU}$

Heat delivered to generator; $\dot{Q}_{gen} = \dot{m}_{water} \times C_{p,water} \times \Delta T_{gen}$

Heat gained by working fluid (water of HRU);

$$\dot{Q}_{sensible\ gain} = \frac{400 \times C_{p,water}}{time} \times \left\{ \frac{(T_{solar\ initial} - T_{solar\ final}) + (T_{HRU\ initial} - T_{HRU\ final}) + (T_{gen.\ initial} - T_{gen.\ final})}{3} \right\}$$

4.6.2 Scheffler Dish Calculation:

According to Munir et al. (2010), the ‘solar inclination’ or seasonal angle deviation of sun:-

$$\delta = \frac{180}{\pi} \left[\begin{aligned} & (0.006918 - 0.399912) \cos \frac{(n-1).2\pi}{365} + 0.070257 \sin \frac{(n-1).2\pi}{365} - 0.006758 \cos \frac{2(n-1).2\pi}{365} \\ & + 0.000907 \sin \frac{(n-1).2\pi}{365} - 0.002679 \cos \frac{3(n-1).2\pi}{365} + 0.001488 \sin \frac{3(n-1).2\pi}{365} \end{aligned} \right]$$

Where, $n = n^{\text{th}}$ day of the year

While, the aperture area (A_s) is:

$$A_s = \text{Reflector, area} \times \cos \left\{ 43.23 - \frac{\delta}{2} \right\}$$

Patil et al. (2011) introduced the Energy efficiency of solar dishes as follows:

$$\begin{aligned} \eta_{\text{energy}} &= \frac{\text{Total power obtained by sun}}{\text{Power given by radiation}} \\ &= \frac{E_p}{\text{Beam radiation} \times \text{Aperture area}} = \frac{E_p}{\text{Average DNI} \times \text{Aperture area}} \\ \therefore \eta_{\text{energy}} &= \frac{\dot{m}_{\text{water}} \times C_{p,\text{water}} \Delta T_{\text{solar}}}{\text{DNI}_{\text{avg}} \times A_s} \end{aligned}$$

Pridasawas and Lundqvist (2004) formulated the Exergy efficiency of solar dishes:

$$\begin{aligned} \eta_{\text{exergy}} &= \frac{\text{Exergy gained by water}}{\text{Exergy input to scheffler collector}} \\ \therefore \eta_{\text{exergy}} &= \frac{\dot{E}_{x_{\text{out}}}}{\dot{E}_{x_{\text{in}}}} = \frac{\dot{E}_p - \dot{m}_{\text{water}} C_{p,\text{water}} T_{\text{ambient}} \ln \left(\frac{T_{\text{out/solar}}}{T_{\text{in/solar}}} \right)}{f \sigma T_{\text{sun}}^4 + (1-f) \sigma T_{\text{planet}}^4 - \sigma T_{\text{SC}}^4} \end{aligned}$$

Where, Exergy gained by water:

$$\dot{E}_{xO} = \dot{E}_p - \dot{m}_w C_{pw} T_{amb} \ln \left(\frac{T_f}{T_i} \right)$$

Exergy input to the collector: $\dot{E}_{xi} = f \sigma T_{\text{sun}}^4 + (1-f) \sigma T_{\text{planet}}^4 - \sigma T_{\text{SC}}^4$

Where, f = sunlight dilution factor = 2.16×10^{-5} on earth

σ = Stefan boltzmann constant = $5.670373 \times 10^{-8} \text{ W/m}^2 \text{ K}^4$

T_{sun} = Temperature of sun = 5800 K, T_{planet} = Temperature of planet/earth = 288 K

T_{sc} = Temperature of scheffler collector

∴ ED of SC = Exergyin –Exergy out

$$\therefore \text{Exergy efficiency; } \eta_{exergy} = \frac{\dot{E}x_o}{\dot{E}x_{in}}$$

Heat loss factor as per Bhirud and Tandale (2006):

$$\text{Heat loss factor; } FU_L = \frac{DNI}{(T_m - T_a)} \text{ (W/m}^2\text{K)}$$

$$\text{Where, mean temperature } T_m = \frac{T_{in/solar} + T_{out/solar}}{2}$$

4.6.3 Required Producer Gas And Biomass Calculation:

For the gasifier; Air inflow rate: $\dot{Q}_{air\ inflow} = \frac{\pi}{4} d_{pipe} V_{air}$ (m³/hr)

Producer gas flow rate in the gasifier;

$$\dot{Q}_{PG} = \dot{m}_{fuel} = 364.4 \times \sqrt{\Delta h} \text{ ((m}^3\text{/hr)}$$

Where,

$$\Delta h = \text{Manometer height (m)}$$

According to Sridhar et al. (2001), the air in flow in the producer gas run engine can be calculated from the following expression;

$$(\dot{m}_{air} + \dot{m}_{fuel}) \times C_{p,exhaust} \times \Delta T_{exhaust} = \dot{Q}_{exhaust}^{actual}$$

∴ The Air-fuel ratio is estimated by Martinez et al. (2012);

$$\therefore \text{A/F ratio} = \frac{\dot{m}_{air}}{\dot{m}_{fuel}}$$

Remaining heat = required heat for VAM (cooling capacity) - heat given to generator
Dasappa et al. (2011) reported the production of producer gas equivalent to biomass as follows;

$$BCR \times CV_{biomass} = \dot{m}_{PG} \times CV_{PG}$$

$$\text{Where, } CV_{PG} = \sum (\text{Volume\%} \times LHV_{components})$$

∴ The required biomass in kW to produce PG (in kW) for remaining heat will be;

$$= \frac{\dot{Q}_{remaining}}{PG_{equivalent}}$$

∴ Requirement of biomass per hour = $\frac{\text{required biomass in kW}}{\text{CV of biomass}} = \text{(kg/hr)}$

$$\dot{m}_{biomass}^{required} = \frac{\dot{m}_{biomass}^{required} (kW)}{CV_{biomass}} (kg / hr)$$

∴ Total BCR = BCR + Required biomass/hour

$$\therefore \text{Total SFC} = \frac{BCR_{total}}{Power_{electric}} (kg/kWhr)$$

4.6.4 Evaluation of HRU (In Case of Counter or Cross Flow Heat Exchanger):

Al-attab and Zainal (2010) states that;

$$\text{Heat duty for hot fluid; } \dot{Q}_h = \dot{m}_h C_{ph} (T_{h1} - T_{h2})$$

$$\text{And heat duty for cold fluid; } \dot{Q}_c = \dot{m}_c C_{pc} (T_{c2} - T_{c1})$$

$$\therefore \text{From energy balance; } \dot{Q}_h = \dot{Q}_c = \dot{m}_c C_{pc} (T_{c2} - T_{c1})$$

Decide C_{min} or C_{max} by the product $\dot{m}_h C_{ph}$ or $\dot{m}_c C_{pc}$

$$\therefore \text{Heat capacity ratio; } R = \frac{C_{min}}{C_{max}}$$

∴ Effectiveness; ε

If $\dot{m}_h C_{ph} < \dot{m}_c C_{pc}$

$$\varepsilon = \frac{q_{actual}}{q_{max}} = \frac{\dot{m}_h C_{ph} (T_{h1} - T_{h2})}{C_{min} (T_{h1} - T_{c1})} = \frac{(T_{h1} - T_{h2})}{(T_{h1} - T_{c1})}$$

And if $\dot{m}_h C_{ph} > \dot{m}_c C_{pc}$

$$\varepsilon = \frac{q_{actual}}{q_{max}} = \frac{\dot{m}_c C_{pc} (T_{c2} - T_{c1})}{C_{max} (T_{h1} - T_{c1})} = \frac{(T_{c2} - T_{c1})}{(T_{h1} - T_{c1})}$$

$$\therefore (\Delta T)_{LMTD} = \frac{\theta_i - \theta_o}{\ln(\theta_i / \theta_o)} = \frac{(T_{h1} - T_{c2}) - (T_{h2} - T_{c1})}{\ln\left\{\frac{(T_{h1} - T_{c2})}{(T_{h2} - T_{c1})}\right\}}$$

Specifications of HRU are as follows;

Length of drum = 1.6002 m, Exhaust pipe diameter = 0.1524 m,

Producer gas pipe diameter = 0.1016 m, Diameter of drum = 0.331042 m

Area of heat transfer; $A = 2\pi r \times \text{length of drum}$,

Where, r = Radius of exhaust pipe

$$\therefore A = \pi \times 0.1524 \times 1.6002 = 0.766 \text{ m}^2$$

$$\therefore \dot{Q} = UA(\Delta T)_{LMTD}$$

$$\therefore U = \frac{UA}{(\Delta T)_{LMTD}} \left(\frac{kW}{m^2 K} \right)$$

Exergy Analysis of HRU;

Patel and Ramana (2013) introduced following model for entropy generation,

$$\text{If } \dot{m}_h C_{ph} < \dot{m}_c C_{pc}$$

\therefore The entropy generation from the system;

$$S_{gen} = C_{min} \ln \left[1 - \varepsilon \left(1 - \frac{1}{T_R} \right) \right] + C_{max} \ln [1 + \varepsilon R (T_R - 1)]$$

$$\text{Where, } T_R = \frac{T_{h1}}{T_{c1}} = \text{Temperature ratio,}$$

Exergy Destruction in HRU; $HRU_{ED} = T_0 S_{gen}$

Exergy Efficiency/Effectiveness of HRU;

Ghazikhani et al. (2014) reported the exergy analysis like so;

$$\eta_{II} = \frac{\text{Exergy}_{out}}{\text{Exergy}_{in}} = \frac{\text{Exergy}_{water}}{\text{Exergy}_{exhaust}} = \frac{\dot{m}_w [(h_{out} - h_{in}) - T_0 (S_{out} - S_{in})]}{-\dot{m}_{exht} [(h_{out,exht} - h_{in,exht}) - T_0 (S_{out,exht} - S_{in,exht})]}$$

Where, Change in enthalpy/entropy of exhaust gas is;

$$\Delta h_{exht} = h_{out,exht} - h_{in,exht} = \frac{1}{28.9} \left[\begin{array}{l} 28.11(T_{h2} - T_{h1}) + 0.9835 \times 10^{-3} (T_{h2}^{-2} - T_{h1}^{-2}) + 0.16 \times 10^{-5} (T_{h2}^{-3} - T_{h1}^{-3}) \\ - 0.49 \times 10^{-9} (T_{h2}^{-4} - T_{h1}^{-4}) \end{array} \right]$$

And entropy;

$$\Delta S_{exht} = S_{out,exht} - S_{in,exht} = \frac{1}{28.9} \left[\begin{array}{l} 28.11 \ln \left(\frac{T_{h2}}{T_{h1}} \right) + 0.1967 \times 10^{-2} (T_{h2} - T_{h1}) + 0.2401 \times 10^{-5} (T_{h2}^2 - T_{h1}^2) \\ - 0.655 \times 10^{-9} (T_{h2}^3 - T_{h1}^3) \end{array} \right] - R \ln \left(\frac{P_{h2}}{P_{h1}} \right)$$

In Case of Shell and Tube Heat Exchanger: heat transfer as per Gomez et al. (2009):

$$\dot{Q} = FUA(\Delta T)_{LMTD}$$

Where, LMTD correction factor,

$$F = \frac{\sqrt{(1+R)}}{(1-R)} \times \frac{\ln \left\{ \frac{1-\varepsilon R}{1-\varepsilon} \right\}}{\ln \left[\frac{2-\varepsilon \left\{ (1+R) - \sqrt{(R+1)} \right\}}{2-\varepsilon \left\{ (1+R) + \sqrt{(R+1)} \right\}} \right]}$$

And heat transfer area of the pipe (A):

$$= \pi \times \text{Diameter of pipe} \times \text{Length of drum} \times \text{No. of pass} \times \text{No. of tubes per pass}$$

4.6.5 Evaluation of Chemical Exergy of Producer Gas:

The chemical exergy is calculated as per Mountouris et al. (2006):

$$\bar{\epsilon}_{ch,M} = \sum_i x_i \bar{\epsilon}_{ch,i} + \bar{R}T_0 \sum_i x_i \ln x_i$$

$$\begin{aligned} \bar{\epsilon}_{ch,M} = & \{x_{co} \epsilon_{ch,co} + x_{co_2} \epsilon_{ch,co_2} + x_{H_2} \epsilon_{ch,H_2} + x_{CH_4} \epsilon_{ch,CH_4} + x_{N_2} \epsilon_{ch,N_2}\} \\ & + \bar{R}T_0 \{x_{co} \ln_{,co} + x_{co_2} \ln_{co_2} + x_{H_2} \ln_{H_2} + x_{CH_4} \ln_{CH_4} + x_{N_2} \ln_{N_2}\} \end{aligned}$$

Chemical exergy of the species are taken by the reference Zhang et al. (2013).

$$\text{No of moles } (x) = \frac{\text{Volume of gas}}{\text{Molar volume of gas}}$$

The physical exergy is calculated as:

$$\bar{\epsilon}_{ph,M} = (\bar{h} - \bar{h}_0) - T_0 (\bar{S} - \bar{S}_0)$$

$$\therefore \text{Exergy of PG; } Ex_{PG} = \bar{\epsilon}_{ch,M} + \bar{\epsilon}_{ph,M}$$

4.6.6 Evaluation of Solid Fuel and Efficiency of Gasifier: Centeno et al. (2012)

gives;

$$\text{The energy efficiency of the gasifier; } \eta_{energy} = \frac{\dot{Q}_{PG} \times CV_{PG}}{BCR \times CV_{biomass}}$$

Exergy of solid fuel (wood) is taken by Zhang et al. (2013);

Higher heating value (HHV) of solid fuel (wood) :

$$HHV = 0.3491C + 1.1783H + 0.1005S - 0.1034O - 0.0151N - 0.0211Ash \text{ (MJ/kg)}$$

Lower heating value (LHV) of wood:

$$LHV = HHV - 9m_H h_{fg}$$

Where, m_H = mass fraction of hydrogen in solid fuel,

h_{fg} = Enthalpy of vaporization at NTP

\therefore Exergy of solid fuel:

$$\epsilon_{solid} = \phi_{dry} [LHV + m_w h_{fg}]$$

$$\text{Where, } \phi_{dry} = \frac{1.044 + 0.016\left(\frac{H}{C}\right) - 0.3493\left(\frac{O}{C}\right)\left\{1 - 0.0531\left(\frac{H}{C}\right)\right\} + 0.0493\left(\frac{N}{C}\right)}{\left\{1 - 0.4124\left(\frac{O}{C}\right)\right\}}$$

And m_w = mass fraction of moisture

Kanogolu and Dincer (2009) concept provides the following efficiency equation;

$$\text{Exergy efficiency of gasifier: } \eta_{exergy} = \frac{Ex_{PG}}{BCR \times \varepsilon_{solid}}$$

ED of gasifier = Exergy of wood - Exergy of PG

$$ED_{gasifier} = \varepsilon_{solid} - Ex_{PG}$$

4.6.7 Evaluation of Exergy Destruction of Gas Cooling and Cleaning Unit:

Guo et al. (2010) describes the irreversibilities as follows;

$$\text{For HE-1 regenerator; } \dot{E}_{D,regen} = T_o \left[\dot{m}_h C_{ph} \ln \left(\frac{T_{h,out}}{T_{h,in}} \right) + \dot{m}_c C_{pc} \ln \left(\frac{T_{c,out}}{T_{c,in}} \right) \right]$$

Where, mass flow rate of air

$$\dot{m}_{air} = \dot{m}_c = \frac{\dot{m}_{PG} C_{PG} (T_{PGin} - T_{PGo})}{C_{air} (T_{a,o} - T_{a,in})}$$

$$\text{For HE-2 Air cooler; } \dot{E}_{D,AC} = T_o \left[\dot{m}_h C_{ph} \ln \left(\frac{T_{h,out}}{T_{h,in}} \right) + \dot{m}_c C_{pc} \ln \left(\frac{T_{c,out}}{T_{c,in}} \right) \right]$$

Where, the mass flow rate of air is also calculated by the energy balance.

$$\text{For HE-2 Water cooler; } \dot{E}_{D,WC} = T_o \left[\dot{m}_h C_{ph} \ln \left(\frac{T_{h,out}}{T_{h,in}} \right) + \dot{m}_c C_{pc} \ln \left(\frac{T_{c,out}}{T_{c,in}} \right) \right]$$

The exergy destruction according to Sahin et al. (2010);

For Fabric filter: For the single stream

$$\dot{E}_{D,FL} = \dot{m}_h C_{ph} (T_{h,n} - T_{h,out}) - T_o \dot{m}_h C_{ph} \ln \left(\frac{T_{h,in}}{T_{h,out}} \right)$$

For Paper filter: For the single stream

$$\dot{E}_{D,PL} = \dot{m}_h C_{ph} (T_{h,n} - T_{h,out}) - T_o \dot{m}_h C_{ph} \ln \left(\frac{T_{h,in}}{T_{h,out}} \right)$$

4.6.8 Evaluation of Exergy Destruction of Electric Generator and Heat Engine:

The concept of Agarwal and Karimi (2012) provides the idea of the generation of expressions of the exergy destructions in the following components of the plant;

$$\dot{E}_{D,electric} = \dot{W}_E - \dot{P}_E$$

Or

$$\dot{E}_{D,engine} = \dot{E}_{PG} - \left(\dot{m}_{exht} h_{exht} + \dot{m}_{exht} h_{air} - T_0 \dot{m}_{exht} S_{exht} + T_0 \dot{m}_{exht} S_{air} + \dot{W}_E \right)$$

4.6.9 Evaluation of the VAM: According to Kong et al. (2010);

Desired effect (Energy output); $Q_E = \dot{m}_r (h_{out} - h_{in})$

Expenditure; $Q_{in} = \dot{m}_w (h_4 - h_5)$

∴ Energetic COP; $COP_I = \frac{Q_E}{Q_{in}}$

Exergetic COP;

Exergy out (Desired effect); $\Delta \dot{E}_{out} = \dot{m}_r [(h_{in} - h_{out}) - T_o (s_{in} - s_{out})]$

Exergy in (Expenditure); $\Delta \dot{E}_{in} = \dot{m}_r [(h_4 - h_5) - T_o (s_4 - s_5)]$

∴ Exergetic COP; $COP_{II} = \frac{\dot{E}_{out}}{\dot{E}_{in}}$

Kaynakli and Yamankaradeniz (2007) state exergy destruction in different components;

For generator; $\dot{E}_{D,gen} = T_o [\dot{m}_w (s_4 - s_5) + \dot{m}_{ss} (s_{12} - s_7) + \dot{m}_r (s_7 - s_6)]$

For pump; $\dot{E}_{D,p} = \dot{m}_{ss} [T_o (s_{out} - s_{in})]$

For solution heat exchanger; $\dot{E}_{D,SHE} = T_o [\dot{m}_{ws} (s_7 - s_8) + \dot{m}_{ss} (s_{12} - s_{11})]$

For throttle valve-1; $\dot{E}_{D,TV1} = T_o [\dot{m}_r (s_{in} - s_{out})]$

For throttle valve-2; $\dot{E}_{D,TV2} = T_o [\dot{m}_r (s_{in} - s_{out})]$

For absorber; $\dot{E}_{D,A} = T_o [\dot{m}_a (s_j - s_i) + \dot{m}_{ss} (s_{10} - s_9) + \dot{m}_r (s_9 - s_{15})]$

For condenser; $\dot{E}_{D,C} = T_o [\dot{m}_r (s_6 - s_{13}) + \dot{m}_c (s_k - s_l)]$

For evaporator; $\dot{E}_{D,evp} = T_o [\dot{m}_r (s_{14} - s_{15}) + \dot{m}_e (s_p - s_q)]$

4.6.10 Performance of VAM with Atmospheric Temperature:

The doctrine of Mazouz et al. (2014) has been used to derive first and second law COP of VAM with respect to ambient temperature;

$$COP_I = \frac{T_E}{T_{atm} - T_E} \times \frac{T_G - T_{atm}}{T_G}$$

$$COP_{II} = COP_I \times \frac{\left(\frac{T_0}{T_E} - 1\right)}{\left(1 - \frac{T_0}{T_G}\right)}$$

4.6.11 Combined Analysis of Hybrid System: Pihl et al. (2010) provides the overall efficiencies of the hybrid system;

Overall energy and exergy efficiency of the system;

Overall energy efficiency; $\eta_{o,en} = \frac{P_E + \dot{Q}_E}{E_{in}}$

Overall exergy efficiency $\eta_{o,ex} = \eta_{o,en} \times \frac{1}{\left(1 - \frac{T_o}{T_{grate}}\right)}$

Where, $\dot{Q}_E = \dot{m}(h_{ga} - h_{fa})$ and $E_{in} = \dot{Q}_{Supplied} + \dot{Q}_{Solar}$

T_{grate} = Temperature above the grate of gasifier

4.6.12 Heat Balance Sheet of Co-generation system: The philosophy of Minciuc et al. (2003) has been used in preparation of the heat balance sheet;

Heat supplied is calculated as follows:-

$$Q_s = \text{Biomass consumption rate} \times \text{CV of fuel used}$$

$$\text{Solar heat given by radiation} = \text{Average DNI} \times A_s$$

$$\therefore \text{Total heat supplied } (\dot{Q}_{total}) = \text{Heat supplied by biomass} + \text{Heat supplied by solar}$$

(i) **Heat used in gasification (Q_1):**-It can be calculated from

$$\dot{Q}_1 = \dot{m}_{biomass} CV_{biomass} - \dot{m}_{pg} CV_{pg}$$

$$\text{Percentage of heat utilized in gasifier} = \left(\frac{\dot{Q}_1}{\dot{Q}_{total}}\right) \times 100$$

$$\text{Average heat (\%)} \text{ used in gasification, } \dot{Q}_{avg,1} = \frac{\dot{Q}_{15.24} + \dot{Q}_{23.62} + \dot{Q}_{27.432} + \dot{Q}_{32.004} + \dot{Q}_{38.862}}{5}$$

(ii) **Heat used in HE-1(regenerator):**-It can calculate from; $\dot{Q}_2 = \dot{m}_{pg} C_{pg} (T_{g,in} - T_{g,out})$

$$\text{Percentage of heat utilized in HE-1(regenerator)} = \left(\frac{\dot{Q}_2}{\dot{Q}_{total}}\right) \times 100$$

$$\text{Average heat (\%), } \dot{Q}_{avg,2} = \frac{\dot{Q}_{15.24} + \dot{Q}_{23.62} + \dot{Q}_{27.432} + \dot{Q}_{32.004} + \dot{Q}_{38.862}}{5}$$

(iii) Heat used in HE-2 (Air cooler); $\dot{Q}_3 = \dot{m}_{pg} C_{pg} (T_{g,in} - T_{g,out})$

$$\text{Percentage of heat utilized in HE-2(Air cooler)} = \left(\frac{\dot{Q}_3}{\dot{Q}_{total}} \right) \times 100$$

$$\text{Average heat, } \dot{Q}_{avg,3} = \frac{\dot{Q}_{15.24} + \dot{Q}_{23.62} + \dot{Q}_{27.432} + \dot{Q}_{32.004} + \dot{Q}_{38.862}}{5}$$

(iv) Heat used in HE-2 (Water cooler); $\dot{Q}_4 = \dot{m}_{pg} C_{pg} (T_{g,in} - T_{g,out})$

$$\text{Percentage of heat utilized in HE-2(Water cooler)} = \left(\frac{\dot{Q}_4}{\dot{Q}_{total}} \right) \times 100$$

$$\text{Average heat, } \dot{Q}_{avg,4} = \frac{\dot{Q}_{15.24} + \dot{Q}_{23.62} + \dot{Q}_{27.432} + \dot{Q}_{32.004} + \dot{Q}_{38.862}}{5}$$

(v) Heat used in fabric filter; $\dot{Q}_5 = \dot{m}_{pg} C_{pg} (T_{g,in} - T_{g,out})$

$$\text{Percentage of heat utilized in fabric filter} = \left(\frac{\dot{Q}_5}{\dot{Q}_{total}} \right) \times 100$$

$$\text{Average heat, } \dot{Q}_{avg,5} = \frac{\dot{Q}_{15.24} + \dot{Q}_{23.62} + \dot{Q}_{27.432} + \dot{Q}_{32.004} + \dot{Q}_{38.862}}{5}$$

(vi) Heat used in paper filter; $\dot{Q}_6 = \dot{m}_{pg} C_{pg} (T_{g,in} - T_{g,out})$

$$\text{Percentage of heat utilized in paper filter} = \left(\frac{\dot{Q}_6}{\dot{Q}_{total}} \right) \times 100$$

$$\text{Average heat, } \dot{Q}_{avg,6} = \frac{\dot{Q}_{15.24} + \dot{Q}_{23.62} + \dot{Q}_{27.432} + \dot{Q}_{32.004} + \dot{Q}_{38.862}}{5}$$

(vii) Heat equivalent to brake power; $\dot{Q}_7 = \frac{P_{electric}}{\eta_{generator}}$

Where, the electric generator efficiency is; $\eta_{gen} = 0.8$

$$\text{Percentage of heat equivalent to brake power} = \left(\frac{\dot{Q}_7}{\dot{Q}_{total}} \right) \times 100$$

$$\text{Average heat, } \dot{Q}_{avg,7} = \frac{\dot{Q}_{15.24} + \dot{Q}_{23.62} + \dot{Q}_{27.432} + \dot{Q}_{32.004} + \dot{Q}_{38.862}}{5}$$

(viii) Heat equivalent to electric power; $\dot{Q}_8 = VI\sqrt{3}$

$$\text{Percentage of heat equivalent to electric power} = \left(\frac{\dot{Q}_8}{\dot{Q}_{total}} \right) \times 100$$

$$\text{Average heat, } \dot{Q}_{avg,8} = \frac{\dot{Q}_{15.24} + \dot{Q}_{23.62} + \dot{Q}_{27.432} + \dot{Q}_{32.004} + \dot{Q}_{38.862}}{5}$$

(ix) Heat lost due to exhaust; $\dot{Q}_9 = (\dot{m}_{air} + \dot{m}_{fuel}) \times C_{p,exhaust} \times \Delta T_{exhaust}$

$$\text{Percentage of heat lost due to exhaust} = \left(\frac{\dot{Q}_9}{\dot{Q}_{total}} \right) \times 100$$

$$\text{Average heat, } \dot{Q}_{avg,9} = \frac{\dot{Q}_{15.24} + \dot{Q}_{23.62} + \dot{Q}_{27.432} + \dot{Q}_{32.004} + \dot{Q}_{38.862}}{5}$$

(x) Heat used in solar collector; $\dot{Q}_{10} = \dot{m}_{water} \times C_{p,water} \times \Delta T$

$$\text{Percentage of heat used in solar collector} = \left(\frac{\dot{Q}_{10}}{\dot{Q}_{total}} \right) \times 100$$

$$\text{Average heat, } \dot{Q}_{avg,10} = \frac{\dot{Q}_{15.24} + \dot{Q}_{23.62} + \dot{Q}_{27.432} + \dot{Q}_{32.004} + \dot{Q}_{38.862}}{5}$$

(xi) Heat used in HRU; $\dot{Q}_{11} = \dot{m}_{water} \times C_{p,water} \times \Delta T$

$$\text{Percentage of heat used in HRU} = \left(\frac{\dot{Q}_{11}}{\dot{Q}_{total}} \right) \times 100$$

$$\text{Average heat, } \dot{Q}_{avg,11} = \frac{\dot{Q}_{15.24} + \dot{Q}_{23.62} + \dot{Q}_{27.432} + \dot{Q}_{32.004} + \dot{Q}_{38.862}}{5}$$

(xii) Heat used in generator; $\dot{Q}_{12} = \dot{m}_{water} \times C_{p,water} \times \Delta T$

$$\text{Percentage of heat used in generator} = \left(\frac{\dot{Q}_{12}}{\dot{Q}_{total}} \right) \times 100$$

$$\text{Average heat, } \dot{Q}_{avg,12} = \frac{\dot{Q}_{15.24} + \dot{Q}_{23.62} + \dot{Q}_{27.432} + \dot{Q}_{32.004} + \dot{Q}_{38.862}}{5}$$

(xiii) Heat used in condenser; $\dot{Q}_{13} = \dot{m}_{ammonia} (h_{gc} - h_{fc})$

$$\text{Percentage of heat used in condenser} = \left(\frac{\dot{Q}_{13}}{\dot{Q}_{total}} \right) \times 100$$

$$\text{Average heat, } \dot{Q}_{avg,13} = \frac{\dot{Q}_{15.24} + \dot{Q}_{23.62} + \dot{Q}_{27.432} + \dot{Q}_{32.004} + \dot{Q}_{38.862}}{5}$$

(xiv) Heat used in evaporator; $\dot{Q}_{14} = \dot{m}_{ammonia} (h_{ga} - h_{fa})$

$$\text{Percentage of heat used in evaporator} = \left(\frac{\dot{Q}_{14}}{\dot{Q}_{total}} \right) \times 100$$

$$\text{Average heat, } \dot{Q}_{avg,14} = \frac{\dot{Q}_{15.24} + \dot{Q}_{23.62} + \dot{Q}_{27.432} + \dot{Q}_{32.004} + \dot{Q}_{38.862}}{5}$$

(xv) Heat used in TV₁; $\dot{Q}_{15} = \dot{m}_{ws} C_w (T_8 - T_9)$

$$\text{Percentage of heat used in TV}_1 = \left(\frac{\dot{Q}_{15}}{\dot{Q}_{total}} \right) \times 100$$

$$\text{Average heat, } \dot{Q}_{avg,15} = \frac{\dot{Q}_{15.24} + \dot{Q}_{23.62} + \dot{Q}_{27.432} + \dot{Q}_{32.004} + \dot{Q}_{38.862}}{5}$$

(xvi) Heat used in TV₂; $\dot{Q}_{16} = \dot{m}_{ammonia} (h_{fc} - h_{fa})$

$$\text{Percentage of heat used in TV}_2 = \left(\frac{\dot{Q}_{16}}{\dot{Q}_{total}} \right) \times 100$$

$$\text{Average heat, } \dot{Q}_{avg,16} = \frac{\dot{Q}_{15.24} + \dot{Q}_{23.62} + \dot{Q}_{27.432} + \dot{Q}_{32.004} + \dot{Q}_{38.862}}{5}$$

(xvii) Heat used in pump; $\dot{Q}_{17} = \dot{m}_{ss} C_{ammonia} (T_{11} - T_{10})$

$$\text{Percentage of heat used in pump} = \left(\frac{\dot{Q}_{17}}{\dot{Q}_{total}} \right) \times 100$$

$$\text{Average heat, } \dot{Q}_{avg,17} = \frac{\dot{Q}_{15.24} + \dot{Q}_{23.62} + \dot{Q}_{27.432} + \dot{Q}_{32.004} + \dot{Q}_{38.862}}{5}$$

(xviii) Heat used in SHE; $\dot{Q}_{18} = \dot{m}_{ss} C_{ammonia} (T_{12} - T_{11})$

$$\text{Percentage of heat used in SHE} = \left(\frac{\dot{Q}_{18}}{\dot{Q}_{total}} \right) \times 100$$

$$\text{Average heat, } \dot{Q}_{avg,18} = \frac{\dot{Q}_{15.24} + \dot{Q}_{23.62} + \dot{Q}_{27.432} + \dot{Q}_{32.004} + \dot{Q}_{38.862}}{5}$$

(xix) Heat used in absorber; $\dot{Q}_{19} = \dot{m}_a C_w (T_{out,cw} - T_{in,cw})$

$$\text{Percentage of heat used in absorber} = \left(\frac{\dot{Q}_{19}}{\dot{Q}_{total}} \right) \times 100$$

$$\text{Average heat, } \dot{Q}_{avg,19} = \frac{\dot{Q}_{15.24} + \dot{Q}_{23.62} + \dot{Q}_{27.432} + \dot{Q}_{32.004} + \dot{Q}_{38.862}}{5}$$

(xx) Unaccounted heat loss; $\dot{Q}_{20} = \dot{Q}_{total} - (\dot{Q}_1 + \dot{Q}_2 + \dot{Q}_3 + \dot{Q}_4 + \dots + \dot{Q}_{19})$

$$\text{Percentage of unaccounted heat loss} = \left(\frac{\dot{Q}_{20}}{\dot{Q}_{total}} \right) \times 100$$

$$\text{Average heat, } \dot{Q}_{avg,20} = \frac{\dot{Q}_{15.24} + \dot{Q}_{23.62} + \dot{Q}_{27.432} + \dot{Q}_{32.004} + \dot{Q}_{38.862}}{5}$$

4.6.13 Exergy Balance Sheet: Dai et al. (2009) provides the exergy balance as follows;

Total exergy supplied is calculated as follows:-

Total exergy supplied ($\dot{E}x_{total}$) = Exergy input in gasifier + Exergy input by solar

$$\dot{E}x_{total} = \bar{E}x_{input,gasifier} + \dot{E}x_{input,solar}$$

∴ Exergy destruction of all components has been calculated in above exergy calculations.

∴ The percentage of Exergy Destruction (ED) of all components:

(i) **Percentage of Exergy output of electric generator,**

$$\dot{E}x_{out,gen} = \left(\frac{\dot{E}x_{out,gen}}{\dot{E}x_{ergy\ total}} \right) \times 100$$

$$\text{Average exergy, } \dot{E}x_{avg,gen} = \frac{\dot{E}x_{15.24} + \dot{E}x_{23.62} + \dot{E}x_{27.432} + \dot{E}x_{32.004} + \dot{E}x_{38.862}}{5}$$

(ii) **Percentage of Exergy output of VAM,** $\dot{E}x_{out,VAM} = \left(\frac{\dot{E}x_{out,VAM}}{\dot{E}x_{ergy\ total}} \right) \times 100$

$$\text{Average exergy, } \dot{E}x_{avg,VAM} = \frac{\dot{E}x_{15.24} + \dot{E}x_{23.62} + \dot{E}x_{27.432} + \dot{E}x_{32.004} + \dot{E}x_{38.862}}{5}$$

(iii) **Percentage of exergy destruction of gasifier,** $\dot{E}_{D1} = \left(\frac{\dot{E}_{D\ gasifier}}{\dot{E}x_{ergy\ total}} \right) \times 100$

$$\text{Where, } \dot{E}_{D\ gasifier} = \varepsilon_{solid} - \dot{E}x_{PG}$$

$$\text{Average ED, } \dot{E}_{D\ avg,1} = \frac{\dot{E}_{D15.24} + \dot{E}_{D23.62} + \dot{E}_{D27.432} + \dot{E}_{D32.004} + \dot{E}_{D38.862}}{5}$$

(iv) **Percentage of exergy destruction of HE-1(regenerator),**

$$\dot{E}_{D2} = \left(\frac{\dot{E}_{D\ HE-1}}{\dot{E}x_{ergy\ total}} \right) \times 100$$

$$\text{Average ED, } \dot{E}_{D\ avg,2} = \frac{\dot{E}_{D15.24} + \dot{E}_{D23.62} + \dot{E}_{D27.432} + \dot{E}_{D32.004} + \dot{E}_{D38.862}}{5}$$

(v) **Percentage of exergy destruction of HE-2 (Air cooler),**

$$\dot{E}_{D3} = \left(\frac{\dot{E}_{D\ HE-2AC}}{\dot{E}x_{ergy\ total}} \right) \times 100$$

$$\text{Average ED, } \dot{E}_{D\ avg,3} = \frac{\dot{E}_{D15.24} + \dot{E}_{D23.62} + \dot{E}_{D27.432} + \dot{E}_{D32.004} + \dot{E}_{D38.862}}{5}$$

(vi) **Percentage of exergy destruction of HE-2 (Water cooler),**

$$\dot{E}_{D4} = \left(\frac{\dot{E}_{D\ HE-2WC}}{\dot{E}x_{ergy\ total}} \right) \times 100$$

$$\text{Average ED, } \dot{E}_{D\ avg,4} = \frac{\dot{E}_{D15.24} + \dot{E}_{D23.62} + \dot{E}_{D27.432} + \dot{E}_{D32.004} + \dot{E}_{D38.862}}{5}$$

Where, in case of regenerator, air cooler and water cooler, the ED is given by;

$$\dot{E}_{D,regen/AC/WC} = T_o \left[\dot{m}_h C_{ph} \ln \left(\frac{T_{h,out}}{T_{h,in}} \right) + \dot{m}_c C_{pc} \ln \left(\frac{T_{c,out}}{T_{c,in}} \right) \right]$$

(vii) **Percentage of exergy destruction of fabric filter,** $\dot{E}_{D5} = \left(\frac{\dot{E}_{D,FL}}{\dot{E}_{xergy_{total}}} \right) \times 100$

Average ED, $\dot{E}_{D,avg,5} = \frac{\dot{E}_{D15.24} + \dot{E}_{D23.62} + \dot{E}_{D27.432} + \dot{E}_{D32.004} + \dot{E}_{D38.862}}{5}$

(viii) **Percentage of exergy destruction of paper filter,** $\dot{E}_{D6} = \left(\frac{\dot{E}_{D,PL}}{\dot{E}_{xergy_{total}}} \right) \times 100$

Average ED, $\dot{E}_{D,avg,6} = \frac{\dot{E}_{D15.24} + \dot{E}_{D23.62} + \dot{E}_{D27.432} + \dot{E}_{D32.004} + \dot{E}_{D38.862}}{5}$

In case of above filters; $\dot{E}_{D,FL/PL} = \dot{m}_h C_{ph} (T_{h,n} - T_{h,out}) - T_o \dot{m}_h C_{ph} \ln \left(\frac{T_{h,in}}{T_{h,out}} \right)$

(ix) **Percentage of exergy destruction of an engine,** $\dot{E}_{D7} = \left(\frac{\dot{E}_{D,engine}}{\dot{E}_{xergy_{total}}} \right) \times 100$

Average ED, $\dot{E}_{D,avg,7} = \frac{\dot{E}_{D15.24} + \dot{E}_{D23.62} + \dot{E}_{D27.432} + \dot{E}_{D32.004} + \dot{E}_{D38.862}}{5}$

Where, $\dot{E}_{D,engine} = \dot{E}_{PG} - (\dot{m}_{exht} h_{exht} + \dot{m}_{exht} h_{air} - T_o \dot{m}_{exht} S_{exht} + T_o \dot{m}_{exht} S_{air} + \dot{W}_E)$

(x) **Percentage of exergy destruction of electric generator,**

$$\dot{E}_{D8} = \left(\frac{\dot{E}_{D,gen}}{\dot{E}_{xergy_{total}}} \right) \times 100$$

Average ED, $\dot{E}_{D,avg,8} = \frac{\dot{E}_{D15.24} + \dot{E}_{D23.62} + \dot{E}_{D27.432} + \dot{E}_{D32.004} + \dot{E}_{D38.862}}{5}$

Where, $\dot{E}_{D,electric} = \dot{W}_E - \dot{P}_E$

(xi) **Percentage of exergy lost due to exhaust,** $\dot{E}_{D9} = \left(\frac{\dot{E}_{D,exht}}{\dot{E}_{xergy_{total}}} \right) \times 100$

Average ED, $\dot{E}_{D,avg,9} = \frac{\dot{E}_{D15.24} + \dot{E}_{D23.62} + \dot{E}_{D27.432} + \dot{E}_{D32.004} + \dot{E}_{D38.862}}{5}$

Where, $\dot{E}_{D,exht} = \dot{m}_{exht} [(h_{out,exht} - h_{in,exht}) - T_o (S_{out,exht} - S_{in,exht})]$

(xii) **Percentage of exergy destruction of solar collector,**

$$\dot{E}_{D10} = \left(\frac{\dot{E}_{D,SC}}{\dot{E}_{xergy_{total}}} \right) \times 100$$

Average ED, $\dot{E}_{D,avg,10} = \frac{\dot{E}_{D15.24} + \dot{E}_{D23.62} + \dot{E}_{D27.432} + \dot{E}_{D32.004} + \dot{E}_{D38.862}}{5}$

$$\text{Where, } \dot{E}_{D,SC} = \dot{E}x_{in} - \dot{E}x_{out}$$

$$\text{(xiii) Percentage of exergy destruction of HRU, } \dot{E}_{D11} = \left(\frac{\dot{E}_{D,HRU}}{\dot{E}xergy_{total}} \right) \times 100$$

$$\text{Average ED, } \dot{E}_{D,avg,11} = \frac{\dot{E}_{D15,24} + \dot{E}_{D23,62} + \dot{E}_{D27,432} + \dot{E}_{D32,004} + \dot{E}_{D38,862}}{5}$$

$$\text{Where, } \dot{E}_{D,HRU} = T_o S_{gen}$$

$$\text{(xiv) Percentage of exergy destruction of generator, } \dot{E}_{D12} = \left(\frac{\dot{E}_{D,gen}}{\dot{E}xergy_{total}} \right) \times 100$$

$$\text{Average ED, } \dot{E}_{D,avg,12} = \frac{\dot{E}_{D15,24} + \dot{E}_{D23,62} + \dot{E}_{D27,432} + \dot{E}_{D32,004} + \dot{E}_{D38,862}}{5}$$

$$\text{Where, } \dot{E}_{D,gen} = T_o [\dot{m}_w(s_4 - s_5) + \dot{m}_{ss}(s_{12} - s_7) + \dot{m}_r(s_7 - s_6)]$$

$$\text{(xv) Percentage of exergy destruction of condenser, } \dot{E}_{D13} = \left(\frac{\dot{E}_{D,condenser}}{\dot{E}xergy_{total}} \right) \times 100$$

$$\text{Average ED, } \dot{E}_{D,avg,13} = \frac{\dot{E}_{D15,24} + \dot{E}_{D23,62} + \dot{E}_{D27,432} + \dot{E}_{D32,004} + \dot{E}_{D38,862}}{5}$$

$$\text{Where, } \dot{E}_{D,C} = T_o [\dot{m}_r(s_6 - s_{13}) + \dot{m}_c(s_k - s_l)]$$

$$\text{(xvi) Percentage of exergy destruction of evaporator, } \dot{E}_{D14} = \left(\frac{\dot{E}_{D,evaporator}}{\dot{E}xergy_{total}} \right) \times 100$$

$$\text{Average ED, } \dot{E}_{D,avg,14} = \frac{\dot{E}_{D15,24} + \dot{E}_{D23,62} + \dot{E}_{D27,432} + \dot{E}_{D32,004} + \dot{E}_{D38,862}}{5}$$

$$\text{Where, } \dot{E}_{D,evp} = T_o [\dot{m}_r(s_{14} - s_{15}) + \dot{m}_e(s_p - s_q)]$$

$$\text{(xvii) Percentage of exergy destruction of TV}_1, \dot{E}_{D15} = \left(\frac{\dot{E}_{D,TV1}}{\dot{E}xergy_{total}} \right) \times 100$$

$$\text{Average ED, } \dot{E}_{D,avg,15} = \frac{\dot{E}_{D15,24} + \dot{E}_{D23,62} + \dot{E}_{D27,432} + \dot{E}_{D32,004} + \dot{E}_{D38,862}}{5}$$

$$\text{(xviii) Percentage of exergy destruction of TV}_2, \dot{E}_{D16} = \left(\frac{\dot{E}_{D,TV2}}{\dot{E}xergy_{total}} \right) \times 100$$

$$\text{Average ED, } \dot{E}_{D,avg,16} = \frac{\dot{E}_{D15,24} + \dot{E}_{D23,62} + \dot{E}_{D27,432} + \dot{E}_{D32,004} + \dot{E}_{D38,862}}{5}$$

$$\text{Where, } \dot{E}_{D,TV1,2} = T_o [\dot{m}_r(s_{in} - s_{out})]$$

$$\text{(xix) Percentage of exergy destruction of pump, } \dot{E}_{D17} = \left(\frac{\dot{E}_{D,pump}}{\dot{E}xergy_{total}} \right) \times 100$$

$$\text{Average ED, } \dot{E}_{D_{avg,17}} = \frac{\dot{E}_{D15.24} + \dot{E}_{D23.62} + \dot{E}_{D27.432} + \dot{E}_{D32.004} + \dot{E}_{D38.862}}{5}$$

$$\text{Where, } \dot{E}_{D,Pump} = \dot{m}_{ss} [T_o (s_{out} - s_{in})]$$

$$\text{(xx) Percentage of exergy destruction of SHE, } \dot{E}_{D18} = \left(\frac{\dot{E}_{D,SHE}}{\dot{E}_{xergy_{total}}} \right) \times 100$$

$$\text{Average ED, } \dot{E}_{D_{avg,18}} = \frac{\dot{E}_{D15.24} + \dot{E}_{D23.62} + \dot{E}_{D27.432} + \dot{E}_{D32.004} + \dot{E}_{D38.862}}{5}$$

$$\text{Where } \dot{E}_{D,SHE} = T_o [\dot{m}_{ws} (s_7 - s_8) + \dot{m}_{ss} (s_{12} - s_{11})]$$

$$\text{(xxi) Percentage of exergy destruction of absorber, } \dot{E}_{D19} = \left(\frac{\dot{E}_{D,absorber}}{\dot{E}_{xergy_{total}}} \right) \times 100$$

$$\text{Average ED, } \dot{E}_{D_{avg,19}} = \frac{\dot{E}_{D15.24} + \dot{E}_{D23.62} + \dot{E}_{D27.432} + \dot{E}_{D32.004} + \dot{E}_{D38.862}}{5}$$

$$\text{Where, } \dot{E}_{D,absorber} = T_o [\dot{m}_a (s_j - s_i) + \dot{m}_{ss} (s_{10} - s_9) + \dot{m}_r (s_9 - s_{15})]$$

(xxii) Percentage of unaccounted exergy loss;

Unaccounted exergy loss;

$$\dot{E}_{D20} = \dot{E}x_{total} - (\dot{E}x_{out,gen} + \dot{E}x_{out,VAM} + \dot{E}_{D1} + \dot{E}_{D2} + \dot{E}_{D3} + \dot{E}_{D4} + \dots + \dot{E}_{D19})$$

$$\therefore \text{Percentage of unaccounted exergy loss, } \dot{E}_{D20} = \left(\frac{\dot{E}_{D,unaccountal}}{\dot{E}_{xergy_{total}}} \right) \times 100$$

$$\text{Average ED, } \dot{E}_{D_{avg,20}} = \frac{\dot{E}_{D15.24} + \dot{E}_{D23.62} + \dot{E}_{D27.432} + \dot{E}_{D32.004} + \dot{E}_{D38.862}}{5}$$

The various parameters have been calculated to predict the individual and combined performance of the system, and the performance has been evaluated on the basis of the energy and the exergy methods. The sample calculations have been represented in the Appendix-A with all formulae used. The Exergy analysis has been chosen for the performance evaluation of the ‘new hybrid cold storage cum power generation system’ because it differentiates the work and heat in terms of exergy destruction, or the change in energy quality. Thus, the exergy analysis has been proven a powerful tool in the thermodynamic analysis to determine the maximum performance of the system and to identify each equipment of the complex system separately for the main exergy loss, which shows the directions that must be taken for the potential improvements in the overall efficiency of the new hybrid co-generation system.

CHAPTER-V

RESULTS AND DISCUSSION

The performance of the 'new hybrid cold storage cum power generation system' and its components has been evaluated at the different electric loads. The generated electrical load can be utilized to meet the demands of end uses. The rejected heat of power plant together with the thermal power input from the scheffler collector is used in vapour absorption machine (VAM) for getting the refrigeration effect. Thus, this robust system plays an important role in the hybrid energy utilization and provides us full benefits efficiently. Traditionally, combined heating and power (CHP) systems, which have power generation below 500 kW, are classified as micro-scale systems. With the development of compact and micro-scale absorption chillers, the combined cooling and power (CCP) system has become feasible for power requirements less than 15 kW. This hybrid system has many technical and commercial challenges, but the integration of the VAM with power generator can support us in:

- Meeting the increased demand of energy at some extent.
- Learning the way of the integration of the different kind of energies
- Making the commercialization of exhaust gas waste heat with emissions reduction and cost elimination for meeting the energy demand in remote areas.

In this hybrid system, the mixed wood pieces (biomass) was used for the running the gasifier, which had the moisture content of 25% and approximate size of $65 \times 40 \times 35$ mm³. The producer gas composition by volume had been taken as; CO = $20 \pm 2\%$, CO₂ = $12 \pm 1\%$, CH₄ = $3 \pm 1\%$, H₂ = $20 \pm 2\%$ & N₂ = 45%. The CV of the PG and biomass are considered 5.415 MJ/m³ and 18.6 MJ/m³ respectively, while the thermodynamic properties of the NH₃-H₂O mixture for the VAM had been taken from NH₃-H₂O mixture chart. The collected and calculated data have been depicted in Appendices-A, B and C. These data are also used in making the different diagrams for the evaluation of the system. In order to clarify the ideal and the real performance of the system, the energy and exergy analysis had been performed. The exergy destruction (ED) due to the irreversibility in each component has been clearly depicted in the figures. The performance of the hybrid system and its individual

components has been investigated and the whole assessment has been divided into following six categories to meet the objectives:

5.1 EVALUATION OF GASIFIER

The gasifier has been evaluated at the different electrical loads. The different parameters such as biomass consumption rate, specific fuel consumption, pressure inside reactor, efficiency, etc are measured to assess the performance of the downdraft gasifier.

5.1.1 Biomass Consumption Rate and Specific Fuel Consumption

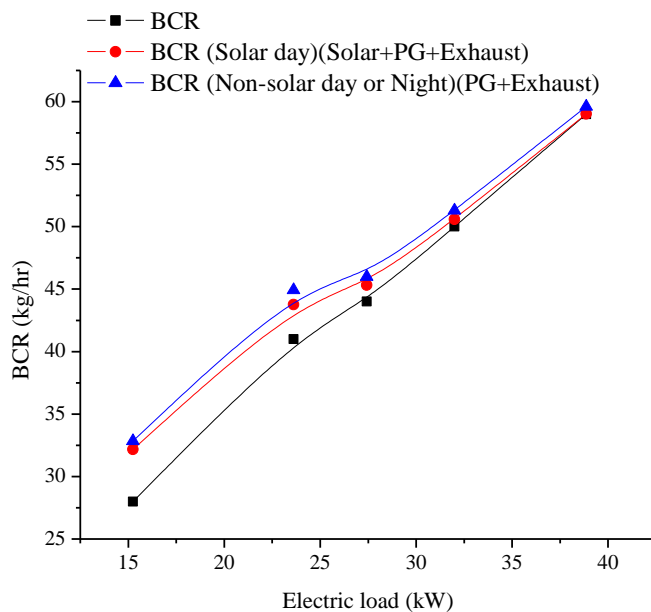


Fig 5.1 Variation of biomass consumption rate at different loads

Figure 5.1 shows the biomass consumption rate (BCR) is in increasing order with respect to increase in the electric load due to the increase in the biomass gasification. This increase in biomass gasification meets the requirement of the producer gas (PG) for the engine and vapour absorption machine (VAM). The exhaust gas from the engine, producer gas and solar energy are used in the combined form for operating the VAM. In the solar day, the BCR is something less than the night because the PG consumption rate is less for the day and remaining amount of energy demand is fulfilled by the solar energy, while in the night only PG consumption can meet the demand of energy so in the night the BCR is greater than others BCRs. At the maximum load, the exhaust gas gives the ample amount of energy for the VAM,

therefore, all BCRs appear meeting at one point in graph and the PG consumption rate reduces. The biomass consumption rate is 59 kg/hr for operating the internal combustion engine, while it is 59.02 kg/hr for the solar day and for the night 59.62 kg/hr at the maximum electric load of 38.86 kW.

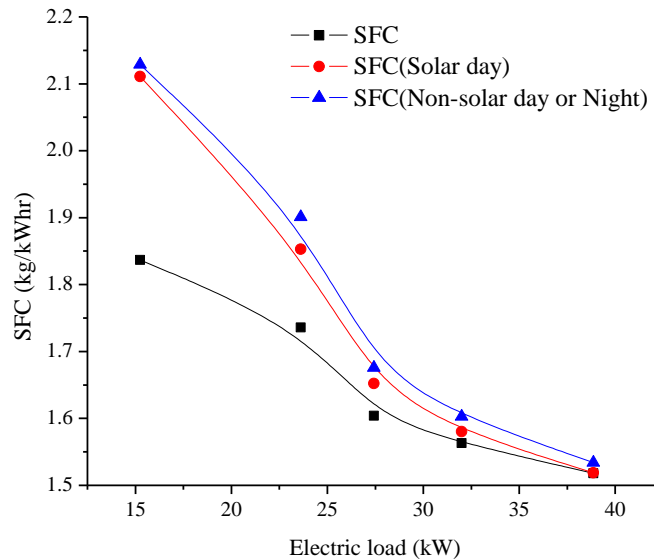


Fig 5.2 Variation of specific fuel consumption at different loads

Specific fuel consumption (SFC) is the measurement of fuel consumed for the unit power output. It is measured on the basis of biomass consumption rate and electric load applied to the engine. The figure 5.2 shows that the specific fuel consumption decreases with increase in the load. The reason for the steep fall in SFC is that the frictional power remains fundamentally constant while indicated power increases continuously. Therefore, brake power increases more rapidly than fuel consumption rate there by the specific fuel consumption falls steeply. The SFC for the day and night are greater than the SFC for engine because of the more biomass consumption rate for these, while the brake power cannot be increased due to the design considerations of the engine. All the specific fuel consumptions at maximum load are found to be equal. The reason for this is that the same quality exhaust gas produces from the approximately same BCRs at the maximum load for operating the VAM in night and day. The value of SFC is about 1.52 kg/kWhr at this load. This figure may be helpful in preparation of algorithm to get the electric power demand and needful cooling in the VAM. Accordingly, the SFC at the particular demand is multiplied by the electric load to obtain the required BCR.

5.1.2 Temperature, Reactor Pressure, Calorific Value of Producer Gas and Specific Gas Production

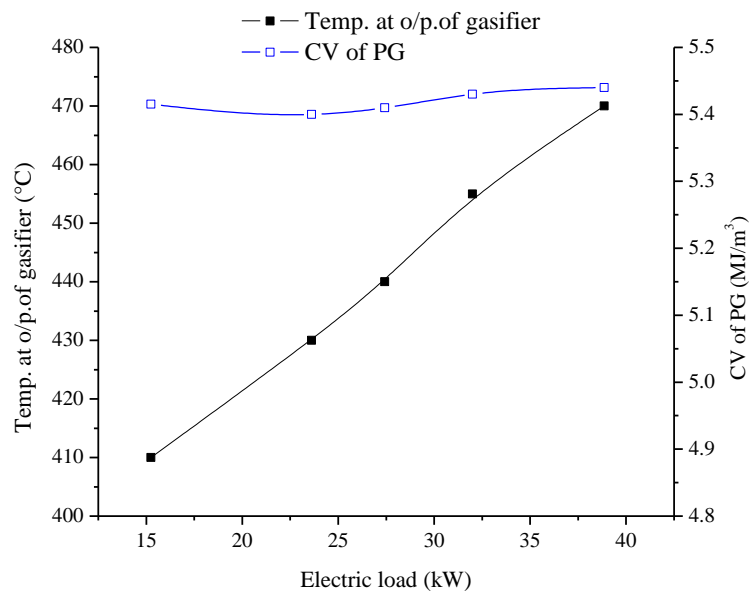


Fig 5.3 Variation of CV and PG temperature at different loads

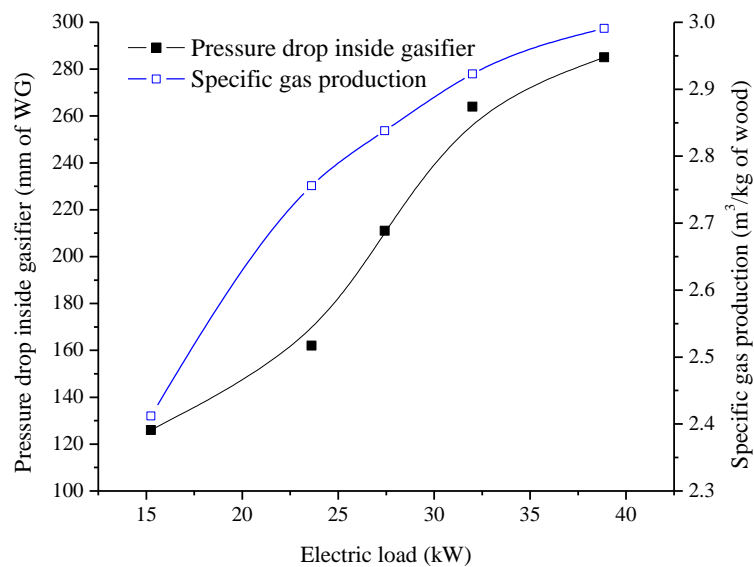


Fig 5.4 Variation of reactor pressure and specific gas production with load

Figure 5.3 indicates the slight variation of the calorific value (CV) of the producer gas (PG) and its temperature with respect to electric load. The temperature of the PG increases with increase in electric load. It is the proof of improvement in the quality of PG while, the CV of PG fluctuates with the load. The first one reason for this is that the hydrogen content of producer gas increases up to 40% moisture in wood while,

beyond 40%, it will decrease. Since the fuel wood used is comparatively dry (25% moisture), the hydrogen content in the gas is acceptable and the second one reason is the variation in the carbon monoxide content due to the CO formation by the endothermic reaction, while the third one reason is defective design of air-in manifold of gasifier. These above three reasons are responsible for the variation in calorific value of the PG. In the producer gas sample, the composition of these contents by volume varies so the CV of the PG has slight changes in a particular fashion.

Figure 5.4 shows the variation of reactor pressure of gasifier and specific gas production with the electric load. The reactor pressure of gasifier increases with the increase in the load, which indicates the production of producer gas rises inside the gasifier to meet the requirement. This variation in the reactor pressure may be due to the formation of large quantity of charcoal on the charcoal bed. The charcoal formation is very needful for gasification but it should not chock the charcoal bed, otherwise, air nozzles will give the back fires if this bed chocked then comb rotor should be operated manually for 5 to 10 minutes. Since the rise in reactor pressure also directs to the improvement in quantity of the PG, so the specific gas production increases with increase in load. The quantity of PG per kilogram of biomass during gasification increases with the load as the maximum dilution of producer gas takes place because of the presence of nitrogen (or air). Nearly 50-60% of gas is composed of non-combustible nitrogen. Thus it may be advantageous to use oxygen instead of air for gasification. However the cost and availability of the oxygen is a limiting factor in this regard.

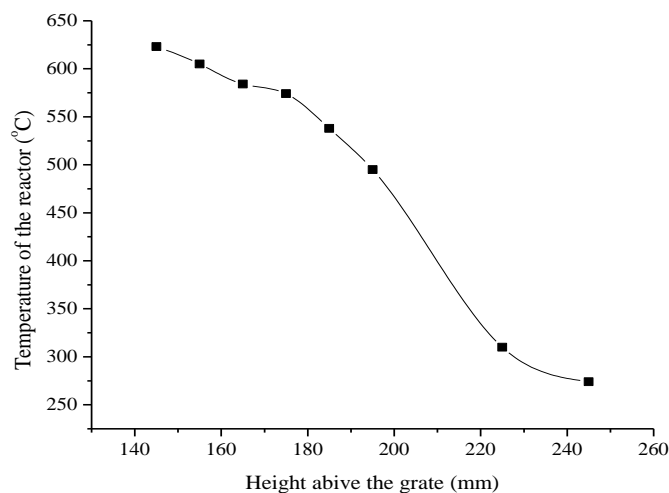


Fig 5.5 Variation of reactor temperature above the grate

Figure 5.5 indicates the variation of reactor temperature above the grate of the downdraft gasifier. The temperature inside the reactor has been measured at the height of 145 mm, 155 mm, 165 mm, 175 mm, 185 mm, 195 mm, 225 mm and 245 mm above the grate using the K-type thermocouple. The temperature profile has been found to be 623°C, 605°C, 584°C, 574°C, 538°C, 495°C, 310°C and 274°C above the respective height from the reduction zone, while, the temperature of grate was recorded with variation of 1310°C to 1360°C. The recorded temperature profile becomes nearly stable in some time inside the gasifier. It reflects that the quality of producer gas improves and the gasifier is operating smoothly for the longer duration.

5.1.3 Energy and Exergy Efficiency of Downdraft Gasifier

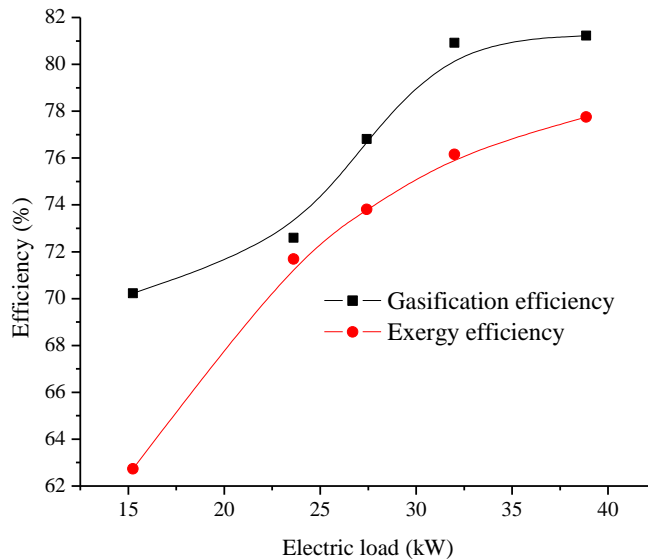


Fig 5.6 Effect of load on energy and exergy efficiency

Figure 5.6 shows the energy (or gasification) efficiency of the gasifier increases with the increase in the electric load. This is because of the significant increase in the energy outputs of producer gas. Therefore, the energy efficiency of the gasifier increases. The exergy efficiency of the gasifier also increases, due to the fact that the amount of chemical exergy associated with the producer gas increases as output of the gasifier increases. Since the energy output of gasifier is more than the amount of the exergy associated with the output as producer gas, the energy efficiency is greater than the exergy efficiency in increasing trend of efficiencies. The energy efficiency

falls suddenly at 23.62 kW of load upto 72.59% but in increasing trend, while further values of efficiency increase slightly. It occurs because of the variation in the calorific value of the producer gas as shown in figure 5.3. These values change the energy output so the changes occur in the energy efficiency.

5.2 EVALUATION OF GAS COOLING & CLEANING UNIT AND SCHEFFLER SOLAR DISC

5.2.1 Evaluation of Gas Cooling & Cleaning Unit (Condition of Producer Gas)

The gas cooling & cleaning unit is assessed by the measurement of temperature and pressure and tar content when gas passes through the different stages of filters.

5.2.1.1 Temperature and Pressure of Producer Gas

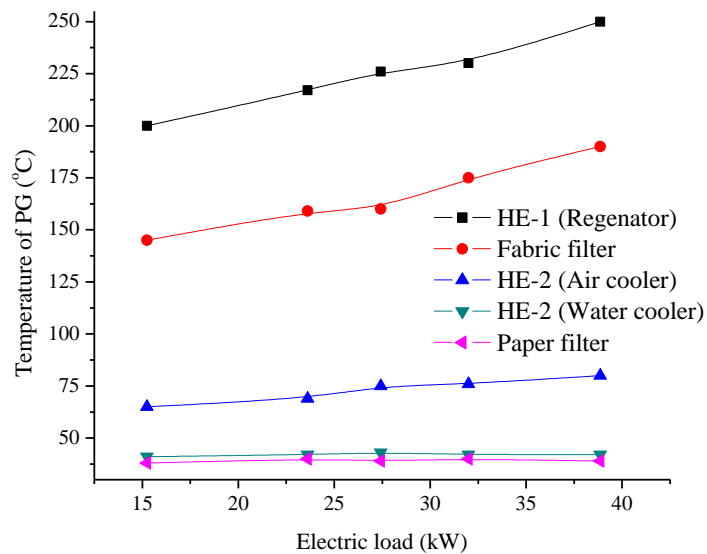


Fig 5.7 Variation of temperature of producer gas at different loads

Figure 5.7 shows the temperature at the outlet of the heat exchanger-1 i.e. HE-1 (regenerator), fabric filter and HE-2 (Air cooler) increases appreciably with increase in the load, while that of the HE-2 (water cooler) and paper filter is almost constant. The appreciable rise in the temperature after HE-1 (regenerator), fabric filter and HE-2 (Air cooler) is the indication of the quality improvement of the producer gas and there is not so much condensation of tar with increases of load, owing to that the

energy and exergy output of PG increases. The slight variation in temperature at the outlet of the HE-2 (water cooler) and paper filter depicts the steady and smooth operation or performance in all the filters. The temperature of about 39°C is obtained after paper filter and now this filtered quality producer gas can be fed to the internal combustion engine.

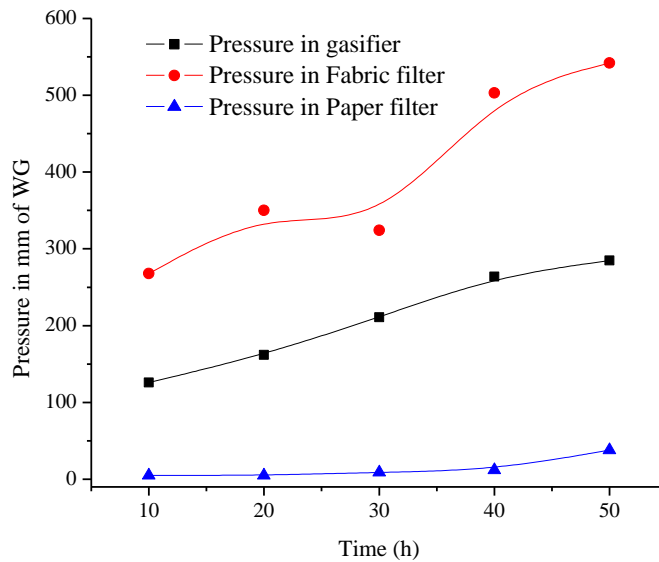


Fig 5.8 Variation in pressure of gasifier and different filters

Figure 5.8 shows the variation of pressure of gasifier and in the different filters with increase in time, it is approximately constant after the stabilization of the system up to the maximum output. The temperature and pressure nearly steady state indicates the stabilization of system that is meaningful. It has been observed that pressure drop across the gasifier and filters increases with time, which shows the blockage of the cleaning area of gasifier and filters and deposition of the tar and particulates in to the filter media. It has been seen that the pressure drop is low in paper filter, medium in gasifier and high in fabric filter. For filters it occurs due to the size of media used in filters and that of the tar and particulates while, for gasifier, it happens because of the production of the producer gas there by its more for fabric filter than the gasifier (here the gasifier is working for both gasification as well as filter). The fluctuation in the pressure drop in gasifier is showing the improper layering of the biomass. The pressure drop with electric load also increases; it means that the large amount of producer gas is filtered out. If the filters show the increase or constant pressure drop

then they are considered well-functioning. Whenever the decrease in the pressure drop occurs then the filters or gasifier must be cleaned for reuse and the time at what it happens; that is called the time of operation or the time of use of the filters and gasifier.

5.2.1.2 Tar Contents and Composition of Producer Gas

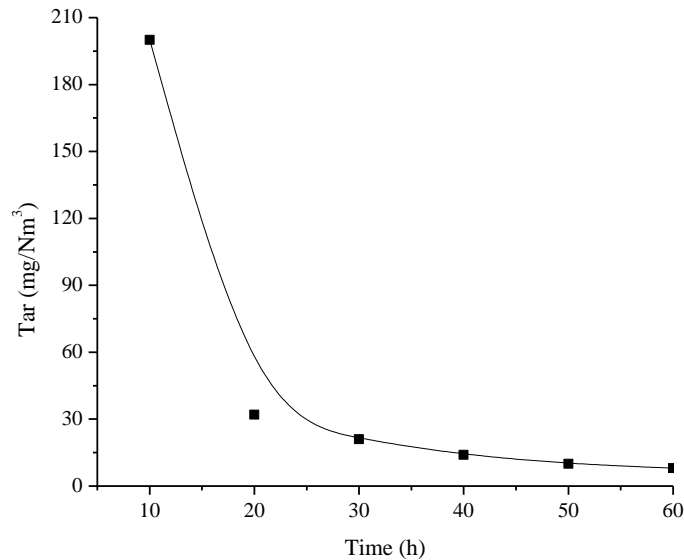


Fig 5.9 Variation of tar content of producer gas at different filters

Figure 5.9 states the tar level measured in the producer gas at the outlet of gasifier and filters. It is measured 200 mg/Nm^3 at the outlet of the gasifier, while it is 32 mg/Nm^3 , 21 mg/Nm^3 , 14 mg/Nm^3 , 10 mg/Nm^3 and 8 mg/Nm^3 at the outlet of HE-1 (regenerator), fabric filter, HE-2 (air cooler), HE-2 (water cooler) and paper filter respectively. The tar with producer gas travels in heat exchangers and precipitates. The travelling of PG along with exchange of heat with cold fluid which reduces the temperature of gas, while precipitation condenses the amount of tar from PG in such a way that the heat exchangers are used as gas cooling and cleaning unit. The tar measurement after gasifier reflects the performance of the reactor while, tar generated after paper filter indicates the quality of gas that can be used in the engine. The quality of producer gas in terms of tar after cleaning and cooling unit is 8 mg/Nm^3 . This graph is also showing the time of cleaning for the filters during the utility. If the filter's efficiency in terms of tar is calculated then it will be in the increasing order. The efficiency of the paper filter is 80%, which is the highest efficiency among filters.

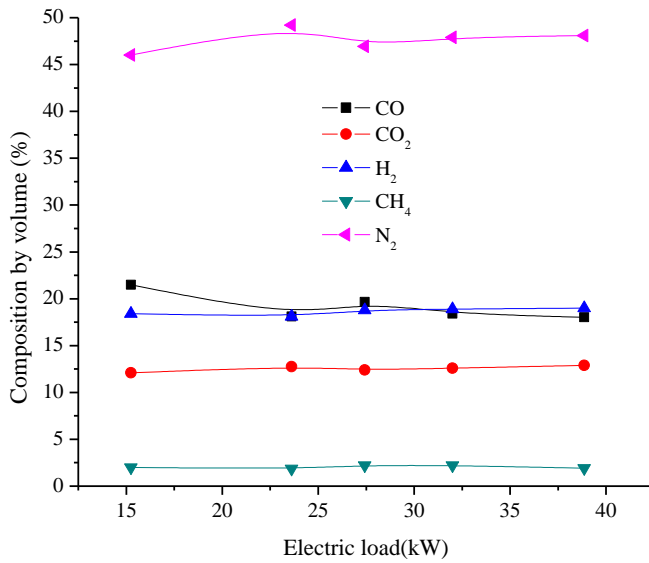


Fig 5.10 Variation of composition of producer gas at different loads

Figure 5.10 indicates the composition of PG at different loads. Since the CO formation reactions are endothermic and therefore high temperatures need for CO formation. H₂ formation is governed not only by water (moisture), but also by CH₄ formation reactions. At the low temperatures, H₂ is formed by exothermic water (moisture) and CO reaction but consumed for CH₄ formation. At high temperature, the higher H₂ content in the producer gas can also be seen which is produced by endothermic water and char reaction. The presence of considerable amount of CO₂ in producer gas is mainly due to short residence time and moderate temperature in reduction zone of the down draft gasifier, while the large amount of N₂ is present because the air is used in combustion zone. Since the heating values of hydrocarbons (CH₄, C₂H₄ and C₂H₆) are very high, even very small change in amount will vary the heating value of producer gas considerably.

5.2.2 Evaluation of Scheffler Disc

5.2.2.1 Solar Temperature, Radiations and Solar Power

Figure 5.11 depicts the variation of water temperature and beam radiation with time. The detail of change in solar temperature gain for water on June 25, 2012 has been -

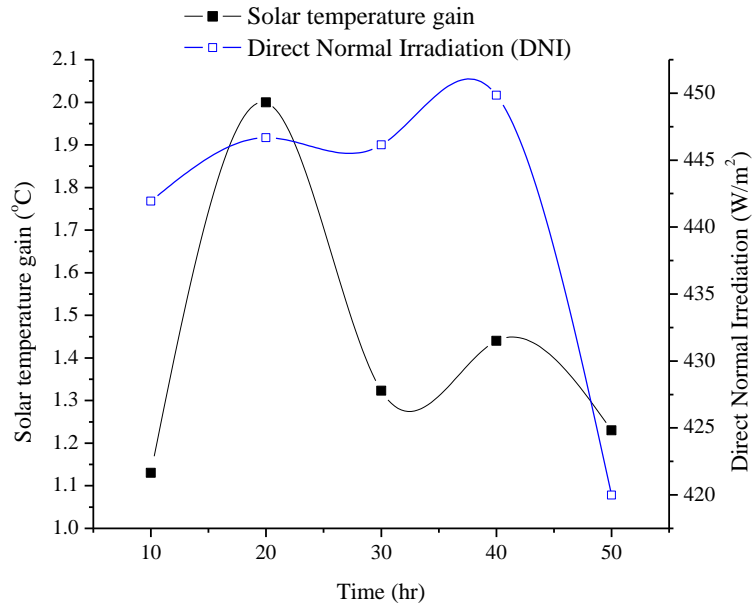


Fig 5.11 Variation of solar temperature gain and beam radiations with time

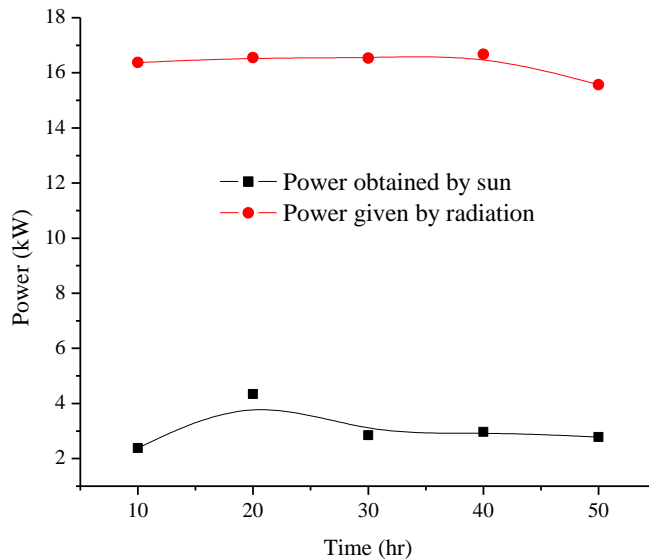


Fig 5.12 Variation of power obtained and given by beam radiations with time

- shown in figure 5.11. The variation in the temperature is due to the deviation in the intensity of the solar energy on that day. There may also be the other reasons such as reflectance and absorbance of the scheffler collector, incident rays, water quantity, time of operation, dish area, ambient temperature, wind speed, dish position, acceleration due to gravity etc. The deviation in the intensity of solar radiation plays a key role for the variation in the direct normal irradiation (DNI). Since the radiation

heat transfer coefficient goes on fluctuating as the solar temperature gain fluctuates with time so this also may be the reason for the variation in DNI.

Figure 5.12 states the variation of power obtained by sun and power given by radiation against the time. Since the power obtained by sun and power given by radiation depend upon solar radiation and the variation in the DNI encounter because of the deviation in intensity of solar energy, which has been explained in above figure therefore, the power obtained or gain goes on decreasing as the time increases. The other one reason for decreasing the power obtained by sun can be that the solar radiation is not absorbed properly by the receiver which also decreases the power obtained by sun. The increase in the wind heat transfer coefficient may also cause the decrease in power gain. The power obtained by sun at the maximum DNI of 449.84 W/m^2 is 2.97 kW. Similarly, the power given by radiation at the maximum DNI is 16.67 kW. This shows a huge difference of 13.7 kW which affects the VAM cooling drastically.

5.2.2.2 Heat Loss Factor and Heat Absorbed by Receiver

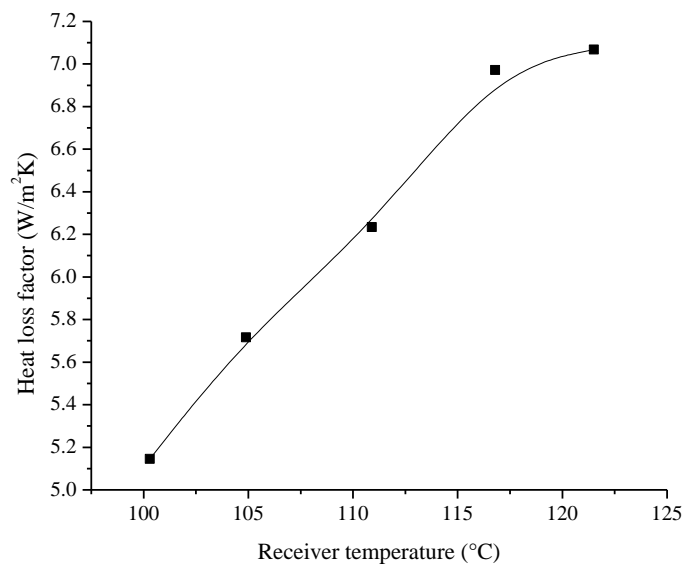


Fig 5.13 Variation of heat loss with receiver temperature

Figure 5.13 indicates the variation of heat loss factor against the receiver temperature. The heat loss factor increases with increase in the receiver temperature. The reason for this is that the cosine losses for the scheffler collector increases with receiver temperature there by the aperture area reduce and the heat loss factor increases. In

other words, incident of sun light rays on collector to receiver always goes decreasing over the day or in the days of summer season, owing to the design considerations of the scheffler collector. It means that this collector can efficiently be used in the winter season. This nature of collector affects the power obtained (output) by sun, due to which the heat loss factor increases with the increase in temperature of receiver.

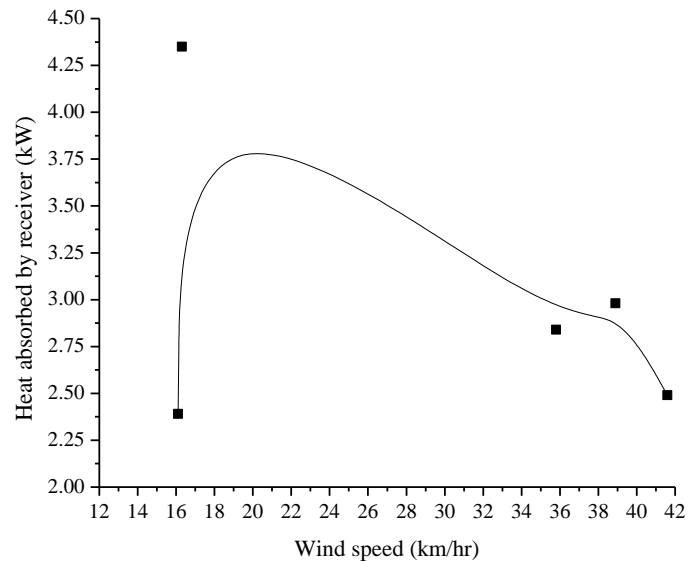


Fig 5.14 Variation of heat absorbed by receiver with wind velocity

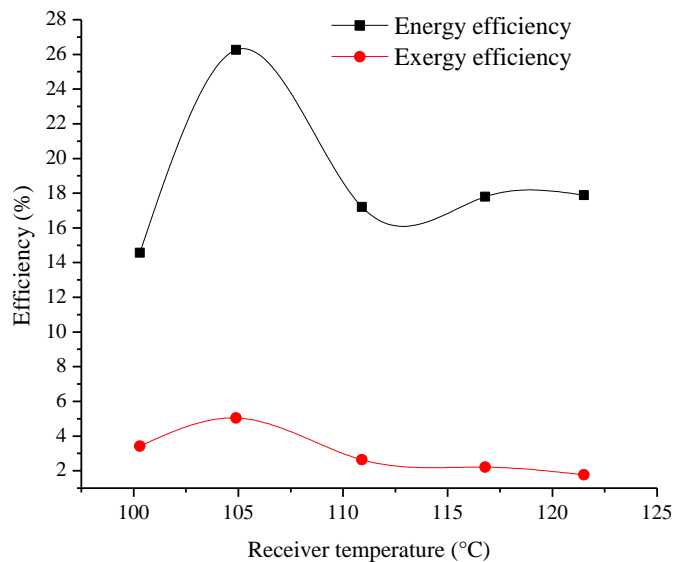


Fig 5.15 Variation of energy and exergy efficiency with receiver temperature

Figure 5.14 shows the variation of heat absorbed by receiver with wind velocity which states that the heat absorbed by the receiver goes on increasing first and then decreasing as wind velocity increases, because firstly, the heat loss is less due to small increase in wind velocity there by not so disperse of heat over the receiver and later the heat loss increases with significant increase in wind velocity, as a result, the heat absorbed by receiver firstly increases and subsequently decreases with increase of wind velocity.

5.2.2.3 Energy and exergy efficiency of scheffler collector

Figure 5.15 shows the variation of energy and exergy efficiency against the receiver temperature. These both of the efficiencies go on decreasing as receiver temperature increases; however both the efficiencies suddenly increase in beginning because of the increase in mass flow rate of water. When the mass flow rate is established in regular way then the efficiencies decrease. It also occurs due to the decrease in the difference of mean and atmospheric temperature, and design considerations of the scheffler collector due to which the heat loss factor increases. The energy efficiency of collector decreases because of the energy output decreases, similarly the exergy efficiency also decreases as the exergy destruction increases there by the exergy output decreases. These efficiencies can be increased if all the heat losses are minimized.

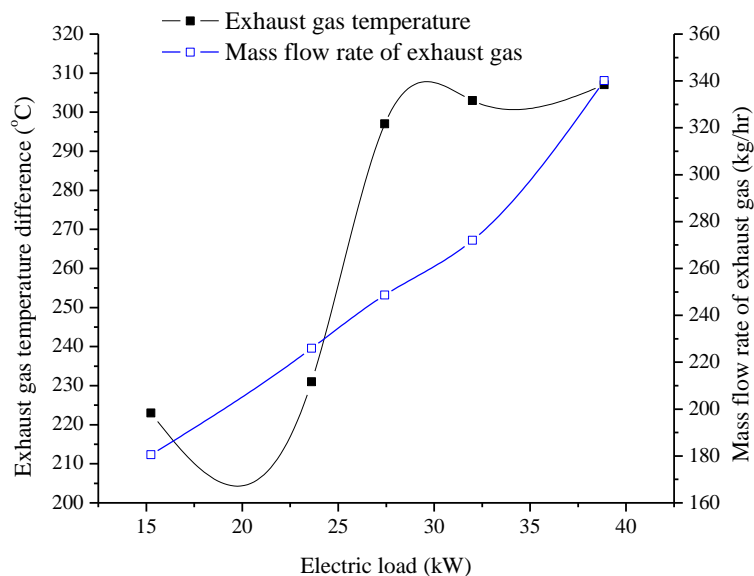


Fig 5.16 Variation of exhaust gas temperature and mass flow rate with load

5.3 PERFORMANCE ANALYSIS OF EXHAUST GAS AND ITS EMISSION CHARACTERISTICS

5.3.1 Exhaust Gas and Mass Flow Rate

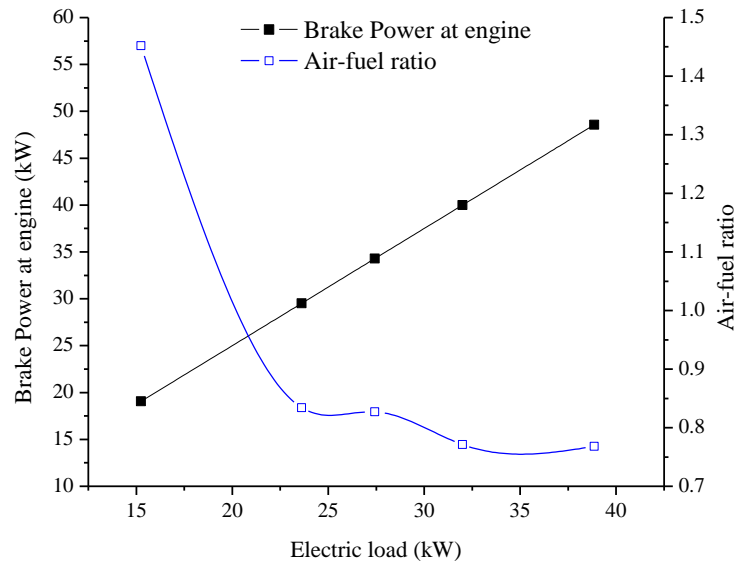


Fig 5.17 Variation of air-fuel ratio and brake power output with load

Figure 5.16 shows the variation of temperature and mass flow rate of exhaust gas against the electric load. The rise in exhaust gas temperature indicates that the heat carried away by the exhaust gas and its quality increases with increase in electric load. The relative proportion of the air and fuel in the engine are very important from the viewpoint of the combustion, the efficiency of the engine and mass flow rate of the exhaust gas. The air and producer gas flow rate is varied in engine through manually operated valves to maintain the required output. The mass flow rate of exhaust gas also increases because the producer gas flow rate increases with increase in load there by the air-fuel ratio decreases and the power output increases with load, which is obvious. This has been shown in the figure 5.17.

Figure 5.18 indicates the variation of heat used of exhaust gas in the HRU with exhaust gas temperature. The exhaust gas heat used increases with increase in exhaust gas temperature, which represents as the quality of exhaust gas increases, the heat used in the water of the HRU increases. This is the indication of better performance of the exhaust gas and it can be used to achieve the required output in the system.

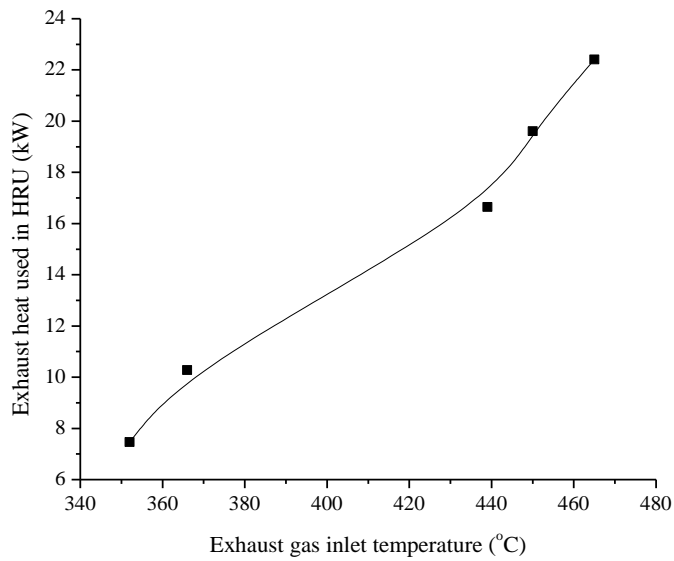


Fig 5.18 Variation of exhaust gas heat used with exhaust gas temperature

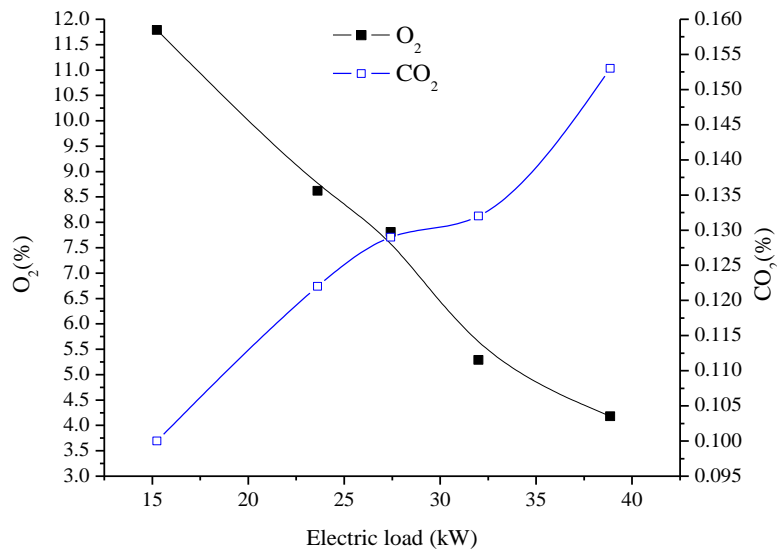


Fig 5.19 Variation of oxygen and carbon dioxide with load

5.3.2 Exhaust Gas Emission: Following figures show that the exhaust gas emissions samples have oxygen, nitrogen oxides and carbon dioxide:

Figure 5.19 shows that the exhaust gas emissions samples have oxygen and carbon dioxide at the different output of electric load. The oxygen emission level is in decreasing order because air-fuel ratio reduces with increase of load, while the carbon dioxides emissions increase due to the complete combustion of the producer gas in the

engine up to the maximum power output, there by the carbon monoxide emissions are zero in the samples, while the amount of carbon dioxide emission at the maximum output of the producer gas engine is very small as compared to that of the fossil fuel run engine.

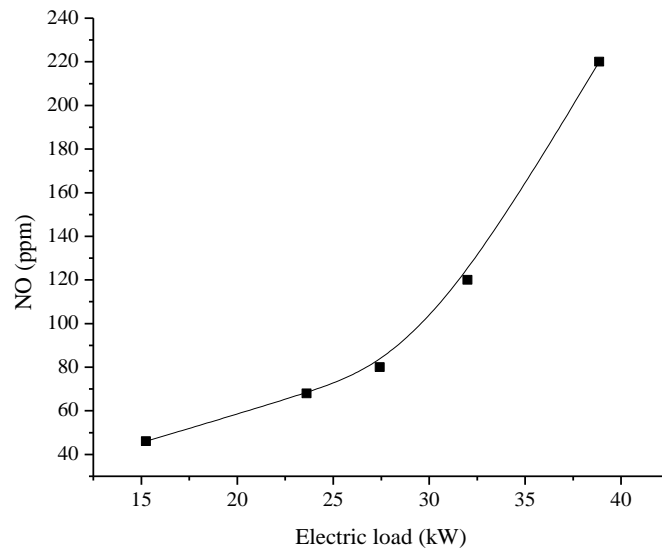


Fig 5.20 Variation of nitrous oxide with load

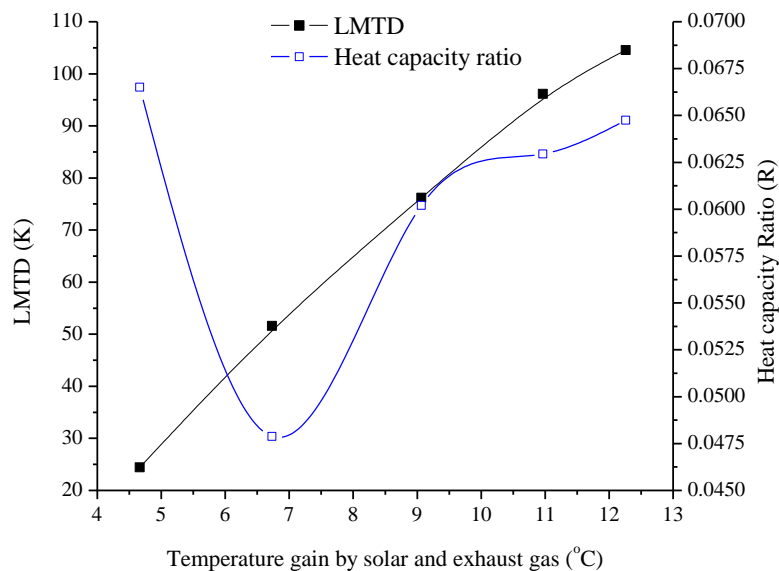


Fig 5.21 Effect of input temperature on LMTD and heat capacity ratio

Figure 5.20 indicates the nitrous oxides emissions increase with increase in load. Since, the nitrogen oxides emission depends upon the temperature and the combustion

duration of the producer gas in the engine cylinder. The atmospheric nitrogen exists as a stable diatomic molecule (N_2) at low temperature, but the diatomic nitrogen (N_2) molecules break into monatomic nitrogen (N) at very high temperature and have the reactions, as a result the formation of nitrous oxides occur. Therefore, nitrogen oxides emissions are very small in quantity in the environment, but in increasing order with increase of load.

5.4 ASSESSMENT OF HEAT RECOVERY UNIT (HRU)

5.4.1. On the Basis of Solar Energy and Engine's Exhaust

5.4.1.1 LMTD and Heat Capacity Ratio (R)

Figure 5.21 shows effect of temperature gain by solar and exhausts gas on logarithmic mean temperature difference (LMTD) and heat capacity ratio (R). The LMTD is a logarithmic mean of temperature difference between hot and cold fluids. The increase in the LMTD indicates the increase in heat transfer between the hot and cold fluids, and the performance of the HRU improves. In figure, once the heat capacity ratio dips and then increases. This is due to the fact that the imbalanced heat transfer between the fluids and the significant leak of heat to the surrounding occurs. At the high temperature gain by solar and exhaust, the HRU experiences the more recovery of heat (either by insulation or surrounding) subsequently, the degradation of energy reduces and therefore, the heat capacity ratio of the HRU increases.

5.4.1.2 Efficiencies and Overall Heat Transfer Coefficient (U)

Figure 5.22 indicates the effects of temperature gain by solar and exhausts gas on efficiencies and overall heat transfer coefficient. The energy efficiency decreases with increase in temperature gain by solar and exhaust gas because the temperature difference between exhaust gas waste heat inlet and cold water inlet in the HRU increases. On the other hands, the energy output decreases so energy efficiency decreases, while the exergy efficiency of the HRU increases, due to the fact that the amount of exergy associated with the output or actual heat transfer increases. Since the LMTD increases, the overall heat transfer coefficient of the HRU almost decreases. In the figure, the fluctuation in the overall heat transfer coefficient occurs because the increase in the sensible heat is not as sharp as in the LMTD.

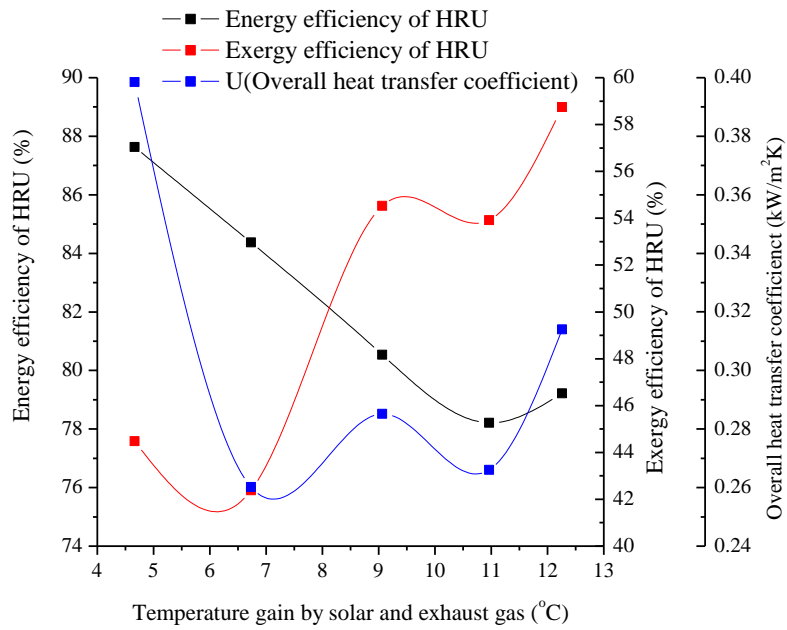


Fig 5.22 Effect of input temperature on efficiencies and overall heat transfer coefficient

5.4.2. On the Basis of Producer Gas

5.4.2.2 LMTD and Heat Capacity Ratio (R)

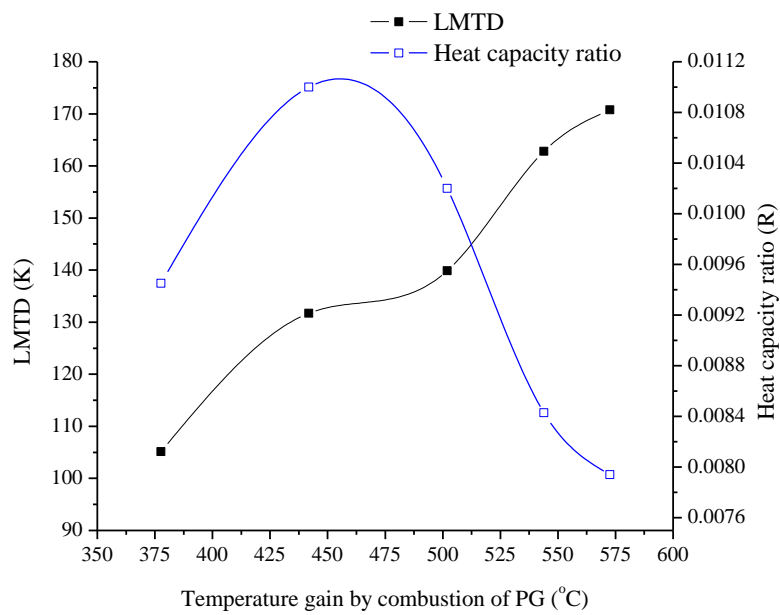


Fig 5.23 Effect of input temperature on LMTD and heat capacity ratio

Figure 5.23 shows effect of temperature gain by combustion of producer gas (PG) on logarithmic mean temperature difference (LMTD) and heat capacity ratio (R). The increase in the LMTD depicts the increase in heat transfer between the hot and cold fluids. The LMTD of the HRU operated by the PG is more than that of the temperature gain by the solar and exhaust because the heat is generated by the combustion in PG operation of the HRU, in this way, the improvements in the performance of the HRU are observed. In figure, once the heat capacity ratio goes up and then decreases. This is due to the fact that the imbalanced heat transfer between the fluids and the significant leak of heat to the surrounding occurs. At the high temperature gain by combustion of producer gas (PG), the HRU experiences the less recovery of heat because of the loss of the heat through the insulation or surrounding subsequently, the degradation of energy increases and therefore, the heat capacity ratio of the HRU decreases.

5.4.2.2 Efficiencies and Overall Heat Transfer Coefficient (U)

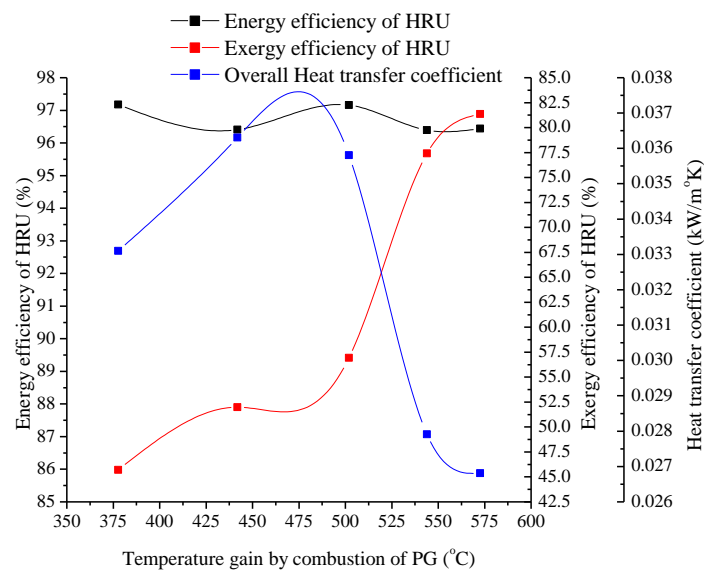


Fig 5.24 Effect of input temperature on efficiencies and overall heat transfer coefficient

Figure 5.24 indicates the effects of temperature gain by combustion of producer gas on efficiencies and overall heat transfer coefficient. The energy efficiency slightly fluctuates with increase in temperature gain by combustion of producer gas because the increase in the temperature difference between producer gas inlet and cold water inlet in the HRU is not smooth, as a result the energy output has an uneven nature.

The exergy efficiency of the HRU increases with temperature input through the combustion of the PG. The reason for this is that the amount of exergy associated with the output or actual heat transfer of the HRU increases. The overall heat transfer coefficient (U) of the HRU almost decreases with input temperature of the PG because of the increase in the LMTD in earlier figure. In the present figure, the fluctuation in the overall heat transfer coefficient occurs due to the fact that the increase in the LMTD of the HRU is not as smooth as in the sensible heat transfer between the hot and cold fluid of the system.

5.4.3. Comparison of Waste Heat Recovery with Overall Energy and Exergy Loss

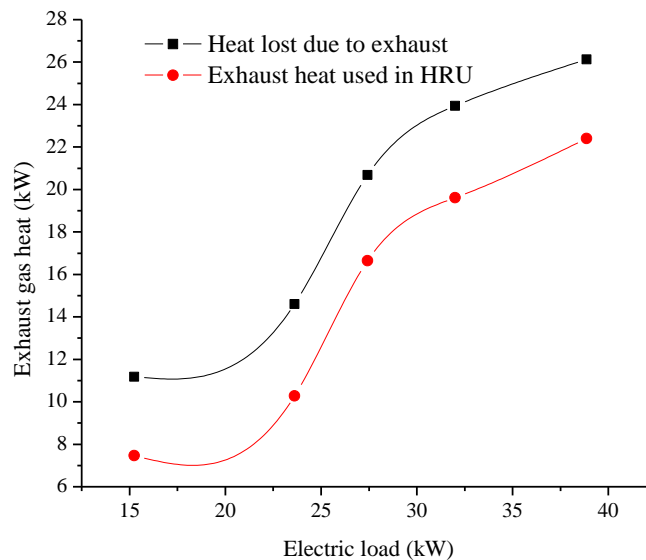


Fig 5.25 Variation of exhaust heat used or lost at different loads

Figure 5.26 shows the variation of heat used or loss in the different components at the different loads. Out of 100% input energy supplied to the system, around 6.95% to 8.15% of energy is lost through exhaust gas but in the HRU about 4.63% to 6.99% of input energy is used. **In figure 5.25** the heat lost due exhaust is from 11.18 kW to 26.13 kW, while 7.46 kW to 22.41 kW energy is used in the HRU for vapour absorption machine (VAM). About 1.16% to 2.32% (or around 3.72 kW) of energy is lost in the HRU. This loss of the heat in the HRU is very less, which shows the effective utilization of the exhaust heat and solar energy in the HRU. In figure.5.25.there is the significant percentage of heat used in the HRU than that of the

others components of the system, therefore the HRU reflects the better performance. The unaccounted heat loss varies from 4.81% to 11.49%. Almost 38.98% of the total input energy is used in the various components of the system.

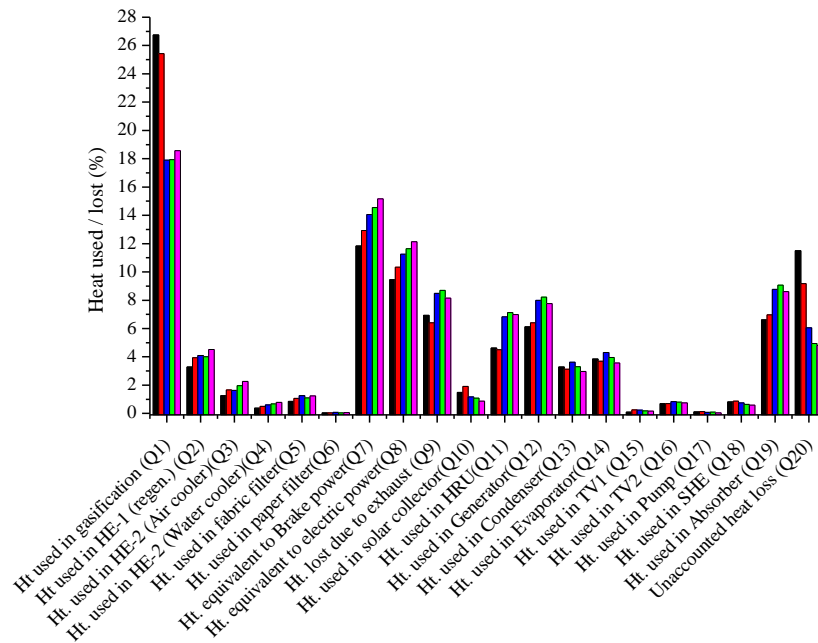


Fig 5.26 Percentage distribution of input energy at different loads

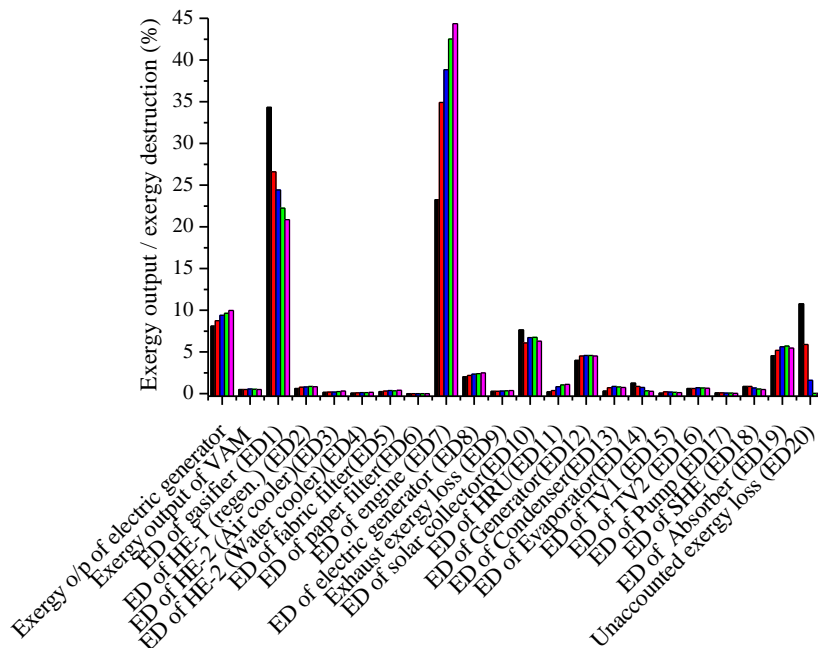


Fig 5.27 Percentage distribution of input exergy at different loads

Figure 5.27 indicates the percentage distribution of exergy input at different loads. It is found that around 0.213% to 1.102% of input exergy is destructed due to irreversibility in the HRU. This exergy destruction shows very less exergy loss and gives better performance of the HRU. Approximately 80.41% to 88.39% of the total input exergy is destructed due to the irreversibilities in the different components of the system at different electric loads. Around 0.052% to 10.76% of input exergy is lost as unaccounted exergy, which is lower than the above energy loss; therefore it is also the proof of better performance of HRU.

5.5 PERFORMANCE EVALUATION OF COLD STORAGE SYSTEM

5.5.1 Generator Temperature and Absorber Temperature

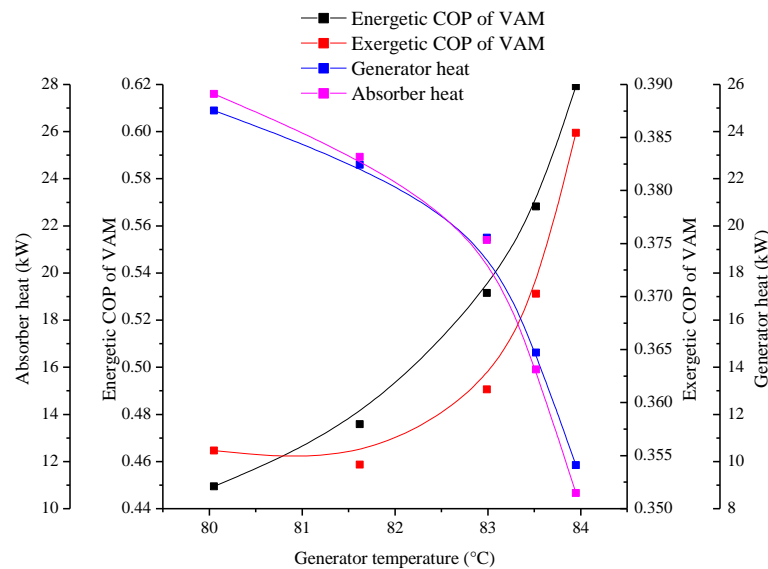


Fig 5.28 Variation of heat used and performance with generator temperature

Figure 5.28 depicts the relationship of different generator temperatures with coefficient of performances, generator and absorber heat. When the generator temperature increases, the generator and absorber heat decrease because as the generator temperature gets higher, the concentration of the solution leaving the generator increases there by the weak solution temperature increases and, hence, the enthalpy (h_9) at the inlet of absorber of figure 4.1 increases which is more than the strong solution in the solution heat exchanger. This enthalpy is responsible for decreasing the generator heat load. Similarly, as the generator temperature rises, the

mass flow rate of refrigerant in the evaporator increases which decreases the concentration of the weak solution in the absorber and owing to that, the absorber heat decreases. The energetic and exergetic COP go on increasing as the generator temperature increases because the input energy and exergy associated with generator decrease, while the energetic COP is more than the exergetic COP which states that the desired energy output is more than exergy output.

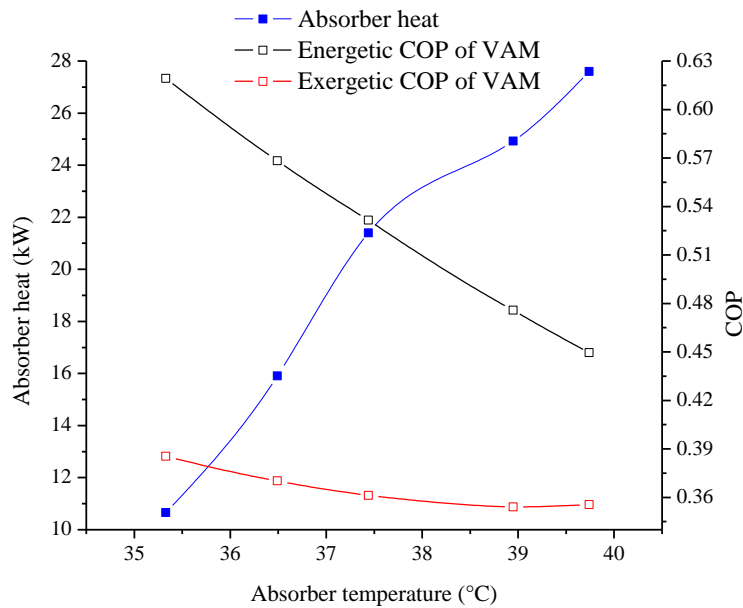


Fig 5.29 Variation of absorber heat and performance with absorber temperature

Figure 5.29 shows the variation of Coefficient of Performances and absorber heat at different absorber temperatures. The absorber heat increases with increase in absorber temperature because the concentration of the weak solution in the absorber increases. This concentration of weak solution approaches the concentration of the strong solution. When the absorber heat increases, the absorption of vapour ammonia refrigerant from the evaporator in aqua-ammonia solution of absorber decreases there by amount of energy and exergy associated with refrigeration output decreases and, hence the energetic and exergetic COP reduce with increase in absorber temperature.

5.5.2 Evaporator Temperature and Condenser Temperature

Figure 5.30 indicates the energetic and exergetic COP of the VAM increase with increase in the evaporator temperature. The first reason is that there is a huge temperature difference between the refrigerant and cooling body at the low temperature of the evaporator and, as the temperature of the evaporator increases,

there is a reduction in heat transfer temperature difference. This results in an increase in the energetic and exergetic COP from low to high temperature of the evaporator. The second reason is that the refrigeration output of the VAM increases and, therefore, the energetic COP and exergetic COP increase with increase in the evaporator temperature.

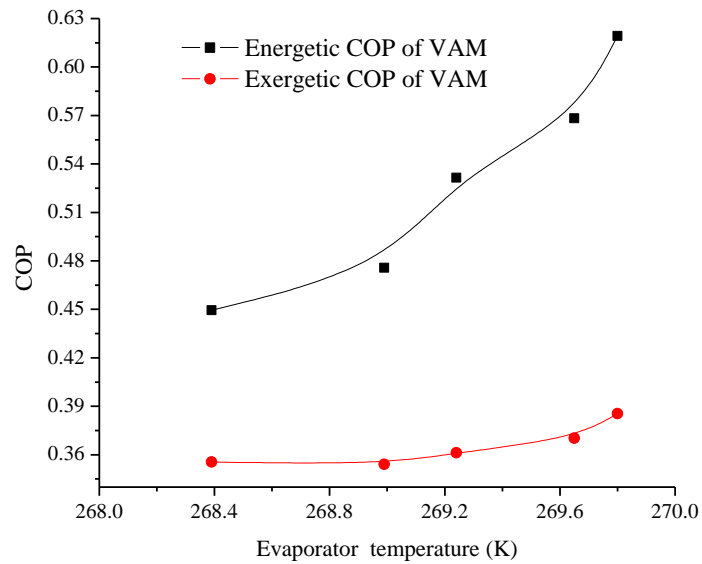


Fig 5.30 Variation of Coefficient of Performances with evaporator temperature

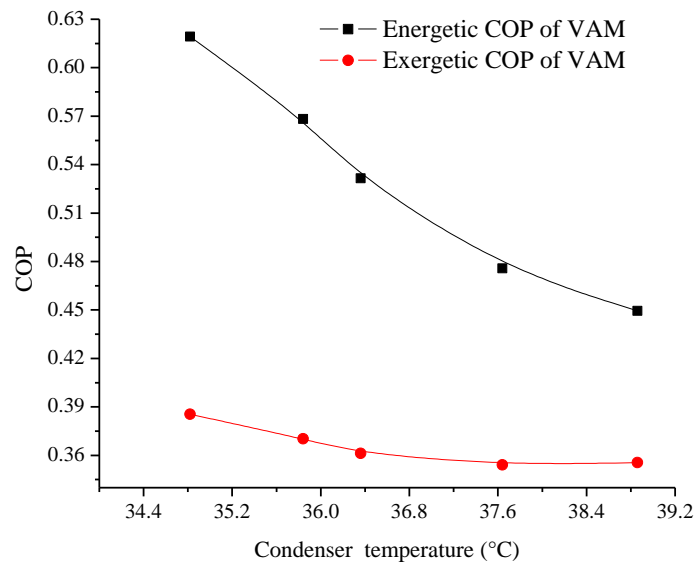


Fig 5.31 Variation of Coefficient of Performances with condenser temperature

Figure 5.31 shows the variation in performances against the condenser temperature of VAM. The enthalpy of the ammonia vapour (h_6) of fig. 4.1 leaving the generator increases with increasing the generator temperature. The heat used in condenser also rises, which increases the condenser temperature and reduces the refrigeration output. The reason for this is that as the condenser temperature increases, the condenser pressure also increases subsequently the back pressure on the generator increases. Thus, the mass flow rate of the vapour ammonia decreases resulting in a decrease in the refrigeration output of the VAM, as a result the energetic and exergetic COP reduce with decreasing the energy and exergy associated with the refrigeration output.

5.5.3 Ambient Temperature and Time for Steady State

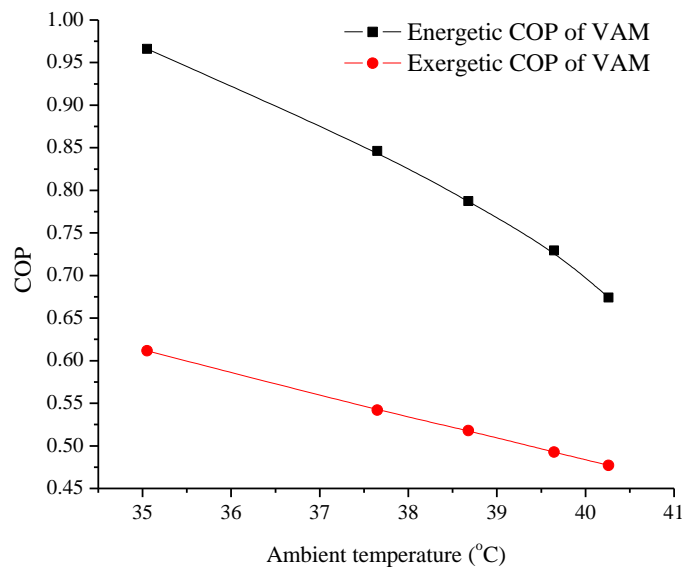


Fig 5.32 Variation of Coefficient of Performance with ambient temperature

Figure 5.32 shows the variation of energetic and exergetic COP against ambient temperature. As ambient temperature rises, the temperatures of the condenser and absorber increase and the heat of the generator rises, this gets worse the performance of the system. This is also the cause of a decrease in Coefficient of Performances. The air-cooled absorber and air-cooled condenser capacity are also affected by the ambient temperature. As an increase of ambient temperature occurs causes a decrease on the condenser capacity and an increase in condenser temperature. The high pressure of the condenser decreases the concentration of the strong solution, which

increases the heat of both the generator and absorber. The enthalpy of the saturated liquid (h_{13}) of figure 4.1 leaving the condenser increases with increasing condenser temperature. Thus, it causes an increase in the absorber temperature and the concentration of the weak solution approaches the concentration of the strong solution. Therefore, the heat of the absorber increases that decreases the energetic and exergetic COP.

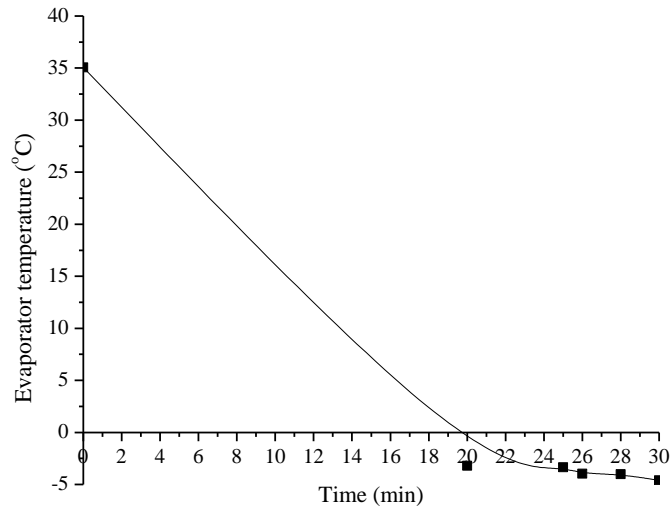


Fig 5.33 Variation of evaporator temperature with time

Figure 5.33 depicts the variation of evaporator temperature against time. The time required to reach steady state for evaporator temperature with respect to time has been given in graph. In the cold storage, the temperature falls up to 0°C in approximately in twenty minutes, while the negative temperature gets in next fifteen minutes. Therefore, it shows the time after which the cold storage must be used for preservation of perishable commodities.

5.6 COMBINED ANALYSIS OF THE SYSTEM

5.6.1. Energy and Exergy Analysis

Figure 5.34 shows that out of 100% input biomass and solar energy supplied to the system, around 14.83% is available as the useful energy output from the electric generator and the VAM, while 7.74% energy is lost to the environment via exhaust, however, 6.02% part of the exhaust energy is used in the HRU. The percentage of

energy loss in the HRU is 1.72%, which is very less; it means the HRU is functioning well. The maximum amount of heat 21.31% is used in the gasification, while a little heat 0.052% is used in the paper filter. The heat equivalent to the brake power of the engine is 13.71%. The unaccounted losses in the system are 7.29%, i.e. maximum amount of heat is used in the components of the system. These unaccounted energy losses shown at the different loads in figure 5.26 are in decreasing order, so it's a proof of better utilization of heat in the system and it works well at the high electric load because the unaccounted loss is less at this testing load. Nearly 36.30% of the total input energy by solar and biomass is used in the various components of the hybrid system.

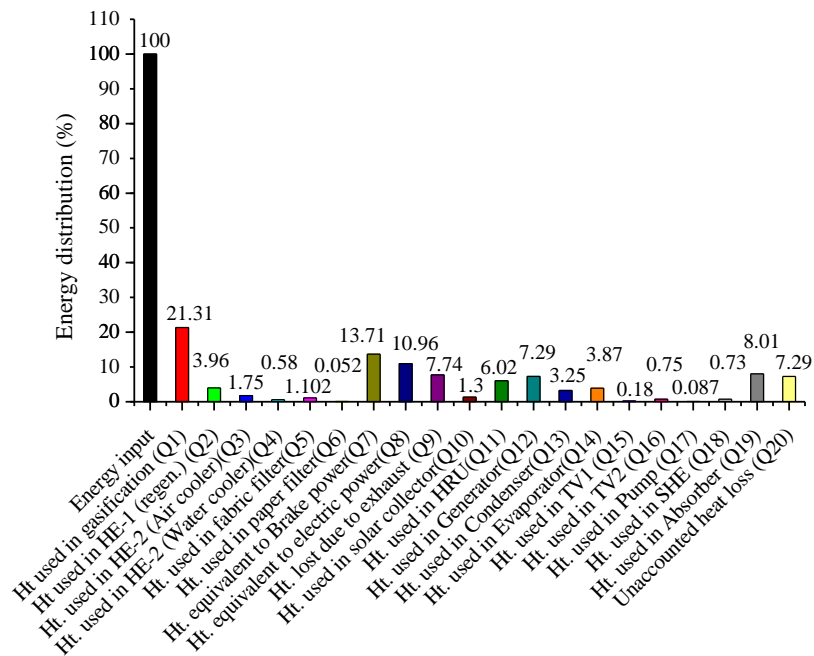


Fig 5.34 Percentage distribution of total input energy for the hybrid system

Figure 5.35 indicates the exergetic analysis of the system. It is found that 3.67% of the total (100%) input exergy is lost as unaccounted exergy. Around 9.68% is available as exergy output from the electric generator and VAM. Approximately 86.35% of the input exergy is destructed due to the irreversibilities in the different components of the hybrid system. 3.67% exergy is lost as unaccounted exergy, which is lower than 7.29% unaccounted energy loss of the input energy. Similarly, 0.32% exhaust exergy is lost in environment, which is lower than 7.74% exhaust energy loss. This is the proof of the deeper investigation of the second law over the first law. The particular component of the maximum irreversibility can be pointed out by the second law

analysis. It is found that the percentage of the exergy destruction is highest in the engine. The irreversible processes in the engine are due to combustion, heat transfer, mixing, friction, etc., which destroy a significant fraction of the fuel exergy. The exergy destruction in the engine increases with increasing octane rating and engine speed. The exergy destruction because of the combustion can be reduced by taking some design precautions to increase the combustion temperature such as preheating the intake air and decreasing the amount of additional air. However, these precautions may lead to a rise in the exhaust gas temperature, thereby causing a higher exergy loss associated with the exhaust gas. These exergy losses can be reduced by the concentrations of CO and unburned HC in the exhaust gas. The next largest exergy destruction occurs in the gasifier, Scheffler collector, absorber, generator, electric generator and HRU. In the gasifier, the main reasons for inefficiencies are chemical reactions. Heating of inert chemical components, mixing of streams with differences in temperature, pressure and chemical composition as well as pressure drop due to friction are also the cause of exergy destruction. The increase in gasification temperature increases the relative amount of combustion and internal heat transfer in gasifier; thus there is an increase in the exergy destruction within the gasifier. The exergy destruction in an adiabatic gasifier can be reduced by preheating the reactants with air and by reducing the temperature of producer gas at outlet. The significant loss in the gasifier emphasizes the need of the good gasifier design for the better performance. The exergy destruction in the Scheffler collector is due to its fixed focus, so the huge temperature difference between working medium (water) and solar collector is obtained. The irreversibility of the solar collector can be reduced by the right choice or the proper design of the concentrating collector so that the minimum temperature could be maintained between the working mediums. If a generator is designed with a minimum pressure drop, but maximum heat transfer efficiency then the exergy destruction can be obtained lower, while the absorber would be designed with maximum pressure drop for low exergy destruction. The exergy destruction in the electric generator occurs due to friction, eddy currents and metallurgical limitations. It can be reduced by proper design of electric generator and excellent choice of material for the manufacturing of the generator. The reason for the irreversibility of the HRU is a larger temperature difference between the working fluids (water and exhaust gases). This leads to more entropy generation due to the heat transfer. The Irreversibility in condenser and evaporator is insignificant, because

in the condenser and evaporator, the low quality energy is lost. The exergy destruction in other components of the hybrid system is much lower than the above components. Therefore, the engine, gasifier, Scheffler collector, absorber, generator, electric generator and HRU need special attention for the proper design from the second law point of view, so that the hybrid exhaust gas heat and renewable energy could be utilized effectively.

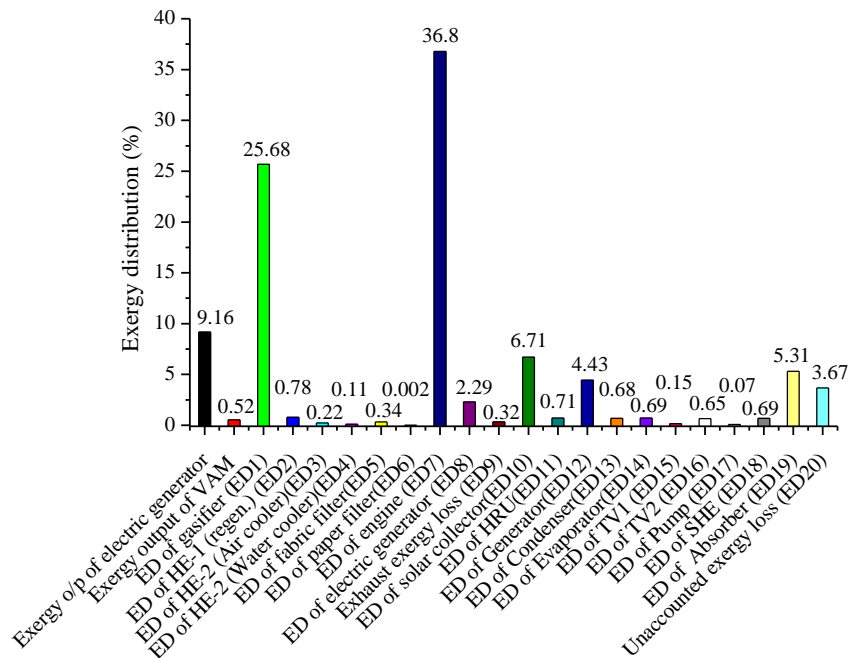


Fig 5.35 Percentage distribution of total input exergy for the hybrid system

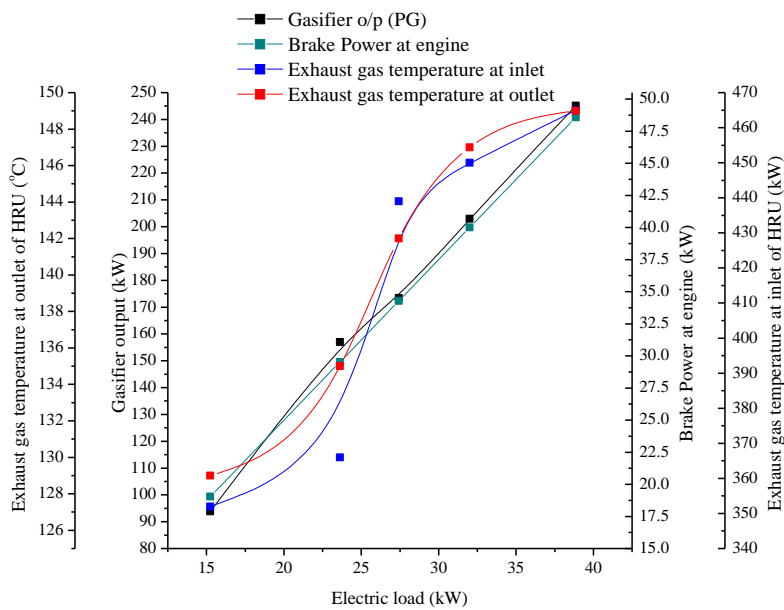


Fig 5.36 Effect of electric load on Gasifier output, Brake power and exhaust gas temperature

5.6.2. Gasifier Output, Brake Power and Exhaust Gas Temperature

Figure 5.36 shows the gasifier output, brake power, and exhaust gas temperature at inlet and outlet of HRU increase with the increase in electric load. As the electric load increases, the biomass gasification in gasifier increases to meet the demand of the producer gas (PG) for the engine, therefore, the gasifier output as well as brake power output at engine increase. On the other hand, there are some design considerations for the downdraft gasifier and engine, owing to that, the biomass gasification in reactor of gasifier and brake power at the crank shaft of engine increase with increase in electric load. The quality of the exhaust gas from engine improves with increase in the electric output, so the temperature of the exhaust gas increases at the inlet and outlet of the HRU. The exhaust gas temperature at the inlet of HRU increases rapidly as the electric output of the generator increases and corresponding the outlet temperature also increases, but the variations are smaller. The increase in performance parameters with increasing the electric load shows that the performance of the system improves at the maximum design load for the system.

5.6.3. Power Outputs and Overall Efficiency at Exhaust Gas Temperature

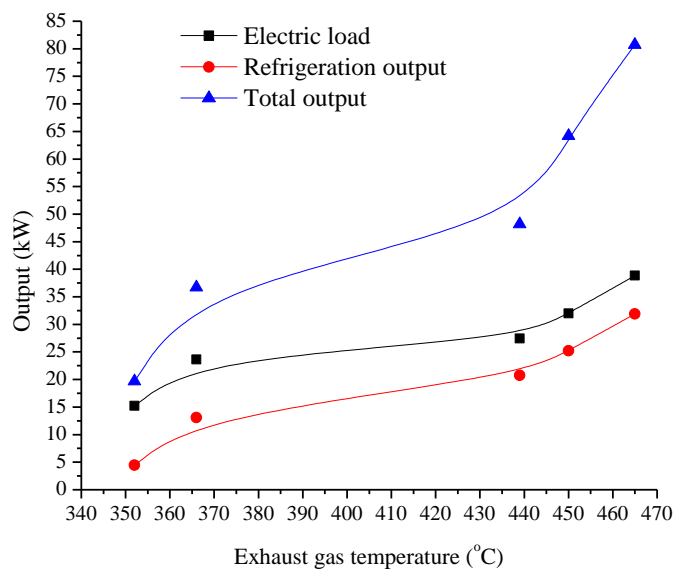


Fig 5.37 Effect of Exhaust gas temperature on Electric output, Refrigeration and total output

Figure 5.37 indicates the variation of electric output, total output and the refrigeration output of the VAM with the increase in exhaust gas temperature. The electric power output increases with increasing the exhaust gas temperature. The reason is that the

heat carried away by the exhaust gas increases with the increase in the electric output. This indicates that the rise in temperature of the exhaust gas and the quality of energy is improved resulting in an increase in the engine power output which increases the electric output. Subsequently, the refrigeration output of the VAM increases with increasing the exhaust gas temperature. This is due to the fact that the higher temperature at the exit of the HRU because of giving the maximum amount of heat by solar and exhaust gas to the HRU, owing to this, the supply of heat to the VAM is greater and consequently, there is the higher mass flow rate of the refrigerant to the condenser through the generator and so it is for the evaporator of the VAM. When the mass flow rate of refrigerant increases, it gives the larger refrigerating effect at the evaporator of the VAM. It has also been observed that the increase in the exhaust gas temperature causes a higher total output of the hybrid system because the rate of increase in the electric power output is much effective than the refrigeration output of the VAM.

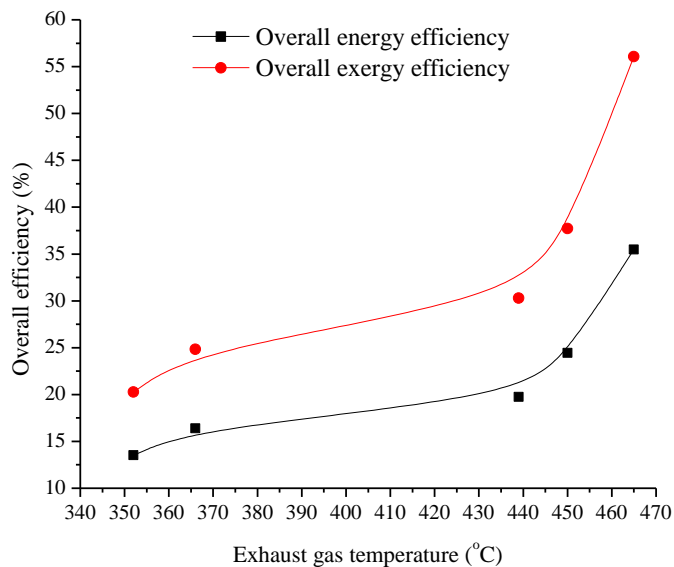


Fig 5.38 Effect of exhaust gas temperature on overall energy and exergy efficiency

Figure 5.38 shows the overall energy and exergy efficiency of the new hybrid cold storage cum power generator system increase with the increase in the exhaust gas temperature. This is because of the increase in the exhaust gas temperature. The increase in exhaust gas temperature shows the improvement in the quality of the exhaust gas waste heat and correspondingly, the quality heat is given to the generator of the VAM. This reflects the significant increase in the refrigeration outputs of

VAM. Therefore, the overall energy efficiency of the system increases. The overall exergy efficiency of the hybrid system also increases, due to the fact that the amount of exergy associated with the power output of the electric generator is much greater than the amount of the exergy associated with the refrigeration output of the VAM. The overall exergy efficiency of this system is more than the overall energy efficiency. It is due to fact that the exergy associated with the output of the hybrid system at the low temperature is higher than the energy output.

5.6.4. Power Outputs and Overall Efficiency at Evaporator Temperature

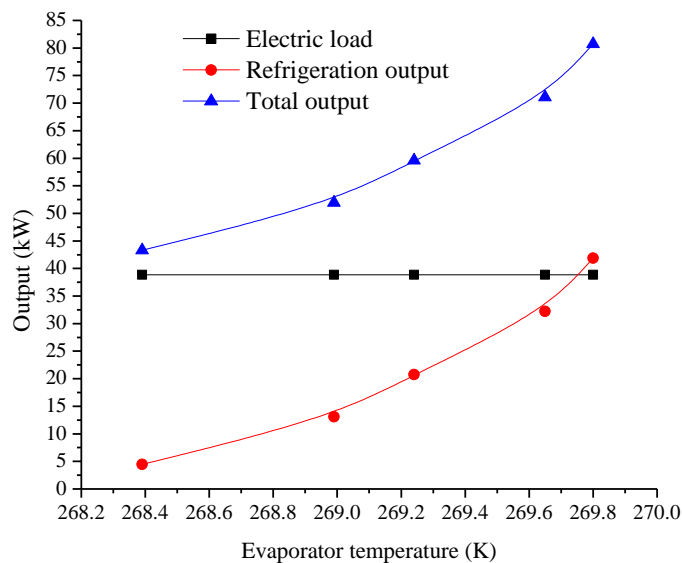


Fig 5.39 Effect of Evaporator temperature on Electric output, Refrigeration and total output

Figure 5.39 shows the increase in the evaporator temperature which causes a significant increase in the refrigeration output of the VAM and total output. In the VAM, the refrigeration capacity increases due to the exhaust heat given to the generator through HRU. Now, the ammonia vapor drives off the solution due to this heat at high pressure leaving behind the hot weak solution in the generator and the high velocity refrigerant ammonia vapor, coming from the generator goes to the condenser. This increased mass flow rate of refrigerant passes through the evaporator also; therefore, there is an increase in the refrigeration output of VAM. The engine power output does not change by the change in evaporator temperature, so the electric power output is constant. The total output is mostly affected by the increase in the refrigeration output of VAM, owing to that, the overall output increases.

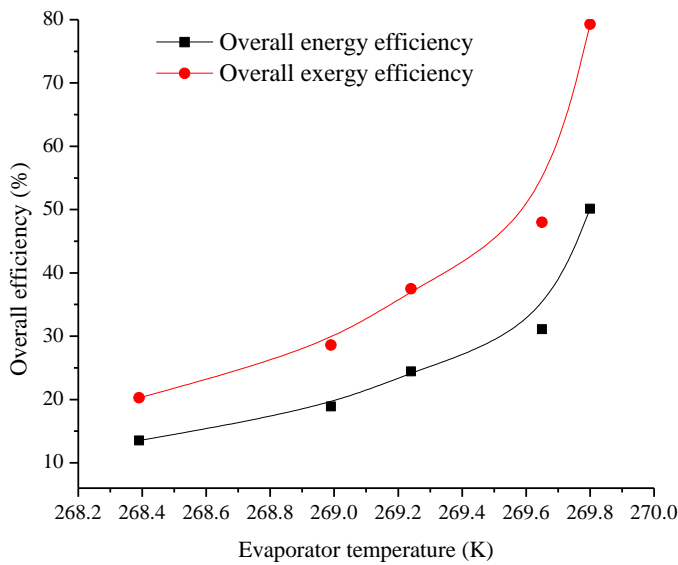


Fig 5.40 Effect of evaporator temperature on overall energy and exergy efficiency

Figure 5.40 indicates the overall energy and exergy efficiency of the hybrid system increase with increase in the evaporator temperature. The first reason is that the finite heat transfer temperature difference between the refrigerant and cooling body reduces from the low temperature to higher temperature of the evaporator. This results in an increase in the overall energy and exergy efficiency of the system with increase in the temperature of the evaporator. The second one reason is that the reduction of the total energy and exergy output is less as compared to that of the energy and exergy input, therefore, the overall energy and exergy efficiency of the hybrid system increase, as the temperature of evaporator increases.

5.6.5. Power Outputs and Overall Efficiency at Condenser Temperature

Figure 5.41 shows the temperature of the condenser increases with the decrease in the refrigeration capacity of VAM because as the temperature of the condenser increases, the condenser pressure also increases subsequently the back pressure on the generator increases. Thus, the mass flow rate of the vapor refrigerant decreases resulting in a decrease in the refrigeration output of the VAM. Further, it is found that the engine power output is constant with the increase in the condenser temperature because the operating conditions for engine do not change, so the electric power output is constant. It can also be seen that as the condenser temperature increases, the total power output of the system decreases as the total power output is mostly dominated

by the VAM refrigeration output, so the total power output decreases with the increase in the condenser temperature.

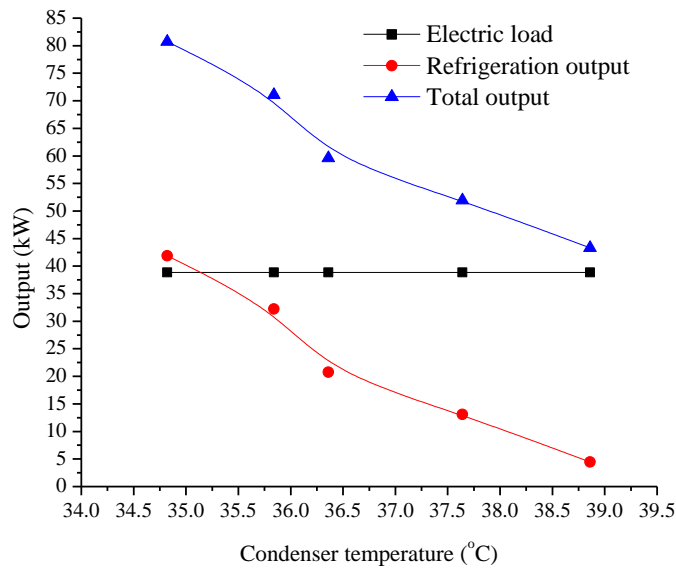


Fig 5.41 Effect of condenser temperature on Electric output, Refrigeration and total output

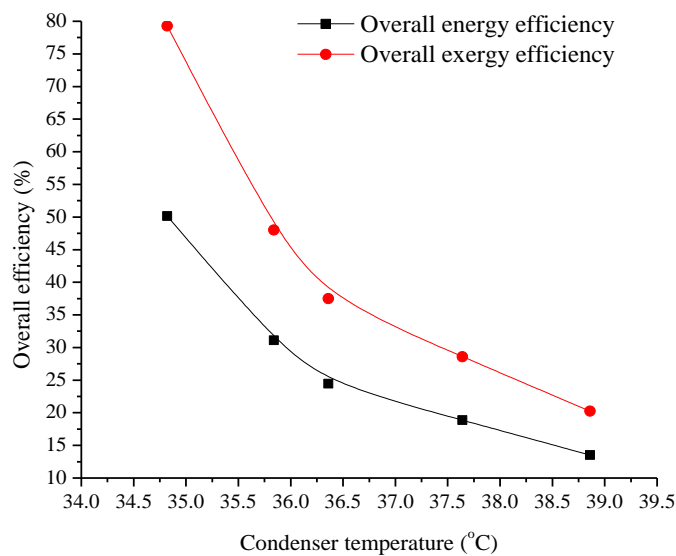


Fig 5.42 Effect of condenser temperature on overall energy and exergy efficiency

Figure.5.42 indicates that the overall energy and exergy efficiency of the hybrid system decrease with the increase in the condenser temperature because the energy and exergy associated with the total power output decrease with the increase in the condenser temperature. In addition, because the refrigeration output decreases with increase in the condenser temperature and the electric power output is constant, the

energy and exergy efficiency of the system decrease with increasing condenser temperature.

The energetic performance analysis is often misleading and deviates from the reality of the phenomenon, while the exergetic analysis takes into account not only the quantity of energy consumed but also the quality of energy conversion. Practically, the each component of the new hybrid cold storage cum power generation system is associated with the irreversibilities. This is the main cause of exergy loss of the individual components as well as of the whole system and due to this, a big part of the hybrid input renewable fuel energy-exhaust gas waste heat has to waste for the generation of the required output of energy. The irreversibilities in the hybrid system can be decreased by the good design of its individual components considering the maximum possible all designing factors. The reduction in the irreversibilities gives better performance and the effective utilization of total input energy.

CHAPTER-VI

CONCLUSIONS

The comparison has been made on the basis of first and second law analysis of the above **investigation of the individual components** with analogous previous research work and the following conclusions have been drawn from this analysis:

6.1 For Gasifier and Producer Gas:

- Wood is found to be effective fuel for generation of producer gas.
- The pressure drop across the filters increases with increase in duration of test, which indicates that the tar and particulates have been filtered out from the producer gas. The producer gas cooling-cleaning unit gives a quality gas with the tar content below the limit of 8 mg/Nm^3 for the applications of internal combustion engine. This value is lower than that of the 'wet packed bed scrubber-based producer gas cooling and cleaning system'.
- The gasification efficiency is found between 70.22% and 81.22%, while the exergy efficiency is limited to the range of 62.73% to 77.75%, which are greater than 'the biomass downdraft gasifier coupled with reciprocating internal combustion engines'. It shows the satisfactory functioning of the gasifier.
- The grate temperature of gasifier varies between the range of 1310°C to 1360°C , which is adequate to the proper gasification.

6.2 For Scheffler Collector:

- The results of power obtained by sun and power given by radiation are analogous, which reflects the proper functioning between sheffler collector and energy receiver.
- The scheffler collector can efficiently be used in winter season because of the low value of cosine losses in winter.
- The effective performance of the scheffler collector is noticed with the normal wind velocity.
- There is always variation in the solar temperature gain and the DNI due to the unavoidable and uncontrollable reasons.

- The scheffler collector has maximum energy and exergy efficiency of 26.25% and 5.05%, which are better than that of the previously coined parabolic trough. It means that Scheffler collectors can be used effectively in this hybrid technology.

6.3 For Vapour Absorption Machine (VAM):

- This conclusion has been made by the experimental investigation's results of the Vapour Absorption Machine (VAM) under the various operating conditions with varying evaporator, generator, condenser and absorber temperatures and it has been found that high performance of the system is obtained at "high evaporator and generator temperatures" and also at "low condenser and absorber temperatures".
- The generator must be designed for a minimum pressure drop with maximum heat transfer efficiency, while the absorber must be designed for maximum pressure drop with minimum heat transfer efficiency for low exergy destruction in both the components, thus the more cooling can be maintained in evaporator at the low temperature of the hybrid solar energy-exhaust gas waste heat.
- It has been noticed from the above discussion that the performance of the cold storage is effective at the normal atmospheric temperature.
- The energetic COP of the vapour absorption machine is found to lie between 0.45 and 0.62, while the exergetic COP lies between 0.36 and 0.39. The Coefficients of Performance (COP) of the VAM are higher in comparison to a single stage ammonia-water vapour absorption refrigeration chiller, which show the effective utilization of available input energy resources and provide a better replacement to the traditional refrigerants.

6.4 For Exhaust Heat and Waste Heat Recovery Unit (HRU):

- 'The exhaust gas heat used' increases with increase in exhaust gas temperature, which represents the quality improvement and better performance can be harnessed from the exhaust gas waste heat.

- The percentage of energy loss and exergy destruction is very less in the HRU in individual and combined analysis, which demonstrates the effective utilization of the hybrid solar energy-exhaust gas waste heat in the HRU.
- The waste heat recovery unit operated from the producer gas has energy and exergy efficiencies of 96.44% and 81.35% respectively, which are more than a 'biomass fuel powered stainless steel high temperature heat exchanger'. The HRU powered by exhaust gas and solar energy also indicates the better energy and exergy analysis than a 'double pipe counter flow heat exchanger'. It is the proof of successful use of 'combustion heat of the PG' and 'hybrid solar energy-exhaust gas waste heat' in the HRU.

6.5 For Combined Analysis of the Hybrid System:

In the combined analysis, the performance of the 'new hybrid cold storage cum power generation system' has been studied by the energetic and exergetic method. The above hybrid system has been compared with the performance of 'the novel combined power and ejector-refrigeration cycle' and, 'the combined power and ejector-absorption refrigeration cycle' in this study. The following conclusions can be derived from the above analysis:

- The overall energy efficiency of the hybrid cold storage cum power generation system is slightly higher than 'the novel combined power and refrigeration cycle' and 'the combined power and ejector-absorption refrigeration cycle'; while an overall exergy efficiency is significantly higher than the 'both of the above cycles', because of the higher heat source temperature for the hybrid system.
- Most exergy destructions occur in the engine, gasifier, scheffler collector, absorber, generator, electric generator and the HRU of the 'hybrid cold storage cum power generation system'. The exergy destructions in the components are higher than 'the novel combined power and refrigeration cycle' and 'the combined power and ejector-absorption refrigeration cycle'. The reason is that the friction and larger temperature difference between the working fluids are maintained in the number of components of the hybrid system than the both the cycles mentioned above.

- Approximately 86.35% of the total input exergy is destructed due to the irreversibilities in the different components of this new hybrid system, 3.99% of the total input exergy is lost to 'the environment and as an unaccounted exergy' and 9.68% is available as the useful exergy output, whereas 15.03% of the total input energy is lost to 'the environment and as an unaccounted energy', 38.98% of the total input energy is used in the different components of the system and 14.83% is available as the useful energy output. The exhaust exergy loss of the hybrid system to the environment is significantly lower than 'the novel combined power and refrigeration cycle' and 'the combined power and ejector-absorption refrigeration cycle'.
- The exergy destruction in the gasifier, scheffler collector, evaporator and the SHE is higher at low heat source temperature and drops with increasing temperature, while the trends of the irreversibility for the others components of the system are opposite.
- In the exhaustive analysis, the parametric evaluation shows that the electric load, exhaust gas temperature, evaporator temperature and condenser temperature have significant effects on the total power output, refrigeration output, energy and exergy efficiency.
- The renewable energy power plant associated with the VAM based on the hybrid solar energy-exhaust gas waste heat provides significantly higher overall energy and exergy efficiencies and hence shows the effective utilization of 'the hybrid solar energy-exhaust gas waste heat'.
- The refrigerants used in 'hybrid cold storage cum power generation system' are of the zero ODP and negligible GWP hence are favourable to the environment.
- The emission sample of exhaust gas waste heat from renewable energy power plant for the production of cooling reduces the problems related to the global environment such as the greenhouse effect, and thus inversely, this technology has also a huge scope to save the fossil fuel.

It can be concluded through the above discussions that, the 'new hybrid cold storage cum power generation system' is admissible from the viewpoint of the global environment, thermodynamics and the technology.

CHAPTER-VII

SCOPE FOR FUTURE WORK

Based on the above study, the 'new hybrid cold storage cum power generation system' can be reflected in the several ways as per their feasibility in the near future. The co-generation technology can specially be a boon to save energy. The main future scopes of the 'new hybrid system' can be grouped as follows:

7.1 Extended HRU Design For Multi-heat Resources

Many types of heat sources can be used to drive the absorption machine, such as steam, hot water, exhaust gas, oil, LPG and natural gas. Among them the most widely used heating media are steam, natural gas and hot water. From a research perspective, the several researchers like Mustafi et al. (2006), Shiba and Bejan (2001), Al-attab and Zainal (2010), Lee and Bae (2008), Gomez et al. (2009), Ghazikhani et al. (2014) etc. indicate towards the universal design of the heat recovery unit in the forthcoming time, in which the HRU would be designed to adapt any type of heat source associated with vapor absorption machine. The extended heat recovery unit using various heat sources can meet the cooling demand to a great extent.

7.2 System Integration For Application

Many cogeneration concepts with heating system can be converted into tri-generation, but the selection of one over another requires detailed study of long-term technical and economic performance. On the basis of the hybrid system developed in this thesis, the researchers such as Sedigh and Saffari (2012), Minciuc et al. (2003), Kong et al. (2005), Coronado et al. (2011), Agarwal et al. (2012) etc. have recommended an integrated designed heat exchanger after the exhaust gas or HRU that can be installed for the heating purpose, which maximize the overall efficiency and lowers the capital cost as well as finally reduces the associated operational and maintenance fees.

7.3 Formation Of Chemical And Fertilizers

More than a few investigators like Franco and Giannini (2005), Soheli and Jack (2011), Shabangu et al. (2014), Banapurmath and Tewari (2009), Prasad et al. (2009), Sezer (2011), Liaquat et al. (2013) etc. have introduced the sample of conversion of producer gas into the chemicals and fertilizers. They declared that the producer gas

will be used for the production of chemicals like methanol and formic acid due to the scarcity of the fossil fuels, these chemicals will be in economical feasible proposition. Another important application, the ash of gasifier has been addressed recently as fertilizer. The ash contained high total content of calcium, iron, phosphorus, potassium, sulphur, magnesium and minor amounts of heavy metals, such as zinc, copper, chromium and nickel. The use of ash as fertilizer could also be a way to increase the level of organic carbon in the soil of farm. If a char's fraction is left un-gasified in the solid residuals and these are amended to farm soil.

7.4 Co-generation Technology For Residential Use

The high energy consumption is the challenge, which is faced by existing technologies for cooling and power generation, thus, future developments of renewable energy based building-integrated cooling and power systems on energy saving are attractive and crucial. Some of the novel integrated system may become good alternatives to the present conventional technologies. The idea of design and fabrication of building-integrated cogeneration system taken from references such as Lior (2002), Jurado et al. (2003), Jankes et al. (2012), Ahrenfeldt et al. (2013) etc. will be a smart system. The power developed by renewable energy could be easily integrated with the central grid network via smart metres. The DC power systems for residential application should be a good solution. The refrigeration effect generated in the VAM by its exhaust can easily be used as central cooling system for the buildings.

7.5 Integration With Energy Storage

Thermal energy storage is one of the most promising ways for energy saving in the buildings. The integrated envelopes with building of phase change material (PCM) as energy storage is provided by a few researchers like Sardeshpande and Pillai (2012), Wu and Wang (2006), Kawabata et al. (2012), Kumar et al. (2015) etc. in the several ways. The PCM can be integrated with almost every part of the building envelope, such as PCM ceilings, PCM walls, PCM windows and PCM floors. Several PCM applications in the buildings such as active heating and night cooling can be achieved by this technology.

In India, it is required to have a joint financial effort of the government to a rapid introduction of the co-generation technology for the massive scale utilization so that the energy related problems can be dealt easily in the near future.

LIMITATIONS

- The high gasification temperature (800-1300°C) is required for proper gasification of biomass.
- The tar content after producer gas cooling-cleaning unit is limited to 8 mg/Nm³. Therefore the internal combustion engine cannot be maintenance free.
- There are various processes of operations in engines, so exergy destruction always exists and provides lower efficiency.
- The maximum generation of electric power is 38.86 kWe with -5°C temperature of the VAM. So it can be set up as a micro-scale plant.
- The maximum temperature by the scheffler collector can be achieved 125°C, which is lower than its designed value due to irreversibilities.
- The maximum temperature in the HRU is maintained of 316°C with the help hybrid solar energy-exhaust gas waste heat.
- The ammonia boils at -33.34°C at the atmospheric pressure, so the minimum required temperature can be obtained in the VAM. If the temperature is maintained below the above boiling temperature, the pressure in the evaporator is lower than the atmospheric pressure and the suction volume is very large when a refrigerant with high boiling temperature is used.
- The pressure in the condenser is very high with low boiling point of refrigerant.
- The performance of the hybrid system is low due to the very high pressure ratio of the vapour absorption machine (VAM).
- The maximum temperature of exhaust gas is limited to 465°C because of the design considerations of the engine.
- The combustion of producer gas gives temperature of 674.25°C, which establishes the better performance of the HRU.
- The robust hybrid co-generation technology is required broad area for installation. So it is suitable for commercial buildings and societies.

CONTRIBUTIONS

This robust system plays an important role in the hybrid renewable energy utilization and provides us full benefits efficiently. However, it has many technical and commercial challenges, but the integration of the VAM with power generator can support the nation in the following ways:

- Increased energy and exergy efficiency of the system increases the energy saving.
- It provides a way to use any kinds of hybrid energies.
- Control the emissions easily
- Decentralize the power which can eliminate the distribution and transmission cost and losses with meeting the energy shortages.
- It can support in fuel saving also.
- This system can be used in power generation and cooling purpose for commercial buildings specially.

REFERENCES

1. Abdollahpour, A., Ahmadi, Md.H. and Mohammadi, A.H. (2014) 'Thermodynamic model to study a solar collector for its application to Stirling engines', *Energy Conversion and Management*, Vol. 79, pp. 666-673.
2. Agarwal, B.K and Karimi, M.N. (2012) 'Thermodynamic performance assessment of a novel waste heat based triple effect refrigeration cycle', *International Journal of Refrigeration*, Vol. 35, pp. 1647-1656.
3. Ahrenfeldt, J., Thomsen, T.P., Henriksen, U. and Clausen, L.R. (2013) 'Biomass gasification cogeneration-A review of state of the art technology and near future perspectives', *Applied Thermal Engineering*, Vol. 50, No. 2, pp. 1407-1417.
4. Al-attab, K.A. and Zainal, Z.A. (2010) 'Performance of high-temperature heat exchangers in biomass fuel powered externally fired gas turbine systems', *Renewable Energy*, Vol. 35, pp. 913-920.
5. Alotaibi, S., Sen, M., Goodwine, B. and Yang, K.T. (2004) 'Controllability of cross-flow heat exchangers', *International Journal of Heat and Mass Transfer*, Vol. 47, No. 5, pp. 913-924.
6. Andersen, S.O. and Lupinacci, J.M. (1988) 'Implication of CFCs on environmental quality and opportunities for engineering solutions', *International Journal of Refrigeration*, Vol. 11, No. 4, pp. 253-256.
7. Anis, A. and Zainal, Z.A. (2011) 'Tar reduction in biomass producer gas via mechanical, catalytic and thermal methods: A review', *Renewable and Sustainable Energy Reviews*, Vol. 15, No. 5, pp. 2355-2377.
8. Arena, U. (2012) 'Process and technological aspects of municipal solid waste gasification. A review', *Waste Management*, Vol. 32, pp. 625-639.
9. Asadullah, M. (2014) 'Barriers of commercial power generation using biomass gasification gas: A review', *Renewable and Sustainable Energy Reviews*, Vol. 29, pp. 201-215.
10. Baliga, B.N., Dasappa, S., Shrinivasa, U. and Mukunda, H.S. (1993) 'Gasifier based power generation: Technology and economics', *Sadhan*, Vol. 18, Part-1, pp. 57-75.
11. Balki, M.K., Sayin, C. and Canakci, M. (2014) 'The effect of different alcohol fuels on the performance, emission and combustion characteristics of a gasoline engine', *Fuel*, Vol. 115, pp. 901-906.

12. Banapurmath, N.R. and Tewari, P.G. (2009) 'Comparative performance studies of a 4-stroke CI engine operated on dual fuel mode with producer gas and Honge oil and its methyl ester (HOME) with and without carburetor', *Renewable Energy*, Vol. 34, pp. 1009-1015.
13. Baratieri, M., Baggio, P., Bosio, B., Grigiante, M. and Longo, G.A. (2009) 'The use of biomass syngas in IC engines and CCGT plants: A comparative analysis', *Applied Thermal Engineering*, Vol. 29, pp. 3309-3318.
14. Barea, A.G., Leckner, B., Perales, A.V., Nilsson, S. and Cano, D.F. (2013) 'Improving the performance of fluidized bed biomass/waste gasifiers for distributed electricity: A new three-stage gasification system', *Applied Thermal Engineering*, Vol. 50, No. 2, pp.1453–1462.
15. Belgiorno, V., De, F.G., Della, R.C. and Napoli, R.M.A. (2003) 'Energy from gasification of solid wastes', *Waste management*, Vol. 23, pp. 1-15.
16. Beziel, M. and Stephan, K. (1995) 'Temperature distribution in the outlet of cross-flow heat exchangers', *International Journal of Heat and Mass Transfer*, Vol. 38, No. 2, pp. 371-380.
17. Bhattacharya, S.C. and Dutta, A. (2000) 'Two-stage gasification of wood with preheated air supply: A promising technique for producing gas of low tar content', 1999 ISES Solar World Congress, *Progress in Energy and combustion Science*, Vol. 1, pp. 557-561.
18. Bhave, A.G., Vyas, D.K. and Patel, J.B. (2008) 'A wet packed bed scrubber based producer gas cooling and cleaning system', *International Journal of Renewable energy*, Vol. 33, pp. 1716-1720.
19. Bhoi, P.R. and Channiwala, S.A. (2008) 'Optimization of producer gas fired premixed burner', *Renewable energy*, Vol. 33, pp. 1209-1219.
20. Bhirud, N. and Tandale, M.S. (2006) 'Field evaluation of a fixed-focus concentrators for industrial oven' *Advances in Energy Research*.
21. Blik, A., Swaaij, W.P.M. and Westerterp, K.R. (1984) 'Small industrial-scale producer gas units', *Progress in Energy and combustion Science*, Vol. 10, No. 3, pp. 341-357.
22. Boyle, S. (1994) 'Making a renewable energy future a reality. Case studies in successful renewable energy development', *International Journal of Renewable energy*, Vol. 5, pp. 1322 -1333.

23. Buckinx, G., Rogiers, F. and Baelmans, M. (2013) 'Thermal design and optimization of small-scale high effectiveness cross-flow heat exchangers', *International Journal of Heat and Mass Transfer*, Vol. 60, pp. 210-220.
24. Calm, J.M. (2002) 'Options and outlook for chiller refrigerants', *International Journal of Refrigeration*, Vol. 25, No. 6, pp. 705-715.
25. Calm, J.M. (2002) 'Emissions and environmental impacts from air-conditioning and refrigeration systems', *International Journal of Refrigeration*, Vol. 25, No. 3, pp. 293-305.
26. Calm, J.M. (2006) 'Comparative efficiencies and implications for greenhouse gas emissions of chiller refrigerants', *International Journal of Refrigeration*, Vol. 29, pp. 833-841.
27. Calm, J.M. (2008) 'The next generation of refrigerants – Historical review, considerations, and outlook', *International Journal of Refrigeration*, Vol. 31, No. 7, pp. 1123-1133.
28. Centeno, F., Mahkamov, K., Lora, E.E.S. and Andrade, R.V. (2012) 'Theoretical and experimental investigations of a downdraft biomass gasifier-spark ignition engine power system', *Renewable Energy*, Vol. 37, pp. 97–108.
29. Chandak, A., Somani, S.K. and Suryaji, P.M. (2011) 'Comparative Analysis of SK-14 and PRINCE-15 Solar Concentrators', *Proceedings of the World Congress on Engineering*, ISSN: 2078-0958, Vol. 8, July 6-8.
30. Chen, G., Andries, J. and Spliethoff, H. (2003) 'Biomass conversion into fuel gas using circulating fluidised bed technology: the concept improvement and modelling discussion', *Renewable energy*, Vol. 28, pp. 985-994.
31. Cho, H., Mago, P.J., Luck, R. and Chamra, L.M. (2009) 'Evaluation of CCHP systems performance based on operational cost, primary energy consumption, and carbon dioxide emission by utilizing an optimal operation scheme', *International Journal of Applied energy*, Vol. 86, No. 12, pp. 2540-2549.
32. Chua, H.T., Toh, H.K., Malek, A., Ng, K.C. and Srinivasan, K. (2000) 'A general thermodynamic framework for understanding the behaviour of absorption chillers', *International Journal of Refrigeration*, Vol. 23, pp. 491-507.
33. Coronado, C.R., Yoshioka, J.T. and Silveira, J.L. (2011) 'Electricity, hot water and cold water production from biomass. Energetic and economical analysis of the compact system of co-generation run with wood gas from a small downdraft gasifier', *International Journal of Renewable Energy*, Vol. 36, pp.1861-1868.

34. Dafle, V.R. and Shinde, N.N. (2012) 'Design, Development & Performance Evaluation Of Concentrating Monoaxial Scheffler Technology For Water Heating And Low Temperature Industrial Steam Application', *International Journal of Engineering Research and Applications*, ISSN: 2248-9622, Vol. 2, pp. 848-852.
35. Dai, Y.P., Wang, J.F. and Gao, L. (2009) 'Exergy analysis, parametric analysis and optimization for a novel combined power and ejector refrigeration cycle', *Applied Thermal Engineering*, Vol. 29, pp. 1983-1990.
36. Dasappa, S., Subbukrishna, D.N., Suresh, K.C., Pual, P.J. and Prabhu, G.S. (2011) 'Operational experience on a grid connected 100 kWe biomass gasification power plant in Karnataka, India', *Energy for Sustainable Development*, Vol. 15, No. 3, pp. 231-239.
37. Dawoud, B. (2007) 'A hybrid solar assisted adsorption cooling unit for vaccine storage', *International Journal of renewable energy*, Vol. 32, No. 6, pp. 947-964.
38. Devotta, S., Asthana, S. and Joshi, R. (2004) 'Challenges in recovery and recycling of refrigerants from Indian refrigeration and air-conditioning service sector', *Atmospheric Environment*, Vol. 38, pp. 845-854.
39. Dincer, I., Edin, M. and Ture, I.E. (1995) 'Performance evaluation of a solar powered absorption refrigeration system', *International Journal Energy conversion management*, Vol. 37, No. 1, pp. 51-58.
40. Dixit, T. and Ghosh, I. (2013) 'Two-stream cross flow heat exchangers in thermal communication with the surroundings – A generalized analysis', *International Journal of Heat and Mass Transfer*, Vol. 66, pp. 1-9.
41. Dorfling, C., Hornung, C.H., Hallmark, B., Beaumont, R.J.J., Fovargue, H. and Mackley, M.R. (2010) 'The experimental response and modelling of a solar heat collector fabricated from plastic microcapillary films', *Solar Energy Materials & Solar Cells*, Vol. 94, pp. 1207-1221.
42. Dutsadee, N., Homdoug, N., Ramaraj, R., Santisouk, K. and Inthavideth, S. (2015) 'Performance analysis of power generation by producer gas from refuse derived fuel-5 (RDF-5)', *International Journal of Sustainable and Green Energy*, Vol. 4, No. 1-1, pp. 44-49.
43. Dweepson, Subramanian, S.C., Kumar, J.A. and Sakthivel, S. (2014) 'An Experimental Assessment of Performance and Exhaust Emission Characteristics by addition of Hydroxy (HHO) gas in Twin cylinder C.I. Engine', *International*

- Journal of Innovative Research in Science, Engineering and Technology, Vol. 3, No. 2(S), pp. 60-67.
44. Fagernas, L., Brammer, J., Wilen, C., Lauer, M. and Verhoeff, F. (2010) 'Drying of biomass for second generation synfuel production', *Biomass and Bioenergy*, Vol. 34, No. 9, pp.1267–77.
 45. Fakheri, A. (2014) 'Efficiency analysis of heat exchangers and heat exchanger networks', *International Journal of Heat and Mass Transfer*, Vol. 76, pp. 99-104.
 46. Faith, L., Piper, M. and Skye, B. (2014) 'Wood Gas from the Suction Gasifier: A Practical Investigation', *International Journal of Research in Applied Sciences*, ISSN: 2356-5675, Vol. 03, pp. 22-28.
 47. Fischer, S.K. (1993) 'Total equivalent warming impact: a measure of the global warming impact of CFC alternatives in refrigerating equipment', *International Journal of Refrigeration*, Vol. 16, N. 6, pp. 423-428.
 48. Franco, A. and Giannini, N. (2005) 'Perspectives for the use of biomass as fuel in combined cycle power plants', *International Journal of thermal Sciences*, Vol. 44, pp. 163-177.
 49. Garg, A. and Sharma, M.P. (2013) 'Performance Evaluation of Gasifier Engine System Using Different Feed Stocks', *International Journal of Emerging Technology and Advanced Engineering*, ISSN-2250-2459, Vol. 3, pp. 188-191.
 50. Gassner, M. and Marechal, F. (2009) 'Thermodynamic comparison of the FICFB and Viking gasification concepts', *Energy*, DOI:10.1016/j.energy.2009.05.011, pp. 1-18.
 51. Ghazikhani, M., Hatami, Md., Ganji, D.D., Bandpy, M.G., Behravan, A. and Shahi, G. (2014) 'Exergy recovery from the exhaust cooling in a DI diesel engine for BSFC reduction purposes', *Energy*, Vol. 65, pp. 44-51.
 52. Ghazikhani, M., Hatami, Md., Safari, B. and Ganji, D.D. (2014) 'Experimental investigation of exhaust temperature and delivery ratio effect on emissions and performance of a gasoline–ethanol two-stroke engine', *Case Studies in Thermal Engineering*, Vol. 2, pp. 82-90.
 53. Gomez, L.C., Navarro, H.A., de Godoy, S.M., Campo, A. and Jabardo, J.M.S. (2009) 'Thermal characterization of a cross-flow heat exchanger with a new flow arrangement', *International Journal of Thermal Sciences*, Vol. 48, No. 11, pp. 2165-2170.

54. Gonzalez, F.O.C., Mahkamov, K., Lora, E.E.S., Andrade, R.V. and Jaen, R.L. (2013) 'Prediction by mathematical modeling of the behavior of an internal combustion engine to be fed with gas from biomass, in comparison to the same engine fueled with gasoline or methane', *International Journal of Renewable Energy*, Vol. 60, pp. 427-432.
55. Guo, Z.Y., Liu, X.B., Tao, W.Q. and Shah, R.K. (2010) 'Effectiveness-thermal resistance method for heat exchanger design and analysis', *International Journal of Heat and Mass Transfer*, Vol. 53, pp. 2877-2884.
56. Gupta, P. and Atrey, M.D. (2000) 'Performance evaluation of counter flow heat exchangers considering the effect of heat in leak and longitudinal conduction for low-temperature applications', *Cryogenics*, Vol. 40, pp. 469-474.
57. Hagos, F.Y., Aziz, A.R.A. and Sulaiman, S.A. (2014) 'Effect of Air-fuel Ratio on the Combustion Characteristics of Syngas (H₂: CO) in Direct-injection Spark-ignition Engine', *Energy Procedia*, Vol. 61, pp. 2567-2571.
58. Hagos, F.Y., Aziz, A.R.A. and Sulaiman, S.A. (2014) 'Trends of Syngas as a Fuel in Internal Combustion Engines', *Advances in Mechanical Engineering*, Vol. 2014, Article ID 401587, pp. 1-10, <http://dx.doi.org/10.1155/2014/401587>.
59. Hasler, P. and Nussbaumer, Th. (1999) 'Gas cleaning for IC engine applications from fixed bed biomass gasification', *Biomass and Bioenergy*, Vol. 16, No. 6, pp. 385-395.
60. Hasler, P. and Nussbaumer, T. (2000) 'Sampling and analysis of particles and tars from biomass gasifiers', *Biomass and Bioenergy*, Vol. 18, pp. 61-66.
61. Hassan, S., Mohd Nor, F., Zainal, Z.A. and Miskam, M.A. (2011) 'Performance and Emission Characteristics of Supercharged Biomass Producer Gas-diesel Dual Fuel Engine', *Journal of Applied Sciences*, Vol. 11, pp. 1606-1611.
62. Homdoug, N., Tippayawong, N. and Dussadee, N. (2015) 'Performance and emissions of a modified small engine operated on producer gas', *Energy Conversion and Management*, Vol. 94, pp. 286-292.
63. Homdoug, N., Tippayawong, N. and Dussadee, N. (2015) 'Performance investigation of a modified small engine fuelled with producer gas', *Maejo International Journal of Science and Technology*, ISSN 1905-7873, Vol. 9, No. 1, pp. 10-20.

64. Hsieh, W.D., Chen, R.H., Wu, T.L. and Lin, T.H. (2002) 'Engine performance and pollutant emission of an SI engine using ethanol-gasoline blended fuels', *Atmospheric Environment*, Vol. 36, pp. 403-410.
65. Huang, W., Hu, P. and Chen, Z. (2012) 'Performance simulation of a parabolic trough solar collector', *Solar Energy*, Vol. 86, No. 2, pp. 746-755.
66. Islam, Md. R., Wijesundera, N.E. and Ho, J.C. (2006) 'Heat and mass transfer effectiveness and correlations for counter-flow absorbers', *International Journal of Heat and Mass Transfer*, Vol. 49, No. 21-22, pp. 4171-4182.
67. Jankes, G.G., Trninic, M.R. and Stamenic, M.S. (2012) 'Biomass gasification with CHP production a review of the state-of-the-art technology and near future perspectives', *Thermal Science*, Vol. 16, pp. S115-S130.
68. Jaojaruek, K., Jarungthammachote, S., Gratuito, M.K.B., Wongsuwan, H. and Homhual, S. (2011) 'Experimental study of wood downdraft gasification for an improved producer gas quality through an innovative two-stage air and premixed air/gas supply approach', *Bioresource Technology*, Vol. 102, No.7, pp. 4834 - 40.
69. Jayasimha, B.K. (2006) 'Application of Scheffler reflectors for process industry', *International Solar Cooker Conference*, Granada, Spain.
70. Jordan, C.A. and Akay, G. (2012) 'Occurrence, composition and dew point of tars produced during gasification of fuel cane bagasse in a downdraft gasifier', *Biomass and Bioenergy*, Vol. 42, pp. 51-58.
71. Jurado, F., Cano, A. and Carpio, J. (2003) 'Modelling of combined cycle power plants using biomass', *Renewable Energy*, Vol. 28, pp. 743-753.
72. Kalam, M.A. and Masjuki, H.H. (2011) 'An experimental investigation of high performance natural gas engine with direct injection', *Energy*, Vol. 36, pp. 3563-3571.
73. Kanoglu, M. Isik, S.K. and Abusoglu, A. (2005) 'Performance characteristics of a Diesel engine power plant', *Energy Conversion and Management*, Vol. 46, pp. 1692-1702.
74. Kanogolu, M. and Dincer, I. (2009) 'Performance assessment of cogeneration plants', *Energy conversion and management*, Vol. 50, pp. 76-81.
75. Kapale, U.C. and Chand, S. (2006) 'Modeling for shell-side pressure drop for liquid flow in shell-and-tube heat exchanger', *International Journal of Heat and Mass Transfer*, Vol. 49, No. 3-4, pp. 601-610.

76. Kawabata, M., Kurata, O., Iki, N., Furutani, H. and Tsutsumi, A. (2012) 'Advanced integrated gasification combined cycle (A-IGCC) by exergy Recuperation technical challenges for future generations', *Journal of Power Technologies*, Vol. 92, No. 2, pp. 90-100.
77. Kaynakli, O. and Yamankaradeniz, R. (2007) 'Thermodynamic analysis of absorption refrigeration system based on entropy generation', *Current Science*, Vol. 92, No. 4, pp. 472-479.
78. Khaliq, A., Agarwal, B.K. and Kumar, R. (2012) 'First and second law investigation of waste heat based combined power and ejector absorption refrigeration cycle', *International Journal of Refrigeration*, Vol. 35, pp. 88-97.
79. Khan, J.U.R., Yaqub, M. and Zubair, S.M. (2003) 'Performance characteristics of counter flow wet cooling towers', *Energy Conversion and Management*, Vol. 44, pp. 2073-2091.
80. Kline, S.J., and McClintock, F.A. (1953) 'Describing Uncertainties in Single-Sample Experiments', *Mechanical Engineering*, Vol. 75, No. 1, pp. 3-8.
81. Kong, D., Liu, J., Zhang, L., He, H. and Fang, Z. (2010) 'Thermodynamic and Experimental Analysis of an Ammonia-Water Absorption Chiller', *Energy and Power Engineering*, Vol. 2, pp. 298-305.
82. Kong, X.Q., Wang, R.Z., Wu, J.Y., Huang, X.H., Huangfu, Y., Wu, D.W. and Xu, Y.X. (2005) 'Experimental investigation of a micro-combined cooling, heating and power system driven by a gas engine', *International Journal of Refrigeration*, Vol. 28, pp. 977-987.
83. Korakianitis, T., Namasivayam, A.M. and Crookes, R.J. (2011) 'Natural-gas fueled spark-ignition (SI) and compression-ignition (CI) engine performance and emissions', *Progress in Energy and Combustion Science*, Vol. 37, pp. 89-112.
84. Kumar, A., Kumar, N., Baredar, P. and Shukla, A. (2015) 'A review on biomass energy resources, potential, conversion and policy in India', *Renewable and Sustainable Energy Reviews*, Vol. 45, pp. 530-539.
85. Kumar, M.L.S.D. and Reddy, K.V.K. (2010) 'Effect of fuel injection pressure on full load performance of diesel-producer gas dual fuel engine', *Indian Journal of Science and Technology*, ISSN: 0974- 6846, Vol. 3, No. 10, pp. 1056-1061.
86. Kumar, N. Vishwanath, G. and Gupta, A. (2011) 'An exergy based unified test protocol for solar cookers of different geometries', *World Renewable Energy Congress*, Sweden, pp. 3741-3748, 8-13 May.

87. Lee, S. and Bae, C. (2008) 'Design of a heat exchanger to reduce the exhaust temperature in a spark-ignition engine', *International Journal of Thermal Sciences*, Vol. 47, No. 4, pp. 468-478.
88. Liaquat, A.M., Masjuki, H.H., Kalam, M.A., Fattah, I.M.R., Hazrat, M.A., Varman, M., Mofijur, M. and Shahabuddin, M. (2013) 'Effect of coconut biodiesel blended fuels on engine performance and emission characteristics', 5th BSME International Conference on Thermal Engineering, *Procedia Engineering*, Vol. 56, pp. 583-590.
89. Lior, N. (2002) 'Thoughts about future power generation systems and the role of exergy analysis in their development', *Energy conversion and management*, Vol. 43, pp. 1187-1198.
90. Luo, X., Li, M. and Roetzel, W. (2002) 'A general solution for one-dimensional multi-stream heat exchangers and their networks', *International Journal of Heat and Mass Transfer*, Vol. 45, No. 13, pp. 2695-2705.
91. Malik, A. and Mohapatra, S.K. (2013) 'Biomass-based gasifiers for internal combustion (IC) Engines-A review', *Indian Academy of Sciences*, Vol. 38, No. 3, pp. 461-476.
92. Mangani, F., Maione, M., Lattanzi, L. and Arduini, J. (2000) 'Atmospheric measurements of the halogenated hydrocarbons involved in global change phenomena', *Atmospheric Environment*, Vol. 34, No. 29-30, pp. 50303-50309.
93. Martinez, J.D., Mahkamov, K., Andrade, R.V. and Lora, E.E.S. (2012) 'Syngas production in downdraft gasifiers and its application using internal combustion engines', *International Journal of renewable energy*, Vol. 38, pp.1-9.
94. Mawire, A. and Taole, S.H. (2014) 'Experimental energy and exergy performance of a solar receiver for a domestic parabolic dish concentrator for teaching purposes', *Energy for Sustainable Development*, Vol. 19, pp. 162-169.
95. Mazouz, S., Mansouri, R. and Bellagi, A. (2014) 'Experimental and thermodynamic investigation of an ammonia/water diffusion absorption machine', *International Journal of Refrigeration*, Vol. 45, pp. 83-91.
96. McKendry, P. (2002) 'Energy production from biomass (part 1): overview of biomass', *Bio-resource Technology*, Review paper, Vol. 83, pp. 37-46.
97. McLinden, M.O., Kazakov, A.F., Brown, J.S. and Domanski, P.A. (2014) 'A thermodynamic analysis of refrigerants: Possibilities and tradeoffs for Low-GWP refrigerants', *International Journal of Refrigeration*, Vol. 38, pp. 80-92.

98. McMullan, J.T. (2002) 'Refrigeration and the environment-issues and strategies for the future', *International Journal of Refrigeration*, Vol. 25, No. 1, pp. 89-99.
99. Minciuc, E., Corre, O.L., Athanasovici, V., Tazerout, M. and Bitir, I. (2003) 'Thermodynamic analysis of tri-generation with absorption chilling machine', *Applied Thermal Engineering*, Vol. 23, pp. 1391-1405.
100. Mohanraj, M., Jayaraj, S. and Muraleedharan, C. (2009) 'Environment friendly alternatives to halogenated refrigerants-A review', *International Journal of greenhouse gas control*, Vol. 3, pp. 108-119.
101. Mohod, A.G. Gadge, S.R. and Madansure, V.N. (2003) 'Liberation of Carbon Monoxide Through Gasifier-IC Engine System' *IE(I) Journal-ID*, Vol 84.
102. Mondol, J.D., Smyth, M. and Zacharopoulos, A. (2011) 'Experimental characterisation of a novel heat exchanger for a solar hot water application under indoor and outdoor conditions', *Renewable Energy*, Vol. 36, pp. 1766-1779.
103. Mountouris, A., Voutsas, E. and Tassios, D. (2006) 'Solid waste plasma gasification: Equilibrium model Development and exergy analysis', *Energy Conversion and Management*, Vol. 47, pp. 1723–1737.
104. Mountouris, A., Voutsas, E. and Tassios, D. (2008) 'Plasma gasification of sewage sludge: Process development and energy optimization', *Energy Conversion and Management*, Vol. 49, No. 8, pp. 2264-2271.
105. Mukhopadhyay, K. (2004) 'An assessment of a biomass gasification based power plant in the sunderbans', *Biomass and Bioenergy*, Vol. 27, pp. 253-64.
106. Mukunda, H.S., Dasappa, S., Paul, P.J., Rajan, N.K.S. and Shrinivasa, U. (1994) 'Gasifiers and combustors for biomass–technology and field studies', *Energy Sustainable Development*, Vol. 1, No. 3, pp. 27-38.
107. Mukunda, H.S., Paul, P.J., Dasappa, S., Shrivasa, U., Sharan, H., Buehler, R., Hasler, P. and Kaufmann, H. (1994) 'Results of an Indo-Swiss programme for qualification and testing of a 300kW IISc-Dasag gasifier' *Energy for sustainable Development*, Vol. 1, No.4, pp. 46-49.
108. Munir, A., Hensel, O. and Scheffler, W. (2010) 'Design principle and calculations of scheffler fixed focus concentrator for medium temperature applications', *International Journal of Solar Energy*, Vol. 84, pp. 1490-1502.
109. Murillo, S., Miguez, J.L., Porteiro, J., Gonzalez, L.M.L., Granada, E. and Moran, J.C. (2005) 'LPG: Pollutant emission and performance enhancement for spark-

- ignition four strokes outboard engines', *Applied Thermal Engineering*, Vol. 25, pp. 1882-1893.
110. Mustafi, N.N., Miraglia, Y.C., Raine, R.R., Bansal, P.K. and Elder, S.T. (2006) 'Spark-ignition engine performance with 'Power-gas' fuel (mixture of CO/H₂): A comparison with gasoline and natural gas', *Fuel*, Vol. 85, No.12/13, pp. 1605-12.
111. Narayanan, S.P. and Venkatarathnam, G. (1999) 'Performance of a counter-flow heat exchanger with heat loss through the wall at the cold end', *Cryogenics*, Vol. 39, pp. 43-52.
112. Navarro, H.A. and Gomez, L.C. (2005) 'A new approach for thermal performance calculation of cross-flow heat exchangers', *International Journal of Heat and Mass Transfer*, Vol. 48, No. 18, pp. 3880-3888.
113. Nene, A.A. and Suyambazhahan, S. (2012) 'Thermal Efficiency Optimization Applied to Scheffler Solar Concentrator', *Proceedings of International Conference on Control System and Power Electronics, CSPE*, pp. 593-598.
114. Ogulata, R.T. and Doba, F. (1998) 'Experiments and entropy generation minimization analysis of a cross-flow heat exchanger', *International Journal of Heat and Mass Transfer*, Vol. 41, No. 2, pp. 373-381.
115. Ohta, T.N., Baba, A., Takahashi, T. and Shinohara, M. (2006) 'Waste heat recovery device for internal combustion engine, US Patent No. US 6990805 B2, pp. 1-6.
116. Padilla, R.V., Demirkaya, G., Goswami, D.Y., Stefanakos, E. and Rahman, M.M. (2010) 'Analysis of power and cooling cogeneration using ammonia-water mixture', *Energy*, Vol. 35, No. 12, pp. 4649-4657.
117. Paethanom, A., Nakahara, S., Kobayashi, M., Prawisudha, P. and Yoshikawa, K. (2012) 'Performance of tar removal by absorption and adsorption for biomass gasification', *Fuel Processing Technology*, Vol. 104, pp. 144–154.
118. Panwar, N.L., Kothari, R. and Tyagi, V.V. (2012) 'Thermo chemical conversion of biomass – Eco friendly energy routes', *Renewable and Sustainable Energy Reviews*, Vol. 16, pp. 1801-1816.
119. Patel, R.D. and Ramana, P.V. (2013) 'Energy & Exergy Analysis of Heat Exchanger', *International Journal of Scientific & Engineering Research*, Vol. 4, No. 6, pp. 1382-1389.

120. Pathak, B.S., Kapatel, D.V., Bhoi, P.R., Sharma, A.M. and Vyas, D.K. (2007) 'Design and Development of Sand Bed Filter for Upgrading Producer Gas to IC Engine Quality Fuel', *International Energy Journal*, Vol. 8, pp. 15-20.
121. Patil, R.J., Awari, G.K. and Singh, M.P. (2011) 'Performance analysis of scheffler reflector and formulation of mathematical model', *VSRD Technical & Non- Technical Journal*, Vol. 2, No. 8, pp. 390-400.
122. Patil, R.J. Awari, G.K. and Singh, M.P. (2012) 'Comparative Study of Mathematical Modeling and Simulation of Scheffler Reflector', *International Journal for Technical Research & Development*, Vol. 1, No. 1, pp. 13-28.
123. Phate, M.R, Gadkari, D.M., Avachat, S.S. and Tajne, A.D. (2014) 'Experimental Analysis of 2.7 m² Scheffler Reflector and Formulation of a Model', *International Journal of Engineering Trends and Technology*, ISSN: 2231-5381, vol. 12, No. 1, pp. 1-5.
124. Phate, M.R. and Bhortake, R.V. (2014) 'Predicting and Analyzing the Efficiency of Portable Scheffler Reflector By Using Response Surface Method', *International Journal of Mechanical Engineering*, ISSN: 2277-7059, Vol. 4, No. 2, pp. 5-13.
125. Pihl, E., Heyne, S., Thunman, H. and Johnsson, F. (2010) 'Highly efficient electricity generation from biomass by integration and hybridization with combined cycle gas turbine (CCGT) plants for natural gas', *Energy*, Vol. 35, No. 10, pp. 4042-4052.
126. Pirc, A., Sekavčnik, M. and Mori, M. (2012) 'Universal Model of a Biomass Gasifier for Different Syngas Compositions', *Journal of Mechanical Engineering*, DOI:10.5545/sv-jme.2011.101, Vol. 58, No. 5, pp. 291–299.
127. Prasad, C.S.N., Reddy, K.V.K., Kumar, B.S.P., Ramjee, E., Hebbel, O.D. and Nivendgi, M.C. (2009) 'Performance and emission characteristics of a diesel engine with castor oil', *International Indian Journal of Science and Technology*, ISSN: 0974- 6846, vol. 2, No. 10, pp. 25-31.
128. Prasanna, U.R. and Umanand, L. (2011) 'Optimization and design of energy transport system for solar cooking application', *Applied Energy*, Vol. 88, pp. 442-451.
129. Pratihari, A.K., Kaushik, S.C. and Agarwal, R.S. (2012) 'Performance evaluation of a small capacity compression absorption refrigeration system', *International Journal of Applied Thermal Engineering*, Vol. 42, pp. 41-48.

130. Pridasawas, W. and Lundqvist, P. (2004) 'An exergy analysis of a solar-driven ejector refrigeration system', *International Journal of solar Energy*, Vol. 76, pp. 369-379.
131. Prins, M.J., Ptasinski, K.J. and Janssen, F.J.J.G. (2003) 'Thermodynamics of gas-char reactions: first and second law analysis', *Chemical Engineering Science*, Vol. 58, pp. 1003-1011.
132. Pulat, E., Etemoglu, A.B. and Can, M. (2009) 'Waste-heat recovery potential in Turkish textile industry: Case study for city of Bursa', *Renewable and Sustainable Energy Reviews*, Vol. 13, pp. 663-672.
133. Raman, P. and Ram, N.K. (2013) 'Performance analysis of an internal combustion engine operated on producer gas, in comparison with the performance of the natural gas and diesel engines', *Energy*, Vol. 63, pp.317-333.
134. Rapagna, S., Gallucci, K., Marcello, M.D., Matt, M., Nacken, M. and Heidenreich, S. (2010) 'Gas cleaning, gas conditioning and tar abatement by means of a catalytic filter candle in a biomass fluidized-bed gasifier', *Bioresource Technology*, Vol. 101, No. 18, pp. 7123–7130.
135. Rashidi, M.M., Bég, O.A. and Aghagoli, A. (2012) 'Utilization of waste heat in combined power and ejector refrigeration for a solar energy source', *International Journal of Applied Math and Mechanics*, Vol. 8, No. 17, pp. 1-16.
136. Rathore, N.S., Panwar, N.L. and Chiplunkar, V.Y. (2008) 'Industrial Application of Biomass Based Gasification System', *World applied sciences Journal*, Vol. 5, No. 4, pp. 406-409, ISSN 1818-4952.
137. Rathore, N.S., Panwar, N.L. and Chiplunkar, V.Y. (2009) 'Design and Techno-Economic Evaluation of Biomass Gasifier for Industrial Thermal Applications', *African Journal of Environmental Science and Technology*, Vol. 3, No. 1, pp. 006-012.
138. Reed, T.B., Walt, R., Ellis, S., Das A. and Deutch, S. (1999) 'Superficial Velocity – The Key to Down draft Gasification: The Biomass Energy Foundation', *The National Renewable Energy Laboratory*, Presented at 4th Biomass Conference of the Americas; Oakland.
139. Rocha, M.S., Andreos, R. and Moreira, F.R.S. (2012) 'Performance Test of two Small tri-generation pilot plants', *Applied thermal Engineering*, Vol. 41, pp. 84-91.

140. Rutherford, J.P. and Williamson, C.J. (2006) 'Integrated Advanced Biomass Gasifiers into the New Zealand wood industry', NZ Journal of Forestry, (refereed articles) pp. 35-41.
141. Sadhukhan, K., Chowdhuri, A.K. and Mandal, B.K. (2012) 'Computer based thermodynamic properties of Ammonia-Water Mixture for the Analysis of Power and Refrigeration Cycles', International Journal of Thermodynamics, ISSN 1301-9724/e-ISSN 2146-1511, Vol. 15, No. 3, pp. 133-139.
142. Sahin, B., Ust, Y., Teke, I. and Erdem, H.H. (2010) 'Performance analysis and optimization of heat exchangers: a new thermos-economic approach', Applied Thermal Engineering, Vol. 30, pp. 104-109.
143. Sahoo, P.K., Das, L.M., Babu, M.K.G., Arora, P., Singh, V.P., Kumar, N.R. and Varyani, T.S. (2009) 'Comparative evaluation of performance and emission characteristics of jatropha, karanja and polanga based biodiesel as fuel in a tractor engine', Fuel, Vol. 88, pp. 1698-1707.
144. Saidura, R., BoroumandJazi, G., Mekhlif, S. and Jameel, M. (2012) 'Exergy analysis of solar energy applications', Renewable and Sustainable Energy Reviews, Vol. 16, pp. 350-356.
145. Sardeshpande, V. and Pillai, I.R. (2012) 'Effect of micro-level and macro-level factors on adoption potential of solar concentrators for medium temperature thermal applications', Energy for Sustainable Development, Vol. 16, No. 2, pp. 216-223.
146. Scheffler, W. (2006) 'Introduction to the revolutionary design of Scheffler reflectors', In: SCIs International Solar Cooker Conference, Granada, Spain.
147. Sedigh, S. and Saffari, H. (2012) 'Thermodynamic analysis of triple effect absorption refrigeration systems', International Journal of Energy & Technology, Vol. 4, No. 7, pp. 1-8.
148. Sezer, I. (2011) 'Thermodynamic, performance and emission investigation of a diesel engine running on dimethyl ether and diethyl ether', International Journal of Thermal Sciences, Vol. 50, pp. 1594-1603.
149. Shabangu, S., Woolf, D., Fisher, E.M., Angenent, L.T. and Lehmann, J. (2014) 'Techno-economic assessment of biomass slow pyrolysis into different biochar and methanol concepts', Fuel, Vol. 117, pp. 742-748.
150. Shackley, S., Carter, S., Knowles, T., Middelink, E., Haeefele, S., Sohi, S., Cross, A. and Haszeldine, S. (2012) 'Sustainable gasification-biochar systems? A case-

- study of rice-husk gasification in Cambodia, Part I: Context, chemical properties, environmental and health and safety issues', *Energy Policy*, Vol. 42, pp. 49-58.
151. Sharma, D. and Panwar, N.L. (2009) 'Performance Evaluation of Biomass based Natural Draft Gasifier System for Thermal Application', *IE(I) Journal-AG*, Vol.90, pp 34-38.
 152. Shashikantha, Klose, W. and Parikh, P.P. (1994) 'Development of a 15 kW spark ignition producer gas engine and some investigations of its in-cylinder processes', *International Journal of Renewable Energy*, Vol. 5, pp. 835-837.
 153. Sheth, P.N. and Babu, B.V. (2009) 'Experimental studies on producer gas generation from wood waste in a downdraft biomass gasifier', *Bio-resource Technology*, Vol. 100, No. 12, pp. 3127–3133.
 154. Shiba, T. and Bejan, A. (2001) 'Thermodynamic optimization of geometric structure in the Counter-flow heat exchanger for an environmental control system', *Energy*, Vol. 26, pp. 493-511.
 155. Simeone, E., Nacken, M., Haag, W., Heidenreich, S. and Jong, W.D. (2011) 'Filtration performance at high temperatures and analysis of ceramic filter elements during biomass gasification' *Biomass and Bioenergy*, Vol. 35, 87–104.
 156. Singh, R.N., Singh, S.P. and Pathak, B.S. (2007) 'Performance of Renewable Fuel Based CI engine', *Agricultural Engineering International: the CIGR Ejournal*, Manuscript EE 0014, Vol. IX.
 157. Singh, R.N., Singh, S.P. and Pathak, B.S. (2007) 'Investigations on operation of CI engine using producer gas and rice bran oil in mixed fuel mode', *International Journal of Renewable Energy*, Vol. 32, No. 9, pp. 1565–1580.
 158. Soheli, M.I. and Jack, M.W. (2011) 'Thermodynamic analysis and potential efficiency improvements of a biochemical process for lignocellulosic biofuel production', *World Renewable Energy Congress 2011 Sweden*, pp. 8–13.
 159. Sovacool, B.K. (2008) 'Valuing the greenhouse gas emissions from nuclear power: A critical survey', *Energy Policy*, Vol. 36, pp. 2940-2953.
 160. Sridhar, G., Paul, P.J. and Mukunda, H.S. (2001) 'Biomass derived producer gas as a reciprocating engine fuel-an experimental analysis', *Biomass and Bioenergy*, Vol. 21, pp.61-72.
 161. Sridhar, G., Dasappa, S., Sridhar, H.V., Paul, P.J. and Rajan, N.K.S. (2005) 'Gaseous Emissions Using Producer Gas as Fuel in Reciprocating Engines', *SAE International*, Vol. 01, pp. 1732-1738.

162. Srihirin, P., Aphornratana, S. and Chungpaibulpatana, S. (2001) 'A review of absorption refrigeration technologies', *Renewable and Sustainable Energy Reviews*, Vol. 5, pp. 343-372.
163. Strzalka, R., Erhart, T.G. and Eicker, U. (2013) 'Analysis and optimization of co-generation system based on biomass combustion', *International Journal of Applied Thermal Engineering*, Vol. 50, No. 2, pp. 1418-1426.
164. Sun, D.W. (1999) 'Comparative study of the performance of an ejector refrigeration cycle operating with various refrigerants', *Energy Conversion and Management*, Vol. 40, pp. 873-884.
165. Sun, Z.G. (2008) 'Experimental investigation of integrated refrigeration system with gas engine, compression chiller and absorption chiller', *Energy*, Vol. 33, pp. 431-437.
166. Suple, Y.R. and Suraskar, N.N. (2012) 'Design and Fabrication of Manually Track Parabolic Solar Disc for In-House Cooking', *International Journal of Modern Engineering Research (IJMER)*, ISSN: 2249-6645, Vol. 2, No. 6, pp. 4228-4230.
167. Tao, T., Hongfei, Z., Kaiyan, H. and Mayere, A. (2011) 'A new trough solar concentrator and its performance analysis', *Solar Energy*, Vol. 85, No. 1, pp. 198-207.
168. Thakkar, V. (2013) 'Status of Parabolic Dish Solar Concentrators', *International Journal of Enhanced Research in Science Technology & Engineering*, ISSN: 2319-7463, Vol. 2, No. 6, pp. 42-50.
169. Tighe, C.J., Gruar, R.I., Ma, C.Y., Mahmud, T., Wang, X.Z. and Darr, J.A. (2012) 'Investigation of counter-current mixing in a continuous hydrothermal flow reactor', *Journal of Supercritical Fluids*, Vol. 62, pp. 165-172.
170. Tyagi, S.K., Wang, S., Singhal, M.K., Kaushik, S.C. and Park, S.R. (2007) 'Exergy analysis and parametric study of concentrating type solar collectors', *International Journal of Thermal Sciences*, Vol. 46, pp. 1304-1310.
171. Vaezi, M., Fard, M. P., Moghiman, M. and Charmchi, M. (2008) 'Modeling biomass gasification: A new approach to utilize renewable sources of energy', *Proceedings of ASME-IMECE 2008, Boston, Massachusetts, USA*.
172. Vaezi, M., Fard, M.P., Moghiman, M. and Charmchi, M. (2012) 'On a methodology for selecting biomass materials for gasification purposes', *Fuel Processing Technology*, Vol. 98, pp. 74-81.

173. Varshney, R., Bhagoria, J.L. and Mehta, C.R. (2010) 'Small scale biomass gasification technology in India-An overview', *Journal of Engineering, Science and Management Education*, Vol. 3, pp. 33-40.
174. Varshney, R., Bhagoria, J.L. and Mehta, C.R. (2011) 'Experimental investigation on a biomass briquette based throatless downdraft gasifier', *International Journal of Applied Engineering Research*, Dindigul, ISSN - 0976-4259, Vol. 2, No. 2, pp. 554-561.
175. Wang, R.Z. (2001) 'Performance improvement of adsorption cooling by heat and mass recovery operation', *International Journal of Refrigeration*, Vol. 24, No. 7, pp. 602-611.
176. Wu, D.W. and Wang, R.Z. (2006) 'Combined cooling, heating and power: A review', *Progress in Energy and Combustion Science*, Vol. 32, pp. 459-495.
177. Wuebbles D.J. (1994) 'The role of refrigerants in climate change', *International Journal of Refrigeration*, Vol. 17, No. 1, pp. 7-17.
178. Yaliwal, V.S., Banapurmath, N.R., Gireesh, N.M. and Tewari, P.G. (2014) 'Production and utilization of renewable and sustainable gaseous fuel for power generation applications: A review of literature', *Renewable and Sustainable Energy Reviews*, Vol. 34, pp.608-627.
179. Yan, Q., Yu, F., Liu, J., Street, J., Gao, J., Cai, Z. and, Zhang, J. (2013) 'Catalytic conversion wood syngas to synthetic aviation turbine fuels over a multifunctional catalyst', *Bioresource Technology*, Vol. 127, pp. 281-290.
180. Yoon, S.J. and Lee, J.G. (2012) 'Hydrogen-rich syngas production through coal and charcoal gasification using microwave steam and air plasma torch', *International journal of hydrogen energy*, Vol. 372, pp. 17093–17100.
181. Zainal, Z.A., Rifau, A., Quadir, G.A. and Seetharamu, K.N. (2002) 'Experimental investigation of a downdraft biomass gasifier', *Biomass and Bioenergy*, Vol. 23, No. 4, pp. 283–289.
182. Zhang, Q., Wu, Y., Dor, L., Yang, W. and Blasiak, W. (2013) 'Thermodynamic analysis of solid waste gasification in the Plasma Gasification Melting process', *Applied Energy*, Vol. 112, pp. 405-413.
183. Zheng, M., Reader, G.T. and Hawley, J.G. (2004) 'Diesel engine exhaust gas recirculation-a review on advanced and novel concepts', *Energy Conversion and Management*, Vol. 45, pp. 883-900.

APPENDIX-A (Sample Calculations)

Table-14. Exhaust calculation:

At electric load 15.24 kW,

$$\begin{aligned} \text{Heat supplied by solar} &= \dot{m}_{\text{water}} \times C_{p,\text{water}} \times \Delta T \\ &= \text{mass flow rate} \times \text{Specific heat of water} \times \Delta T_{\text{average}} \\ &= 1818.467 \times 4.18 \times (121.5 - 120.37) \\ &= 2.39 \text{ kW} \end{aligned}$$

$$\begin{aligned} \text{Heat gained by exhaust in HRU} &= 1818.467 \times 4.18 \times (125.033 - 121.5) \\ &= 7.46 \text{ kW} \end{aligned}$$

$$\begin{aligned} \text{Heat delivered to generator} &= 1818.467 \times 4.18 \times (125.033 - 120.37) \\ &= 9.85 \text{ kW} \end{aligned}$$

Heat gained by working fluid (water of HRU):

$$\begin{aligned} &= \frac{400 \times 4.18}{\text{time}} \times \left[\frac{(T_{\text{solar}}^{\text{initial}} - T_{\text{solar}}^{\text{final}}) + (T_{\text{HRU}}^{\text{initial}} - T_{\text{HRU}}^{\text{final}}) + (T_{\text{gen.}}^{\text{initial}} - T_{\text{gen.}}^{\text{final}})}{3} \right] \\ &= \frac{400 \times 4.18}{30 \times 60} \times \left[\frac{(122 - 119) + (124 - 120) + (128 - 123)}{3} \right] = 3.72 \text{ kW} \end{aligned}$$

Note: Actual heat of exhaust: (By energy balance)

$$\begin{aligned} \dot{Q}_{\text{exhaust}}^{\text{actual}} + \dot{Q}_{\text{solar}} &= \dot{Q}_{\text{gen.}} + \dot{Q}_{\text{gain}}^{\text{sensible}} \\ \dot{Q}_{\text{exhaust}}^{\text{actual}} &= \dot{Q}_{\text{gen.}} + \dot{Q}_{\text{gain}}^{\text{sensible}} - \dot{Q}_{\text{solar}} \\ &= 9.85 + 3.72 - 2.39 = 11.18 \text{ kW} \end{aligned}$$

Table-12. Scheffler dish calculation:

Date: 25/06/2012, nth day of the year, is being denoted by 'n' = 177

According to Munir et al. (2010), 'solar inclination' or seasonal angle deviation of sun:-

$$\delta = \frac{180}{\pi} \left[\begin{aligned} &(0.006918 - 0.399912) \cos \frac{(n-1).2\pi}{365} + 0.070257 \sin \frac{(n-1).2\pi}{365} - 0.006758 \cos \frac{2(n-1).2\pi}{365} \\ &+ 0.000907 \sin \frac{(n-1).2\pi}{365} - 0.002679 \cos \frac{3(n-1).2\pi}{365} + 0.00148 \sin \frac{3(n-1).2\pi}{365} \end{aligned} \right]$$

$$\delta = \frac{180}{\pi} \left[\begin{aligned} &(0.006918 - 0.399912) \times 0.9986 + 0.070257 \times 0.0529 - 0.006758 \times 0.99441 \\ &+ 0.000907 \times 0.0529 - 0.002679 \times 0.98744 + 0.00148 \times 0.15797 \end{aligned} \right]$$

$$\delta = -22.793^\circ$$

Aperture area (A_s) is:

$$A_s = \text{Re } flector, area \times \cos \left\{ 43.23 - \frac{\delta}{2} \right\}$$

$$A_s = 64 \times \cos \left\{ 43.23 - \frac{(-22.793)}{2} \right\}$$

$$= 64 \times 0.579 = 37.056 \text{ m}^2$$

Energy Efficiency of scheffler dishes:

$$\begin{aligned} \eta_{energy} &= \frac{\text{Total power obtained by sun}}{\text{Power given by radiation}} \\ &= \frac{E_p}{\text{Beam radiation} \times \text{Aperture area}} = \frac{E_p}{\text{Average DNI} \times \text{Aperture area}} \end{aligned}$$

Total power obtained by sun:

$$\begin{aligned} E_p &= \text{mass flow rate} \times \text{Specific heat of water} \times \Delta T \\ &= 1818.47 \times 4.18 \times (121.5 - 120.37) = 2.3859341 \text{ kW} \end{aligned}$$

Power given by radiation = Average DNI \times A_s

$$= 441.9295 \times 37.056 = 16.37613 \text{ kW}$$

Efficiency of the scheffler dishes: $\eta_{energy} = \frac{2.385934}{16.37613} = 14.56957322\%$

Exergy Efficiency of scheffler dishes:

$$\eta_{exergy} = \frac{\text{Exergy gained by water}}{\text{Exergy input to scheffler collector}}$$

Exergy gained by water:

$$\begin{aligned} E_{XO} &= E_p - \dot{m}_w C_{pw} T_{amb} \ln \left(\frac{T_f}{T_i} \right) = 4.222891 - 1818.24 \times 4.18 \times (273 + 36.75214) \ln \left(\frac{273 + 121.5}{273 + 120.37} \right) \\ &= 0.509866 \text{ kW} \end{aligned}$$

Exergy input to the collector:

$$E_{Xi} = f \sigma T_{sun}^4 + (1 - f) \sigma T_{planet}^4 - \sigma T_{SC}^4$$

Where, f = sunlight dilution factor = 2.16×10^{-5} on earth

σ = Stefan boltzmann constant = $5.670373 \times 10^{-8} \text{ W/m}^2 \text{ K}^4$

T_{sun} = Temperature of sun = 5800 K

$$T_{planet} = \text{Temperature of planet/earth} = 288 \text{ K}$$

$$T_{sc} = \text{Temperature of scheffler collector}$$

∴ Exergy input;

$$E_{Xi} = 2.16 \times 10^{-5} \times 5.670373 \times 10^{-8} \times (5800)^4 + (1 - 2.16 \times 10^{-5}) \times 5.670373 \times 10^{-8} \times (288)^4 - 5.670373 \times 10^{-8} \times (273 + 121.5)^4 \\ = 14.92369 \text{ kW}$$

∴ ED of SC = Exergyin – Exergy out = 14.92369 - 0.509866 = 14.4138 kW and,

$$\therefore \text{Exergy efficiency; } \quad \therefore \eta_{exergy} = \frac{0.509866}{14.92369} = 3.41649\%$$

Heat loss factor and optical efficiency factor calculation: from **table-13**:

$$\text{Heat loss factor; } FU_L = \frac{DNI}{(T_m - T_a)} = \frac{441.93}{(120.935 - 35.0521)} = 5.145724 \text{ W/m}^2\text{K}$$

$$\text{Where mean temperature, } T_m = \frac{(120.37 + 121.5)}{2} = 120.935^\circ\text{C}$$

Table-4. Required Producer gas and biomass calculation:

In day (solar + Exhaust+ PG required)

$$\text{At 15.24 kW, } \quad (\dot{m}_{air} + \dot{m}_{fuel}) \times C_{p,exhaust} \times \Delta T_{exhaust} = \dot{Q}_{exhaust}^{actual}$$

$$\therefore \dot{Q}_{exhaust}^{actual} = 11.18 \text{ kW, } \rho_{PG} = 1.09 \text{ kg/m}^3 \text{ and } \dot{m}_{fuel/PG} = 67.54 \text{ m}^3 / \text{hr}$$

(From table-14, 4 and 4b)

$$\therefore (\dot{m}_{air} + 67.54 \times 1.09) \times 1.008 \times (352 - 129) = 11.18$$

$$\dot{m}_{air} = 106.86 \text{ kg/hr}$$

$$\therefore \text{Air –fuel ratio is } \frac{\dot{m}_{air}}{\dot{m}_{fuel}} = 1.452$$

$$\therefore \text{BCR} = 28 \text{ kg/hr}$$

∴ 28 kg/hr of biomass gives = 28 × 2.412 m³/hr of PG = 67.54 m³/hr of PG (table-4)

Assume, CV_{Biomass} = 18.6 MJ/kg and CV_{PG} = 5.415 MJ/m³ (from table-5)

$$CV_{PG} = \sum (\text{Volume\%} \times LHV_{components})$$

$$CV_{PG} = \frac{21.5}{100} \times 12.622 + \frac{12.1}{100} \times 0 + \frac{18.4}{100} \times 10.788 + \frac{2}{100} \times 35.814 + \frac{46}{100} \times 0 = 5.415002 \text{ MJ/m}^3$$

$$\therefore \frac{28 \times 18600}{3600} \text{ kW of Biomass gives } = \frac{67.54 \times 5.415002 \times 1000}{3600} \text{ kW of PG}$$

144.67 kW of biomass gives = 101.5914 kW of PG

∴ 1 kW of biomass gives = 0.702228 kW of PG

In day, the heat is given to generator by solar and exhaust:

$$\therefore \dot{Q}_{gen} = 9.85 \text{ kW (from table-14)}$$

∴ For generator the required heat is 25 kW

$$\therefore \text{Remaining heat} = 25 - 9.85 = 15.15 \text{ kW}$$

$$\therefore \text{For 15.15 kW production of PG, required biomass} = \frac{15.15}{0.702228} \text{ kW of biomass}$$

$$= 21.575 \text{ kW of biomass}$$

$$\therefore \text{Requirement of biomass per hour} = \frac{\text{required biomass in kW}}{\text{CV of biomass}} = \frac{21.575}{18600} = 4.176 \text{ kg/hr}$$

$$\therefore \text{Total BCR} = 28 + 4.176 = 32.176 \text{ kg/hr}$$

$$\therefore \text{Total SFC} = \frac{32.176 \text{ kg/hr}}{15.24 \text{ kW}} = 2.1113 \text{ kg/kWhr}$$

In night (Exhaust+ PG required):

∴ 1 kW of biomass gives = 0.6484 kW of PG

In night, the heat is given to generator by the exhaust:

$$\therefore \dot{Q}_{gen} = 7.46 \text{ kW (from table-14)}$$

∴ For generator the required heat is 25 kW

$$\therefore \text{Remaining heat} = 25 - 7.46 = 17.54 \text{ kW}$$

$$\therefore \text{For 17.54 kW production of PG, required biomass} = \frac{17.54}{0.702228} \text{ kW of biomass}$$

$$= 24.979 \text{ kW of biomass}$$

$$\therefore \text{Requirement of biomass per hour} = \frac{\text{required biomass in kW}}{\text{CV of biomass}} = \frac{24.979}{18600} = 4.835 \text{ kg/hr}$$

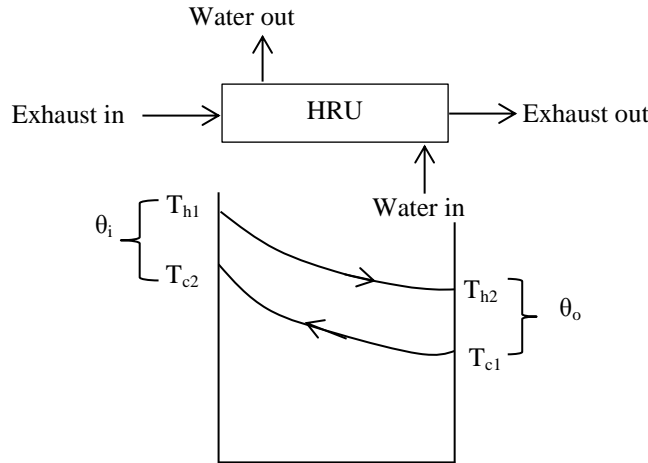
$$\therefore \text{Total BCR} = 28 + 4.835 = 32.835 \text{ kg/hr}$$

$$\therefore \text{Total SFC} = \frac{33.24 \text{ kg/hr}}{15.24 \text{ kW}} = 2.129 \text{ kg/kWhr}$$

Table-16. Evaluation of HRU for solar and exhaust:

At 15.24 kW electric load,

The HRU will work as H.E. then water is considered as cold fluid, while the exhaust gas as the hot fluid.



Then, from table.4, $T_{c1}=121.5^{\circ}\text{C}$, $T_{c2}= 125.033^{\circ}\text{C}$

From table.8, $T_{h1}= 182.133^{\circ}\text{C}$, $T_{h2}= 129^{\circ}\text{C}$.

\therefore Heat duty for hot fluid; $\dot{Q}_h = \dot{m}_h C_{ph} (T_{h1} - T_{h2})$

And heat duty for cold fluid; $\dot{Q}_c = \dot{m}_c C_{pc} (T_{c2} - T_{c1})$

\therefore From energy balance; $\dot{Q}_h = \dot{Q}_c = \dot{m}_c C_{pc} (T_{c2} - T_{c1})$

$$= 1818.467 \times 4.18 \times (125.033 - 121.5)$$

$$= 7.46 \text{ kW}$$

$$\therefore \dot{m}_c C_{pc} = 1818.467 \times 4.18 = 2.114 \text{ kW/K} = C_{\max}$$

$$\text{And so } \dot{m}_h C_{ph} = 0.1404 \text{ kW/K} = C_{\min}$$

$$\therefore \text{Heat capacity ratio; } R = \frac{C_{\min}}{C_{\max}} = \frac{0.1404}{2.114} = 0.0665$$

Effectiveness; $\varepsilon \quad \therefore \dot{m}_h C_{ph} < \dot{m}_c C_{pc}$

$$\varepsilon = \frac{q_{\text{actual}}}{q_{\max}} = \frac{\dot{m}_h C_{ph} (T_{h1} - T_{h2})}{C_{\min} (T_{h1} - T_{c1})} = \frac{(T_{h1} - T_{h2})}{(T_{h1} - T_{c1})} = \frac{182.133 - 129}{182.133 - 121.5} = 0.8763$$

\therefore The nitrogen gas is used in the pipe line of the water so there is no conversion of water into vapour.

\therefore No need of the calculation of latent heat of vaporization of water.

$$\therefore \dot{Q} = \dot{Q}_h = \dot{Q}_c = Q_{\text{sensible}} = 7.46 \text{ kW}$$

$$\therefore (\Delta T)_{LMTD} = \frac{\theta_i - \theta_o}{\ln(\theta_i / \theta_o)} = \frac{(T_{h1} - T_{c2}) - (T_{h2} - T_{c1})}{\ln\left\{\frac{(T_{h1} - T_{c2})}{(T_{h2} - T_{c1})}\right\}} = \frac{(57.1 - 7.5)}{\ln\left\{\frac{57.1}{7.5}\right\}} = 24.435 \text{ K}$$

Specifications of HRU:-

Length of drum = 1.6002 m

Exhaust pipe diameter = 0.1524 m

Producer gas pipe diameter = 0.1016 m

Diameter of drum = 0.331042 m

Area of heat transfer; $A=2\pi r \times \text{length of drum}$,

Where, r = Radius of exhaust pipe

$$\therefore A = \pi \times 0.1524 \times 1.6002 = 0.766 \text{ m}^2$$

$$\therefore \dot{Q} = UA(\Delta T)_{LMTD}$$

$$\therefore U = \frac{7.46 \text{ kW}}{0.766 \text{ m}^2 \times 24.435 \text{ K}} = 0.3985 \frac{\text{ kW}}{\text{ m}^2 \text{ K}}$$

Exergy analysis of HRU

$$\therefore \dot{m}_h C_{ph} < \dot{m}_c C_{pc}$$

\therefore The entropy generation from the system;

$$S_{gen} = C_{min} \ln \left[1 - \varepsilon \left(1 - \frac{1}{T_R} \right) \right] + C_{max} \ln [1 + \varepsilon R (T_R - 1)]$$

Where, $T_R = \frac{T_{h1}}{T_{c1}}$ = Temperature ratio,

$$\begin{aligned} S_{gen} &= 0.1404 \ln \left[1 - 0.8763 \left(1 - \frac{1}{1.15336} \right) \right] + 2.114 \ln [1 + 0.8763 \times 0.0665 (1.15336 - 1)] \\ &= 0.00135 \text{ kW/K} \end{aligned}$$

Exergy destruction in HRU; $HRU_{ED} = T_0 S_{gen} = 298 \times 0.00135 = \mathbf{0.401539309 \text{ kW}}$

Exergy efficiency/effectiveness of HRU; (from the table-17)

$$\begin{aligned} \varepsilon &= \frac{\text{Exergy}_{out}}{\text{Exergy}_{in}} = \frac{\text{Exergy}_{water}}{\text{Exergy}_{exhaust}} = \frac{\dot{m}_w [(h_{out} - h_{in}) - T_0 (S_{out} - S_{in})]}{-\dot{m}_{exht} [(h_{out,exht} - h_{in,exht}) - T_0 (S_{out,exht} - S_{in,exht})]} \\ &= \frac{1818.47 \times [(510.19 - 525.22) - 298(1.5441 - 1.5819)]}{-180.513 \times [-51.5512111 - 298 \times -0.459193593]} = 0.444776126 \end{aligned}$$

Where, Change in enthalpy/entropy of exhaust gas is;

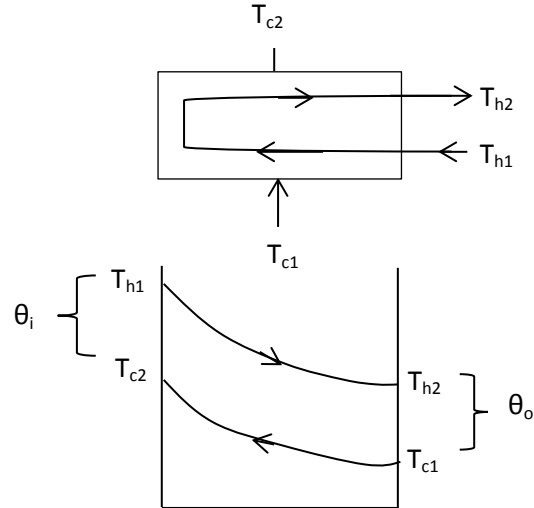
$$\Delta h_{exht} = h_{out,exht} - h_{in,exht} = \frac{1}{28.9} \left[28.11(T_{h2} - T_{h1}) + 0.9835 \times 10^{-3} (T_{h2}^{-2} - T_{h1}^{-2}) + 0.16 \times 10^{-5} (T_{h2}^{-3} - T_{h1}^{-3}) \right] - 0.49 \times 10^{-9} (T_{h2}^{-4} - T_{h1}^{-4})$$

And entropy;

$$\Delta S_{exht} = S_{out,exht} - S_{in,exht} = \frac{1}{28.9} \left[28.11 \ln \left(\frac{T_{h2}}{T_{h1}} \right) + 0.1967 \times 10^{-2} (T_{h2} - T_{h1}) + 0.2401 \times 10^{-5} (T_{h2}^2 - T_{h1}^2) \right] - R \ln \left(\frac{P_{h2}}{P_{h1}} \right) - 0.655 \times 10^{-9} (T_{h2}^3 - T_{h1}^3)$$

Table-18. Evaluation of HRU for producer gas:

Time: 1:30 to 1:59



From table.5, $T_{c1} = 76.93^\circ\text{C}$, $T_{c2} = 80.5^\circ\text{C}$

From table.12b, $T_{h1} = 465.6^\circ\text{C}$, $T_{h2} = 87.894^\circ\text{C}$.

\therefore Heat duty for hot fluid; $\dot{Q}_h = \dot{m}_h C_{ph} (T_{h1} - T_{h2})$

And heat duty for cold fluid; $\dot{Q}_c = \dot{m}_c C_{pc} (T_{c2} - T_{c1})$

\therefore From energy balance;

$$\dot{Q}_h = \dot{Q}_c = \dot{m}_c C_{pc} (T_{c2} - T_{c1})$$

$$= 805.82 \times 4.18 \times (80.5 - 76.93) = 3.34 \text{ kW}$$

$$\therefore \dot{m}_c C_{pc} = 805.82 \times 4.18 = 0.936 \text{ kW/K} = C_{\max}$$

$$\text{And so } \dot{m}_h C_{ph} = 0.008843 \text{ kW/K} = C_{\min}$$

$$\therefore \text{Heat capacity ratio; } R = \frac{C_{\min}}{C_{\max}} = \frac{0.008843}{0.936} = 0.00945$$

Effectiveness; ε $\therefore \dot{m}_h C_{ph} < \dot{m}_c C_{pc}$

$$\varepsilon = \frac{q_{\text{actual}}}{q_{\max}} = \frac{\dot{m}_h C_{ph} (T_{h1} - T_{h2})}{C_{\min} (T_{h1} - T_{c1})} = \frac{(T_{h1} - T_{h2})}{(T_{h1} - T_{c1})} = \frac{465.6 - 87.894}{465.6 - 76.93} = 0.9711$$

∴ The nitrogen gas is used in the pipe line of the water so there is no conversion of water into vapour.

∴ No need of the calculation of latent heat of vaporization of water.

$$\therefore \dot{Q} = \dot{Q}_h = \dot{Q}_c = Q_{\text{sensible}} = 7.46 \text{ kW}$$

$$\therefore (\Delta T)_{LMTD} = \frac{\theta_i - \theta_o}{\ln(\theta_i / \theta_o)} = \frac{(T_{h1} - T_{c2}) - (T_{h2} - T_{c1})}{\ln\left\{\frac{(T_{h1} - T_{c2})}{(T_{h2} - T_{c1})}\right\}} = \frac{(385.1 - 10.964)}{\ln\left\{\frac{385.1}{10.964}\right\}} = 105.13 \text{ K}$$

∴ The heat exchanger has two tubes.

∴ There is need to calculate the correction factor.

$$F = \frac{\sqrt{(1+R)}}{(1-R)} \times \frac{\ln\left\{\frac{1-\varepsilon R}{1-\varepsilon}\right\}}{\ln\left[\frac{2-\varepsilon\left\{(1+R)-\sqrt{(R+1)}\right\}}{2-\varepsilon\left\{(1+R)+\sqrt{(R+1)}\right\}}\right]}$$

$$F = \frac{\sqrt{1.00945}}{(1-0.00945)} \times \frac{\ln\left\{\frac{1-0.9711 \times 0.00945}{1-0.9711}\right\}}{\ln\left[\frac{2-0.9711\left\{(1.00945)-\sqrt{1.00945}\right\}}{2-0.9711\left\{(1.00945)+\sqrt{1.00945}\right\}}\right]}$$

$$F = \frac{3.5514}{0.991 \times \ln\left[\frac{1.9954}{0.04405}\right]} = 0.9398$$

$$\therefore \dot{Q} = FUA(\Delta T)_{LMTD}$$

∴ Heat transfer area of the PG pipe:

$$= \pi \times \text{Diameter of PG pipe} \times \text{Length of drum} \times \text{No. of pass} \times \text{No. of tubes per pass}$$

$$= \pi \times 0.1016 \times 1.6002 \times 2 \times 1 = 1.022 \text{ m}^2$$

$$\therefore U = \frac{3.34 \text{ kW}}{0.9398 \times 1.022 \times 105.13} = 0.0331 \frac{\text{kW}}{\text{m}^2 \text{ K}}$$

Exergy analysis of HRU; ∴ $\dot{m}_h C_{ph} < \dot{m}_c C_{pc}$

∴ The entropy generation from the system;

$$S_{gen} = C_{\min} \ln\left[1 - \varepsilon \left(1 - \frac{1}{T_R}\right)\right] + C_{\max} \ln[1 + \varepsilon R (T_R - 1)]$$

Where, $T_R = \frac{T_{h1}}{T_{c1}}$ = Temperature ratio,

$$S_{gen} = 0.008844 \ln \left[1 - 0.9718 \left(1 - \frac{1}{2.11071} \right) \right] + 0.935647 \ln [1 + 0.9718 \times 0.00945(2.11071 - 1)]$$

$$= 0.003162 \text{ kW/K}$$

Exergy destruction in HRU; $HRU_{ED} = T_0 S_{gen} = 298 \times 0.003162 = 0.94223114 \text{ kW}$

Exergy efficiency/effectiveness of HRU; (from the table-17)

$$\varepsilon = \frac{\text{Exergy}_{out}}{\text{Exergy}_{in}} = \frac{\text{Exergy}_{water}}{\text{Exergy}_{exhaust}} = \frac{\dot{m}_w [(h_{out} - h_{in}) - T_0 (S_{out} - S_{in})]}{-\dot{m}_{exht} [(h_{out,exht} - h_{in,exht}) - T_0 (S_{out,exht} - S_{in,exht})]}$$

$$= \frac{805.52 \times [(337.11 - 322.13) - 298(1.0815 - 1.0389)]}{-73.6186 \times [-367.3811647 - 298 \times -1.049123315]} = 0.456931117$$

Where, Change in enthalpy/entropy of exhaust gas is;

$$\Delta h_{exht} = h_{out,exht} - h_{in,exht} = \frac{1}{28.9} \left[28.11(T_{h2} - T_{h1}) + 0.9835 \times 10^{-3} (T_{h2}^{-2} - T_{h1}^{-2}) + 0.16 \times 10^{-5} (T_{h2}^{-3} - T_{h1}^{-3}) \right. \\ \left. - 0.49 \times 10^{-9} (T_{h2}^{-4} - T_{h1}^{-4}) \right]$$

And entropy;

$$\Delta S_{exht} = S_{out,exht} - S_{in,exht} = \frac{1}{28.9} \left[28.11 \ln \left(\frac{T_{h2}}{T_{h1}} \right) + 0.1967 \times 10^{-2} (T_{h2} - T_{h1}) + 0.2401 \times 10^{-5} (T_{h2}^2 - T_{h1}^2) \right. \\ \left. - 0.655 \times 10^{-9} (T_{h2}^3 - T_{h1}^3) \right] - R \ln \left(\frac{P_{h2}}{P_{h1}} \right)$$

Table-5. Evaluation of chemical exergy of producer gas:

The chemical exergy is calculated as: $\bar{\varepsilon}_{ch,M} = \sum_i x_i \bar{\varepsilon}_{ch,i} + \bar{R} T_0 \sum_i x_i \ln x_i$

$$\bar{\varepsilon}_{ch,M} = \{x_{co} \bar{\varepsilon}_{ch,co} + x_{co_2} \bar{\varepsilon}_{ch,co_2} + x_{H_2} \bar{\varepsilon}_{ch,H_2} + x_{CH_4} \bar{\varepsilon}_{ch,CH_4} + x_{N_2} \bar{\varepsilon}_{ch,N_2}\} + \bar{R} T_0 \{x_{co} \ln x_{co} + x_{co_2} \ln x_{co_2} + x_{H_2} \ln x_{H_2} + x_{CH_4} \ln x_{CH_4} + x_{N_2} \ln x_{N_2}\}$$

Chemical composition by volume: At 15.24kW;

CO=13.508m³/hr (20%), CO₂=8.105m³/hr (12%), H₂=13.508m³/hr (20%),
CH₄=2.026m³/hr (3%), N₂=30.393m³/hr (45%).

$$\text{No of moles } (x_{co}) = \frac{\text{Volume of gas}}{\text{Molar volume of gas}} = \frac{13.508(m^3 / hr)}{22.4(m^3 / kgmol)} = 0.60304kgmol/hr,$$

$$x_{co_2} = 0.3618kgmol / hr , \quad x_{H_2} = 0.60304kgmol / hr , \quad x_{CH_4} = 0.09045kgmol / hr ,$$

$$x_{N_2} = 1.357kgmol / hr$$

Total no of moles of PG =3.01533 kgmol / hr (in table-9)

$$\bar{\varepsilon}_{ch,M} = \{(0.60304 \times 275100 + 0.3618 \times 19870 + 0.60304 \times 236100 + 0.09045 \times 831650 + 1.357 \times 720) / 3600\} \\ + 40.285 \times 298 \{0.60304 \times \ln 0.60304 + 0.3618 \times \ln 0.3618 + 0.60304 \times \ln 0.60304 + 0.09045 \times \ln 0.09045 \\ + 1.357 \times \ln 1.357\} / 3600\}$$

=108.7952kW (chemical exergy of substances are considered from paper of gasifier)

Table-6. Evaluation of mass of constituents of producer gas, molar enthalpy and entropy:

At 15.24kW (at 38°C of temperature of paper filter)

Mass=No of moles × Molecular weight

$$\text{CO} = 0.60304 \text{ kmol/hr} \times 28.01 \text{ Kg/kmole} = 16.8911504 \text{ kg/hr,}$$

$$\text{CO}_2 = 0.3618 \text{ kmol/hr} \times 44.01 \text{ Kg/kmole} = 15.922818 \text{ kg/hr,}$$

$$\text{H}_2 = 0.60304 \text{ kmol/hr} \times 2.016 \text{ Kg/kmole} = 1.21572864 \text{ kg/hr,}$$

$$\text{CH}_4 = 0.09045 \text{ kmol/hr} \times 16.043 \text{ Kg/kmole} = 1.45108935 \text{ kg/hr,}$$

$$\text{N}_2 = 1.357 \text{ kmol/hr} \times 28.016 \text{ Kg/kmole} = 38.00957 \text{ kg/hr.}$$

$$\text{Total mass} = 73.49036 \text{ kg/hr}$$

At temperature 38°C of paper filter, molar enthalpy of PG:

$$\bar{h} = \frac{m_{co} \bar{h}_{co} + m_{co_2} \bar{h}_{co_2} + m_{H_2} \bar{h}_{H_2} + m_{CH_4} \bar{h}_{CH_4} + m_{N_2} \bar{h}_{N_2}}{\sum_i m} \text{ (kJ/kmol)}$$

From table-20 take the values of molar enthalpy of constituents;

$$\bar{h} = \frac{16.8911504 \times 9043.2 + 15.922818 \times 9883.3 + 1.21572864 \times 8839.9 \\ + 1.45108935 \times 10466 + 38.0095 \times 9043.2}{73.49036}$$

$$= 9249.951096 \text{ kJ/kmol}$$

Molar entropy;

$$\bar{S} = \frac{m_{co} \bar{s}_{co} + m_{co_2} \bar{s}_{co_2} + m_{H_2} \bar{s}_{H_2} + m_{CH_4} \bar{s}_{CH_4} + m_{N_2} \bar{s}_{N_2}}{\sum_i m}$$

$$\bar{S} = \frac{16.8911504 \times 198.771 + 15.922818 \times 215.27 + 1.21572864 \times 131.781 \\ + 1.45108935 \times 187.72 + 38.0095 \times 192.73}{73.49036}$$

$$= 197.8949 \text{ kJ/kmol.K}$$

Molar enthalpy and entropy at 25°C and 1 atm; (in table-6)

Volume of PG constituents per kmole:

For H₂, $PV = nRT$

$$0.101325 \times V = n \times \frac{8.3143}{2.016} \times 298$$

$$\left(\frac{V}{n}\right)_{H_2} = 12.129 \text{ m}^3 / \text{kmol},$$

$$\text{Similarly, } \left(\frac{V}{n}\right)_{N_2} = 0.87299 \text{ m}^3 / \text{kmol}, \left(\frac{V}{n}\right)_{CO} = 0.87299 \text{ m}^3 / \text{kmol},$$

$$\left(\frac{V}{n}\right)_{CO_2} = 0.55561 \text{ m}^3 / \text{kmol}, \left(\frac{V}{n}\right)_{CH_4} = 1.5242 \text{ m}^3 / \text{kmol}$$

$$\text{No of moles } (x_{CO}) = \frac{\text{Volume of gas}}{\text{Molar volume of gas}} = \frac{20(\text{m}^3)}{0.87299(\text{m}^3 / \text{kmol})}$$

$$= 22.91 \text{ kmol},$$

$$x_{CO_2} = \frac{12}{0.55561} = 21.598 \text{ kmol}, x_{H_2} = \frac{20}{12.129} = 1.6489 \text{ kmol},$$

$$x_{CH_4} = \frac{3}{1.5242} = 1.9682 \text{ kmol}, x_{N_2} = \frac{45}{0.87299} = 51.546 \text{ kmol}$$

$$\bar{h}_0 = \frac{x_{CO} \bar{h}_{0CO} + x_{CO_2} \bar{h}_{0CO_2} + x_{H_2} \bar{h}_{0H_2} + x_{N_2} \bar{h}_{0N_2} + x_{CH_4} \bar{h}_{0CH_4}}{\sum_i n}$$

$$\bar{h}_0 = \frac{8669 \times 22.91 + 9364 \times 21.598 + 8468 \times 1.6489 + 8669 \times 51.546 + 10018 \times 1.9682}{99.671}$$

$$= 8842.92 \text{ kJ/kmol}$$

$$\bar{S}_0 = \frac{x_{CO} \bar{S}_{0CO} + x_{CO_2} \bar{S}_{0CO_2} + x_{H_2} \bar{S}_{0H_2} + x_{N_2} \bar{S}_{0N_2} + x_{CH_4} \bar{S}_{0CH_4}}{\sum_i n}$$

$$\bar{S}_0 = \frac{197.543 \times 22.91 + 213.685 \times 21.598 + 130.574 \times 1.6489 + 191.502 \times 51.546 + 186.266 \times 1.9682}{99.671}$$

$$= 196.586 \text{ kJ/kmol.K}$$

Evaluation of physical exergy of producer gas: (in table-9)

At 15.24kW (at 38°C of temperature of paper filter)

The physical exergy is calculated as: $\bar{\varepsilon}_{ph,M} = \{(\bar{h} - \bar{h}_0) - T_0(\bar{S} - \bar{S}_0)\} \times n_{PG}$

$$\begin{aligned}\bar{\varepsilon}_{ph,M} &= \{(9249.951 - 8842.92) - 298 \times (197.8949 - 196.586)\} \times 3.01533 \\ &= 0.014221301 \text{ kW}\end{aligned}$$

$$\therefore \text{Exergy of PG} = \bar{\varepsilon}_{ch,M} + \bar{\varepsilon}_{ph,M} = 108.7952 + 0.014221301 = 108.8094 \text{ kW}$$

Table-8 and 9. Evaluation of exergy of solid fuel and exergy efficiency of gasifier:

Exergy of solid fuel (wood):

Higher heating value (HHV) of solid fuel (wood):

$$HHV = 0.3491C + 1.1783H + 0.1005S - 0.1034O - 0.0151N - 0.0211Ash \text{ (MJ/kg)}$$

From table-23

$$HHV = 0.3491 \times 48.7 + 1.1783 \times 6.42 + 0.1005 \times 0.05 - 0.1034 \times 44.2 - 0.0151 \times 0.55 - 0.0211 \times 0.08$$

$$HHV = 19.990608 \text{ MJ/kg}$$

Lower heating value (LHV) of wood:

$$LHV = HHV - 9m_H h_{fg}$$

$$LHV = 19.990608 - 9 \times \left(\frac{6.42}{100}\right) \times \left(\frac{2466.1}{10^3}\right)$$

Where, m_H = mass fraction of hydrogen in solid fuel,

h_{fg} = Enthalpy of vaporization at NTP

$$\therefore LHV = 18.5656954 \text{ (MJ/kg)}$$

$$\therefore \text{Exergy of solid fuel: } \varepsilon_{solid} = \phi_{dry} [LHV + m_w h_{fg}]$$

Where,

$$\phi_{dry} = \frac{1.044 + 0.016\left(\frac{H}{C}\right) - 0.3493\left(\frac{O}{C}\right) \left\{1 - 0.0531\left(\frac{H}{C}\right)\right\} + 0.0493\left(\frac{N}{C}\right)}{\left\{1 - 0.4124\left(\frac{O}{C}\right)\right\}}$$

$$\phi_{dry} = \frac{1.044 + 0.016\left(\frac{6.42}{48.7}\right) - 0.3493\left(\frac{44.2}{48.7}\right) \left\{1 - 0.0531\left(\frac{6.42}{48.7}\right)\right\} + 0.0493\left(\frac{0.55}{48.7}\right)}{\left\{1 - 0.4124\left(\frac{44.2}{48.7}\right)\right\}}$$

$$\phi_{dry} = 1.16256215$$

∴ Exergy of solid fuel:

$$\varepsilon_{solid} = 1.16256215 \times \left[18.5656954 + \left(\frac{25}{100} \right) \times \left(\frac{2466.1}{10^3} \right) \right];$$

Where, m_w = mass fraction of moisture

$$\varepsilon_{solid} = 22.3005235 \text{ MJ/kg}$$

At 15.24 kW

$$\begin{aligned} \text{ED of gasifier} &= \text{Exergy of wood} - \text{Exergy of PG} \\ &= 22.3005235 \times 28 - 108.809421 = 64.638933 \text{ kW} \end{aligned}$$

Exergy efficiency of gasifier:

$$\begin{aligned} &= \frac{\text{Exergy of producer gas (kW)}}{BCR \times \varepsilon_{solid} \times \left(\frac{1000}{3600} \right) (\text{kW})} = \frac{108.8094 (\text{kW})}{28 \times 22.3005235 \times \left(\frac{1000}{3600} \right) \text{kW}} \\ &= 62.73303289\% \end{aligned}$$

Table-10. Evaluation of exergy destruction of cooling unit:

At 15.24kW, Exergy destruction in different components;

For HE-1 regenerator;

$$\dot{E}_{D,regen} = T_o \left[\dot{m}_h C_{ph} \ln \left(\frac{T_{h,out}}{T_{h,in}} \right) + \dot{m}_c C_{pc} \ln \left(\frac{T_{c,out}}{T_{c,in}} \right) \right]$$

$$\begin{aligned} \dot{E}_{D,regen} &= 298 \left[73.6186 \times 1.232 \ln \left(\frac{273 + 200}{273 + 410} \right) + 104.706 \times 1.005 \ln \left(\frac{273 + 226}{273 + 45} \right) \right] \\ &= 1.166287 \text{ kW} \end{aligned}$$

$$\begin{aligned} \text{Where, mass flow rate of air } \dot{m}_{air} &= \frac{\dot{m}_{PG} C_{PG} (T_{PGin} - T_{PGo})}{C_{air} (T_{a,o} - T_{a,in})} = \frac{73.6186 \times 1.232 (410 - 200)}{1.005 \times (226 - 45)} \\ &= 104.706 \text{ kg/hr} \end{aligned}$$

For HE-2 Air cooler

$$\dot{E}_{D,AC} = T_o \left[\dot{m}_h C_{ph} \ln \left(\frac{T_{h,out}}{T_{h,in}} \right) + \dot{m}_c C_{pc} \ln \left(\frac{T_{c,out}}{T_{c,in}} \right) \right]$$

$$\begin{aligned} \dot{E}_{D,AC} &= 298 \left[73.6186 \times 1.232 \ln \left(\frac{273 + 65}{273 + 145} \right) + 1443.95 \times 1.005 \ln \left(\frac{273 + 50}{273 + 45} \right) \right] \\ &= 0.2791359 \text{ kW} \end{aligned}$$

Where, the mass flow rate of air is also calculated by the energy balance.

For HE-2 Water cooler

$$\dot{E}_{D,WC} = T_o \left[\dot{m}_h C_{ph} \ln \left(\frac{T_{h,out}}{T_{h,in}} \right) + \dot{m}_c C_{pc} \ln \left(\frac{T_{c,out}}{T_{c,in}} \right) \right]$$

$$\dot{E}_{D,WC} = 298 \left[73.6186 \times 1.232 \ln \left(\frac{273+41}{273+65} \right) + 236.707 \times 1.005 \ln \left(\frac{273+46}{273+35} \right) \right]$$

$$= 0.13461076 \text{ kW}$$

For Fabric filter: For the single stream

$$\dot{E}_{D,FL} = \dot{m}_h C_{ph} (T_{h,n} - T_{h,out}) - T_o \dot{m}_h C_{ph} \ln \left(\frac{T_{h,in}}{T_{h,out}} \right)$$

$$\dot{E}_{D,FL} = 73.6186 \times 1.232 \{ (273+200) - (273+145) \} - 298 \times 73.6186 \times 1.232 \ln \left(\frac{273+200}{273+145} \right)$$

$$= 0.4575982 \text{ kW}$$

For Paper filter: For the single stream

$$\dot{E}_{D,PL} = \dot{m}_h C_{ph} (T_{h,n} - T_{h,out}) - T_o \dot{m}_h C_{ph} \ln \left(\frac{T_{h,in}}{T_{h,out}} \right)$$

$$\dot{E}_{D,PL} = 73.6186 \times 1.232 \{ (273+41) - (273+38) \} - 298 \times 73.6186 \times 1.232 \ln \left(\frac{273+41}{273+38} \right)$$

$$= 0.0035064 \text{ kW}$$

Table-11. Evaluation of exergy destruction of electric generator and heat engine:

At 15.24kW, Energy efficiency; table-11; $\dot{E}_{D,electric} = \dot{W}_E - \dot{P}_E = 19.05 - 15.24 = 3.81 \text{ kW}$

$$\dot{E}_{D,engine} = \dot{E}_{PG} - (\dot{m}_{exht} h_{exht} + \dot{m}_{exht} h_{air} - T_o \dot{m}_{exht} S_{exht} + T_o \dot{m}_{exht} S_{air} + \dot{W}_E)$$

$$= 108.8094 - \{ 180.513(-51.55121 + 312.2319 - 298 \times -0.459193 + 298 \times 1.7413) + 19.05 \}$$

$$= 43.80671 \text{ kW}$$

Table-20-23. Evaluation of energetic, exergetic COP and exergy destruction of VAM:

At 15.24kW, Energetic COP; **table-21**

Desired effect (Energy output);

$$Q_E = \dot{m}_r (h_{out} - h_{in}) = 17.04 \times (1427.31 - 116.85) / 3600 = 6.20284 \text{ kW}$$

Expenditure;

$$Q_{in} = \dot{m}_w (h_4 - h_5) = 1818.5(525.21 - 505.38) / 3600 = 10.0167224 \text{ kW}$$

$$\therefore \text{Energetic COP}; \quad COP_I = \frac{Q_E}{Q_{in}} = \frac{6.20284}{10.0167224} = 0.619284$$

Now, at 15.24kW, Exergetic COP;

Desired effect (Exergy out);

$$\begin{aligned} \Delta \dot{E}_{out} &= \dot{m}_r [(h_{in} - h_{out}) - T_o (s_{in} - s_{out})] \\ &= 17.04 [(116.85 - 1427.31) - 298 \times (0.46501 - 5.543)] = 0.95983 \text{ kW} \end{aligned}$$

Expenditure (Exergy in);

$$\begin{aligned} \Delta \dot{E}_{in} &= \dot{m}_r [(h_4 - h_5) - T_o (s_4 - s_5)] \\ &= 15.04 [(525.21 - 505.38) - 298 \times (1.5819 - 1.5319)] = 2.49028 \text{ kW} \end{aligned}$$

$$\therefore \text{Exergetic COP}; \quad COP_{II} = \frac{\dot{E}_{out}}{\dot{E}_{in}} = \frac{0.95983}{2.49028} = 0.385431$$

At 15.24kW, Exergy destruction in different components;

For generator

$$\begin{aligned} \dot{E}_{D,gen} &= T_o [\dot{m}_w (s_4 - s_5) + \dot{m}_{ss} (s_{12} - s_7) + \dot{m}_r (s_7 - s_6)] \\ &= 298 [1818.467 \times (1.5819 - 1.5319) + 51.89(1.343 + 0.39989) \\ &\quad + 17.04(-0.39989 - 4.915)] / 3600 = 7.515904 \text{ kW} \end{aligned}$$

For pump

$$\dot{E}_{D,P1} = \dot{m}_{ss} [T_o (s_{out} - s_{in})] = 298 \times 51.89 \times (1.0446 - 1.0053) / 3600 = 0.168807 \text{ kW}$$

For solution heat exchanger

$$\begin{aligned} \dot{E}_{D,SHE} &= T_o [\dot{m}_{ws} (s_7 - s_8) + \dot{m}_{ss} (s_{12} - s_{11})] \\ &= 298 [36.85(-0.39998 + 0.52348) + 51.89(1.343 - 1.0446)] \\ &= 1.6587 \text{ kW} \end{aligned}$$

For throttle valve-1

$$\begin{aligned} \dot{E}_{D,TV1} &= T_o [\dot{m}_r (s_{in} - s_{out})] = 298 \times 36.85 (-0.52348 + 0.569) \\ &= 0.137449 \text{ kW} \end{aligned}$$

For throttle valve-2

$$\begin{aligned} \dot{E}_{D,TV2} &= T_o [\dot{m}_r (s_{in} - s_{out})] = 298 \times 17.04 (1.306 - 0.46501) \\ &= 1.18624 \text{ kW} \end{aligned}$$

For absorber

$$\dot{E}_{D,A} = T_o [\dot{m}_d (s_j - s_i) + \dot{m}_{ss} (s_{10} - s_9) + \dot{m}_r (s_9 - s_{15})]$$

$$= 298[1347.95(0.494-0.40075) + 17.04(-0.569--5.543) + 51.89(1.0053+0.569)]$$

$$= 8.58914 \text{ kW}$$

For condenser

$$\dot{E}_{D,C} = T_o[\dot{m}_r(s_6 - s_{13}) + \dot{m}_c(s_k - s_l)]$$

$$= 298[17.04(4.915-1.306) + 503.83(0.4181-0.5257)] = 0.60305697 \text{ kW}$$

For evaporator

$$\dot{E}_{D,evp} = T_o[\dot{m}_r(s_{14} - s_{15}) + \dot{m}_e(s_p - s_q)]$$

$$= 298[17.04(5.543-0.465) + 515.7681(6.7655-6.8778)]$$

$$= 2.3681226 \text{ kW}$$

Table.24.Performance of VAM wrt atm temperature:

$$COP_I = \frac{T_E}{T_{atm} - T_E} \times \frac{T_G - T_{atm}}{T_G}$$

$$= \frac{269.8}{308.0521 - 269.8} \times \frac{356.95 - 308.0521}{356.95} = 0.966204$$

$$COP_{II} = COP_I \times \frac{\left(\frac{T_o}{T_E} - 1\right)}{\left(1 - \frac{T_o}{T_G}\right)} = 0.966204 \times \frac{\left(\frac{298}{269.8} - 1\right)}{\left(1 - \frac{298}{356.95}\right)} = 0.6115$$

Table.25.Combined analysis of hybrid system at 15.24 kW

Overall energy and exergy efficiency of the system;

Overall energy efficiency; $\eta_{o,en} = \frac{P_E + \dot{Q}_E}{E_{in}} = \frac{15.24 + 41.87}{161.043} = 35.47\%$

Overall exergy efficiency $\eta_{o,ex} = \eta_{o,en} \times \frac{1}{\left(1 - \frac{T_o}{T_{grate}}\right)} = 0.3547 \times \frac{1}{\left(1 - \frac{273 + 25}{273 + 538}\right)} = 56.069\%$

Where, $\dot{Q}_E = \dot{m}(h_{ga} - h_{fa}) = 115.04(1427.31 - 1116.85) = 41.87 \text{ kW}$

$E_{in} = \dot{Q}_{Supplied} + \dot{Q}_{Solar} = 144.6667 + 16.37614 = 161.042 \text{ kW}$

And T_{grate} = Temperature above the grate of gasifier

Similarly, the overall energy and exergy can be calculated at the constant electric load of 38.862 kW.

Table.27.Heat balance sheet at 15.24 kW

Heat supplied is calculated as follows:-

$$Q_s = \text{Biomass consumption rate} \times \text{CV of fuel used}$$

$$= 28 \times 18.6/3600 = 144.6667 \text{ kW}$$

$$\text{Solar heat given by radiation} = \text{Average DNI} \times A_s$$

$$= 441.9295 \times 37.056$$

$$= 16.37614 \text{ kW}$$

$$\therefore \text{Total heat supplied } (Q_{total}) = 144.6667 + 16.37614 = 161.0428067 \text{ kW}$$

(i) Heat used in gasification (Q_1):-It can be calculated from

$$Q_1 = \dot{m}_{biomass} CV_{biomass} - \dot{m}_{pg} CV_{pg} = 28 \text{ kg/hr} \times 18.6 \text{ MJ/kg} - 67.54 \text{ m}^3/\text{hr} \times 5.415002 \text{ MJ/m}^3$$

$$= 43.0753 \text{ kW}$$

$$\text{Percentage of heat utilized in gasifier} = \left(\frac{Q_1}{Q_{total}} \right) \times 100 = 26.7477\%$$

Average heat (%) used in gasification,

$$Q_{avg,1} = \frac{26.7477 + 25.42395 + 17.89213 + 17.9264 + 18.57298}{5} = 21.31264\%$$

(ii) Heat used in HE-1(regenerator):-It can calculate from

$$Q_2 = \dot{m}_{pg} C_{pg} (T_{g,in} - T_{g,out}) = 73.6186 \times 1.232 \{ (273 + 410) - (273 + 200) \} = 5.29072 \text{ kW}$$

$$\text{Percentage of heat utilized in HE-1(regenerator)} = \left(\frac{Q_2}{Q_{total}} \right) \times 100 = 3.28529\%$$

$$\text{Average heat (%), } Q_{avg,2} = \frac{3.28529 + 3.931053 + 4.08755 + 4.0045 + 4.5200218}{5} = 3.965683\%$$

(iii) Heat used in HE-2 (Air cooler); $Q_3 = \dot{m}_{pg} C_{pg} (T_{g,in} - T_{g,out})$

$$= 73.6186 \times 1.232 \{ (273 + 145) - (273 + 65) \} = 2.01551 \text{ kW}$$

$$\text{Percentage of heat utilized in HE-2(Air cooler)} = \left(\frac{Q_3}{Q_{total}} \right) \times 100 = 1.251539\%$$

$$\text{Average heat, } Q_{avg,3} = \frac{1.25154 + 1.661008 + 1.62356 + 1.9626 + 2.260011}{5} = 1.751744\%$$

(iv) Heat used in HE-2 (Water cooler); $Q_4 = \dot{m}_{pg} C_{pg} (T_{g,in} - T_{g,out})$

$$= 73.6186 \times 1.232 \{ (273 + 65) - (273 + 41) \} = 0.604650 \text{ kW}$$

$$\text{Percentage of heat utilized in HE-2(Water cooler)} = \left(\frac{Q_4}{Q_{total}} \right) \times 100 = 0.375462\%$$

$$\text{Average heat, } Q_{avg,4} = \frac{0.37546 + 0.498303 + 0.61122 + 0.67402 + 0.7807311}{5} = 0.587949\%$$

$$\text{(v) Heat used in fabric filter; } Q_5 = \dot{m}_{pg} C_{pg} (T_{g,in} - T_{g,out})$$

$$= 73.6186 \times 1.232 \{(273 + 200) - (273 + 145)\} = 1.3857 \text{ kW}$$

$$\text{Percentage of heat utilized in fabric filter} = \left(\frac{Q_5}{Q_{total}} \right) \times 100 = 0.860433\%$$

$$\text{Average heat, } Q_{avg,5} = \frac{0.86043 + 1.070427 + 1.26065 + 1.09033 + 1.2327331}{5} = 1.102915\%$$

$$\text{(vi) Heat used in paper filter; } Q_6 = \dot{m}_{pg} C_{pg} (T_{g,in} - T_{g,out})$$

$$= 73.6186 \times 1.232 \{(273 + 41) - (273 + 38)\} = 0.07558 \text{ kW}$$

$$\text{Percentage of heat utilized in paper filter} = \left(\frac{Q_6}{Q_{total}} \right) \times 100 = 0.046933\%$$

$$\text{Average heat, } Q_{avg,6} = \frac{0.04693 + 0.036911 + 0.0764 + 0.03965 + 0.061637}{5} = 0.052306\%$$

$$\text{(vii) Heat equivalent to brake power; } Q_7 = \frac{P_{electric}}{\eta_{generator}}$$

$$Q_7 = \frac{15.24}{0.8} = 19.05 \text{ kW}$$

Where, the electric generator efficiency is; $\eta_{gen} = 0.8$

$$\text{Percentage of heat equivalent to brake power} = \left(\frac{Q_7}{Q_{total}} \right) \times 100$$

$$= \left(\frac{19.05}{161.0428067} \right) \times 100 = 11.82915\%$$

$$\text{Average heat, } Q_{avg,7} = \frac{11.8292 + 12.9277 + 14.061 + 14.5471 + 15.16168}{5} = 13.70534\%$$

$$\text{(viii) Heat equivalent to electric power; } Q_8 = VI\sqrt{3} = 440 \times 20\sqrt{3}/1000 = 15.24 \text{ kW}$$

$$\text{Percentage of heat equivalent to electric power} = \left(\frac{Q_8}{Q_{total}} \right) \times 100$$

$$= \left(\frac{15.24}{161.0428067} \right) \times 100 = 9.463322\%$$

$$\text{Average heat, } Q_{avg,8} = \frac{9.46332 + 10.34216 + 11.2488 + 11.6377 + 12.12935}{5} = 10.96427\%$$

$$\text{(ix) Heat lost due to exhaust; } Q_9 = (\dot{m}_{air} + \dot{m}_{fuel}) \times C_{p,exhaust} \times \Delta T_{exhaust}$$

$$Q_9 = (106.86 + 67.54 \times 1.09) \times 1.008 \times (352 - 129) = 11.18 \text{ kW}$$

$$\text{Percentage of heat lost due to exhaust} = \left(\frac{Q_9}{Q_{total}} \right) \times 100$$

$$= \left(\frac{11.18}{161.0428067} \right) \times 100 = 6.942254\%$$

$$\text{Average heat, } Q_{avg,9} = \frac{6.94225 + 6.396203 + 8.479271 + 8.70537 + 8.154583}{5} = 7.735536\%$$

$$\text{(x) Heat used in solar collector; } Q_{10} = \dot{m}_{water} \times C_{p,water} \times \Delta T$$

$$= 1818.467 \times 4.18 \times (121.5 - 120.37)$$

$$= 2.39 \text{ kW}$$

$$\text{Percentage of heat used in solar collector} = \left(\frac{Q_{10}}{Q_{total}} \right) \times 100$$

$$= \left(\frac{2.39}{161.0428067} \right) \times 100 = 1.484077\%$$

$$\text{Average heat, } Q_{avg,10} = \frac{1.48408 + 1.904674 + 1.164577 + 1.08363 + 0.867675}{5} = 1.300926\%$$

$$\text{(xi) Heat used in HRU; } Q_{11} = \dot{m}_{water} \times C_{p,water} \times \Delta T$$

$$= 1818.467 \times 4.18 \times (125.0333 - 121.5) = 7.46 \text{ kW}$$

$$\text{Percentage of heat used in HRU} = \left(\frac{Q_{11}}{Q_{total}} \right) \times 100 = \left(\frac{7.46}{161.0428067} \right) \times 100 = 4.632309\%$$

$$\text{Average heat, } Q_{avg,11} = \frac{4.63231 + 4.501161 + 6.827539 + 7.13084 + 6.992585}{5} = 6.016887\%$$

$$\text{(xii) Heat used in generator; } Q_{12} = \dot{m}_{water} \times C_{p,water} \times \Delta T$$

$$= 1818.467 \times 4.18 \times (125.033 - 120.37) = 9.85 \text{ kW}$$

$$\text{Percentage of heat used in generator} = \left(\frac{Q_{12}}{Q_{total}} \right) \times 100$$

$$= \left(\frac{9.85}{161.0428067} \right) \times 100 = 6.116386\%$$

$$\text{Average heat, } Q_{avg,12} = \frac{6.11639 + 6.402771 + 7.99335 + 8.21447 + 7.769747}{5} = 7.299343\%$$

$$\text{(xiii) Heat used in condenser; } Q_{13} = \dot{m}_{ammonia} (h_{gc} - h_{fc})$$

$$= 17.04 \times (1471.83 - 354.894) = 5.28683 \text{ kW}$$

$$\text{Percentage of heat used in condenser} = \left(\frac{Q_{13}}{Q_{total}} \right) \times 100$$

$$= \left(\frac{5.28683}{161.0428067} \right) \times 100 = 3.282872\%$$

$$\text{Average heat, } Q_{avg,13} = \frac{3.28287 + 3.129609 + 3.62308 + 3.30429 + 2.959899}{5} = 3.259951\%$$

$$\text{(xiv) Heat used in evaporator; } Q_{14} = \dot{m}_{ammonia} (h_{ga} - h_{fa})$$

$$= 17.04 \times (1427.31 - 116.85) = 6.20284 \text{ kW}$$

$$\text{Percentage of heat used in evaporator} = \left(\frac{Q_{14}}{Q_{total}} \right) \times 100$$

$$= \left(\frac{6.20284}{161.0428067} \right) \times 100 = 3.8516715\%$$

$$\text{Average heat, } Q_{avg,14} = \frac{3.85167 + 3.695296 + 4.3082 + 3.95523 + 3.571574}{5} = 3.876395\%$$

$$\text{(xv) Heat used in TV}_1; Q_{15} = \dot{m}_{ws} C_w (T_8 - T_9)$$

$$= 36.85 \times 4.18 (42.05 - 38.73) = 0.14205 \text{ kW}$$

$$\text{Percentage of heat used in TV}_1 = \left(\frac{Q_{15}}{Q_{total}} \right) \times 100 = \left(\frac{0.14205}{161.0428067} \right) \times 100 = 0.088208\%$$

$$\text{Average heat, } Q_{avg,15} = \frac{0.08821 + 0.259218 + 0.24081 + 0.18899 + 0.170596}{5} = 0.189564\%$$

$$\text{(xvi) Heat used in TV}_2; Q_{16} = \dot{m}_{ammonia} (h_{fc} - h_{fa})$$

$$= 17.04 \times (354.894 - 116.85) = 1.1267416 \text{ kW}$$

$$\text{Percentage of heat used in TV}_2 = \left(\frac{Q_{16}}{Q_{total}} \right) \times 100 = \left(\frac{1.1267416}{161.0428067} \right) \times 100 = 0.6996534\%$$

$$\text{Average heat, } Q_{avg,16} = \frac{0.69965 + 0.695687 + 0.83916 + 0.79864 + 0.748616}{5} = 0.756352\%$$

$$\text{(xvii) Heat used in pump; } Q_{17} = \dot{m}_{ss} C_{ammonia} (T_{11} - T_{10})$$

$$= 51.89 \times 4.72 (33.14 - 30.64) = 0.17008 \text{ kW}$$

$$\text{Percentage of heat used in pump} = \left(\frac{Q_{17}}{Q_{total}} \right) \times 100 = \left(\frac{0.17008}{161.0428067} \right) \times 100 = 0.105614\%$$

$$\text{Average heat, } Q_{avg,17} = \frac{0.10561 + 0.123177 + 0.07825 + 0.09024 + 0.039643}{5} = 0.087385\%$$

$$\text{(xviii) Heat used in SHE; } Q_{18} = \dot{m}_{ss} C_{ammonia} (T_{12} - T_{11})$$

$$= 51.89 \times 4.72 (52.58 - 33.14) = 1.32257 \text{ kW}$$

$$\text{Percentage of heat used in SHE} = \left(\frac{Q_{18}}{Q_{total}} \right) \times 100 = \left(\frac{1.32257}{161.0428067} \right) \times 100 = 0.821254\%$$

$$\text{Average heat, } Q_{avg,18} = \frac{0.82125 + 0.868461 + 0.75289 + 0.64782 + 0.586108}{5} = 0.735307\%$$

$$\text{(xix) Heat used in absorber; } Q_{19} = \dot{m}_a C_w (T_{out,cw} - T_{in,cw})$$

$$= 1347.95 \times 4.18 (34.21-27.4) = 10.6585 \text{ kW}$$

$$\text{Percentage of heat used in absorber} = \left(\frac{Q_{19}}{Q_{total}} \right) \times 100 = \left(\frac{10.6585}{161.0428067} \right) \times 100 = 6.618427\%$$

$$\text{Average heat, } Q_{avg,19} = \frac{6.61843 + 6.963069 + 8.77383 + 9.06309 + 8.614719}{5} = 8.006625\%$$

$$\begin{aligned} \text{(xx) Unaccounted heat loss; } Q_{20} &= Q_{total} - (Q_1 + Q_2 + Q_3 + Q_4 + \dots + Q_{19}) \\ &= 161.0428067 - (142.527) = 18.5158 \text{ kW} \end{aligned}$$

$$\text{Percentage of unaccounted heat loss} = \left(\frac{Q_{20}}{Q_{total}} \right) \times 100 = \left(\frac{18.5158}{161.0428067} \right) \times 100 = 11.49744\%$$

$$\text{Average heat, } Q_{avg,20} = \frac{11.4974 + 9.169365 + 6.05757 + 4.93512 + 4.805145}{5} = 7.292928\%$$

Table.28 .Exergy balance sheet at 15.24 kW

Total exergy supplied is calculated as follows:-

$$\begin{aligned} \text{Total exergy supplied (} Ex_{total} \text{)} &= \text{Exergy input in gasifier} + \text{Exergy input by solar} \\ &= 173.44833 + 14.92369 = 188.3720233 \text{ kW} \end{aligned}$$

∴ Exergy destruction of all components has been calculated in above exergy calculations.

∴ The percentage of ED of all components:

(i) Percentage of Exergy output of electric generator,

$$Ex_{out,gen} = \left(\frac{Ex_{out,gen}}{Exergy_{total}} \right) \times 100 = \left(\frac{15.24}{188.3720233} \right) \times 100 = 8.090373 \%$$

Average exergy,

$$Ex_{avg,gen} = \frac{8.090373 + 8.734707 + 9.387899 + 9.634239 + 9.96334}{5} = 9.162112\%$$

(ii) Percentage of Exergy output of VAM, $Ex_{out,VAM} = \left(\frac{Ex_{out,VAM}}{Exergy_{total}} \right) \times 100$

$$= \left(\frac{0.95983}{188.3720233} \right) \times 100 = 0.50954\%$$

Average exergy,

$$Ex_{avg,VAM} = \frac{0.50954 + 0.487276 + 0.56533 + 0.537692 + 0.493647}{5} = 0.518696\%$$

(iii) Percentage of exergy destruction of gasifier, $ED_1 = \left(\frac{ED_1}{Exergy_{total}} \right) \times 100$

$$= \left(\frac{64.6389}{188.3720233} \right) \times 100 = 34.31451\%$$

$$\text{Average ED, } ED_{avg,1} = \frac{34.31451 + 26.58916 + 24.4257 + 22.23662 + 20.84782}{5} = 25.68276\%$$

(iv) **Percentage of exergy destruction of HE-1(regenerator),**

$$\begin{aligned} ED_2 &= \left(\frac{ED_2}{Exergy_{total}} \right) \times 100 \\ &= \left(\frac{1.166287}{188.3720233} \right) \times 100 = 0.61914\% \end{aligned}$$

$$\text{Average ED, } ED_{avg,2} = \frac{0.61914 + 0.786128 + 0.813476 + 0.871178 + 0.833652}{5} = 0.784715\%$$

(v) **Percentage of exergy destruction of HE-2 (Air cooler),**

$$\begin{aligned} ED_3 &= \left(\frac{ED_3}{Exergy_{total}} \right) \times 100 \\ &= \left(\frac{0.279136}{188.3720233} \right) \times 100 = 0.148183\% \end{aligned}$$

$$\text{Average ED, } ED_{avg,3} = \frac{0.148183 + 0.203197 + 0.20057 + 0.254954 + 0.317468}{5} = 0.224874\%$$

(vi) **Percentage of exergy destruction of HE-2 (Water cooler),**

$$\begin{aligned} ED_4 &= \left(\frac{ED_4}{Exergy_{total}} \right) \times 100 \\ &= \left(\frac{0.134611}{188.3720233} \right) \times 100 = 0.07146\% \end{aligned}$$

$$\text{Average ED, } ED_{avg,4} = \frac{0.07146 + 0.093544 + 0.1155 + 0.123322 + 0.146182}{5} = 0.110002\%$$

(vii) **Percentage of exergy destruction of fabric filter,** $ED_5 = \left(\frac{ED_5}{Exergy_{total}} \right) \times 100$

$$= \left(\frac{0.457598}{188.3720233} \right) \times 100 = 0.242923\%$$

$$\text{Average ED, } ED_{avg,5} = \frac{0.24292 + 0.318882 + 0.37817 + 0.336312 + 0.399763}{5} = 0.33521\%$$

(viii) **Percentage of exergy destruction of paper filter,** $ED_6 = \left(\frac{ED_6}{Exergy_{total}} \right) \times 100$

$$= \left(\frac{0.003506}{188.3720233} \right) \times 100 = 0.001861\%$$

$$\text{Average ED, } ED_{avg,6} = \frac{0.00186 + 0.001588 + 0.00325 + 0.001672 + 0.002503}{5} = 0.002174\%$$

(ix) **Percentage of exergy destruction of an engine, $ED_7 = \left(\frac{ED_7}{Exergy_{total}} \right) \times 100$**

$$= \left(\frac{43.806}{188.3720233} \right) \times 100 = 23.25505\%$$

Average ED, $ED_{avg,7} = \frac{23.2551 + 34.92288 + 38.83716 + 42.51091 + 44.47587}{5} = 36.80037\%$

(x) **Percentage of exergy destruction of electric generator,**

$$ED_8 = \left(\frac{ED_8}{Exergy_{total}} \right) \times 100$$

$$= \left(\frac{3.81}{188.3720233} \right) \times 100 = 2.022593\%$$

Average ED, $ED_{avg,8} = \frac{2.02259 + 2.183677 + 2.346975 + 2.40856 + 2.490835}{5} = 2.290528\%$

(xi) **Percentage of exergy lost due to exhaust, $ED_9 = \left(\frac{ED_9}{Exergy_{total}} \right) \times 100$**

$$= \left(\frac{0.54628}{188.3720233} \right) \times 100 = 0.290001\%$$

Average ED, $ED_{avg,9} = \frac{0.290001 + 0.283416 + 0.326971 + 0.34198 + 0.376113}{5} = 0.323696\%$

(xii) **Percentage of exergy destruction of solar collector,**

$$ED_{10} = \left(\frac{ED_{10}}{Exergy_{total}} \right) \times 100$$

$$= \left(\frac{14.4138}{188.3720233} \right) \times 100 = 7.651784\%$$

Average ED, $ED_{avg,10} = \frac{7.65178 + 6.078635 + 6.722758 + 6.761503 + 6.299066}{5} = 6.702749\%$

(xiii) **Percentage of exergy destruction of HRU, $ED_{11} = \left(\frac{ED_{11}}{Exergy_{total}} \right) \times 100$**

$$= \left(\frac{0.40154}{188.3720233} \right) \times 100 = 0.213163\%$$

Average ED, $ED_{avg,11} = \frac{0.21316 + 0.377398 + 0.829405 + 1.044016 + 1.102125}{5} = 0.713221\%$

(xiv) **Percentage of exergy destruction of generator, $ED_{12} = \left(\frac{ED_{12}}{Exergy_{total}} \right) \times 100$**

$$= \left(\frac{7.515907}{188.3720233} \right) \times 100 = 3.989927\%$$

$$\text{Average ED, } ED_{avg,12} = \frac{3.989927 + 4.515573 + 4.56129 + 4.571272 + 4.526628}{5} = 4.432937\%$$

(xv) **Percentage of exergy destruction of condenser,**

$$ED_{13} = \left(\frac{ED_{13}}{Exergy_{total}} \right) \times 100 = \left(\frac{0.603057}{188.3720233} \right) \times 100 = 0.320141\%$$

$$\text{Average ED, } ED_{avg,13} = \frac{0.320141 + 0.70073 + 0.87396 + 0.802838 + 0.741322}{5} = 0.687798\%$$

(xvi) **Percentage of exergy destruction of evaporator,** $ED_{14} = \left(\frac{ED_{14}}{Exergy_{total}} \right) \times 100$

$$= \left(\frac{2.368123}{188.3720233} \right) \times 100 = 1.257152 \%$$

$$\text{Average ED, } ED_{avg,14} = \frac{1.257152 + 0.853937 + 0.73291 + 0.343316 + 0.297932}{5} = 0.69705\%$$

(xvii) **Percentage of exergy destruction of TV₁,** $ED_{15} = \left(\frac{ED_{15}}{Exergy_{total}} \right) \times 100$

$$= \left(\frac{0.137449}{188.3720233} \right) \times 100 = 0.072967\%$$

$$\text{Average ED, } ED_{avg,15} = \frac{0.072967 + 0.20992 + 0.19147 + 0.148667 + 0.132972}{5} = 0.151199\%$$

(xviii) **Percentage of exergy destruction of TV₂,** $ED_{16} = \left(\frac{ED_{16}}{Exergy_{total}} \right) \times 100$

$$= \left(\frac{1.18624}{188.3720233} \right) \times 100 = 0.629733\%$$

$$\text{Average ED, } ED_{avg,16} = \frac{0.629733 + 0.611326 + 0.72704 + 0.689993 + 0.639767}{5} = 0.659572\%$$

(xix) **Percentage of exergy destruction of pump,** $ED_{17} = \left(\frac{ED_{17}}{Exergy_{total}} \right) \times 100$

$$= \left(\frac{0.168807}{188.3720233} \right) \times 100 = 0.089614\%$$

$$\text{Average ED, } ED_{avg,17} = \frac{0.089614 + 0.103145 + 0.06452 + 0.073709 + 0.031946}{5} = 0.072586\%$$

(xx) **Percentage of exergy destruction of SHE,** $ED_{18} = \left(\frac{ED_{18}}{Exergy_{total}} \right) \times 100$

$$= \left(\frac{1.6587}{188.3720233} \right) \times 100 = 0.880545\%$$

$$\text{Average ED, } ED_{avg,18} = \frac{0.880545 + 0.855239 + 0.67956 + 0.557903 + 0.489835}{5} = 0.692615\%$$

(xxi) Percentage of exergy destruction of absorber, $ED_{19} = \left(\frac{ED_{19}}{Exergy_{total}} \right) \times 100$

$$= \left(\frac{8.58914}{188.3720233} \right) \times 100 = 4.559669\%$$

Average ED, $ED_{avg,19} = \frac{4.559669 + 5.189348 + 5.61443 + 5.697368 + 5.452738}{5} = 5.302711\%$

(xxii) Percentage of unaccounted exergy loss;

Unaccounted exergy loss;

$$ED_{20} = Ex_{total} - (Ex_{out,gen} + Ex_{out,VAM} + ED_1 + ED_2 + ED_3 + ED_4 + \dots + ED_{19})$$

$$= 188.3720233 - 168.085 = 20.287 \text{ kW}$$

\therefore Percentage of unaccounted exergy loss = $\left(\frac{ED_{20}}{Exergy_{total}} \right) \times 100$

$$= \left(\frac{20.287}{161.0428067} \right) \times 100 = 10.76966\%$$

Average ED, $ED_{avg,20} = \frac{10.76966 + 5.90036 + 1.601599 + 0.051843 + 0.051511}{5} = 3.674995\%$

Appendix-B (Tables)

(i) Evaluation of gasifier and gas cooling-cleaning unit:

Table-1. Gasifier

Pressure level measurement (in mm of W.G.)

S.No.	Time (hr)	Gasifier		Fabric filter		Paper filter	
		Inlet	Outlet	Inlet	Outlet	Inlet	Outlet
1	10:00:00	254	128	103	-165	-393	-398
2	20:00:00	248	86	25	-325	-332	-337
3	30:00:00	250	39	-1	-325	-307	-316
4	40:00:00	265	1	-75	-578	-493	-505
5	50:00:00	260	-25	-60	-602	-415	-453

Table-2. Gasifier and filters

Temperature measurement in (°C)

S.No.	Time (hr)	HE-1 (Regenerator)				Fabric filter		HE-2 (Air cooler)				HE-2 (Water cooler)				Paper filter	
		Gas inlet	Gas outlet	Air inlet	Air outlet	Inlet	Outlet	Gas inlet	Gas outlet	Air inlet	Air outlet	Inlet	Outlet	Water inlet	Water outlet	Inlet	Outlet
1	10:00:00	410	200	45	226	200	145	145	65	45	50	65	41	35	46	41	38
2	20:00:00	430	217	48	222	217	159	159	69	48	55	69	42	37	48	42	40
3	30:00:00	440	226	48	230	226	160	160	75	48	58	75	43	36	52	43	39
4	40:00:00	455	230	50	240	230	175	175	76	50	60	76	42	38	53	42	40
5	50:00:00	470	250	50	275	250	190	190	80	50	62	80	42	38	52	42	39

Table-3. Engine and generator

Power generation sheet

S.No.	Time (hr)	Voltage (V)			Current (A)			Electric load	BCR	Frequency	Exhaust gas temperature (°C)			RPM
		Phase			Phase						Inlet	RHE	Outlet	
		I	II	III	I	II	III	(kW)	(kg/hr)	(Hz)				
1	10:00:00	220	220	220	20	20	20	15.24	28	49.8	352	182	129	1296
2	20:00:00	228	228	228	31	31	31	23.62	41	49.6	366	233	135	1290
3	30:00:00	229	229	229	36	36	36	27.432	44	49.4	439	271	142	1297
4	40:00:00	230	230	230	42	42	42	32.004	50	50	450	299	147	1295
5	50:00:00	227	227	227	51	51	51	38.862	59	49.9	465	316	149	1292

Table-4. PG/biomass requirement/gasifier efficiency

S.No.	Electric load	Biomass consumption rate (BCR)	P.G. flow rate	P.G. per kg of biomass	Gasification efficiency (η)	BCR (Day) (Solar + PG +Exhaust)	BCR (Night) (PG + Exhaust)	Specific fuel consumption (SFC)	SFC (Day)	SFC (Night)	Air-fuel ratio
	(kW)	(kg/hr)	(m ³ /hr)	(m ³ /kg)	(%)	(kg/hr)	(kg/hr)	(kg/kWhr)	(kg/kWhr)	(kg/kWhr)	
1	15.24	28	67.54	2.412	70.22	32.176	32.835	1.837	2.111	2.129	1.452
2	23.62	41	112.996	2.756	72.59	43.767	44.925	1.736	1.853	1.901	0.834
3	27.432	44	124.872	2.838	80.81	45.318	45.999	1.604	1.652	1.676	0.827
4	32.004	50	146.15	2.923	80.92	50.576	51.289	1.563	1.5803	1.603	0.771
5	38.862	59	176.47	2.991	81.22	59.023	59.6186	1.518	1.5188	1.534	0.768

Table-4a. Calibration data for air

S.No.	Manometer height			Air flow rate
	h_1 (cm)	h_2 (cm)	Δh (m)	V_a (m/s)
1	15.6	16.5	0.009	4.8
2	15.1	16.6	0.015	4.9
3	14.5	17.4	0.029	5.2
4	13.2	17.9	0.047	5.8
5	12.1	18.8	0.067	3.3
	Avg.		0.0334	4.8

Table-4b. Calibration data for PG

S.No.	Electric load	Manometer height for PG			Air flow rate for gasifier
		h_1 (cm)	h_2 (cm)	Δh (m)	V_a (m/s)
	(kW)				
1	15.24	15.5	18.9	0.034	18.52
2	23.62	14.9	24.5	0.096	25.97
3	27.432	14.4	26.2	0.118	29.22
4	32.004	13.1	29.2	0.161	34.74
5	38.862	12.8	36.3	0.235	40.06

Table-5. PG chemical exergy calculation

S.No.	Chemical composition of producer gas by volume (%)						CV of PG (MJ/m ³)	Temp. paper filter (°C)	P.G. flow rate (m ³ /h)	No of moles (kg mole/h)					PG chemical exergy Ech (kW)
	Electric load (kW)	CO	CO ₂	H ₂	CH ₄	N ₂				CO	CO ₂	H ₂	CH ₄	N ₂	
1	15.24	21.5	12.1	18.4	2	46	5.415002	38	67.54	0.60304	0.3618	0.60304	0.09045	1.357	108.7952213
2	23.62	18.1	12.75	18.1	1.85	49.2	5.400769	40	112.996	1.009	0.6053	1.009	0.1513	2.27	182.0253211
3	27.432	19.65	12.4	18.8	2.2	46.95	5.401075	39	124.872	1.115	0.668	1.115	0.16723	2.51	201.1514415
4	32.004	18.4	12.6	18.9	2.2	47.9	5.441288	40	146.15	1.3049	0.7831	1.3049	0.1957	3.545	235.536495
5	38.862	18.02	12.88	19	1.9	48.1	5.4046704	39	176.47	1.575	0.945	1.575	0.2363	3.545	284.1634569

Where the CV of PG constituents, $CV_{CO} = 12.622MJ / m^3$, $CV_{H_2} = 10.788MJ / m^3$, $CV_{CH_4} = 35.814MJ / m^3$

Table-6. Thermal properties of PG

S.No.	Electric load (kW)	Temp. paper filter (°C)	P.G. flow rate (m ³ /hr)	Mass flow rate of gas constituents (kg/h)					Total mass (kg/hr)	Producer gas (PG)			
				\dot{m}_{CO}	\dot{m}_{CO_2}	\dot{m}_{H_2}	\dot{m}_{CH_4}	\dot{m}_{N_2}		\bar{h}_o (kJ/kgmole) at 25°C & 1atm	\bar{S}_o (kJ/kg mole.K) at 25°C & 1atm	\bar{h} (kJ/kg mole)	\bar{S} (kJ/kg moleK)
1	15.24	38	67.54	16.891150	15.92281	1.2157286	1.45108935	38.00957	73.49036	8842.92	196.586	9249.951096	197.8949274
2	23.62	40	112.996	28.26209	26.639253	2.034144	2.4273059	63.5827	122.9455	8842.92	196.586	9329.024964	198.094173
3	27.432	39	124.872	31.23115	29.39868	2.24784	2.68287089	70.3051	135.8656	8842.92	196.586	9284.452547	197.9877058
4	32.004	40	146.15	36.550249	34.464231	2.6306784	3.1396151	99.29545	176.0802	8842.92	196.586	9307.036352	197.5934175
5	38.862	39	176.47	44.11575	41.58945	3.1752	3.7909609	99.29545	191.9668	8842.92	196.586	9284.695105	197.9936636

Table-7. Thermal properties of constituents of PG

S.No.	Pressure	Temp. paper filter	Molar enthalpy of gas constituents, \bar{h} (kJ/kg mole)					Molar entropy of gas constituents, \bar{s} (kJ/kg moleK)				
	(MPa)		\bar{h}_{CO}	\bar{h}_{CO_2}	\bar{h}_{H_2}	\bar{h}_{CH_4}	\bar{h}_{N_2}	\bar{s}_{CO}	\bar{s}_{CO_2}	\bar{s}_{H_2}	\bar{s}_{CH_4}	\bar{s}_{N_2}
		(°C)										
1	0.1053	38	9043.2	9883.3	8839.9	10466	9043.2	198.771	215.27	131.781	187.72	192.73
2	0.1046	40	9101.6	10035.9	8897.7	10538	9101.6	198.96	215.51	131.968	187.96	192.915
3	0.1044	39	9072.4	9959.6	8579.8	10502	9072.4	198.863	215.39	131.875	187.84	192.823
4	0.1063	40	9101.6	10035.9	8897.7	10538	9101.6	198.96	215.51	131.968	187.96	192.915
5	0.1058	39	9072.4	9959.6	8579.8	10502	9072.4	198.863	215.39	131.875	187.84	192.823

Table-8. Average chemical contents of wood fuels

S.No.	Dry matter weight		Moisture (m _w)%	h _{fg} (kJ/kg) at 25°C and 1atm	LHV (MJ/kg)	HHV (MJ/kg)	Φ _{dry}	Exergy of wood/ kg (MJ/kg)
	Matter	(%)						
1	C	48.7	25	2466.1	18.565695	19.990608	1.162562	22.300524
2	H	6.42						
3	O	44.2						
4	N	0.55						
5	S	0.05						
6	Ash	0.08						

Table-9. ED of gasifier

S.No.	Electric load (kW)	BCR (kg/hr)	Exergy of wood per kg (MJ/kg)	Exergy of wood (kW)	PG total no. of moles n_{PG} (kg mole/hr)	Physical exergy, E_{ph} (kW)	Chemical exergy, E_{ch} (kW)	Exergy of PG, E_{PG} (kW)	Exergy efficiency, η_{ex} (%)	Gasification efficiency, η_{en} (%)	ED of gasifier (kW)
1	15.24	28	22.3005	173.4483	3.01533	0.0142213	108.7952	108.80942	62.73303289	70.22	64.638933
2	23.62	41	22.3005	253.9779	5.0446	0.0513728	182.0253	182.07667	71.68997305	72.59	71.901217
3	27.432	44	22.3005	272.5617	5.57523	0.0368994	201.1514	201.1883	73.81386475	76.81	71.373367
4	32.004	50	22.3005	309.7292	7.1336	0.3247984	235.5365	235.8613	76.15081994	80.92	73.867867
5	38.862	59	22.3005	365.4804	7.8763	0.0487464	284.1635	284.21225	77.75067748	81.22	81.316917

Table-10. EDs of filters

S.No.	HE-1 (Regenerator)		HE-2 (Air cooler)	HE-2 (Water cooler)	ED HE-1	ED HE-2	ED HE-2	ED-Fabric F.	ED-Paper F.
	\dot{m}_{PG}	\dot{m}_{air}	\dot{m}_{air}	\dot{m}_{water}	$\dot{E}_{D,regenerator}$	$\dot{E}_{D,Air-cooler}$	$\dot{E}_{D,water-cooler}$	$\dot{E}_{D,fabric-filter}$	$\dot{E}_{D,Paper-filter}$
	(kg/hr)	(kg/hr)	(kg/hr)	(kg/hr)	(kW)	(kW)	(kW)	(kW)	(kW)
1	73.6186	104.706	1443.95	236.707	1.166287	0.2791359	0.13461076	0.4575982	0.0035064
2	123.1656	184.827	1941.24	445.518	2.125812	0.54947653	0.252958	0.8623059	0.0042953
3	136.1105	196.191	1418.26	401.168	2.377026	0.58606883	0.33750767	1.1050286	0.0094916
4	159.3035	231.259	1933.33	532.13	2.893967	0.84693227	0.40966526	1.1171944	0.0055555
5	192.3523	230.559	2161.49	769.409	3.251657	1.2382843	0.57018339	1.559275	0.0097624

Table-11. ED of engine

S.No.	Electric load	Brake Power at engine shaft (\dot{W}_E)	$\dot{E}_{D,electric-generator}$	Exergy of PG, E_{PG}	\dot{m}_{exht}	$\dot{m}_{exht} \times \Delta h_{exht}$	$\dot{m}_{exht} \times \Delta S_{exht}$	$\dot{m}_{exht} \times h_{air}$	$\dot{m}_{exht} \times S_{air}$	$\dot{E}_{D,engine}$
					$(\dot{m}_{PG} + \dot{m}_{air})$	(kW)	(kW)	(kW)	(kW)	
	(kW)	(kW)	(kW)	(kW)	(kg/hr)					(kW)
1	15.24	19.05	3.81	108.809421	180.513	2.5849066	0.02303	15.656088	0.087315527	43.80671
2	23.62	29.525	5.905	182.076673	225.885	5.9810023	0.04008	19.591251	0.109262313	94.43688
3	27.432	34.29	6.858	201.188299	248.674	8.6672354	0.05327	10.360726	0.120285527	113.4845
4	32.004	40.005	8.001	235.861298	271.985	11.169894	0.06494	7.2523516	0.131561237	141.2171
5	38.862	48.5775	9.7155	284.212246	340.079	15.344643	0.07955	3.1974983	0.171111476	173.0374

Where, $\eta_{generator} = 80\%$, $h_{air} = 312.2319 \text{ kJ/kg}$ and $S_{air} = 1.7413477 \text{ kJ/kgK}$ while Δh_{exht} & ΔS_{exht} are taken from HRU evaluation.

(ii) Evaluation of scheffler disc:

Table-12. Scheffler collector efficiency calculation

S.No.	Time (hr)	Solar field flow rate	Solar temperature		Direct beam radiation (DNI)	$T_{atm,(Avg)}$	Power obtained by sun (receiver)	Power given by radiation	η_{energy}	Exergy input	Exergy output	η_{exergy}	$\dot{E}_{D,scheffler-collector}$
			(°C)										
			Inlet (T_{s1})	Outlet (T_{s2})									
		(kg/hr)			(W/m ²)	(°C)	(kW)	(kW)	(%)	(kW)	(kW)	(%)	(kW)
1	010:00:00	1818.47	120.37	121.5	441.9295	36.7521	2.3859	16.3761	14.5696	14.9237	0.5098	3.4165	14.4138
2	020:00:00	1871.38	114.79	116.79	446.6798	37.6495	4.3458	16.5522	26.2549	17.3109	0.8734	5.0455	16.4376
3	030:00:00	1852.16	109.58	110.903	446.1351	38.6769	2.8452	16.5319	17.2103	20.1756	0.5313	2.6334	19.6443
4	040:00:00	1774.38	103.45	104.89	449.8428	39.6451	2.9668	16.6694	17.7977	22.9686	0.5076	2.2097	22.4611
5	050:00:00	1749.37	98.93	100.3	419.9909	40.2606	2.7828	15.5632	17.8804	25.0128	0.4433	1.7722	24.5695

Table-13. Scheffler collector's heat loss factor calculation

S.No.	Time (hr)	Solar temp. difference (ΔT)	Mean temperature (T_m)	Ht. loss factor (FUL)	Wind speed (km/hr)
		($^{\circ}\text{C}$)	($^{\circ}\text{C}$)	(W/m ² K)	
1	010:00:00	1.13	120.935	5.1457	16.1
2	020:00:00	2.00	115.79	5.7164	16.3
3	030:00:00	1.323	110.242	6.2341	35.8
4	040:00:00	1.44	104.17	6.9716	38.9
5	050:00:00	1.23	99.685	7.0677	41.6

(iii) Evaluation of exhaust gas and emission:

Table-14. Exhaust gas calculation

S.No.	Time (min)	Mass flow rate (kg/hr)	Solar inlet temperature ($^{\circ}\text{C}$)	HRU Temperature ($^{\circ}\text{C}$)		$\Delta T_{exht} = (T_{in} - T_{out})$ in HRU	Electric load (kW)	Solar heat (kW)	HRU working fluid heat (kW)	Generator heat (day) (kW)	Exhaust heat to generator (night) (kW)	Actual exhaust heat (kW)
				Inlet	Outlet							
				($^{\circ}\text{C}$)	($^{\circ}\text{C}$)	($^{\circ}\text{C}$)						
1	00 to 30	1818.47	120.37	121.5	125.0333	223	15.24	2.39	3.72	9.85	7.46	11.18
2	31 to 60	1871.38	114.79	116.79	121.52	231	23.62	4.35	4.335	14.623	10.28	14.608
3	61 to 90	1852.16	109.58	110.903	118.645	297	27.43	2.84	4.025	19.493	16.65	20.678
4	91 to 120	1774.38	103.45	104.89	114.414	303	32	2.98	4.33	22.59	19.61	23.94
5	121 to 150	1749.37	99.07	100.3	111.33	316	38.86	2.49	3.72	24.894	22.404	26.124

Table-15. Exhaust gas emissions calculation

S.No.	Electric load	Exhaust gas temperature (°C)			O ₂	CO ₂	NO
		Inlet	RHE	Outlet			
	(kW)				(%)	(%)	(ppm)
1	15.24	352	182	129	11.79	0.1	46
2	23.62	366	233	135	8.62	0.122	68
3	27.432	439	271	142	7.81	0.129	80
4	32.004	450	299	147	5.29	0.142	120
5	38.862	465	316	149	4.18	0.153	220

(iv) Assessment of HRU:

Table-16. HRU ED evaluation for exhaust and solar energy

S.No.	Electric load	Effectiveness	ΔT (LMTD)	U	Heat capacity Ratio (R)	Mass flow rate (kg/hr)	Exhaust gas temperature (°C)		HRU Temperature (water) (°C)		C_{max} (kW/K)	C_{min} (kW/K)	Temp. ratio $T_R = \frac{T_{h_1}}{T_{c_1}}$	Entropy generation	$\dot{E}_{D,HRU}$
	(kW)						(ϵ)	(K)	(kW/m ² K)	(kg/hr)	RHE	Outlet		Inlet	Outlet
							T_{h_1}	T_{h_2}	T_{c_1}	T_{c_2}					
1	15.24	0.8763	24.44	0.3985	0.0665	1818.47	182	129	121.5	125.0333	2.111445722	0.1407617	1.153358682	0.001347447	0.4015393
2	23.62	0.8437	51.57	0.2602	0.04788	1871.38	233	135	116.79	121.52	2.172880111	0.1048747	1.298134893	0.003424637	1.0205419
3	27.432	0.8054	76.21	0.2852	0.0602	1852.16	271	142	110.903	118.645	2.150563556	0.1290672	1.417024613	0.00813279	2.4235714
4	32.004	0.7821	96.13	0.266	0.06295	1774.38	299	147	104.89	114.414	2.060252333	0.1290911	1.513667999	0.011637987	3.4681203
5	38.862	0.7922	104.524	0.314	0.06474	1749.37	316	149	100.3	111.33	2.031212944	0.1341574	1.577819448	0.013350326	3.9783971

Table-17. HRU evaluation for exhaust and solar energy

S.No.	ΔT (Temp. gain)	$\Delta h_{exht} = h_o - h_{in}$ (kJ/kg)	$P_{exht,2}$ (bar)	$P_{exht,1}$ (bar)	$\Delta S_{exht} = S_o - S_{in}$ (kJ/kgK)	\dot{m}_{exht} (kg/hr)	$\dot{E}_{xin/HRU}$ (kW)	HRU Temperature (water) (°C)		Enthalpy at HRU		Entropy at HRU		$\dot{E}_{xout/HRU}$ (kW)	Exergy efficiency Or Effectiveness
								Inlet	Outlet	IN	OUT	IN	OUT		
	(°C)					$(\dot{m}_{PG} + \dot{m}_{air})$		T_{C_1}	T_{C_2}	(kJ/kg)	(kJ/kg)	(kJ/kgK)	(kJ/kgK)		
1	4.6633	-51.5512	4.33	1.347	-0.4591936	180.513	-4.27657	121.5	125.0333	510.19	525.22	1.5441	1.5819	1.90211962	0.4447761
2	6.73	-95.3211	4.89	1.121	-0.6387978	225.885	-5.96341	116.79	121.52	490.18	510.27	1.4932	1.5443	2.527506621	0.4238362
3	9.065	-125.473	8.272	1.453	-0.7712153	248.674	-7.20799	110.903	118.645	465.24	498.06	1.4288	1.5133	3.930180622	0.5452535
4	10.964	-147.845	8.37	1.237	-0.8595201	271.985	-8.18161	104.89	114.414	439.81	480.11	1.3621	1.4673	4.411502987	0.5391973
5	12.26	-162.434	11.454	1.962	-0.8420485	340.079	-8.35985	100.3	111.33	420.43	467.04	1.3106	1.4335	4.852460818	0.5804482

Table-18. HRU ED evaluation for producer gas

S.No.	PG gas temperature (°C)		ΔT (Temp. gain)	Effectiveness	ΔT (LMTD)	U	Heat capacity Ratio (R)	Correction factor (F)	HRU Temperature (water) (°C)		Mass flow rate of water	C_{max} (kW/K)	C_{min} (kW/K)	Temp. ratio $T_R = \frac{T_h}{T_{C_1}}$	Entropy generation (kW/K)	$\dot{E}_{D,HRU}$ (kW)
	Inlet	Outlet							Inlet	Outlet						
	(Th1)	(Th2)	(°C)	(ϵ)	(K)	(kW/m ² K)	(R)	(F)	T_{C_1}	T_{C_2}	(kg/hr)	(Cold fluid)	(Hot fluid)			
1	465.6	87.894	377.706	0.9718	105.13	0.0331	0.00945	0.9398	76.93	80.5	805.82	0.9356466	0.008844	2.11071	0.003162	0.9422311
2	548.4	106.58	441.82	0.9641	131.71	0.03631	0.011	0.9433	90.15	95	817.83	0.9495915	0.010424	2.26188	0.004577	1.3640365
3	618.3	116.35	501.95	0.9716	139.84	0.03581	0.0102	0.9091	101.7	106.8	785.57	0.9121341	0.009268	2.3787	0.004704	1.4016456
4	674.25	130.325	543.925	0.9639	162.79	0.02791	0.00843	0.9584	109.95	114.55	832.55	0.9666831	0.008175	2.47356	0.004526	1.3486589
5	710.5	137.9	572.6	0.9644	170.74	0.02681	0.00794	0.9596	116.75	121.29	850.5	0.987525	0.00783	2.52341	0.004619	1.376527

Table-19. HRU evaluation for producer gas

S.No	$\Delta h_{PG} = h_o - h_{in}$	$P_{PG,2}$	$P_{PG,1}$	$\Delta S_{PG} = S_o - S_{in}$	\dot{m}_{PG}	$\dot{E}_{x_{in}/HRU}$	HRU Temperature (water) (°C)		Enthalpy at HRU (kJ/kg)		Entropy at HRU (kJ/kgK)		$\dot{E}_{x_{out}/HRU}$	Exergy efficiency
	(kJ/kg)	(bar)	(bar)	(kJ/kg.K)	(kg/hr)	(kW)	Inlet	Outlet			IN	OUT		
							T_{C_1}	T_{C_2}						
1	-367.38	4.55	1.457	-1.0491233	73.6186	1.11946	76.93	80.5	322.13	337.11	1.0389	1.0815	0.51152	0.45931
2	-429.74	7.11	1.251	-1.2795939	123.1656	1.65671	90.15	95	377.67	398.09	1.1946	1.2504	0.86136	0.51992
3	-488.23	15.27	1.621	-1.4834239	136.1105	1.74556	101.7	106.8	426.34	447.88	1.3264	1.3834	0.99375	0.56929
4	-529.06	19.17	1.151	-1.6747507	159.3035	1.32668	109.95	114.55	461.2	480.69	1.4183	1.4688	1.02704	0.77415
5	-556.95	31.55	1.389	-1.7841806	192.3523	1.34977	116.75	121.29	490.01	509.29	1.4927	1.5418	1.09814	0.81357

(v) Performance of VAM:

Table-20. Evaluation of VAM

SNo	Electric load (kW)	Pressure (bar)		Ammonia flow rate (kg/hr)	Enthalpy at condenser pressure		Entropy at condenser pressure		Enthalpy at absorber pressure		Entropy at absorber pressure		Energy output	Exergy output
		condenser	Absorber /Evap.		h_{fc}	h_{gc}	S_{fc}	S_{gc}	h_{fa}	h_{ga}	S_{fa}	S_{ga}		
					(kJ/kg)	(kJ/kg)	(kJ/kgK)	(kJ/kgK)	(kJ/kg)	(kJ/kg)	(kJ/kgK)	(kJ/kgK)	(kW)	(kW)
1	15.24	14.1	2.41	17.04	354.894	1471.83	1.306	4.915	116.85	1427.31	0.46501	5.543	6.20284	0.95983
2	23.62	14.34	2.32	23.09	357.83	1472.22	1.315	4.9086	110.11	1425.93	0.4501	5.555	8.43952	1.31767
3	27.432	15	2.3	28.73	365.624	1472.745	1.339	4.892	109.198	1425.67	0.4457	5.558	10.5062	1.65192
4	32.004	15.37	2.16	29.64	369.451	1473.122	1.354	4.882	102.695	1423.79	0.4198	5.581	10.877	1.78616
5	38.862	15.94	2.08	31.12	376.426	1473.479	1.373	4.691	98.96	1422.72	0.4043	5.5939	11.4432	1.92547

Table-21. COP Evaluation of VAM

S.No.	Electric load (kW)	Temperature (°C)		Flow rate of solar water (kg/hr)	Enthalpy at VAM		Entropy at VAM		Energy input (kW)	Exergy input (kW)	COP _I VAM	COP _{II} VAM
		HW VAM IN	HW VAM OUT		IN	OUT	IN	OUT				
					h_4 (kJ/kg)	h_5 (kJ/kg)	S_4 (kJ/kgK)	S_5 (kJ/kgK)				
									Expenditure			
1	15.24	125.033	120.37	1818.467	525.21	505.38	1.5819	1.5319	10.0167	2.49028	0.61925	0.385431
2	23.62	121.52	114.79	1871.37	510.27	481.7	1.5443	1.4714	14.8514	3.55862	0.568264	0.370275
3	27.432	118.645	109.58	1852.16	498.06	459.64	1.5133	1.4142	19.7667	4.57288	0.531509	0.361243
4	32.004	114.414	103.45	1774.38	480.11	433.73	1.4673	1.346	22.8599	5.04348	0.475811	0.354153
5	38.862	111.33	98.93	1749.37	467.04	414.65	1.4335	1.2951	25.4582	5.41663	0.449488	0.355473

Table-22. Entropy Evaluation of VAM

S.No.	Temperature (°C)									Entropy (kJ/kgK)												
	CW Condenser		CW/air Evaporator		WS GEN OUT	WS SHE OUT	WS ABS IN	SS ABS OUT	SS SHE IN	SS GEN IN	Entropy of CW for condenser		Entropy of CW for evaporator		Entropy of CW for absorber		WS GEN OUT	WS SHE OUT	WS ABS IN	SS ABS OUT	SS SHE IN	SS GEN IN
	T_k	T_l	T_p	T_q	[7]	[8]	[9]	[10]	[11]	[12]	S_k	S_l	S_p	S_q	S_i	S_j	[7]	[8]	[9]	[10]	[11]	[12]
1	28.65	36.52	28.65	-3.2	51.34	42.05	38.73	30.64	33.14	52.58	0.4181	0.5257	6.8778	6.7655	0.401	0.494	-0.399	-0.524	-0.5685	1.0053	1.045	1.343
2	29.98	37.12	29.98	-3.35	54.54	47.9	38.56	31.08	33.85	53.38	0.4365	0.5338	6.8821	6.7651	0.401	0.494	-0.358	-0.445	-0.5709	1.0122	1.056	1.355
3	30.76	38.73	30.76	-3.96	55.78	51.21	39.36	32.76	34.69	53.26	0.4472	0.5554	6.8846	6.7626	0.401	0.494	-0.342	-0.402	-0.5599	1.0386	1.069	1.353
4	31.87	39.59	31.87	-4.01	56.64	52.85	39.42	33.16	35.79	54.67	0.4625	0.5669	6.8883	6.7624	0.401	0.494	-0.331	-0.381	-0.5591	1.0449	1.086	1.374
5	31.98	40.91	31.98	-4.61	57.06	54.06	39.13	34.71	36.01	55.23	0.4639	0.5845	6.8886	6.7601	0.401	0.494	-0.326	-0.364	-0.5631	1.0692	1.089	1.383

Where the entropy of absorber are taken at input and output CW temperature 33.4°C and 40.21°C. $C_{p,ice} = 2.11 \text{ kJ / kgK}$

Table- 23. EDs Evaluation of VAM

S.No.	Electric load (kW)	Temperature (°C)				Mass flow rate (kg/hr)							EXERGY DESTRUCTION (kW)							
		Abs.	Gen.	Evap.	cond.	Water	CW	CW	NH3	Air	\dot{m}_{WS}	\dot{m}_{SS}	GEN	PUMP	SHE	TV1	TV2	ABS	Cond.	Evap.
						(solar)	(cond.)	(Abs.)	Ref.	Evap.										
1	15.24	35.33	83.95	-3.2	34.82	1818.47	503.83	1347.95	17.04	515.768	36.85	51.89	7.516	0.169	1.659	0.137	1.186	8.589	0.6031	2.3681
2	23.62	36.49	83.52	-3.35	35.84	1871.37	617.46	2011.17	23.09	768.382	54.59	77.46	12.211	0.279	2.313	0.568	1.653	14.033	1.8949	2.3091
3	27.432	37.44	82.99	-3.76	36.36	1852.16	658.29	2705.94	28.73	991.841	42.68	75.41	13.328	0.189	1.986	0.559	2.124	16.406	2.5538	2.1416
4	32.004	38.95	81.62	-4.01	37.64	1774.38	692.56	3152.04	29.64	1105.644	33.33	71.97	15.185	0.245	1.853	0.494	2.293	18.926	2.6669	1.1405
5	38.862	39.74	80.05	-4.61	38.86	1749.37	566.73	3490.66	31.12	1147.563	31.53	74.52	17.656	0.125	1.911	0.519	2.495	21.268	2.8915	1.1621

Table-24. VAM calculation with respect to atmosphere

S.No.	Temperature (°C)			Heat (kW)				η energy with T_{atm} (%)	η exergy with T_{atm} (%)
	T_{atm}	T_{gen}	T_{evap}	Q_{evap}	Q_{gen}	Q_{cond}	Q_{abs}		
1	308.0521	356.95	269.8	6.20284	9.85	5.2868304	10.6585	96.621	61.15
2	310.6496	356.52	269.65	8.43952	14.623	7.14757364	15.90264	84.619	54.2
3	311.677	355.99	269.24	10.5062	19.493	8.83544065	21.39632	78.975	51.787
4	312.6452	354.62	268.99	10.877	22.59	9.08689123	24.92373	72.933	49.264
5	313.2606	353.05	268.39	11.4432	24.894	9.48341371	27.60126	67.412	47.696

(vi) Combined analysis:

Table-25. Combined analysis

S.No.	COND. Temp.	EVAP. Temp.	Exht gas temp.	NH ₃ flow rate	Enthalpy at absorber pressure		Electric load	Refrigeration output	Total output	Total Energy in	Overall energy efficiency	Grate temp.	$\frac{T_o}{T_{grate}}$	Overall exergy efficiency
					h_{fa}	h_{ga}						T_{grate}		
	(°C)	(°C)	(°C)	(kg/hr)	(kJ/kg)	(kJ/kg)	(kW)	(kW)	(kW)	(kW)	(%)	(K)		(%)
1	34.82	-3.2	352	115.04	116.85	1427.31	15.24	41.8765	57.1165	161.043	35.466	811	0.36745	56.069
2	35.84	-3.35	366	88.09	110.11	1425.93	23.62	32.1974	55.8174	228.386	24.439	847	0.35183	37.706
3	36.36	-3.96	439	56.73	109.19	1425.67	27.432	20.7454	48.1774	243.865	19.756	857	0.34773	30.287
4	37.64	-4.01	450	35.64	102.69	1423.79	32.004	13.0788	45.0828	275.003	16.394	878	0.33941	24.817
5	38.86	-4.61	465	12.11	98.96	1422.72	38.862	4.4529	43.3149	320.397	13.519	896	0.33259	20.256

Table-26. Combined analysis at constant load

S.No.	COND. Temp.	EVAP. Temp.	Exhaust gas temp.	Electric load	NH ₃ flow rate	Refrigeration output	Total output	Total Energy in	Overall energy efficiency	Grate temp.	$\frac{T_o}{T_{grate}}$	Overall exergy efficiency
										T_{grate}		
	(°C)	(°C)	(°C)	(kW)	(kg/hr)	(kW)	(kW)	(kW)	(%)	(K)	(K)	(%)
1	34.82	-3.2	352	38.862	115.04	41.87648	80.73848	161.0428	50.135	811	0.36745	79.258
2	35.84	-3.35	366	38.862	88.09	32.19738	71.05938	228.3855	31.113	847	0.35183	48.003
3	36.36	-3.96	439	38.862	56.73	20.7454	59.6074	243.8653	24.443	857	0.34773	37.473
4	37.64	-4.01	450	38.862	35.64	13.07884	51.94084	275.0027	18.887	878	0.33941	28.592
5	38.86	-4.61	465	38.862	12.11	4.452982	43.314982	320.3965	13.519	896	0.33259	20.256

Table-27. Overall heat balance at different loads

S.No.	Load (kW)	Heat utilized in different components (kW)					Heat utilized in different components (%)					Average (%)
		15.24	23.62	27.432	32.004	38.862	15.24	23.62	27.432	32.004	38.862	
1	Heat supplied by biomass	144.6667	211.8333	227.3333	258.3333	304.8333						
2	Heat supplied by solar	16.37614	16.552167	16.53198	16.66938	15.563183						
3	Total heat supplied	161.04284	228.38547	243.8653	275.0027	320.396483	100	100	100	100	100	100
4	Ht used in gasification (Q1)	43.07525	58.06461	43.6327	49.2982	59.5071903	26.7477	25.42395	17.89213	17.92644	18.57298	21.31264
5	Ht used in HE-1 (regen.) (Q2)	5.290723	8.977954	9.968127	11.01247	14.48199	3.28529	3.931053	4.087554	4.004495	4.520021	3.9656826
6	Ht. used in HE-2 (Air cooler)(Q3)	2.015514	3.793502	3.959303	5.397203	7.240995	1.251539	1.661008	1.623561	1.9626	2.260011	1.7517438
7	Ht. used in HE-2 (Water cooler)(Q4)	0.604654	1.138051	1.490561	1.853585	2.501435	0.375462	0.498303	0.611223	0.674024	0.780731	0.5879486
8	Ht. used in fabric filter(Q5)	1.385666	2.444701	3.074282	2.998446	3.949634	0.860433	1.070427	1.260647	1.090333	1.232733	1.1029146
9	Ht. used in paper filter(Q6)	0.075582	0.0843	0.18632	0.109034	0.197482	0.046933	0.036911	0.076403	0.039648	0.061637	0.0523064
10	Ht. equivalent to Brake power(Q7)	19.05	29.525	34.29	40.005	48.5775	11.82915	12.9277	14.06104	14.54713	15.16168	13.70534
11	Ht. equivalent to electric power(Q8)	15.24	23.62	27.432	32.004	38.862	9.463322	10.34216	11.24883	11.6377	12.12935	10.9642724
12	Ht. lost due to exhaust (Q9)	11.18	14.608	20.678	23.94	26.127	6.942254	6.396203	8.479271	8.705369	8.154583	7.735536
13	Ht. used in solar collector(Q10)	2.39	4.35	2.84	2.98	2.78	1.484077	1.904674	1.164577	1.083626	0.867675	1.3009258
14	Ht. used in HRU(Q11)	7.46	10.28	16.65	19.61	22.404	4.632309	4.501161	6.827539	7.130839	6.992585	6.0168866
15	Ht. used in Generator(Q12)	9.85	14.623	19.493	22.59	24.894	6.116386	6.402771	7.993347	8.214465	7.769747	7.2993432
16	Ht. used in Condenser(Q13)	5.28683	7.1475736	8.835441	9.086891	9.48341371	3.282872	3.129609	3.623082	3.304292	2.959899	3.2599508
17	Ht. used in Evaporator(Q14)	6.20284	8.43952	10.5062	10.877	11.4432	3.851672	3.695296	4.308198	3.955234	3.571574	3.8763948
18	Ht. used in TV1 (Q15)	0.14205266	0.5920164	0.587241	0.519739	0.54658481	0.088208	0.259218	0.240806	0.188994	0.170596	0.1895644
19	Ht. used in TV2 (Q16)	1.1267416	1.5888486	2.046422	2.196291	2.39853942	0.699653	0.695687	0.839161	0.798643	0.748616	0.756352
20	Ht. used in Pump (Q17)	0.17008389	0.2813175	0.190821	0.248169	0.1270152	0.105614	0.123177	0.078248	0.090242	0.039643	0.0873848
21	Ht. used in SHE (Q18)	1.32257	1.98344	1.83603	1.78153	1.87787	0.821254	0.868461	0.752887	0.647823	0.586108	0.7353066
22	Ht. used in Absorber (Q19)	10.6585	15.90264	21.39632	24.92373	27.60126	6.618427	6.963069	8.773827	9.063085	8.614719	8.0066254
23	Unaccounted heat loss (Q20)	18.5158	20.9415	14.7723	13.5717	15.3955	11.49744	9.169365	6.057571	4.935118	4.805145	7.2929278

Table-28. Overall exergy balance at different loads

S.No.	Load (kW)	Exergy distribution in output and exergy destruction (kW)					Exergy distribution in output and exergy destruction (%)					Average (%)
		15.24	23.62	27.432	32.004	38.862	15.24	23.62	27.432	32.004	38.862	
1	Exergy supplied by biomass	173.4483	253.9779	272.5617	309.7292	365.4804						
2	Exergy supplied by solar	14.92369	17.31099	20.1756	22.96859	25.01276						
3	Total exergy supplied	188.37199	271.28889	292.7373	332.6978	390.49316	100	100	100	100	100	100
4	Exergy o/p of electric generator	15.24	23.62	27.432	32.004	38.862	8.090373	8.734707	9.387899	9.634239	9.96334	9.1621116
5	Exergy output of VAM	0.95983	1.31767	1.65192	1.78616	1.92547	0.50954	0.487276	0.565327	0.537692	0.493647	0.5186964
6	ED of gasifier (ED1)	64.638933	71.901217	71.37337	73.86787	81.316917	34.31451	26.58916	24.4257	22.23662	20.84782	25.682762
7	ED of HE-1 (regen.) (ED2)	1.166287	2.125812	2.377026	2.893967	3.251657	0.61914	0.786128	0.813476	0.871178	0.833652	0.7847148
8	ED of HE-2 (Air cooler)(ED3)	0.2791359	0.5494765	0.586069	0.846932	1.2382843	0.148183	0.203197	0.200567	0.254954	0.317468	0.2248738
9	ED of HE-2 (Water cooler)(ED4)	0.13461076	0.252958	0.337508	0.409665	0.57018339	0.07146	0.093544	0.115503	0.123322	0.146182	0.1100022
10	ED of fabric filter(ED5)	0.4575982	0.8623059	1.105029	1.117194	1.559275	0.242923	0.318882	0.378168	0.336312	0.399763	0.3352096
11	ED of paper filter(ED6)	0.0035064	0.0042953	0.009492	0.005556	0.0097624	0.001861	0.001588	0.003248	0.001672	0.002503	0.0021744
12	ED of engine (ED7)	43.806	94.43688	113.4845	141.2171	173.0374	23.25505	34.92288	38.83716	42.51091	44.36289	36.777778
13	ED of electric generator (ED8)	3.81	5.905	6.858	8.001	9.7155	2.022593	2.183677	2.346975	2.40856	2.490835	2.290528
14	Exhaust exergy loss (ED9)	0.54628	0.7664	0.95543	1.13602	1.46703	0.290001	0.283416	0.326971	0.341979	0.376113	0.323696
15	ED of solar collector(ED10)	14.41382	16.43757	19.6443	22.46105	24.5695	7.651784	6.078635	6.722758	6.761503	6.299066	6.7027492
16	ED of HRU(ED11)	0.401539309	1.0205419	2.423571	3.46812	4.29883778	0.213163	0.377398	0.829405	1.044016	1.102125	0.7132214
17	ED of Generator(ED12)	7.515907	12.21081	13.32835	15.18532	17.65611	3.989927	4.515573	4.561286	4.571272	4.526628	4.4329372
18	ED of Condenser(ED13)	0.60305697	1.8948817	2.553753	2.666949	2.89152638	0.320141	0.70073	0.873957	0.802838	0.741322	0.6877976
19	ED of Evaporator(ED14)	2.3681226	2.3091785	2.141611	1.140461	1.1620817	1.257152	0.853937	0.732911	0.343316	0.297932	0.6970496
20	ED of TV1 (ED15)	0.137449	0.567657	0.559479	0.493858	0.518656	0.072967	0.20992	0.191467	0.148667	0.132972	0.1511986
21	ED of TV2 (ED16)	1.18624	1.65312	2.12445	2.29209	2.49541	0.629733	0.611326	0.727039	0.689993	0.639767	0.6595716
22	ED of Pump (ED17)	0.168807	0.278921	0.188517	0.244854	0.124606	0.089614	0.103145	0.064515	0.073709	0.031946	0.0725858
23	ED of SHE (ED18)	1.6587	2.3127	1.9857	1.8533	1.9106	0.880545	0.855239	0.679555	0.557903	0.489835	0.6926154
24	ED of Absorber (ED19)	8.58914	14.0328	16.4057	18.9261	21.2684	4.559669	5.189348	5.61443	5.697368	5.452738	5.3027106
25	Unaccounted exergy loss (ED20)	20.287	15.9555	4.6799	0.17222	0.20092	10.76966	5.90036	1.601599	0.051843	0.051511	3.6749946

APPENDIX-C

(Uncertainty analysis)

Uncertainty analysis proposed by Kline and McClintok (1953) has been used for prediction of uncertainty interval associated with experimental result, based on observations of scatter in raw data used in calculating the result.

If a parameter is calculated using certain measured quantities as:

$$Y = y(x_1 + x_2 + x_3 + \dots + x_n)$$

Thus uncertainty measured of y quantity is given by:

$$\frac{\delta y}{y} = \left[\left(\frac{\delta y}{\partial x_1} \cdot \delta x_1 \right)^2 + \left(\frac{\delta y}{\partial x_2} \cdot \delta x_2 \right)^2 + \left(\frac{\delta y}{\partial x_3} \cdot \delta x_3 \right)^2 + \dots + \left(\frac{\delta y}{\partial x_n} \cdot \delta x_n \right)^2 \right]^{1/2}$$

Where,

$\delta x_1, \delta x_2, \delta x_3, \dots$ are uncertainties measurements of x_1, x_2, x_3, \dots

δy is known as absolute uncertainty,

$\frac{\delta y}{y}$ is known as relative uncertainty

As a sample, the uncertainty intervals of various equipments used for the measurement of various parameters are given below:

(i) Uncertainty in time measurement during feed rate:

$$\text{Uncertainty} = \frac{\delta t}{t}$$

Where, t = time in second

$$t = 30 \text{ min}$$

$$\delta t = 0.05 \text{ s}$$

$$\text{Uncertainty} = \frac{\delta t}{t} = \frac{0.05}{30 \times 60} = 2.7 \times 10^{-5} = 0.0027\%$$

(ii) Uncertainty in measurement of grate area:

$$\frac{dA}{A} = \left[2 \left(\frac{\delta d}{d} \right)^2 \right]^{1/2} = \left[2 \left(\frac{0.5}{300} \right)^2 \right]^{1/2}$$

$$= 0.236\%$$

where, A is the area of grate

d is the diameter of grate

(iii) Uncertainty in volume measurement of trough for measuring density

$$\frac{dV}{V} = \left[\left(\frac{\delta a}{a} \right)^2 + \left(\frac{\delta b}{b} \right)^2 + \left(\frac{\delta c}{c} \right)^2 \right]^{1/2} = \left[\left(\frac{0.5}{400} \right)^2 + \left(\frac{0.5}{400} \right)^2 + \left(\frac{0.5}{200} \right)^2 \right]^{1/2} = 0.279\%$$

Where, a is the length of trough, b is the breadth of trough and c is the height of trough.

(iv) Uncertainty in measurement of Biomass Consumption Rate (BCR):

$$\begin{aligned}\frac{dBCR}{BCR} &= \frac{50}{40500} \\ &= 0.123\%\end{aligned}$$

(v) Uncertainty in measurement of temperature of oxidation zone

$$\begin{aligned}\frac{dT}{T} &= \frac{0.005}{1400} \\ &= 3.57 \times 10^{-4}\%\end{aligned}$$

(vi) Uncertainty in measurement of temperature of reduction zone

$$\begin{aligned}\frac{dT}{T} &= \frac{0.005}{800} \\ &= 6.25 \times 10^{-4}\%\end{aligned}$$

(vii) Uncertainty in measurement of area of orifice

$$\begin{aligned}\frac{dA}{A} &= \left[2 \left(\frac{\delta d}{d} \right)^2 \right]^{\frac{1}{2}} \\ &= \left[2 \left(\frac{0.05}{250} \right)^2 \right]^{\frac{1}{2}} = 2.83 \times 10^{-2}\%\end{aligned}$$

(viii) Uncertainty in measurement of area of pipe

$$\begin{aligned}\frac{dA}{A} &= \left[2 \left(\frac{\delta d}{d} \right)^2 \right]^{\frac{1}{2}} \\ &= \left[2 \left(\frac{0.05}{500} \right)^2 \right]^{\frac{1}{2}} \\ &= 1.41 \times 10^{-2}\%\end{aligned}$$

(ix) Uncertainty in measurement of gasifier efficiency

$$\begin{aligned}\frac{d\eta}{\eta} &= \left[\left(\frac{\delta \dot{m}_{PG}}{\dot{m}_{PG}} \right)^2 + \left(\frac{\delta \dot{m}_b}{\dot{m}_b} \right)^2 + \left(\frac{\delta CV_{PG}}{CV_{PG}} \right)^2 + \left(\frac{\delta CV_b}{CV_b} \right)^2 \right]^{\frac{1}{2}} \\ &= \left[\left(\frac{0.5}{125.62} \right)^2 + \left(\frac{0.5}{44.45} \right)^2 + \left(\frac{0.001}{5.16} \right)^2 + \left(\frac{0.001}{19.99} \right)^2 \right]^{\frac{1}{2}} \\ &= \left[1.58 \times 10^{-5} + 1.27 \times 10^{-4} + 3.76 \times 10^{-8} + 2.51 \times 10^{-9} \right]^{\frac{1}{2}} \\ &= 1.43\%\end{aligned}$$

(x) Uncertainty in measurement of effectiveness of the HRU

$$\begin{aligned}\frac{d\varepsilon}{\varepsilon} &= \left[\left(\frac{\delta T_{h_1}}{T_{h_1}} \right)^2 + \left(\frac{\delta T_{h_2}}{T_{h_2}} \right)^2 + \left(\frac{\delta T_{c_1}}{T_{c_1}} \right)^2 \right]^{\frac{1}{2}} \\ &= \left[\left(\frac{0.005}{260.21} \right)^2 + \left(\frac{0.005}{139.62} \right)^2 + \left(\frac{0.005}{110.88} \right)^2 \right]^{\frac{1}{2}} \\ &= \left[3.69 \times 10^{-10} + 1.28 \times 10^{-9} + 3.76 \times 10^{-8} + 2.03 \times 10^{-9} \right]^{\frac{1}{2}} = 0.0203\%\end{aligned}$$

(xi) Uncertainty in measurement of COP of the VAM

$$\begin{aligned}\frac{dCOP}{COP} &= \left[\left(\frac{\delta \dot{m}_r}{\dot{m}_r} \right)^2 + \left(\frac{\delta \dot{m}_{ws}}{\dot{m}_{ws}} \right)^2 + \left(\frac{\delta h_{in}}{h_{in}} \right)^2 + \left(\frac{\delta h_{out}}{h_{out}} \right)^2 + \left(\frac{\delta h_4}{h_4} \right)^2 + \left(\frac{\delta h_5}{h_5} \right)^2 \right]^{\frac{1}{2}} \\ &= \left[\left(\frac{0.001}{25.93} \right)^2 + \left(\frac{0.005}{1813} \right)^2 + \left(\frac{0.001}{107.56} \right)^2 + \left(\frac{0.001}{1425.08} \right)^2 + \left(\frac{0.001}{496.14} \right)^2 + \left(\frac{0.001}{459.02} \right)^2 \right]^{\frac{1}{2}} \\ &= \left[1.49 \times 10^{-9} + 7.61 \times 10^{-12} + 8.64 \times 10^{-11} + 4.92 \times 10^{-13} + 4.06 \times 10^{-12} + 4.75 \times 10^{-12} \right]^{\frac{1}{2}} \\ &= 3.99 \times 10^{-3}\%\end{aligned}$$

(xii) Uncertainty in measurement of efficiency of the scheffler

$$\begin{aligned}\frac{d\eta}{\eta} &= \left[\left(\frac{\delta \dot{m}_w}{\dot{m}_w} \right)^2 + \left(\frac{\delta DNI}{DNI} \right)^2 + \left(\frac{\delta T_{in}}{T_{in}} \right)^2 + \left(\frac{\delta T_{out}}{T_{out}} \right)^2 + 2 \right]^{\frac{1}{2}} \\ &= \left[\left(\frac{0.005}{1813.15} \right)^2 + \left(\frac{0.001}{440.92} \right)^2 + \left(\frac{0.005}{109.42} \right)^2 + \left(\frac{0.005}{110.88} \right)^2 + 2 \right]^{\frac{1}{2}} \\ &= \left[7.61 \times 10^{-12} + 5.14 \times 10^{-12} + 4.92 \times 10^{-13} + 2.09 \times 10^{-9} + 2.03 \times 10^{-9} + 2 \right]^{\frac{1}{2}} \\ &= 1.41\%\end{aligned}$$

(xiii) Uncertainty in measurement of voltage

$$\frac{dV}{V} = \frac{0.005}{226.8} = 2.205 \times 10^{-5}$$

(xiv) Uncertainty in measurement of electric load

$$\frac{dP}{P} = \frac{0.005}{27.432} = 1.82 \times 10^{-4}$$

(xv) Uncertainty in measurement of air velocity

$$\frac{dVel}{Vel} = \frac{0.001}{4.8} = 2.08 \times 10^{-4}$$

APPENDIX-D (Brief Biodata)

BRIEF PROFILE OF THE RESEARCH SCHOLAR

Anil Kumar is currently an Assistant Professor in Mechanical & Automation Engineering Department, Amity School of Engineering & Technology, Bijwasan New Delhi and he has received his B.E. in Mechanical Engineering from Government Engineering College Jabalpur (M.P.) and M. Tech. in Thermal Engineering from Rajeev Gandhi Technical University Bhopal (M.P.). He is pursuing his Ph.D. under the supervision of Prof. (Dr.) Raj Kumar, Department of Mechanical Engineering, YMCA University of Science & Technology, Faridabad, Haryana, India. His topic of the research is “*Experimental investigation of hybrid cold storage system cum power generator*”. The experimental investigation is performed at the Solar Energy Centre, Gwalpahari, Gurgaon, for experimental investigation. His research area is Thermal Engineering, New and renewable energy, and Refrigeration and Air Conditioning. He has about fifteen years of experience of teaching and research, including research work on New and renewable energy at Central Institute of Agricultural Engineering, Bhopal (MP) and Solar Energy Centre, Gurgaon (HR). Recently, he has published many research articles in the national, International Journals and conferences. He has taught nearly fifteen subjects at the technical graduation level (Bachelor of Engineering / Bachelor of Technology).

APPENDIX-E (List of Publications)

List of published Papers in International Journals (5)

S.No.	Title of the paper along with, volume, Issue No, year of publication	Publishers	Impact Factor	Referred or Non-referred	Whether you paid any money or not for publication	Remarks
1	Energy and exergy analysis of compact power generation and hybrid solar energy-waste heat based triple effect ejector-vapour absorption refrigeration cycle, 2013, Vol.21, No.4, pp.1-14	World Scientific	2.3 (GISI) (Newly added in SCI)	Referred	No	Available online at world scientific website
2	Performance Evaluation of Downdraft Gasifier for Generation of Engine Quality Gas, 2013, Vol. 1, No.2, pp. 50-54	HR Publication USA	-----	Referred	No	Available online at HR Publication website
3	Thermodynamic analysis of a novel compact power generation and waste heat operated absorption, ejector-jet pump refrigeration cycle, 2014, Vol.28, No.9, pp.3895-3902	Springer	0.703 (SCI)	Referred	No	Available online at world spriger website
4	Thermodynamic analysis of biomass based integrated refrigeration cycle, 2015, Vol.16, No.02, pp.214-238	Inderscience	0.847 (SCI)	Referred	No	Available online at inderscience website
5	Comparative thermodynamic analysis of compact co-generation and triple effect refrigeration cycle (2016)	Taloy & Francis	0.247 (Scopus) (Newly added in SCI)	Referred	No	Recently accepted

List of National Conference Papers (3)

S.No.	Title of the paper	Name Of Organization	Year	Name Of Conference	Whether you paid any money or not for publication	Remarks
1	Performance investigation of a compact tri-generation system based on renewable energy power plant exhaust gas waste heat utilization	YMCAUST Faridabad	2012	TAME 2012	Ph.D. scholar charges	Available online at organization website
2	Performance Evaluation of Downdraft Gasifier for Power Generation and internal combustion S.I. Engine applications	RITS, Bhopal	2013	NCETRES 2013	Ph.D. scholar charges	Available at institute's website
3	Performance evaluation of concentrating solar reflector for water heating and low temperature industrial application	Rawal Institute Faridabad	2015	NCRTME 2015	Ph.D. scholar charges	Available online at institute's website